UNIVERSITÉ DU QUÉBEC

THÈSE

PRÉSENTÉE À

L'UNIVERSITÉ DU QUÉBEC À CHICOUTIMI

COMME EXIGENCE PARTIELLE

DU DOCTORAT EN RESSOURCES MINÉRALES

PAR

TANGFU XIAO

ENVIRONMENTAL IMPACT OF THALLIUM RELATED TO THE MERCURY-THALLIUM-GOLD MINERALIZATION IN SOUTHWEST GUIZHOU PROVINCE, CHINA

AOÛT 2001

Bibliothèque
Paul-Émile-Boulet

UQAC
Université du Québec
à Chicoutimi

Mise en garde/Advice

Afin de rendre accessible au plus grand nombre le résultat des travaux de recherche menés par ses étudiants gradués et dans l'esprit des règles qui régissent le dépôt et la diffusion des mémoires et thèses produits dans cette Institution, **l'Université du Québec à Chicoutimi (UQAC)** est fière de rendre accessible une version complète et gratuite de cette œuvre.

Motivated by a desire to make the results of its graduate students' research accessible to all, and in accordance with the rules governing the acceptation and diffusion of dissertations and theses in this Institution, the **Université du Québec à Chicoutimi (UQAC)** is proud to make a complete version of this work available at no cost to the reader.

L'auteur conserve néanmoins la propriété du droit d'auteur qui protège ce mémoire ou cette thèse. Ni le mémoire ou la thèse ni des extraits substantiels de ceux-ci ne peuvent être imprimés ou autrement reproduits sans son autorisation.

The author retains ownership of the copyright of this dissertation or thesis. Neither the dissertation or thesis, nor substantial extracts from it, may be printed or otherwise reproduced without the author's permission.

ABSTRACT

Toxic metals associated with metal mineralization and mining are critical targets for environmental studies. Thallium, as a typical toxic metal, has received less attention from a geo-environmental perspective since thallium deposits are relatively rare.

This study focuses on natural accumulation of thallium associated with Hg-Tl-(Au) mineralization in the Lanmuchang area in southwest Guizhou Province, China, as a case study for thallium hazard in a geo-environmental perspective. It aims at understanding of the occurrence, the transfer processes and the environmental impacts of thallium related to natural processes and human activity. The distribution and dispersion of thallium together with mercury and arsenic in bedrock, sulfide ore, coals, soil, sediment, ground and surface waters, crops and vegetation have been examined.

This study shows that the Lanmuchang area can be characterized as a specific geological context of thallium, mercury and arsenic accumulations. The extensive occurrences of sulfide minerals, such as lorandite, cinnabar, realgar, orpiment and pyrite are the primary carriers of Tl, Hg and As in the rocks and ores. Thallium occurs either as isomorphous substitution in the structure of sulfide minerals of mercury ores, arsenic ores coals, or as a pure thallium mineral lorandite.

Tl, Hg and As accumulations are characterized by their high concentrations in rocks/ores, soils, sediments, (sub)surface waters and various crops. The range of thallium concentrations are 33–35000 ppm in sulfide ores, 12–46 ppm in coals, 33–490 ppm in host rocks, 25–1100 ppm in secondary minerals, and 6–330 ppm in outcropped host rocks. Thallium concentrations in soils in the mineralized area range from 53 to 282 ppm, from 21 to 100 ppm in alluvial deposits or foundation soils, from 40 to 46 ppm in slope wash material, and from 2.2 to 29 ppm in undisturbed natural soil. A high concentration has also been observed in sediments, ranging from 10 to 3700 ppm. Thallium concentrations are also high in the deep groundwater of the thallium- mineralized area (13.4–1102 μg/l), decreasing away from the area to a background level of less than 0.005 μg/l. In stream water, thallium concentration ranges from 0.3 to 33 μg/l, with marked high contents in downstream sections which likely originated from an unidentified groundwater discharge. In the edible parts of various vegetables and cereals, thallium ranges from 0.21 to 494 ppm (dry weight). The uptake of thallium is more pronounced in vegetables than in cereals, and the highest accumulation occurs in green cabbage.

The dispersion of thallium together with mercury and arsenic in the specific ecosystem of Lanmuchang is constrained by the original Tl-Hg-As sulfide mineralization, the specific topography and hydro-geomorphology, and by the disturbance of human activity. High values of thallium are concentrated in the mineralized and mining area; away from this area, thallium concentrations decreases gradually to a background level. Thallium

from bedrocks is accumulated in soils, sediments and waters within the Lanmuchang watershed area.

The recognition of natural sources and the definition of specific geochemical baselines for toxic metals have been used to help discriminate the relative contributions of thallium due to past and present mining versus natural processes. High geochemical baseline concentrations in outcropped rocks and in soils indicate that both the natural erosion or leaching of outcropped host rocks and soils associated with the Tl mineralized area and the mining activities contribute to the high thallium accumulations in arable soils and in the aqueous system.

The uptake of thallium in arable soils is species-dependent. Thallium contents in the edible parts of crops decreases in the following order: green cabbage > chilli > Chinese cabbage > rice > corn. The highest level of thallium in green cabbage can reach up to 494 ppm in dry weight. Tl contents in crops are much higher than Hg and As, and is likely favoured by the substitution of Tl^+ for K^+ as these two ions have similar ionic radii.

The pathways of Tl into the human body are mainly through the food chain, and dermal and inhalation exposures which are less pronounced. Due to high uptake of Tl by crops, the principal pathway of thallium into the food chain is through the consumption of crops grown in contaminated soils. The daily uptake content of Tl through consumption of locally planted Tl rich crops is estimated to be around 2.7 mg, which is 60 times more than the daily ingestion in thallium-free background areas. Tl levels in drinking water is below the safe drinking limit, and poses no risk to human health under current conditions. Hg and As play an insignificant role in the health problems of the Lanmuchang area.

The socio-economic conditions in the Lanmuchang area enhance the environmental impact of thallium in the ecosystem. Nutritional deficiency, rather than the climatic factor, combined with exposure to high Tl contents in soils and crops is capable of causing thallotoxicosis that prevailed in the 1960's and 1970's.

In order to alleviate the problem or the reoccurrence of a major problem, the local population should be made aware of the thallium hazard and of some of the easily applicable steps to reduce the dispersion of thallium. Also, plans for development should incorporate the results obtained from this investigation. Remediation in a geo-environmental context such as Lanmuchang is complex, but steps should be taken like introducing Tl-hyperaccumulating plants for thallium removal and not planting crops like cabbage which have a tendency to accumulate high amounts of thallium.

Finally, this study not only contributes new knowledge towards the understanding of thallium dispersion processes but also emphasizes the necessity of undertaking investigations in thallium prone areas and studying the effects of prolonged Tl exposure on human health.

RÉSUMÉ

Les métaux toxiques associés à la minéralisation et à l'exploitation minière sont des cibles de choix pour les études environnementales. Le thallium, pourtant un métal toxique par excellence, n'a pas retenu beaucoup d'attention à cet effet, sans doute à cause de la rareté relative des dépôts de ce métal.

L'objet de cette étude est l'accumulation naturelle du thallium en association avec les minéralisations de type Hg-Tl-(Au) dans la région de Lanmuchang, dans le sud-ouest de la province de Guizhou en Chine, dans la perspective géo-environnementale d'une étude de cas sur les dangers du thallium. Plus précisément, cette étude vise à mettre en lumière les manifestations du thallium, ses processus de transfert et ses impacts environnementaux, en référence à la fois aux processus naturels et aux activités humaines. Dans ce sens, on a examiné la distribution et la dispersion du thallium, de même que celles du mercure et de l'arsenic, dans le substratum rocheux, les minerais sulfurés, le charbon, les sols, les sédiments, les eaux souterraines et de surface, la végétation et les produits agricoles.

Cette étude montre que la région de Lanmuchang est géologiquement propice à l'accumulation du thallium, du mercure et de l'arsenic. On y note une présence importante de minéraux sulfurés tels que la lorandite, le cinabre, le réalgar, l'orpiment et la pyrite, qui agissent comme les hôtes principaux de Tl, Hg et As dans le roc et les minerais. Le thallium se présente soit comme substitution isomorphique dans la structure de minéraux sulfurés des minerais de mercure et d'arsenic, et dans les charbons, ou comme un minéral purement de thallium, la lorandite.

Les accumulations de Tl, Hg et As se caractérisent par de fortes concentrations de Tl, Hg et As dans le roc, les minerais, les sols, les sédiments, les eaux de surfaces ou souterraines, de même que dans diverses plantes. La concentration de thallium dans les minerais sulfurés varie de 33 à 35000 ppm, de 12 à 46 ppm dans les charbons, de 33 à 490 ppm dans les roches hôtes, de 25 à 1100 ppm dans les minéraux secondaires, et de 6 à 330 ppm dans les affleurements de roches hôtes. Dans les sols des zones minéralisées, la concentration de thallium varie de 53 à 282 ppm; dans les dépôts alluviaux ou les sols de fondation, elle varie de 21 à 100 ppm; dans les matériaux soliflués, elle se situe entre 40 et 46 ppm; dans les sols vierges, on observe des valeurs entre 2.2 et 29 ppm. Des valeurs élevées de concentration en thallium ont été observées dans les sédiments du lit d'un cours d'eau, allant de 10 à 3700 ppm. La concentration en thallium est également élevée dans l'eau souterraine profonde provenant de la zone minéralisée en thallium (13.4–1102 µg/l), diminuant progressivement aux valeurs normales (0.005 µg/l) avec l'éloignement de cette zone. La concentration de thallium dans les cours d'eau varie de 0.3 à 33 µg/l, avec des valeurs remarquablement élevées en aval d'une décharge d'eau souterraine non identifiée. Dans les divers légumes et céréales comestibles, le contenu de thallium varie de 0.21 à 494

ppm (poids à sec). L'absorption de thallium est plus importante pour les légumes que pour les céréales, et la concentration maximale en thallium est atteinte dans le chou vert.

La dissémination du thallium, de même que celle du mercure et de l'arsenic, dans l'écosystème spécifique à Lanmuchang est contrôlée par la minéralisation originelle des sulfures de Tl-Hg-As, par la topographie et l'hydro-géomorphologie propres au territoire, et par les perturbations de l'activité humaine. On observe de fortes concentrations de thallium dans les zones minières et minéralisées. En dehors de ces zones, les concentrations diminuent graduellement, pour s'établir à un niveau normal. Le thallium en provenance du substratum rocheux s'accumule dans le sol et les sédiments, et il est dispersé par les eaux du bassin versant de Lanmuchang.

On s'est servi de l'identification des sources naturelles et de la définition des niveaux géochimiques de base des métaux toxiques pour faire la part des choses entre d'une part, la contribution relative des activités minières passées et actuelles, et d'autre part, celle des processus naturels. Des concentrations géochimiques de base élevées dans les roches de surface et dans les sols indiquent que l'érosion naturelle ou lessivage de ces roches et de ces sols, en association avec la zone minéralisée en Tl et les activités minières, sont des facteurs déterminants de l'accumulation élevée de thallium dans les terres arables et sa concentration élevée dans le système aquatique.

Le transfert du thallium dans les terres arables dépend des types de culture. La concentration de thallium dans les éléments comestibles des récoltes s'établit comme suit en ordre décroissant: chou vert > chili > chou chinois > riz > maïs. La concentration la plus élevée, 494 ppm en mesure à sec, s'observe pour le chou vert. Le contenu en Tl est beaucoup plus élevé que celui de Hg et As dans les récoltes, cet écart semblant être favorisé par la substitution de K^+ par Tl^+, ces deux ions ayant à peu près le même rayon.

L'assimilation du Tl dans le corps humain se fait principalement par le biais de la chaîne alimentaire, les vecteurs d'assimilation dermiques et respiratoires étant moins importants. Étant donné la concentration élevée de Tl dans les récoltes, la principale assimilation de thallium dans la chaîne alimentaire est la consommation de produits agricoles provenant de sols locaux contaminés. La consommation quotidienne de Tl par le biais de produits contaminés localement est estimée à 2.7 mg en moyenne, ce qui est 60 fois plus élevées que celle de régions sans thallium. Par ailleurs, le niveau de Tl dans l'eau potable est inférieur à la norme de nocivité, et ne pose donc pas de risque pour la santé dans les présentes conditions. Hg et As n'ont pas de rôle significatif à jouer sur la santé de la population dans la région de Lanmuchang.

Les conditions socio-économiques de cette région amplifient l'impact environnemental du thallium sur l'écosystème. La déficience nutritionnelle, plutôt que le facteur climatique, combinée avec une exposition aux concentrations élevées de Tl dans les sols et les récoltes, peuvent bien avoir causé la thalloxicose des années 60 et 70.

Il est nécessaire que l'on prenne conscience des dangers du thallium, ce qui, avec l'introduction de mitigation par étapes faciles à appliquer, va conduire à une réduction de la dispersion de ce métal et des problèmes conséquents. On devrait tenir compte des résultats de cette étude dans l'élaboration des plans de développement de cette région. C'est un problème complexe que de trouver un remède dans un contexte géo-environnemental tel que celui de Lanmuchang, mais on devrait développer des initiatives telles que l'introduction de plantes hyperaccumulantes de Tl, afin de réduire la concentration de thallium dans l'environnement, de même que le remplacement de la culture d'aliments comme le chou vert qui a une forte tendance à accumuler le thallium.

Cette étude non seulement apporte une meilleure compréhension des processus de dispersion du thallium, mais elle souligne également la nécessité d'entreprendre des études dans des régions susceptibles d'être affectées par le thallium, et d'étudier les effets sur la santé humaine d'une exposition prolongée au Tl.

摘要

与金属矿化和采矿活动相关的毒害金属元素是环境学研究中的热点。铊作为一个典型的毒害元素，但由于自然界中铊矿床十分稀少，铊在地质-环境研究中长期以来未引起重视。

该研究以中国黔西南滥木厂地区为例，研究了与 Hg-Tl-Au 矿化有关的铊的自然富集及其环境危害，查明了铊在自然过程和人类活动影响下的分布、迁移及其环境效应，并研究了铊及其共生的汞和砷在基岩、硫化物矿石、煤、土壤、水系沉积物、地下水和地表水以及农作物中的分布与分散规律。

该研究表明滥木厂地区是一个独特的铊、汞和砷的天然富集区。普遍发育的硫化物矿物，比如红铊矿、辰砂、雄黄、雌黄和黄铁矿等，是围岩和矿石中铊、汞、砷的主要载体。铊主要以类质同像赋存在汞矿、砷矿和煤矿中的硫化物矿物晶格中；或者以单一的红铊矿存在。

铊、汞和砷在滥木厂地区的富集主要表现在它们在围岩、矿石、土壤、水系沉积物、地下水、地表水和农作物中的含量很高。铊的含量在硫化物矿石中高达 33-35000 ppm，在煤矿中为 12-46 ppm，在围岩中为 33-490 ppm，在次生矿物中为 25-1100 ppm，在地表裸露的围岩中为 6-330 ppm。铊的含量在矿化区的土壤中为 53-282 ppm，在冲击沉积物或地基土壤中为 21-100 ppm，在残坡积物中为 40-46 ppm，在未扰动的自然土壤中为 2.2-29 ppm。铊在水系沉积物中的含量达 10-3700 ppm。铊在矿化区的深层地下水中的含量很高(13.4-1102 μg/l)，随着远离矿化区，地下水中铊的含量逐渐下降，直到降至背景值(<0.005 μg/l)。在地表溪流水中，铊的含量为 0.3-33 μg/l。铊在下游溪流水中的含量远远高于中上游，这可能是由于富含铊的地下水在下游河床渗流造成的。在蔬菜和谷类农作物(可食部分)中，铊的含量为 0.21-494 ppm(干重)。铊在蔬菜中比在谷类作物中更加富集，在甘蓝菜中最为富集。

铊，连同汞和砷，在滥木厂地区生态环境中的分散范围主要集中在滥木厂汇水盆地中。铊的分散受 Hg-Tl-As 硫化物的原生矿化、特定的地貌和水文地形特征以及人类活动扰动的制约。铊的高含量集中在滥木厂矿化区和采矿区；远离矿化区和采矿区，铊的含量渐趋降低，直至背景值。原岩释放出来的铊富集在滥木厂汇水盆地内的土壤、水系沉积物和水体中。

毒害金属自然来源的识别和地球化学本底值的厘定被用来识别铊分别源于过去/现在采矿活动和自然作用过程的相对贡献。铊在裸露岩石和土壤中的高的地球化学本底值表明，表生环境下与铊矿化相关的裸露岩石和土壤的自然风化淋滤过程和采矿活动都可促使铊在耕作土壤和水环境中富集。

耕作土壤中的铊被农作物吸收程度与农作物的种类有关。铊在农作物可食部分中的含量由高到低的次序是：甘蓝菜 >辣椒 >中国大白菜 >水稻 >玉米。铊在甘蓝菜中的含量可高达 494 ppm(干重)。铊在农作物中的含量远

远高于汞和砷。这可能是由于 Tl^+与 K^+的离子半径很相近，Tl^+易于替换农作物中 K^+的缘故。

铊在滥木厂地区进入人体的主要途径是食物链，其次是皮肤和呼吸接触，但后者的表现不明显。由于铊可被农作物强烈吸收，铊进入食物链的最主要途径是通过食用种植在铊污染的土壤上的农作物。通过食用当地富铊的农作物，滥木厂地区村民的日平均摄入铊量的估算值为 2.7 mg，比不富铊的背景区的村民日摄入量高出 60 多倍。铊在滥木厂地区饮用水中的含量低于现行的安全值，在现有条件下尚未造成健康危害。汞和砷在滥木厂地区的食物链中富集不明显，因而对人体健康的危害不显著。

滥木厂地区落后社会-经济状况加剧了铊在生态环境中的环境影响。相对于气候因素，村民的营养贫乏，连同铊在土壤和蔬菜和谷物中的富集，是促使该地区 20 世纪 60 年代和 70 年代盛行的慢性铊中毒的主要原因。

为了治理现有的铊污染问题或防止新的铊污染出现，滥木厂地区的居民应该对铊的危害引起重视。此外，当地的发展规划应该考虑和利用该研究获得的成果。环境治理在滥木厂这样一个特定的地质-环境单元内虽然很复杂，但是应该采取一些简单易行的措施去减少铊的扩散及其危害。例如，栽种对铊超常富集的植物以减少土壤中易吸收的铊的含量，以及不要栽种和食用易于富集铊的甘蓝菜等。

最后，该研究不但提供了了解铊在生态环境中分散过程的新知识，而且还强调了在铊的富集区进行铊危害调查及铊对人体健康影响的长期效应的必要性。

ACKNOWLEDGEMENTS

This doctoral program is funded by the Canada-China joint Special University Linkage Consolidation project of AUCC-CIDA "Geo-environment and its impact on socio-economic development - Guizhou Province, in alliance with the Pearl River Delta, P.R. of China" (Project No. 01–282/19156) under the auspice of Université du Québec à Chicoutimi (UQAC) and Institute of Geochemistry, Chinese Academy of Sciences (IGCAS).

This thesis is supervised by Prof. Jayanta Guha (UQAC), Dr. Dan Boyle (Geological Survey of Canada, Ottawa) and Prof. Alain Rouleau (UQAC). Discussion and instruction from them have benefited me very much in classroom, fieldwork, document search, laboratory analysis, thesis compilation, and humanity. They are good paragons of virtue and learning in both my life and research. I hereby should particularly express my great condolence to the loss of Dr. Boyle who unfortunately passed away in the summer of 2000. His instruction in field sampling, document collection and laboratory analysis arrangement has ensured this thesis to progress timely and successfully.

I also would like to express my appreciation to the experts at the IGCAS of China side. Instructive discussions with Prof. Yetang Hong and Prof. Baoshan Zheng for fieldwork and academic presentation, and financial support for field work from Prof. Congqiang Liu, the director of the IGCAS have ensured the work of my doctoral program in China to proceed smoothly.

I should appreciate particularly Mr. Jianhong Qian at the Lanmuchang township for constant help during almost 3 months field sampling. The friendship from him and his families made each of my field trip very productive. The local officials of Lanmuchang township also gave me helpful support for collection of local demography information and the access to underground Tl-mining sites for sampling thallium ores.

Dr. Conrad Grégoire, Mr. Peter Bélanger and Ms. Judy Vaive at the Geological Survey of Canada, Ottawa are acknowledged for the arrangement of rock, soils, sediment, water, crops and vegetation sample analysis. Dr. Grégoire also provided with me with a constructive review of the thesis manuscript. Mr. Bélanger gave me much useful information on the analysis protocols.

Many thanks should also go to Dr. Colin Dunn, the consultant of the Activation Laboratories Ltd. in Ancaster, Ontario and Dr. Eric Hoffman, the general manager of the Activation Laboratories Ltd. for releasing useful thallium references and vegetation analysis protocol.

Dr. Matthew Leybourne at the University of Texas at Dallas is also acknowledged for his constructive review of the section on hydrogeochemistry. Ms. Diana Coonrod and

Prof. Alain Rouleau also helped me considerably for English correctiond and French abstract edition of this thesis.

Many thanks are also due to Prof. Huangzhang Lu, Prof. Jacques Carignan, Prof. Denis Roy, Dr. Paul Bédard, Madam Candide Girard, Dr. Zhiwei Bao, Dr. Dijiang Guo, and Dr. Jingan Chen for their help and discussions throughout the doctoral program. Prof. Yangeng Wang from the Guizhou Geological Survey, China is acknowledged for supplying for the unpublished data of the regional geological survey.

Finally, special thanks should go to my lovely wife, Zhonghua Yang. Her constant encouragement and care in my life and research has also contributed to the production of this thesis.

TABLE OF CONTENTS

LIST OF TABLES

LIST OF FIGURES

CHAPTER 1

BACKGROUND AND OBJECTIVES

1.1 Background and significance of thallium study

Resources, environment and human activity are the three most important factors in socio-economic development. The utilization of natural resources, like minerals, gas, oil, etc., can benefit humans by providing metals, specific materials and energy. However, the mining and smelting associated with the recovery of the natural resources may damage the environment by introducing large amounts of chemical pollutants to the environment. Among the pollutants, the heavy metals are often predominant. On the other hand, the natural processes related to the emplacement of mineral resources may cause some damages to the environment in terms of the presence in excess of certain elements toxic to human health. Thus, this link between mineral resources and the environment has a strong impact on humans.

A thorough understanding of the environmental processes that affect mineral deposits and mine wastes has become increasingly important as the World wrestles with how to meet our current demand for metals without compromising the environment, and how to mitigate the damage caused by the mining practices of previous generations. Regulatory requirements are dominated by empirical approaches to environmental problems associated with mining, but mitigation and reclamation can be enhanced greatly

by a theoretical and conceptual understanding of the processes that affect the availability, transport, and fixation of metals and their environmental effects.

The excess of certain chemical elements in the environment, which may produce some health problems to the humans, is well known. Such element-related health problems include high fluoride in drinking water or foods producing dental problems (Dissanayake, 1991; Apambire et al., 1997; Zheng et al., 1999), high arsenic triggering skin cancers (Tseng et al., 1968; Chowdhury et al., 1999; Zheng et al., 1999), an excess of selenium leading to the Keshan Disease and Cashin-Beck Disease (Yang and Xia, 1995; Johnson et al., 2000), elevated Ce and Mg deficiency causing the endomyocardial fibrosis (Smith et al., 1998), and thallium (Tl) intoxication through ingestion or inhalation by humans causing problems of alopecia and disorder of the central nervous system (Bank et al., 1972; Zitko, 1975a,b; Emsley, 1978; Schoer, 1984; Zhou and Liu, 1985). Such chemical element related health problems have raised the importance of the impact of specific element contamination and stimulated a greater awareness and interest for geological, geochemical, environmental and medical scientific researches worldwide. The integration of the study of the geological environment and natural processes coupled with industrial activities affecting the concentration and transport of toxic metals and their impacts on human health can be defined as "geo-environmental" research (Guha, 1999).

The environmental aspects of heavy metals have been widely documented during the past few decades. Problems posed by the increased concentrations of toxic metals in the environment include hazards to human health by imparting toxicity to most plants and animals. The focus of research has been on metals such as Hg, As, Cd, Cr, Cu, Pb, Zn, Co

and Ni. However, Tl, one of the extremely toxic metals, has often been neglected in the geo-environmental studies or regulations, although its high toxicity was recognized soon after its discovery in 1861.

Thallium, with the atomic number 81 and the atomic weight 204.39, occurs between mercury and lead in Group IIIA of the Periodic Table (Table 1-1). Some of its physical and chemical properties are shown in Table 1-2. Tl was first discovered in 1861 by the English chemist William Crookes (1832–1919), who, while doing a spectroscopic examination of seleniferous residues from a sulfuric acid plant in Tilkerode in the Hars Mountains (Germany), noticed a beautiful green line in the emission spectrum never seen before (Weeks, 1968). He correctly concluded that he had discovered a new element and named it "thallium", alluding to the Greek word "thallos" (a budding twig), a word which is frequently used to express the beautiful green tint of young vegetation in spring. Metallic thallium was first prepared in 1862 by the French chemist Claude-August Lamy (1820–1878). From further experimental studies, Lamy pointed out that the Tl could form two series of salts representing Tl^{+} (thallous) and Tl^{3+} (thallic) oxidation states. The discovery of this new metal aroused interest amongst many research workers.

Thallium has a wide use in various fields (Downs, 1993a). The past medical uses of Tl included treatment for gonorrhea, syphilis, dysentery, tuberculosis and ring worm of the scalp. It was also extensively employed as a rat poison (outlawed in the United States after the 1970's). The semiconductor industry is the main user of (metallic) Tl, but substantial quantities also go into the production of cardiac imaging, highly refractive optical glass, and some alloys. Small amounts are used in superconductivity research,

radiation detection equipment and photosensitive devices. Tl compounds also have a wide range of industrial uses. Thallium chloride is used as a catalyst in chlorination. The solution of Tl acetate is used in separating ore constituents by flotation due to its high specific gravity. Tl nitrate is used as with other compounds as signals at sea and in the production of fireworks, photocells and as an oxidizing agent in organic synthesis. Tl oxide is used in the manufacture of highly refractory glass. Tl sulfate is used in the semiconductor industry, in low range thermometers, optical systems, and photoelectric cells. The increasing use of Tl in emerging technologies has enhanced the world market price of Tl up to 1278$US/kg (99.9990% pure Tl granules) in 1998 (U.S. Geological Survey, 1999). The increasing use and bright market of Tl has also raised new concerns about health risks and environmental toxicology of this element.

The toxicity of thallium became immediately apparent and was recognized by W. Crooks in 1863, C.A. Lamy in 1863, J.J. Pualet in 1863, L. Grandeau in 1863 and B. Stadion in 1868 (Nriagu, 1998). In spite of these earlier studies, thallium was used therapeutically for syphilis in 1883, for night sweats of tuberculosis in 1898, for depilation in 1897, for ringworm of the scalp in 1919, and as a pesticide in 1920. In the late 1920's, "Koremlu-Cream", a depilatory cream containing nearly 5% thallium, entered the United States market and became the source of thallium poisoning for a number of people (Schoer, 1984; Nriagu, 1998). By 1934, 778 cases of thallium poisoning, including 46 fatalities, had been reported in the scientific literature. In the 1950's, Swedish workers in 4 families were affected by rodenticides containing thallium. Indications of thallium poisoning in an employee of a pigment factory was reported from Germany, and in the United States 15

workers suffered from thallium poisoning through handling gravity solutions prepared from thallium salts (Schoer, 1984). Between 1953 and 1959, more than 130 children in Texas alone were reported to have shown effects of thallium from contact with rodenticides (Reed et al., 1963). Other cases of thallium poisoning were reported from exposure to thallium related to a cement plant in 1979 in Lengerich, Germany (Dolgner et al., 1983), from high thallium in water and vegetables in Southwest Guizhou, China in 1960's–1970's (Zhou and Liu, 1985), from two cases of criminal poisoning by using Tl_2SO_4 at Beijing University and Tsinghua University, China (Zhou, 1998), and from the Chemirtg, Ukraine in 1989 where children suffered from thallium poisoning (Anonymous, 1989).

The toxicity of thallium during the biochemical process has been well documented (See Chapter 4.4). The lethal dosage for a single ingestion for an adult is 0.1–5 gram, and it is more toxic to mammals than most other metals including Cd, Hg, Cu, Pb and Zn (Zitko, 1975a). The main symptoms of thallium poisoning are body pains in the legs and joints, stomachs problems, central nervous system effects, eye disorders with failing eyesight, total blindness, hair loss and even death (Schoer, 1984; Feldman and Levisohn, 1993; Mulkey and Oehme, 1993; Meggs et al., 1994).

As compared to epidemic and aetiological studies in medical science, issues related to thallium are less frequently considered in the geoscience literature from a geo-environmental perspective. Indeed, a study using a geo-environmental perspective may have yielded a better understanding of the occurrence, transfer processes and the potentials of thallium related environmental hazard due to natural processes and human perturbation in the geosphere and biosphere, and the effective means of remediation. Even in the

geoscience literature, many researchers neglected thallium as a toxic element in the classification of toxic/non-toxic elements (Plant and Raiswell, 1987; Edmunds and Smedley, 1996; Dissanayake and Chandrajith, 1999). In this respect, it seems that in the field of geo-environmental studies, thallium as an issue lags far behind when compared to the fields of medicine and biology. As a result, there is still insufficient information available on Tl geochemistry related to natural mineralization as compared to industrial-induced sources in the literature.

What is the cause for the paucity of geo-environmental study of thallium in geoscience literature? Two reasons may explain the situation: (1) that thallium occurs typically in nature in very low concentrations. The average abundance of thallium in crust is only 0.45 ppm, but it is higher than mercury (0.08 ppm) (a toxic metal), silver (0.07 ppm), cadmium (0.2 ppm) and gold (0.004 ppm) (Taylor, 1964). In contrast to these elements forming commercial ores, thallium does not occur in a native form and is rarely enriched in specific mineral species, and its minerals and commercial ore deposits are very rare. (2) The other reason is that very few studies have been carried out on thallium for its behavior in geological environments and its impact on both the ecosystem and humans. As a result, very few data concerning the occurrence and distribution of thallium in nature are available in the geoscience literature. Although some sparse data on thallium are available in some environmental studies, this information lacks the full insight on the effects of thallium on an ecosystem related to both natural thallium mineralization and human perturbation.

As stated earlier, the mineralization of thallium and its ores are very rare in nature. The few unusual cases of thallium mineralization, thallium minerals and/or ores reported are from the Allchar deposit in Yugoslavia, which has a unique Sb-As-Tl mineralization (Zyka, 1971; Jankovic, 1989; Rieck, 1993; Percival and Radtke, 1994); the Carlin deposit in Nevada with Au-As-Tl mineralization (Percival and Radtke, 1993); the Lengenbach deposit in Switzerland with Pb-Zn-As-Ba-Tl mineralization (Hofmann and Knill, 1996), the Nanhua deposit in Yuannan, China, with As-Tl mineralization (Zhang et al., 1996), and the Lanmuchang deposit in Guizhou, China, with the Hg-Tl mineralization (Chen,1989a,b; Chen et al., 1996; Li, 1996; Zhang et al., 1997). The geology and mineralogy of thallium in these mineralized areas are well documented. However, the studies of geo-environmental aspects of thallium are very limited or less documented, and few successful case studies related to the natural occurrence have been published to date. Also lacking is a comprehensive discussion or identification of the problem, in a geo-environmental perspective. A complete understanding of the behavior of thallium in a local ecosystem is a necessity and would contribute to the remediation of heath related problems.

1.2 Presence of Tl in the fragile ecosystem in Southwest Guizhou

The southwest part of Guizhou Province, China, presents a unique karst terrain. There are two main characteristics of the karst terrains in this area, which influence the ecosystem. First, the surface drainage system is generally poorly developed while the groundwater is in abundance. Second, the supergene environment is characterized by meager soils for farmland, poor forest coverage, and wide distribution of surface rocks. The

first two characteristics make this area a vulnerable ecosystem, while the mineral resources impact on the ecosystem through natural processes of dispersion of metal. This fragile ecosystem with its natural geological features can be further affected by human activity (e.g. mining) that introduces toxic metals from the rocks into the soils, the aquatic systems and the vegetation, and may markedly change the primary environment.

Southwest Guizhou is one of the poorest areas of Guizhou Province, one of China's poorest provinces, but it has abundant mineral resources and minerals. The minerals are an important source for regional development. Among the minerals, gold and coal are predominant. Coal mining has a history covering hundreds of years, mainly supplying local domestic energy needs. This coal is known to enrich in arsenic, causing arsenic poisoning (Zheng et al., 1999; Tunney, 2001). Since its discovery in late 1980's, gold was the most sought-after metal and showed certain similarity to the Carlin type deposits in Nevada, USA. The gold mineralization district is characterized by the presence of Hg, As and Tl in variable quantities giving rise to Hg-only and Hg-Tl only deposits in which Au is quasi absent.

In addition to arsenic related health problem, thallium poisoning has also been recognized in this region of Southwest Guizhou Province. The area showing thallotoxicosis is located within the metallegenic belt of Au-Hg-As-coal in Lanmuchang, Xingren County, Southwest Guizhou. Mercury mining started about 350 years ago, but the deposit was commercially explored and exploited as a low-grade large mercury deposit in 1960's (Chen, 1989a,b). However, no documentary record exists of Hg recovery from this deposit, either in ancient times or after 1960's. Sporadic mercury mining was done by local

villagers in the 1970's and ceased in the early 1980's. Thallotoxicosis appeared in the 1960's–1970's, affecting about 189 out of 1076 local residents (Li, 1963; APASSGP and EGLIGCA, 1974; Zhou and Li, 1980; Liu, 1983; Zhou and Liu, 1985). The victims had hair-loss, body pains and vision problems. The cause for the thallium poisoning was recognized as high thallium contents in drinking water (17–40 μg/l) and in vegetables (3.14–48.6 μg/g (dry weight)) related to the mercury mining (Zhou and Liu, 1985). The researchers at that time simply determined the concentrations of thallium in waters, soils and vegetables, but they did not try to understand the geological processes and behaviors of thallium in the ecosystem.

In late 1980's, studies on thallium in the Lanmuchang area were re-initiated due to the first discovery of the thallium minerals lorandite and christite (Chen, 1989a; Li et al., 1989), and the high-grade thallium pockets in orebodies which were recognized as constituting independent high-grade thallium deposits (Chen, 1989b). These studies documented the geology, mineralogy and metallogenesis of thallium, showing a unique suite of sulfide minerals of thallium, arsenic, mercury and pyrite in the ores. In 1994-1997, the thallium ore was the commercial mining target in a small-scale underground mining operation. All of the past and the present mining activities for Hg and Tl have produced a considerable amount of mine wastes and tailings, and no special attempts have ever been made to mitigate the impact of pollution. The hills in the mined area are almost bare with few grasses and scrubs, and the outcrops present a burnt-black color.

In recent years, the high concentrations of Hg, As, and Tl in rocks and soils in the mine area were reported by Chen (1989b) and Li (1996). Although some studies touched

upon the environmental aspects of thallium (Zhang et al., 1997; Zhang et al., 1998), the relative contributions of thallium from both the natural processes and human activities were not clearly delineated, and the behavior of thallium in the geo-environmental cycle, i.e. transfer process from rock-soil-water-vegetation, is not well demonstrated. Indeed, natural processes on sulfide minerals and ores are capable of dispersing the toxic elements into the surrounding areas both by physical transport, and by chemical dispersal in groundwater. It is important to determine the extent and intensity of natural dispersal, both to identify possible current environmental impacts and to assess potential impacts of future mining. In addition, very few of these previous studies are available in the international geo-environmental science literature. Therefore, this unprecedented context of thallium contamination has remained obscure to the international environmental scene.

In fact, in the Lanmuchang area alone, 1453 of residents (census results according to Qian, J.H., personal communication, 2000) live in very close contact with the natural environment of thallium mineralization and mining wastes, and obtain their food and drinking water directly from the mined area and its vicinity. The local residents rely heavily on locally grown crops within the mined area as well as in areas containing known deposits not yet mined. The geochemical pathways of thallium therefore affect the local populations more directly and also present an opportunity to investigate the role of thallium and associated toxic metals to human health risks.

To have a good comparison of thallium dispersion and its environmental impacts related to the thallium mineralization and the mining operations, the area outside the Lanmuchang Hg-Tl mineralized area with a similar stratigraphy and no Tl-Hg-As

mineralization was chosen as the background area. This background area is located about 2-3 km horizontally removed from the Lanmuchang watershed to west and east, with same lithologies as outcrops or from quarries (limestone, siltstone, sandstone, argillite of T_1y, P_2c and P_2l). Based on the 1:50,000 regional geological survey (Guizhou Geological Bureau, 1990a,b), no Tl-Hg-As mineralization and hydrothermal alteration were noted in the background area.

1.3 Objectives

The specific geo-environmental context associated with the thallium contamination in the Lanmuchang area has been chosen for this study and the principal objectives of this study are (1) to describe the occurrence and distribution of thallium in the geo-environmental cycle; (2) to evaluate the relative contributions of thallium due to past and present mining versus natural processes; and (3) to delineate the pathways of Tl from its natural occurrence to the food chain and ultimately into human beings. The results from this study will lead to (1) the documentation of the various processes of dispersion of thallium not noted elsewhere, which are essential to assess accurately how natural and anthropogenic geochemical variations affect the ecosystem and human health; (2) to increase awareness of thallium hazard to eco-health; and (3) help to discover ways to prevent possible thallium damage in similar geo-environmental contexts.

1.4 Presentation

The presentation has been divided into 8 chapters. Following the first chapter which reviews principally the problems related to the specific contexts, the second chapter presents the physiography, climate and demography of the study area. The third chapter describes the geology and hydrogeology including a description of thallium mineralization. In order to examine the general characteristics of thallium behavior, Chapter 4 presents an overview related to thallium geochemistry, with more emphasis on its geochemical behavior in the supergene environment. This is followed by specific characteristics of thallium in the Lanmuchang area including sampling pattern and analysis of results in Chapter 5. Chapter 6 focuses on interpretation of thallium dispersion relating to the Lanmuchang area. Chapter 7 discusses the environmental impacts of thallium dispersion, which is followed by a chapter (Chapter 8) of conclusions.

Table 1-1 Location of thallium in the Periodic Table of Elements

1	1 H												IIIA					2 He
2	3 Li	4 Be											5 B	6 C	7 N	8 O	9 F	10 Ne
3	11 Na	12 Mg											13 Al	14 Si	15 P	16 S	17 Cl	18 Ar
4	19 K	20 Ca		21 Sc	22 Ti	23 V	24 Cr	25 Mn	26 Fe	27 Co	28 Ni	29 Cu	30 Zn	31 Ga	32 Ge	33 As	34 Se	35 Br	36 Kr
5	37 Rb	38 Sr		39 Y	40 Zr	41 Nb	42 Mo	43 Tc	44 Ru	45 Rh	46 Pd	47 Ag	48 Cd	49 In	50 Sn	51 Sb	52 Te	53 I	54 Xe
6	55 Cs	56 Ba	*	71 Lu	72 Hf	73 Ta	74 W	75 Re	76 Os	77 Ir	78 Pt	79 Au	80 Hg	81 Tl	82 Pb	83 Bi	84 Po	85 At	86 Rn
7	87 Fr	88 Ra	**	103 Lr	104 Rf	105 Db	106 Sg	107 Bh	108 Hs	109 Mt	110 Uun	111 Uuu	112 Uub	113 Uut	114 Uuq	115 Uup	116 Uuh	117 Uus	118 Uuo

(Source: http://www.webelements.com)

Table 1-2 Selected physical and chemical properties of thallium (Downs, 1993b)

Atomic number	81
Atomic weight	204.39
Naturally occurring isotopes	^{203}Tl (29.52%), ^{205}Tl (70.48%)
Density (20°C)	11.85 g/cm^3
Melting point	302°C
Boiling point	1453°C
Electron configuration	(Xe)4f^{14}5d^{10}6s^{2}6p^1
Oxidation states	+1, +3

CHAPTER 2

PHYSIOGRAPHY, CLIMATE AND DEMOGRAPHY

2.1 Physiography

The study area is centered on Lanmuchang, a town which belongs to the administrative division of Xingren County, Southwest Guizhou Province, China (Fig 2-1, Fig. 2-2). This town is located at geographical coordinates of 105°30′30″E longitude and 25°31′28″N latitude. The area presents a mountainous topography within the Yunnan-Guizhou Plateau. The topography is generally higher in the northwest and lower in the southeast. The altitude is 1000-1600 meter above sea level (a.s.l.) with a relative relief of 200-600 meters. The karstic topography is characterized by peaks, depressions, valleys, karstic caves, karstic underground rivers and sinkholes.

The study area hosts a number of mineral resources, such as, gold, mercury, arsenic, antimony, thallium and coal (Yang and Dong, 1994; Qian et al., 1995). Among the abundant mineral resources, gold and coal are the two main targets for mining, gold being mined by provincial or private gold companies from several gold deposits and coal being sparsely mined by local farmers for their daily fuel supply. Due to the mining operations, the ecological environment has been disturbed and damaged, and post-mining reclamations are very limited. Being located in a rural mountainous region with no large industrial

production except for gold and coal mining, the area is free of industrial pollutants affecting the ecosystem.

The study area has a fragile ecological environment due to the karstic topography and the warm and humid climate. The fragility is characterized by the following three aspects. First, the study area contains numerous mountains with steep slopes. Many of the slopes are up to 30–50^{o} and some of the slopes are nearly vertical. Furthermore, the forest coverage is lower than 10%. The hills in the study area are almost bare, with sparse grasses, ferns and other woody shrubs (Fig. 2-3). Therefore, the soil erosion and bedrock exposure in the study area are serious, leading to intensive weathering of the rocks. The extensive rocky exposure and steep mountains also constrain the arable areas. The farmland is limited to specific areas, most are sloped lands and a few are flat lands. Soils are thinly developed and till cover is thin, generally ranging 10–50 cm in thickness. Severe erosion of topsoil has occurred owing to the poor coverage of vegetation, and soil nutrition has been depleted over the years and many farmlands are poorly productive. Secondly, the water for irrigation is restricted in the study area due to the abundance of karstic fractures and caves either on the surface or below ground. Rainfall often readily permeates underground through the karstic fractures or caves and only limited amounts of surface water are available for agriculture. Thirdly, deforestation and indigenous mining (especially for coals) expedite soil erosion and promote the introduction of some toxic metals from underground to the surface environment, resulting in damage to the ecological environment.

2.2 Regional climate

The climate in the study area can be categorized as a subtropical continental monsoon climate. It is warm and humid with an annual precipitation of 1300 –1500 millimeters, at its maximum in June, July and August. The annual average temperature is around 14°C, and the highest temperatures (30–35°C) occur in July and August.

2.3 Demography

The distribution of population is very sparse in the study area. Most of the population belongs to the Han group of people and a small portion is made up of Buyi people. The local residents in the remote and rural areas often reside in the depressed or valley areas around which the drinking water sources are available. Each village usually contains 10-30 families and in some villages there are only two families. The local residents are less educated, and the majority of elders are illiterate or semi-literate, whereas the youth often have completed 9-years of compulsory education. The local residents mainly rely on farming, and industry or handicraft industry is rare. The microeconomic character is predominant and merchandise for daily use is mainly exchanged in the weekly mobile market. As a result, the local residents have little communication with outside areas. Meanwhile, the road conditions for transportation in some rural areas are very poor due to the steep topography, and there are no roads for motorized vehicles to reach the villages. Instead, the local residents mainly travel on foot or by horse. However, in recent years, due to gold exploration and mining, some new roads have been built to improve transportation. Also, some richer residents have installed satellite receivers to watch TV programs or

install telephones for convenient communication with the outside world, and thus people in rural areas have more knowledge about the modern world than ever before.

The local residents in the study area depend heavily on the ambient natural environment. They often rely on the farming lands around their dwellings within a radius of 1–2 km. However, the arable lands are limited to small areas, thin soil layers and poor soil nutrition. Some arable areas are often smaller than one square meter between the interspaces of limestone outcrops. Production from these lands usually is very low. The main crops grown in the study area include corn, wheat and rice, while the economic crops are vegetables, rapeseed, buckwheat and fruits. In addition, the residents raise some livestock and fowl. Crops are generally sufficient to support the local population, but some crops (e.g. rice) are still needed from outside the study area. The drinking water supply is from natural water sources such as springs, karstic caves or dug shallow wells around the dwellings. However, water purity treatment is unavailable. The daily energy needs for cooking or heating are obtained from the locally produced coal and dry straw.

The local residents are so closely tied to the surroundings of the natural eco-environment that endemic diseases related to the geo-environments affect the population directly. Chronic thallium poisoning, discerned in the Lanmuchang area in 1960's–1970's, is an obvious endemic case related to the mercury-thallium mineralization and mining. Thallium poisoning, which has affected a large portion of the population and caused symptoms such as, hair loss, body-aches, reduced vision and blindness, was thought to be largely due to high concentrations of thallium in vegetables and in drinking water related to a boom in mercury mining. 189 cases of people suffering from thallium poisoning were

observed in the epidemiological study of Zhou and Liu (1985) and others (e.g. Li, 1963; Lu, 1981; Liu, 1983).

The drinking water problem was alleviated by the construction of a new piped water supply by the township government in 1995. The new water supply pipes groundwater from a karstic spring 2 km west of the study area. About 40 per cent of the villagers use the new pipe water instead of the dug well water, but the other 60 per cent of villagers still rely on the lower cost dug wells as before. All the villagers still rely on the natural water sources around the Hg-Tl mineralized area for agricultural and domestic uses.

Residents using local coal do not show the symptoms of arsenic poisoning from other areas in southwest Guizhou described by Zheng et al. (1999) and Finkelman et al. (1999) where arsenic was shown to be transferred to the food chain through burning of arsenic-rich coal under non-ventilated conditions. This implies that the local coal may contain lower concentrations of arsenic than those in the arsenic poisoning areas studied by Zheng et al. (1999), and that the coal utilization may not be a vital endemic problem in the study area.

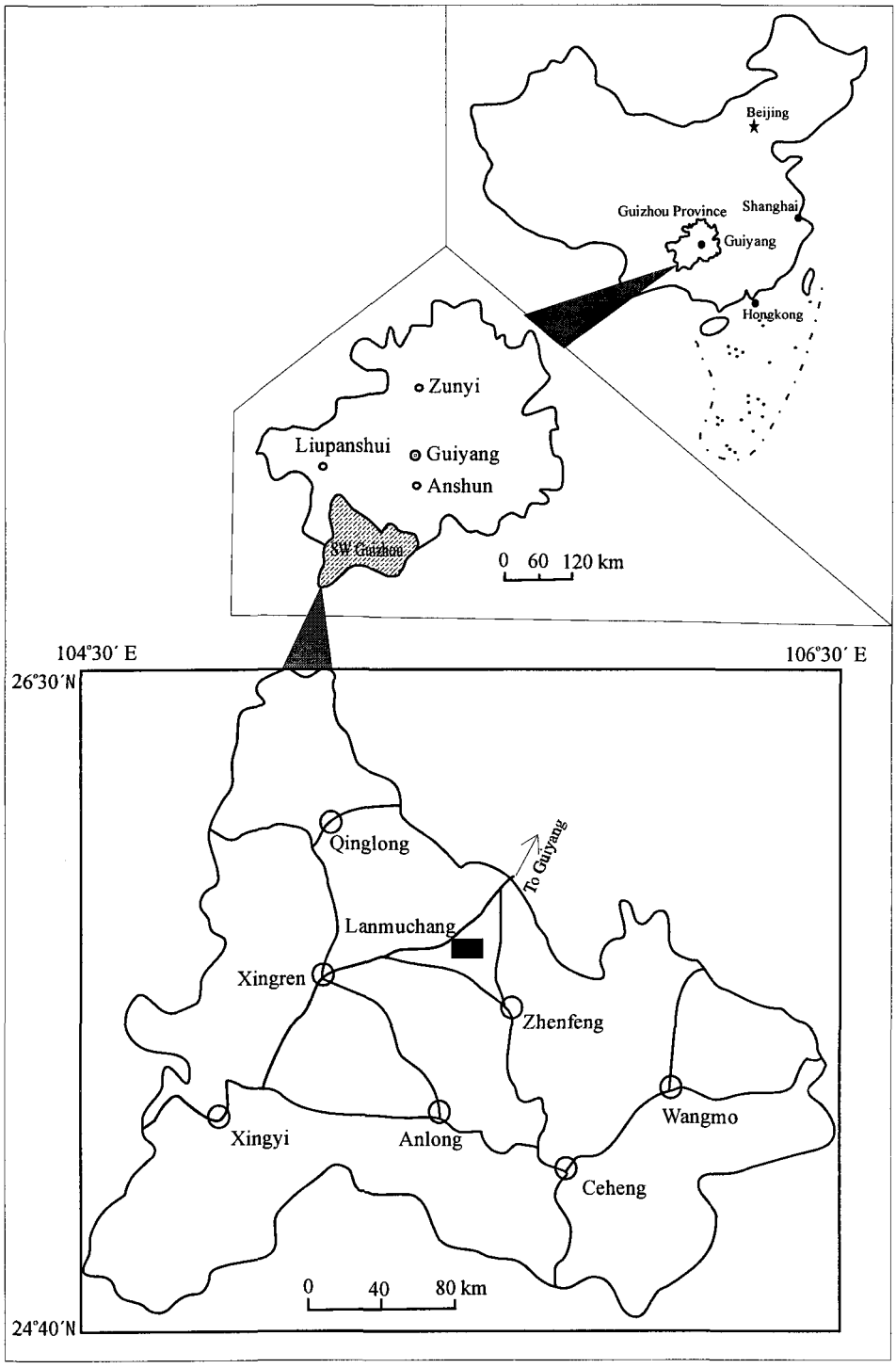

Fig. 2-1 Location of the study area of Lanmuchang

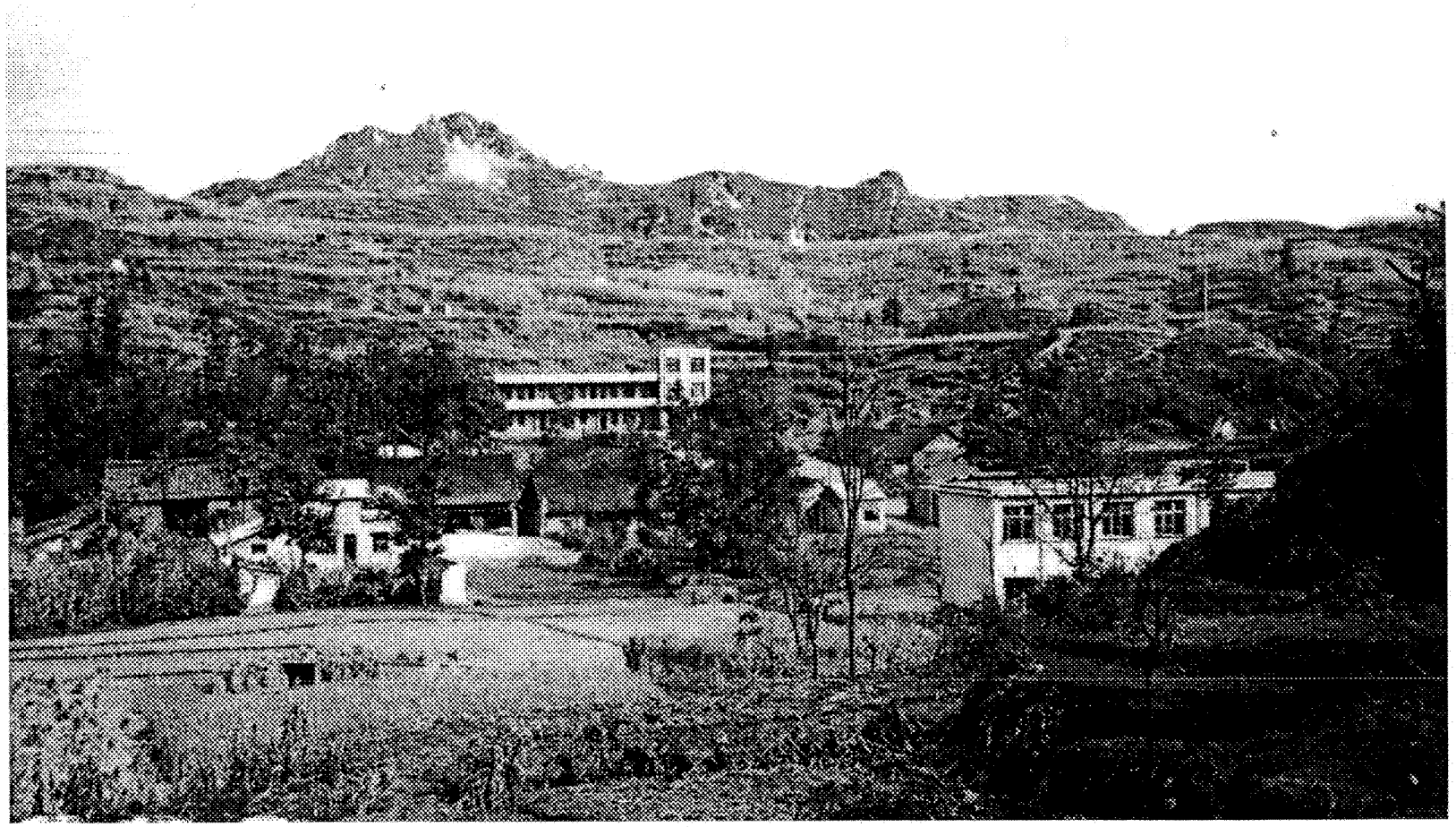

Fig. 2-2 Landscape of the Lanmuchang Hg-Tl mineralized area

Fig. 2-3 Landscape of the Lanmuchang Hg-Tl mineralized area

CHAPTER 3

GEOLOGY AND HYDROGEOLOGY

3.1 Regional geology

The study area is located at the junction of the southwest margin of the "metaplatform" of the Yangtze and west margin of the Youjiang orogen of the South China Fold System (Fig 3-1). The area is made up of sedimentary rocks of Permian and Triassic ages and the alluvium deposit from the Quaternary age. The Permian strata include the Maokou Formation (P_1m) of early Permian age, and the Longtan Formation (P_2l), Changxing Formation (P_2c) and Dalong Formation (P_2d) of late Permian age. The Triassic rocks comprise the Yelang Formation (T_1y) and the Yongningzhen Formation (T_1yn). The contact between the formations is conformable. The lithology of each principal formation starting from the oldest is described in Table 3-1.

The main regional structure is the Huijiabao Anticline (Fig 3-2). This anticline is an EW-trending metallogenic belt of gold, mercury, arsenic, thallium and coal, 18-km long and 5-km wide. The western area of this belt hosts the gold deposits of Zimudang and Taiping Dong and the mercury deposit of Dabatian; the middle part hosts the mercury-thallium

deposit of Lanmuchang, and the east part hosts the gold deposits of Yanshang and Beiyinpo (Fig. 3-2). In addition, a number of minor realgar and orpiment mineralization as well as coal seams occur in the middle and east zone areas of this anticline.

The exposed rocks in the core of the Huijiabao Anticline include the Longtan Formation (P_2l), Changxing Formation (P_2c), Dalong Formation (P_2d) and Yelang Formation (T_1y), and the limb hosts the outcrops of Yelang Formation (T_1y) and the Yongningzhen Formation (T_1yn). The inclination of strata is horizontal to sub-horizontal (5^o–20^o), and the stratigraphies of the two limbs are relatively symmetrical. Around the anticline axis are a number of secondary folds and faults which give rise to favorable ore-forming structures.

3.2 Regional hydrogeology

The groundwater in the region widely occurs as karstic groundwater in limestones and as fracture groundwater in fractures within clastic rocks (Guizhou Hydrogeological Survey, 1985). The lithologies of the aquifers are the inter-bedded median lamina clayey siltstone, claystone and oosparite, argillaceous limestone, and the limestone being predominant.

The groundwater often discharges to the surface through karstic springs, karstic caves and underground rivers. Most of the discharge points have an elevation of about 1000–1400 m a.s.l. (Guizhou Hydrogeological Survey, 1985). The karstification develops

mainly in the horizontal direction, and the strata of folds are nearly flat. These, in turn, can facilitate the storage of groundwater in aquifers. The groundwater is mainly phreatic, but in local aquifers it occurs as artesian flows due to confinement by the permeability barriers. The artesian flow capacity is up to 0.74–11.6 l/s (Guizhou Hydrogeological Survey, 1985). The flow of groundwater is mainly through open channels, and the discharge through the conduits is 92.4 % of the total discharge capacity. Thus, the aquifer is extremely inhomogeneous (Guizhou Hydrogeological Survey, 1985).

The circulation depth of groundwater is constrained by the regional geology and topography. The regional topography, characterized by the peak cluster-valley/depression, favors the shallow and middle depth circulation of groundwater in aquifers in valley/depression areas close to the ridges. The groundwater table is usually down to 50–100 m below ground surface (Guizhou Hydrogeological Survey, 1985). The hydraulic gradient is normally small, and the groundwater often discharges through outlets of underground rivers and karstic springs. The groundwater discharging from the underground rivers and karstic springs is the main water supply for the population (Guizhou Hydrogeological Survey, 1985).

The general flow direction of both groundwater and surface water in the region is from west to east or from north to south (Guizhou Hydrogeological Survey, 1985).

As the groundwater is mainly formed of phreatic groundwater, it is recharged by

rainfall. The main recharging period is in the rainy season, i.e. the months of June-August (Guizhou Hydrogeological Survey, 1985).

The main water quality types of groundwater in the region are composed of HCO_3-Ca, HCO_3-SO_4-Ca and SO_4-Ca. According to the regional hydrogeological survey (Guizhou Hydrogeological Survey, 1985), the groundwater discharging from shallow aquifers is dominated by HCO_3-Ca (>50%), and then HCO_3-Ca/Mg (>36%) and HCO_3-SO_4-Ca/Mg (>14%). The total dissolved solids (TDS) is 0.1–0.5 g/l. However, the groundwater collected from the borehole in deep aquifers is characterized by increasing contents of SO_4, and dominated by HCO_3-Ca/Mg and HCO_3-SO_4-Ca/Mg. The TDS is up to 0.2–1 g/l. In specific zones within P_2l, P_2c and T_1y formation, the TDS increases pronouncedly to 1.3–4.18 g/l, and pH values decrease to 4.10–5.00, due to the presence of sulfides and coal seams. Groundwater chemical composition is dominated by SO_4-Ca.

3.3 Geology of the Lanmuchang area

The Lanmuchang Hg-Tl mineralized area is located at the junction of NE-trending and EW-trending faults within the southwest limb of the Huijiabao Anticline (Fig. 3-2). The outcrops include the Longtan Formation (P_2l), Changxing and Dalong Formation (P_2c+d) of the Permian age, and the Yelang Formation (T_1y) of early Triassic age. The Hg-Tl mineralization mainly occurs in the P_2l and P_2c Formations, and also in the T_1y Formation.

The lithologies of each stratum are the same as those in the regional stratigraphy (Table 3-1). The Longtan Formation is mainly composed of limestone, sandstone, siltstone and argillite stone with laminated inter-bedded coal seams. Almost 10 layers of coal seams occur in this formation. Outcrops of this formation often appears gray to black coal-color, which are good indicators of the presence of coal seams. The Changxing Formation consists of chert-limestone, bioherm stone and argillaceous limestone. The Dalong Formation is made up of calcareous claystone and inter-bedded montmorillonite claystone. The Yelang Formation contains silty stone and claystone, with few occurrences of limestone. In the west and south of the Yelang Formation, just outside the mineralized area, there are large exposures of limestone. The limestone contains several karstic caves, karstic underground rivers and sinkholes formed through the karstification process.

Faults and fractures are well developed in the Lanmuchang area, and trend NE and EW (Fig. 3-3). Among the faults, the nearly NS-trending normal Lanmuchang fault and the NE-trending reverse Huangnijiang fault are the two predominant regional faults in the Lanmuchang area. The Hg-Tl mineralization is structurally located between the two faults and confined by a number of NE-trending and EW-trending secondary faults and fractures. The NE-trending faults are represented by F_1–F_7, and the proven mercury ore bodies mainly occur in the fractured altered zones. The EW-trending faults are represented by Fc and F_6, and the strong Hg-Tl mineralization occurs within these fault zones.

3.4 Hydrogeology of the Lanmuchang area

The Lanmuchang study area is topographically characterized by peak-cluster and depression. The whole area is within a small catchment (Fig. 3-4). One of the main characteristics of hydrogeology in the Lanmuchang area is that the karstic groundwater is predominant. The groundwater, discharging to the surface through karstic springs and karstic underground rivers, is the only natural water source for water supply and irrigation.

The Qingshui (*Chinese word for 'clear water'*) Stream is the only surface water which runs from north to south, very close (about 300 m, Fig. 3-4) to the Lanmuchang Hg-Tl mineralized area. This stream also runs through the densely populated area. The flow rate of the stream ranges from 0.1 to 0.6 m^3/s with an average 0.3 m^3/s. The maximum elevation of the stream water table is up to 1404 m a.s.l. (in flood-flow regime), and the minimum is 1399 m a.s.l. (in base-flow regime). Its sources are mainly from the discharge of three different groundwater outlets (Creeks A, B and C) indicated in the Fig. 3-4 within or around the Tl mineralized area. The upstream is recharged by the karstic cave groundwater (underground river water) and springs (Creek A and B), the middle stream by the karstic springs (Creek C) (Fig. 3-4). All stream water drops into a sinkhole 3 km downstream to join further circulation of groundwater. In the rainy season, the runoff of rainfall also recharges the Qingshui Stream. In addition, some acid mine drainage (AMD) (e.g. Creek D) can overflow from the ancient mine adits to the surface, and be added to the stream, although the volume of this contribution

is very small and the AMD disappears during the dry season. During rain events, the seepage into this sinkhole is not rapid enough to discharge the floodwater from upstream and midstream. Instead, the water inundates the whole sinkhole area and its surroundings, up to an area of 20 hectares.

The potential aquifers in the Lanmuchang area are located in strata of the Triassic Yelang Formation (T_1y) and the Permian Longtan Formation (P_2l).

The Yelang Formation, located above the local base erosion level, is affected by faults and the topography, and does not contain much groundwater in the mineralized area. However, this formation is much thicker at the southern margin of the mineralized area; and some rock units in this area are under the local erosion base, and thus contain groundwater.

The Longtan Formation is directly cut by several large faults and other small fractures, and the groundwater seeps through the fractured zones to the deeper aquifer. The groundwater table is strictly controlled by the faults, and is relatively deep, from 50–150 m under the local streambed which is elevated at 1399–1404 m. In the local fractured zone, the groundwater table is much lower, down to 1226 m in elevation. At the margin of the Hg-Tl mineralized area, especially at the southern margin, the groundwater table is a little higher, up to 1380–1420 m, the maximum being 1448.6 m, with a fluctuation of 2–5 m between winter and summer. As a result, the groundwater at the south margin of the mine area may

discharge to the surface streambed. The Huangnijiang reverse fault, trending NNE, constitutes a hydrogeological conduit facilitating the discharge of groundwater.

The Changxing Formation, confined to the mineralized area, is not a potential aquifer and does not contain groundwater, but infiltrating groundwater can permeate to the deeper aquifers due to the intensive fault and fracture system. This formation just outside the mineralized area and under the local base erosion level can contain groundwater mainly through fissures and karsts.

Due to the particular topography and geological structures, the mercury-thallium ore body is located in the ridge area. Groundwater in the Lanmuchang Hg-Tl mineralized area, recharged by wet season rainfall, drains to the deep parts of the ore bodies in a southwestern direction. The groundwater easily seeps through the faults to deeper strata through the fracture system, resulting in a strong fluctuation of the water table observed during borehole pumping tests (Guizhou Hydrogeological Survey, 1985). The groundwater in deeper hydrological layers is thought to discharge outside the study area with a main flow direction generally to the southwest.

3.5 Thallium mineralization in the Lanmuchang area

The mercury in the Lanmuchang area was first mined about 350 years ago during the early Qing Dynasty (around the 1640's). The mineralization of mercury was proven to be

a large mercury deposit by means of geological surveys and drilling projects during 1957–1960 (Guizhou Geological Bureau, 1960). High concentration of thallium up to 0.011% in the mercury ores was also targeted and evaluated during the mercury exploration project. Thallium in this mercury deposit is enriched enough to be commercially mined, and the geological reserves of metallic thallium were estimated to 391.7 tons.

The thallium sulfide lorandite was first identified as one of the main minerals in the mercury deposit during the 1957–1960 mercury exploration period. However, no further mineralogical investigation was carried out until 1989 when large amounts of thallium sulfides, lorandite, and then the thallium ore body were discovered (Chen, 1989a,b). Since Chen's studies, the Lanmuchang Hg deposit was redefined as a paragenous deposit of mercury and thallium in which thallium is highly enriched to form an independent thallium deposit, one of the very rare thallium ore deposits in the world.

The host strata of thallium-mercury mineralization are mainly the Longtan Formation (P_2l) and the Changxing Formation (P_2c), and the Yelang Formation (T_1y). The host rocks are represented by limestone, argillite, siltstone, mudstone, claystone and layered coal stone. These host rocks are intercalated, interbanded or interdigitated to form the hybrid sedimentary complex which is the favored location for the mineralization of thallium and other metals. The thallium mineralization occurs in several depth zones parallel to the hybrid sedimentary complexes.

The occurrence of the Hg-Tl deposit is constrained by both the lithologies and structures. The Hg-Tl ores occur in the fractured altered zones between faults F_1 and F_7, generally extending through the strata. In a vertical section, the ore bodies rake to the southwest, presenting stratoid, and banded structures, and strike approximately 25° NE, dipping nearly parallel to the host rocks (Fig. 3-5). In horizontal zones, the ore bodies present lens-like and saddle-like structures. The Hg-Tl ores occur in 10–14 different horizons. The individual ore body is generally up to 60–240 m long, 40–80 m wide and 2–5 m thick. The ores often occur in the fractured zone of the strata, the buckling location around the faults, the location of the hybrid sedimentary complex or brecciated rocks, and the fault zones (Fig. 3-6).

Independent thallium ore bodies occur as banded, podiform and bead-shaped morphologies. A thallium ore body was found between the prospecting line VIII–VIII′ and the F_6 fault, (Chen, 1989b; this study). As observed in the underground thallium-mining site, it is 10–17 m long and 4-6 m wide. The ore body is distributed as bead-shaped forms along the NW-trending fault zones. The attitude of the ore body is same as the host rock and the tilt angle is about 25°. In 1997, during a field survey connected to this study, intensive thallium mineralization of some thallium sulfides were observed in an underground adit around the fault Fc. Similarity, during a field survey in 1999, intensive mineralization of thallium sulfide lorandite was discovered in a coal underground mining site around the west side of the fault

F_7. In addition, some thallium mineral has also been found in the tailings or mine wastes on the surface. This indicates that thallium minerals in the Lanmuchang area are very common. This also indicates that thallium is one of the most common mineralized ore metals and constitutes a dominant phase of mineralization in the Lanmuchang, favoring independent thallium ore bodies.

Besides lorandite ($TlAsS_2$), the main minerals containing thallium in the Lanmuchang Hg-Tl deposits are cinnabar, realgar, orpiment, arsenopyrite and pyrite (Chen, 1989b; Li, 1996). Gangue minerals contain quartz, kaolin, barite and calcite. The secondary minerals are melanterite, potash alum, gypsum, limonite, scorodite, etc (Chen, 1989b; Li, 1996; Zhang et al., 1997). What is of more interest is that several other thallium minerals also have been identified in this Hg-Tl deposit. They are christite ($TlHgAsS_3$), imhofite ($Tl_6CuAs_{16}S_{40}$) and raguinite ($TlFeS_2$) (Chen, 1989a; Li, 1996; Li et al., 1989).

The ores are classified into two types. The first type is mainly composed of mercury ores. These ores contain Hg at 0.08–3 % with an average of 0.191 % and Tl at 0.011 % from which thallium can be commercially mined. These ores are rich in pyrite, but the occurrences of realgar, orpiment and lorandite are poor. The gangue minerals are kaolin, barite and calcite. The other type of ores is thallium-rich ores with low quantities of cinnabar. These ores are usually rich in thallium ranging from 5.22–15.97 %, arsenic 1.92–5.87% and Hg only 0.066 %. In the thallium-rich ores, the lorandite is the major thallium-bearing mineral. Pyrite,

marcasite, realgar and orpiment also contain thallium and rank after lorandite for their thallium contents. Kaolinisation and baritization are weak in the altered zones of these ores.

The main thallium sulfide lorandite is easily distinguished by its lead-gray or darker red color and its semi-metallic luster. Lorandite occurs mainly as needle or prismatic crystal. The crystal typically reaches sizes of 5–20 mm long and 0.1–2 mm in diameter. It often occurs as veins, a network of veins or as patches.

The thallium ore is characterized by massive, disseminated, densely veined structures. The hydrothermal alteration of host rocks includes silicification, decalcification, argillisation, pyritization, kaolinization and baritization, and it will be described in detail later in this thesis.

The anthracitic coal has been the focus for the mining for energy since the early Qing Dynasty in Lanmuchang area. The coal seams occurring in the Longtan Formation are thin, often 2–5 cm thick, and are still being sporadically mined by local villagers. Within and around the Hg-Tl mine area some ancient coal mining adits can be observed.

Table 3-1 Description of lithologies of the regional stratigraphy

Formations		Lithology
Yongningzhen Formation (T_1yn)		Gray massive limestone and a small quantity of dolomite.
Yelang Formation (T_1y)	T_1y^3	Median laminar siltstone and argillite, intercalated by biogenic and argillaceous limestone
	T_1y^2	Grey massive limestone intercalated by median and laminar siltstone and claystone.
	T_1y^1	The lower zone is made up of siltstone and claystone, intercalated by dolomitic limestone and calcareous siltstone; the middle zone contains median massive limestone and argillaceous limestone, intercalated by argillaceous dolomite and calcareous siltstone; the upper zone is made up of median laminar siltstone, dolomitic limestone and argillite.
Dalong Formation (P_2d)		Thin-bedded calcareous claystone. Intercalated by 2-4 layers of gray-white montmorillonite claystone. This formation often interdigitates with P_2c formation (7–10 m).
Changxing Formation (P_2c)		The lower zone is composed of massive chert limestone; the middle zone consists of thin-bedded argillaceous limestone; the upper zone is made up of median massive biogenic limestone
Longtan Formation (P_2l)		Limestone, sandstone, siltstone and argillite and inter-bedded coal seam. The lower zone is mainly composed of sandy argillite, coal seam, median lamina of siltstone and sandstone. This zone is the main host for coal seams. The upper zone mainly consists of dark argillites, massive siliceous limestone.
Maokou Formation (P_1m)		Grayish massive biogenic limestone

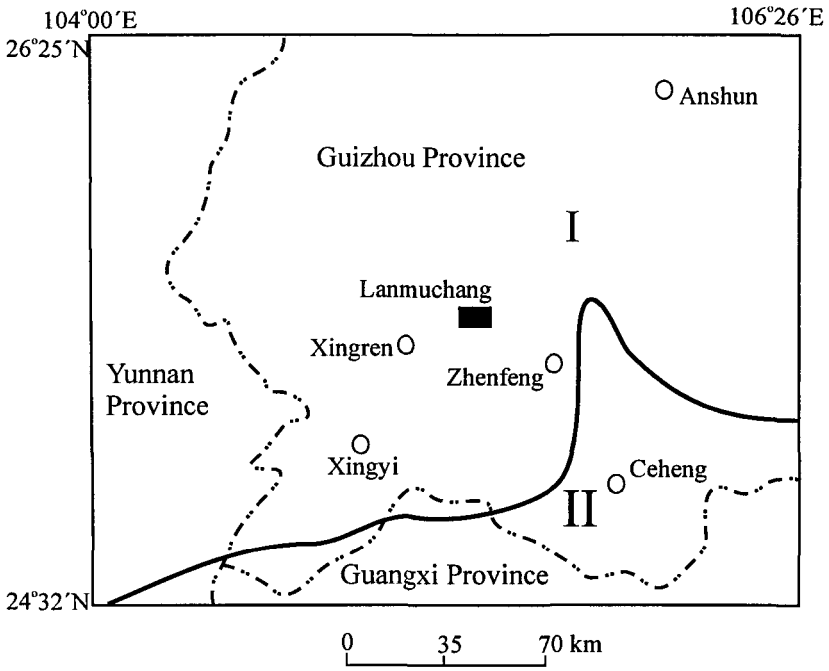

Fig. 3-1 Sketch map of Southwest Guizhou Province showing the tectonic context I-Yangtz craton; II-Youjiang orogenic belt (after Wang et al., 1994)

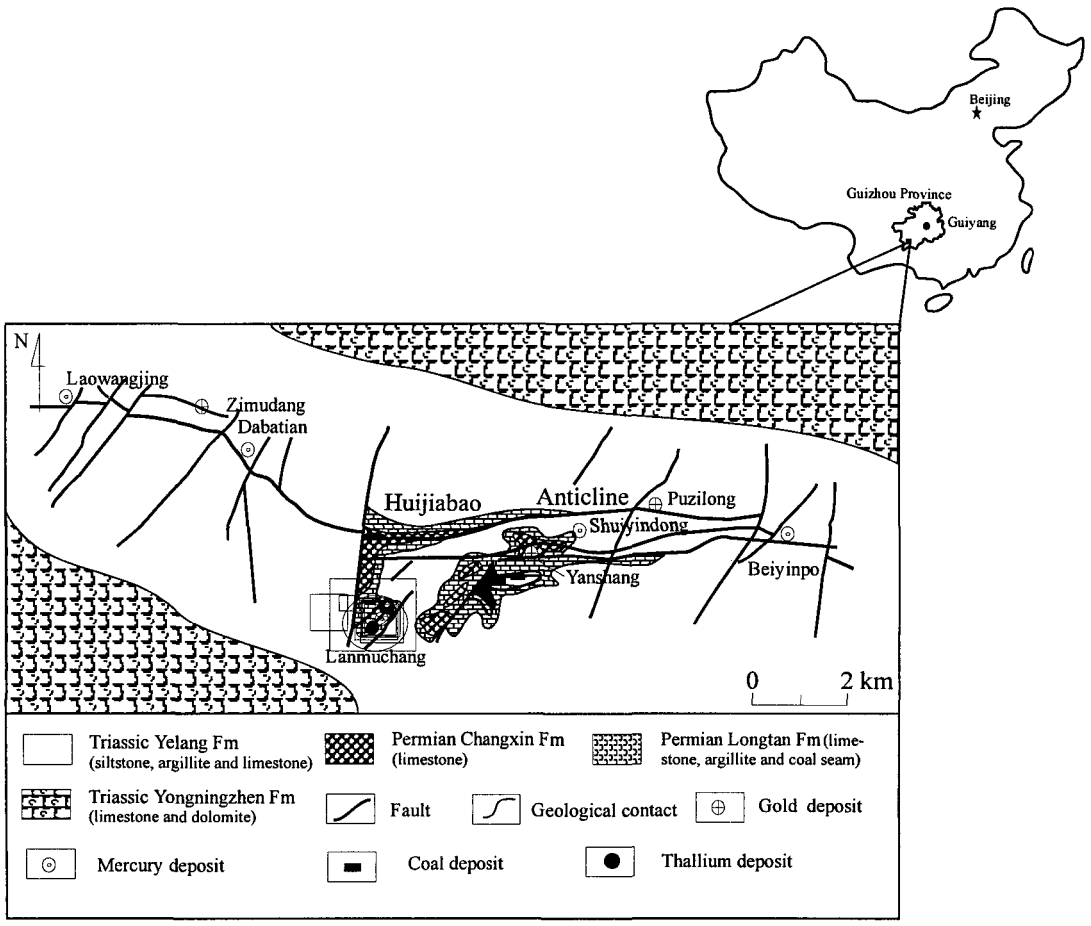

Fig. 3-2 Geological sketch map of Huijiabao anticline metallogenic belt in Southwest Guizhou, China (modified after Wang et al., 1994)

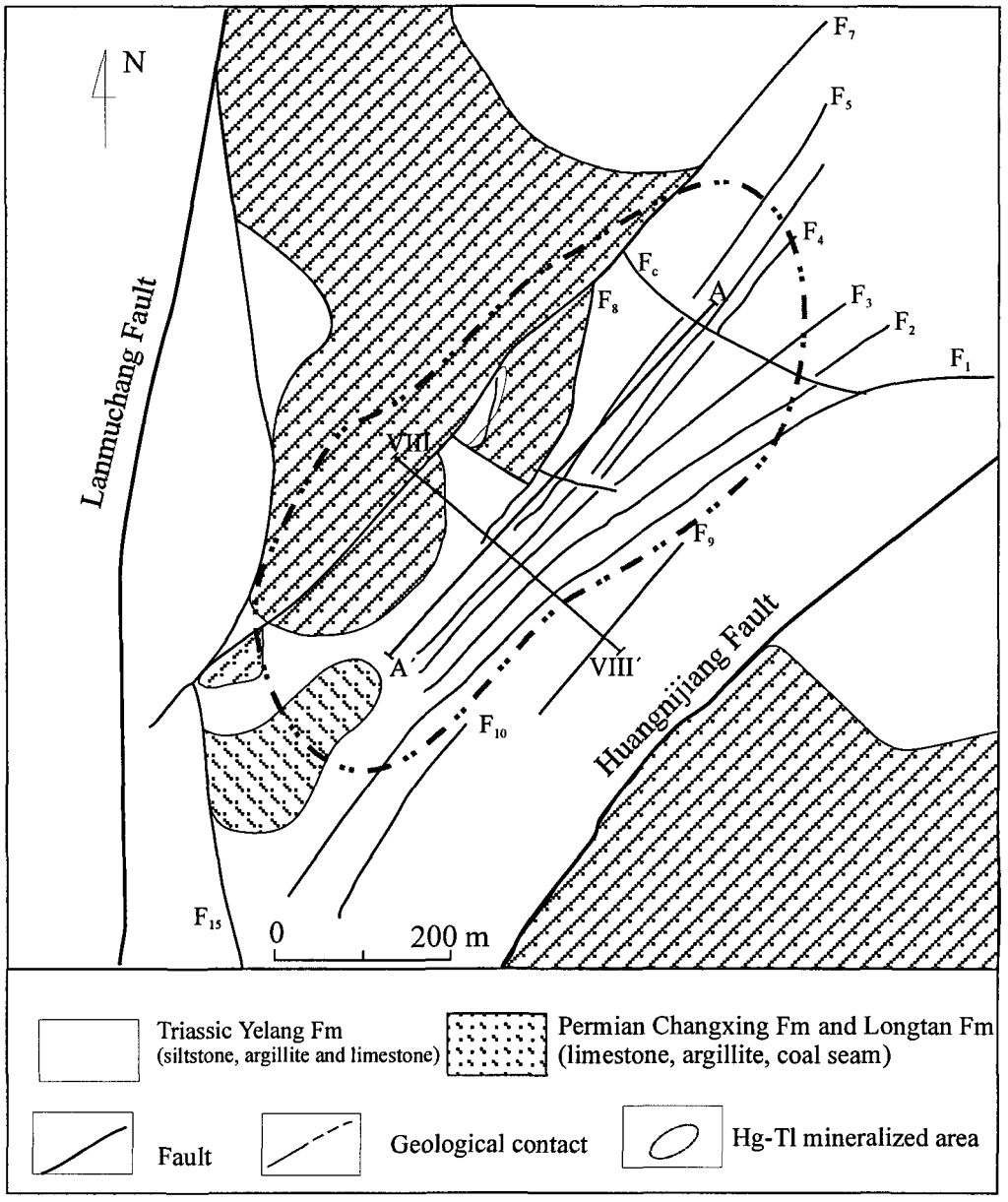

Fig. 3-3 Geological sketch map of Lanmuchang area (after Chen, 1989b)

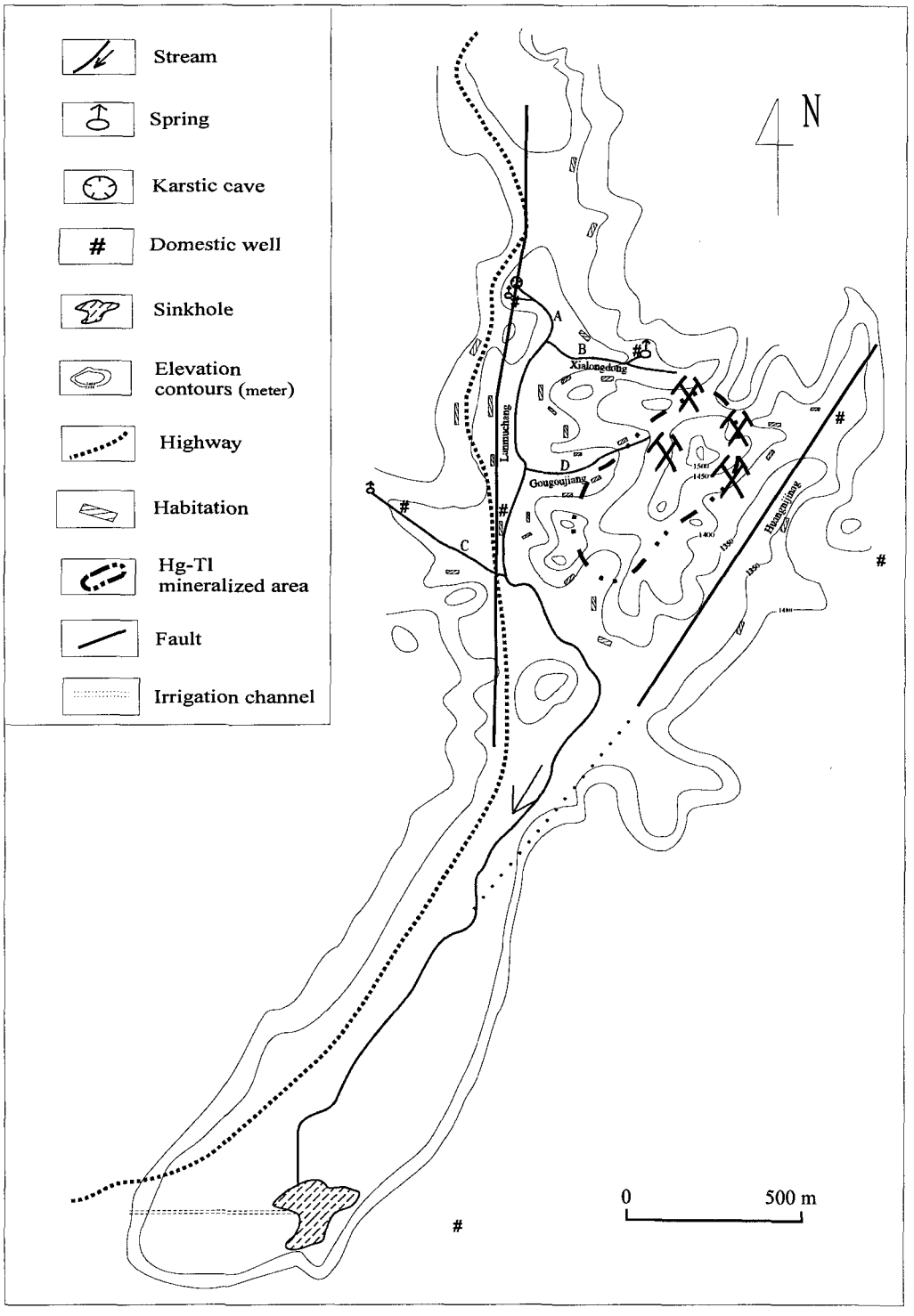

Fig. 3-4 Topography of the Lanmuchang watershed (based on scale 1:50,000 topography map)

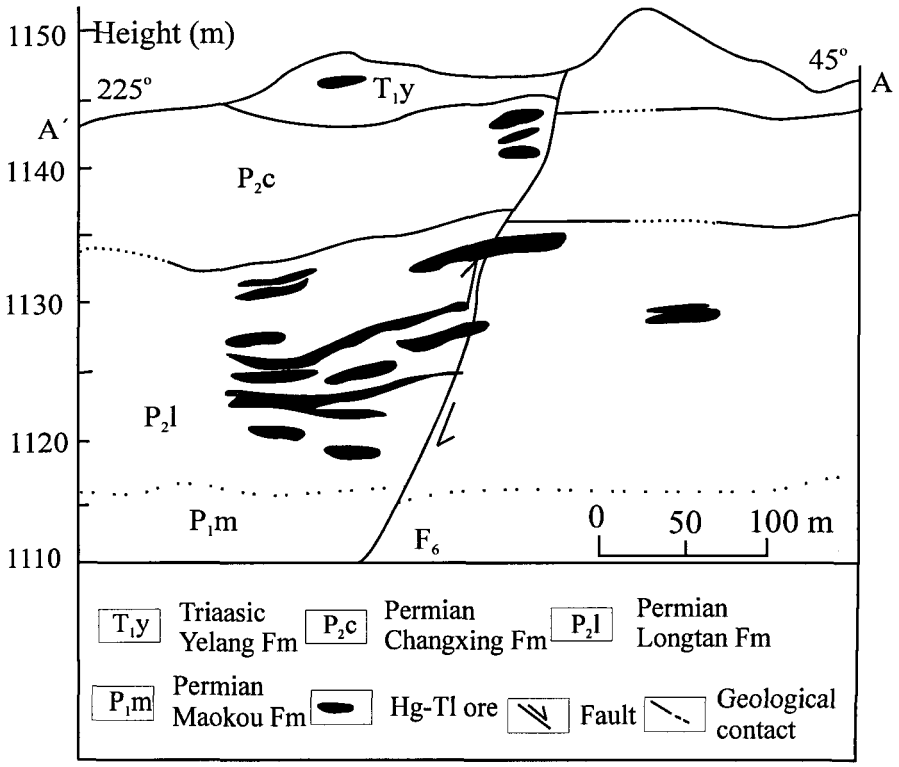

Fig. 3-5 Vertical section of Lanmuchang Hg-Tl deposit
(A-A´ represents the section ligne in Fig. 3-3) (After Chen, 1989b)

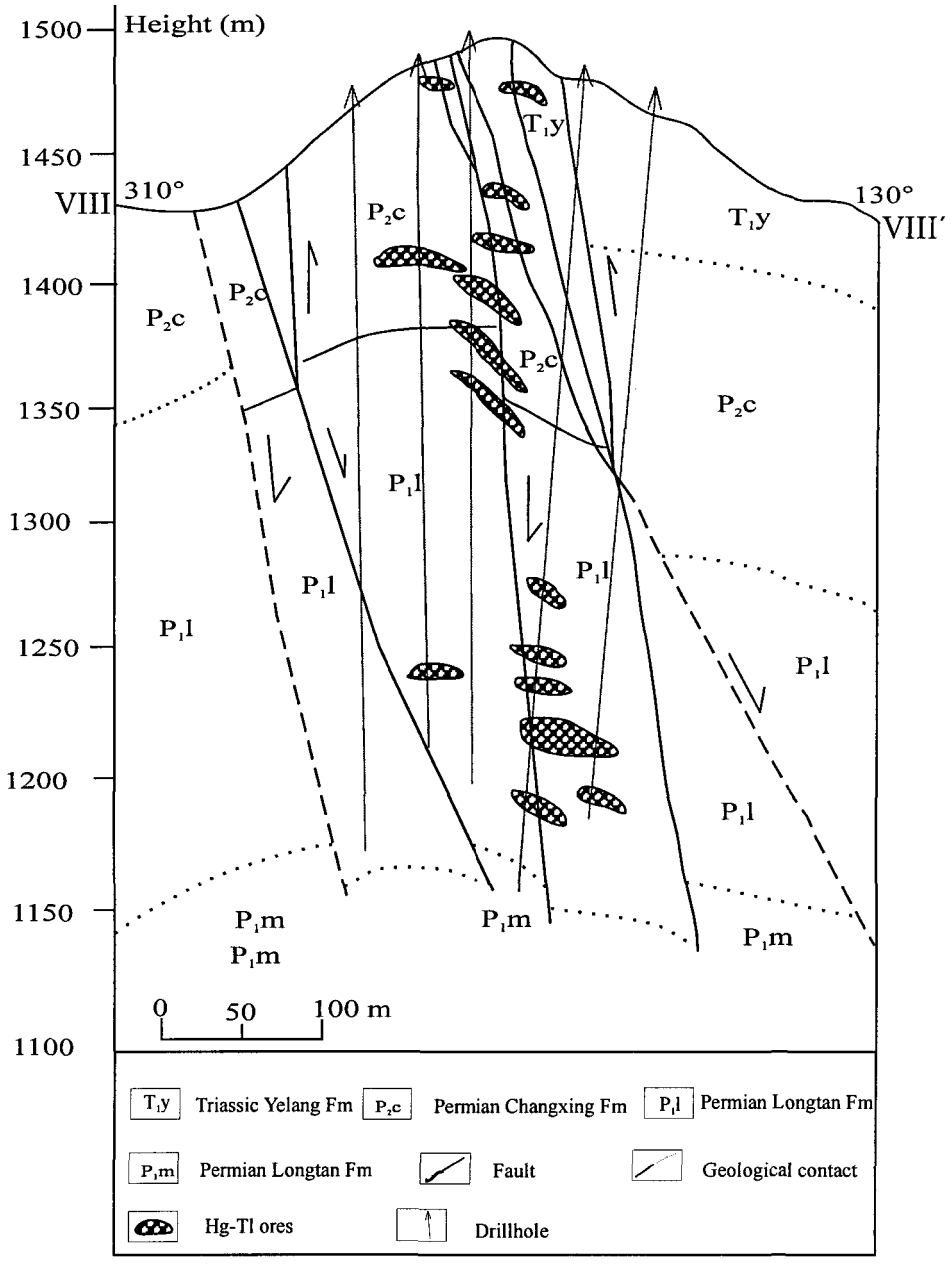

Fig. 3-6 Profile of mercury-thallium deposit through drillholes

(VIII-VIII′ represents the section ligne in Fig. 3-3) (After Chen, 1989b)

CHAPTER 4

GEOCHEMISTRY OF THALLIUM IN SPECIFIC GEO-ENVIRONMENTS

4.1 Rocks

4.1.1 Lithogeochemistry of thallium

Thallium is widely distributed in nature, but generally occurs in very low concentration. Its abundance in the crust is only 0.45 ppm, but it exceeds those of mercury (0.08 ppm), silver (0.07 ppm), cadmium (0.2 ppm) and gold (0.004 ppm) (Taylor, 1964). In contrast to these elements, however, thallium does not occur in a native form and is rarely enriched in specific minerals.

Thallium exists in two oxidation states in nature: as Tl^{+} or thallous species and Tl^{3+} or thallic species. Tl^{+} shows a much closer affinity to the ions K^{+}, Rb^{+} and Pb^{2+} which have quite similar crystal ionic radii (Table 4-1). Therefore, both thallium and rubidium, as well as potassium are readily concentrated in the late stage of magmatic and hydrothermal fluids (Calderoni et al., 1983). Due to a similar ionic radius and identical electric charge, it can substitute for K^{+} and Rb^{+} in silicates such as feldspars and micas that contain large alkali ions with high coordination numbers (Shaw, 1952). The order of ionic radii is $K^{+} < Tl^{+} < Rb^{+}$, but Tl^{+} has the higher electronegativity. Tl is concentrated more in residual melts than K^{+} and Rb^{+} because the Tl-O bond is more covalent and weaker than either the K-O or Rb-

O bonds. Also, the geochemical behavior of Tl during magmatic and hydrothermal processes is controlled largely by the relative abundance of K. To this extent, thallium is a rare lithophile element. On the other hand, thallium is also a chalcophile element occurring not only in oxide, but also in sulfide minerals. Tl often forms paragenetic associations with Cu, Pb, Zn, Ag and In in hypogene processes, while under supergene conditions, Tl tends to hydrolyze and form complexes with chlorides, sulfates and bicarbonates (De Albuquerque and Shaw, 1972). Commercially important Tl accumulations have only been found in sulfide deposits and this points out to a more pronounced chalcophile character of Tl. The great affinity of Tl to sulfur is evident from the chemistry of Tl minerals most of which are all sulfides or selenides with the exception of avicennite (Tl_2O_3), dorallcharite ($(Tl,K)Fe_3^{3+}(SO_4)_2(OH)_6$), monsmedite ($H_8K_2Tl_2(SO4)_8 \cdot 11H_2O$) and perlialite ($K_8TlAl_{12}Si_{24}O_{72} \cdot 20(H_2O)$) (see more in Section 4.1.4).

4.1.2 Distribution of thallium in various rocks

The abundance of thallium in common igneous rocks is listed in Table 4-2. The thallium content of ultramafic rocks is typically low, and is in the range of 0.05–0.6 ppm. The thallium content of mafic rocks increases slightly, ranging from 0.1 to 0.27 ppm. A definite increase in thallium levels is observed in the intermediate rocks relative to mafic and ultramafic rocks. Most values are in the range of 0.15–0.83 ppm and the higher values are found more frequently in the more acid rocks (syenite, monzonite and dacite) (De Albuquerque and Shaw, 1972). Most granitic rocks contain thallium in the range of 0.73–3.2 ppm, showing that these rocks are more enriched in Tl relative to the more mafic

rocks. The thallium content of alkalic rocks is generally low, ranging from 1.2–1.5 ppm. As for the volcanic and hypabyssal rocks, rhyolites and obsidians show contents of thallium mostly in the range of 1.0–1.6 ppm, similar to these of granitic rocks (De Albuquerque and Shaw, 1972).

Data for thallium in metamorphic rocks are not readily available. The concentrations of thallium in the principal metamorphic rocks are cited in Table 4-3. According to Heinrichs et al. (1980), the average concentration of thallium in the common metamorphic rocks is 0.653 ppm. Granites contain more than twice the amount of Tl than upper crustal metamorphic rocks. This is to be expected from its partition coefficients for the silicates in gneisses, etc., and a related granitic melt. The felsic (salic) granulites from the lower crust are depleted in Tl relative to upper crustal metamorphic rocks. The appreciable depletion of Tl in high-K (felsic) granulites relative to upper crust metamorphic rocks seems to be compensated by an accumulation of Tl in granitic rocks. Therefore, the losses and gains probably can be explained by the same process, by partial melting of gneisses and mica schists at intermediate crustal levels and the formation of granitic melts. The latter intruded into the upper crust leaving restites as one of the potential sources of felsic to intermediate granulites. Low-K granulites are close to mafic rocks in Tl content.

The thallium content of sedimentary rocks is generally in the range of 0.1 to 3.0 ppm (Table 4-4). The range 0.27–0.48 ppm is suggested for the average concentration value of Tl in sedimentary rocks by Heinrichs et al. (1980). The highest values for the concentration of this element are found in clay, sandstone and shale. Argillaceous rocks may be relatively rich in thallium, with contents up to 2.2–3.0 ppm. The dark and

especially the black shales have high values and a large dispersion of Tl. In these rocks Tl is more closely related to sulfur than to the organic carbon. The concentration of Tl increases from quartzitic sandstones to shales with increasing clay mineral fraction (Heinrichs et al., 1980).

Argillaceous rocks with high carbonaceous content have concentrations of thallium about twice the value for normal pelitic rocks (Shaw, 1952, 1957). Thallium is concentrated due to the reducing conditions in which such rocks were formed.

The leading role in the concentration of thallium in the sedimentary cycle is played by its chalcophile tendency and sorption (Voskresenskaya et al., 1962). The possibility of thallium being adsorbed in clay minerals to a considerable extent was pointed out by Shaw (1957) and, according to Shaw (1952), the relative degree of adsorption of the large univalent ions in clay is Rb > K > Tl.

The association of thallium with manganese in the sedimentary cycle is a consequence of the oxidizing environment precipitation (Shaw, 1957). The same also seems to be valid for iron.

The coherence of thallium and rubidium appears to extend to sedimentary rocks. The average Rb/Tl ratios for shales and sandstones are approximately 140 and 40, respectively. The concentrations of Tl and Rb are controlled by the abundance of illitic mica. In rocks free of potassium minerals, plagioclase is the major host of Tl and Rb. The sulfide fraction of black shale is high in Tl. According to Valiyev (1984), thallium as carbonate is present in silicate minerals and probably also in biogenic carbonates as isomorphous components, these being accompanied by the adsorbed form on the finely

divided hydroxides of iron and manganese. There may also be a contribution from the dispersed organic matter in the carbonates.

The significant correlations between Tl and K, Rb, Pb and Bi were also observed (Heinrichs et al., 1980). The degree of in interrelationship among the large ions K^+, Rb^+, Tl^+, Pb^{2+} and Bi^{3+} differs according to the mineral composition of the host rocks. Three groups of typical rocks (Table 4-5) characterize the different partitioning of the metals. Group (a) is characterized by plagioclase acting as a host mineral in the absence of major K minerals, group (b) is indicated by the predominance of trioctahedral mica (and K-feldspar) as major host mineral whereas the group (c) is associated with the dioctahedral mica as a host.

As for the oceanic sediments, the pelagic sediments have greatly accumulated some Tl. The factor of enrichment of Tl in Atlantic and Pacific clays relative to near shore deposits is close to 2.8. Deep sea sediments contain usually low amounts of thallium (Table 4-6), with the exception of manganese nodules which may show concentrations of this element as high as 600 ppm and an average concentration of about 100 ppm (Ahrens et al., 1967; Iskowitz et al., 1982).

Based on the data of 2000 magmatic, metamorphic and sedimentary rocks samples and rock-forming minerals of the Earth's crust and the upper mantle, Heinrichs et al. (1980) computed the average abundance of thallium and other related metals (Table 4-7), and developed a conceptual model for the transport process of thallium in the Earth. The Earth's upper mantle contains very low concentrations of Tl compared to the continental crust. This is suggested by the release of thallium from energetically unfavorable lattice

sites during partial melting of the mantle materials. Thallium is then transported into the crust via magma as reflected by the high Tl in magmatic rocks. Tl is also accumulated in the upper crust relative to the lower continental crust by a factor of 3.2. This is mainly caused by the higher concentrations of Tl in granites and lower abundance in granulites relative to gneisses and schists. Furthermore, Tl, Rb and K can form large ions with bulk coefficients less than 1 for the partition between metamorphic rocks and anatectic granific melts. The major hosts of Rb and Tl in rocks are minerals with 12-coordinated potassium sites in mica, such as biotite, K-feldspar and plagioclase.

4.1.3 Thallium behavior in various geological processes

Enrichment of Tl is generally observed in rocks affected by metasomatic processes (Table 4-2). Potassium metasomatism is believed to be responsible for the high thallium content. A marked enrichment of thallium is also charactered in rocks occurring in fault zones. Hydrothermal alteration frequently leads to thallium enrichment: the altered rocks contain slightly higher amounts of Tl than the unaltered rocks.

Enrichment of Tl in the country rocks surrounding intrusions of magmatic rocks and hydrothermal mineral deposits has been observed in different regions. Thallium enrichment is sometimes related to the formation of greisen and micas, which seem to be the main thallium carriers. The mineralogical assemblage of the country rock is, apparently, an important factor controlling the distribution of thallium. Limestones show a much more pronounced enrichment than sandstones or quartzites, if these rocks are not converted to

greisen. The high volatility of the thallium halides plays a major role in the distribution of thallium.

Thallium is probably not lost from the rock unit during metamorphism. But this possibility cannot be totally excluded. The rock from the zone of highest thermal alteration is not lower in Tl than the unaltered shales from the Basel area, Switzerland (Marowsky and Wedepohl, 1971). The scattering of the Tl concentrations around the shale average of about 1 ppm seems to be normal for phyllites, schists and gneisses (Marowsky and Wedepohl, 1971). Tl is enriched in hydrothermal alteration zones where it is preferentially hosted by micas (De Albuquereque and Shaw, 1971).

An interesting fact about the behavior of thallium is that during the processes of ore deposition, thallium is readily concentrated in the sulfide minerals (Table 4-8). The ore minerals from polymetallic sulfide deposits show the highest concentrations of thallium. Enrichment of Tl is accompanied by concentration of metals such as As, Sb and Ag. The critical factor governing the distribution of thallium in mineral deposits appears to be the sorption of this element in sulfide gels, with isomorphism playing a secondary role. This explains the concentration of Tl in sphalerite rather than in galena. Ore minerals which crystallized from colloform solutions show strong enrichment of Tl.

Based on the distributions of Tl in the Au-Ag-U-Cu-Mo mineralized areas in northeastern Washington and central Montana, Ikramuddin et al. (1983) showed significantly higher Tl in the hydrothermal altered rocks than in unaltered rocks. The lower ratios of K/Rb and K/Tl were suggested as pathfinders of metal mineralizations (Ikramuddin et al., 1983).

As for the behavior of thallium during the weathering and alteration of rocks, thallium is largely retained during the weathering processes, and, probably as a result of this, enrichment of thallium may be observed in the products of weathering. Thallium tends to readily deplete during the alteration of K-alkaline rocks, but it is more enriched in the Fe-rich Mn-bearing sedimentary rocks. Thus, the Fe/Mn-rich sediments are regarded as powerful scavengers of thallium (Calderoni et al., 1985a).

Thallium tends to disperse during oxidation of sulfide ores and many oxidized minerals are very poor in thallium. Therefore, the oxidized zone of ore deposits is poorer in thallium than the sulfide zone. In some instance, minerals from the oxidized zone of ore deposits show appreciable enrichment in thallium. Mimetite may concentrate thallium, probably due to the formation of the nearly insoluble compounds $TlAsO_3$ and $TlAsO_4$. Of much more importance as thallium carriers are jarosite, which may form thallium-rich varieties, and manganese oxides, especially psilomelane. Thallium seems to precipitate together with manganese, probably as Tl_2O_3, in strong oxidizing environments. It seems possible that the observed enrichment of thallium in jarosite is a consequence of the substitution of thallium for K in the structure of this mineral (De Albuquerque and Shaw, 1972). The enrichment of thallium in gossans in sulfide deposits was also observed, and therefore, the Tl was suggested as a pathfinder in the oxidizing zones for prospecting (Calderoni et al., 1985b).

4.1.4 Mineralization of thallium

The first thallium mineral was discovered in 1866 by Baron Nils Addf Erik Nordenskiold (Weeks, 1968). During an analysis of selenium minerals (eucairite and berselianite) from Skrikerum in Sweden, the new mineral was named cookesite [$(Cu,Tl,Ag)_2Se$], in honor of William Cookes, the discoverer of the element thallium (Weeks, 1968). Since that time, many thallium-containing minerals have been identified and described (Table 4-9).

The number of already identified Tl minerals is more than 40, but these specific Tl-rich minerals are extremely rare in nature. They are only formed during epithermal stages and hydrothermal processes or under supergene conditions (Vlasov, 1966; Sobott et al., 1987). Instead, thallium generally occurs as a trace element in other minerals, mainly associated with potassium, rubidium and cesium in magmatic, metasomatic and pegmatitic low-temperature formations, with iron and various nonferrous metals in meso- and epithermal deposits as well as in supergenetic manganese precipitations.

There are generally two types of thallium mineralization in sulfide deposits: sulfide deposits containing Tl minerals and sulfide deposits without independent Tl minerals but thallium as a trace element in other sulfide minerals. In the first type, it is interesting to note that in sulfide deposits thallium occurs almost exclusively together with As, Sb, Cu, Pb, Fe, Hg and Ag (Fig 4-1). Thallium is predominantly associated with arsenic and/or antimony by forming Tl sulfosalts and Tl-bearing sulfosalts (Table 4-9).

Remarkably high Tl concentrations and seemingly missing independent Tl minerals are the characteristics of sulfide deposits of the second type. Bulk chemical analyses yield high contents of Tl for low-temperature sphalerites and colloform

pyrites/marcasites and noticeably lower contents for galena (Voskresenskaya, 1969). This is regarded as evidence for a co-precipitation and adsorption of Tl to colloidal metal sulfide gels while the contents of Tl in galenas are explained as some sort of self-purification during the process of (re)crystallization (Voskrenskaya and Karpova, 1958). Thallium may be present in these sulfides as minor inclusions of Tl minerals and not so much by forming limited solid solutions. Solid solutions do occur in sulfosalt structures and a coupled substitution of Tl and As or Sb for Pb (Tl + As, Sb $\rightarrow$ 2Pb) has been proved by crytal structure determination for rathite, hutchinsonite and chabourneite (Sobott et al., 1987). Shah et al. (1994) pointed out that the thallium exhibits lithophile behavior in the rocks of the Cu mineralized area and no chalcophile behavior was observed, and that Tl is more enriched than K in the mineralized metavolcanics. Lu (1983) reported high Tl concentrations with an average 800 ppm in the ores from the Kosaka mine, Japan. Murao and Itoh (1992) also determined high contents of thallium (23–55 ppm) in pyrite-containing ores of Kuroko-type deposits in Japan. The thallium is widely distributed in the Neogene metallogenic province of southeastern Europe, and is associated with sulfides of lead and zinc, but more often with and Sb-As mineralization. The concentrations of thallium range from 10 ppm to >1% (Table 4-8) and in local places form thallium ores of economic size (Jankovic, 1989).

Famous localities which produced thallium minerals include the Allchar deposit, Macedonia, Yugoslavia, the Lengenbach deposit, Wallis, Switzerland, the Jas Roux, Hautes Alpes, France, and the Carlin deposit, Nevada, U.S.A. (Table 4-10). These deposits contain the natural parageneses of Tl-As-Sb-S. All the thallium sulfides and sulfosalts are naturally

formed at low temperatures equilibrium phase assemblages at 100 and 200°C (Sobott, 1995).

Thallium also tends to enrich in coals. The distribution of thallium in various coals are listed in Table 4-11. The average value of Tl in coal was estimated to <0.2–1 ppm by Swaine (1990). In Swiss coals, the higher concentration of thallium was explained by the fact that thallium is probably present as sulfides or associated with other sulfides, mainly pyrites since the pyrite and other fine-grained sulfide minerals are very common in Swiss coals (Hugi et al., 1993). In China, thallium in coal range in concentration from 0–0.88 ppm except for the higher concentration of 1.37 ppm in Tangshan coal (Table 4-11). The latter is due to high mineral contents in the coals (Zhuang et al., 1999).

Tl is strongly enriched in pyrites from coals in Central Asia. Thallium occurs in the sulfide phase in coal rather than in coal itself. Thallium may also occur in the secondary silica minerals that were introduced in coals from the surrounding rocks (Feng et al., 1999). According to Bouska (1981), thallium is not firmly held in the organic mass of the coal because complexes of Tl with humic and fulvic acids are soluble and would not retain Tl during coalification. Pyrite from the coal is richer in thallium than the same mineral from the enclosing sedimentary rocks.

4.1.5 Summary

The distribution of thallium in the earth's crust shows that its concentration tends to increase with increasing acidity of magmatic rocks and with increasing clay content of sedimentary rocks. Common Tl contents in mafic rocks range from 0.05 to 0.4 ppm and in

acid rocks from 0.5 to 2.3 ppm. Calcareous sedimentary rocks contain as little as 0.01 to 0.14 ppm thallium.

In geochemical processes, Tl is known to occur in two oxidation states, +1 and +3. The cation Tl^+ is highly associated with K^+ and Rb^+, and is incorporated into various minerals, mainly sulfides. During weathering Tl is readily mobilized and transported together with alkaline metals. However, Tl is most often fixed *in situ* by clays and gels of Fe/Mn oxides.

4.2 Water

4.2.1 Hydrogeochemistry of thallium

Thallium exists in two oxidized states in natural waters: Tl^+ and Tl^{3+}. The redox equations governing thallium are presented in Table 4-12. As inferred from these standard electrode potentials, Tl^+ is likely to be the dominant species in aqueous environments and Tl^{3+} would be expected to exist only in the extremely strong oxidizing and highly acidic environments.

Brookins (1986, 1988) published the first Eh–pH diagram for thallium. This diagram configuration suggests thallium is immobile under transitional and oxidizing conditions, be it acidic or alkaline, being precipitated as one or more of the thallium oxide phases. However, Brookin's thallium diagram cannot be considered correct to reflect the true distribution of thallium in aqueous environment because some of the calculations result in phase transitions outside the normal Eh–pH space.

Vink (1993) revised Brookin's diagram for 25°C and 1 atm total pressure, within the normal pH limits between 0 and 14 and Eh limits between –0.8 and +1.4 V (Fig. 4-2). In this new diagram, the species Tl^+ now occupies almost all of the Eh–pH space. Thallium oxides (Tl_2O_3, avicennite, and Tl_2O_4, an unstable phase) occur only under very alkaline or oxidizing conditions whereas simple sulfide Tl_2S occurs under very alkaline reducing conditions. The new diagram was calculated for a thallium activity of 10^{-8}M (approximately 2 ppb), and contoured for activity 10^{-6}M (approximately 204 ppb). Increase in activities results in a minor increase of the oxide fields and a substantial increase of the Tl_2S field.

The new diagram suggests that Tl^+ must be considered to be a very mobile element under almost all natural (sub) surface conditions in waters, while only under extremely oxidizing and alkaline conditions will the Tl^{3+} species exist. This agrees well with the empirical observation of De Albuquerque and Shaw (1972) who pointed out that thallium tends to disperse readily during oxidation of thallium-bearing sulfide deposits. This is also entirely in line with the speculations of Shaw (1952). Based on their studies of thallium behaviors in rocks and sediments, both researchers speculated that thallium is probably transported in solution as Tl^+ and therefore is relatively quite mobile.

According to the calculation of temperature dependence (25°C–100°C) of the Eh–pH diagram of thallium (Vink, 1998), it is concluded that an increase in temperature only increases the stability field of Tl^+, or in other words an increase in temperature enhances the mobility of thallium in waters. This would also indicate that when dealing with problems of thallium-polluted surface water or groundwater remediation, measures

involved with elevated temperatures should not be considered because that process only increases the mobility of thallium.

The aqueous species of Tl^+ and Tl^{3+} were discussed by Kaplan and Mattigod (1998). Complexes between Tl^+ and most ligands are generally neutral or anionic, and relatively weak. Though thallium complexes are rather weak, potassium can be readily displaced by thallium from essentially all organic ligands (Sager, 1994). Tl^{3+} forms compounds with nearly all ligands that are more stable than those of Tl^+. The Tl^{3+} inorganic complexes are generally of the form of TlX_4^- or TlX_6^{3-} (X =halogen, sulfate, nitrate, acetate, etc.). The hydrolysis of Tl^{3+} starts at very low pH values. Tl^{3+} hydroxide is rather insoluble in water.

Some understanding of aqueous speciation of Tl^+ in natural water systems can be gained by the illustration of geochemical models. For example, Kaplan and Mattigod (1998) used the geochemical speciation model GEOCHEM-PC (Parker et al., 1995) to compute the distributions of Tl^+ species in natural waters. The natural water system chosen for computation include groundwater, river water, eutrophic lake water, bog water and seawater, and represent a range of conditions of pH, Tl^+ contents, dissolved organic carbon, and major metal and ligand concentrations. Their geochemical compositions and pH values are listed in Table 4-13.

The computation results (Table 4-14) showed that a major fraction (about 90%) of the total dissolved Tl^+ in a typical groundwater would exist in free ionic (uncomplexed) form with minor fraction (< 5% each) as complexes with bicarbonate and sulfate ligands. In typical river water, the free ionic form would constitute about 83% of the total dissolved

thallium, whereas about 16% would exist as an organic complex (Tl-fulvate). In typical eutrophic lake waters, almost a fifth of dissolved thallium would exist as organic complexes. In typical bog waters, the organic bound fraction constitutes a significant fraction (about 67%) of total dissolved thallium. In some bogs, with higher concentrations of dissolved organics (400 mg/l), almost all thallium (about 96%) would exist as organic complexes (Kaplan and Mattigod, 1998). In typical seawater, only about 52% of total dissolved thallium would exist in free ionic form whereas about 36% and 11% would be complexed with chloride (about 31% as $TlCl^0$ and about 5% as $TlCl_2^-$) and sulfate ligands, respectively. These computation results showed that Tl^+ would exist predominantly as free ionic species (77–90%) in common (sub)surface waters (pH =7–8). However, in highly acidic bog water, organically complexed thallium would constitute a major fraction (68–96%) of dissolved Tl^+. In seawater, inorganic complexes of Tl^+ was predicted to constitute almost 50% of the dissolved Tl^+, implying that in other inorganic-ligand-dominated systems, such as alkaline lake and brines, inorganic-ligand-bound Tl^+ would dominate Tl^+ dissolved speciation (Kaplan and Mattigod, 1998).

Tl^+ is the major aqueous species of dissolved thallium in seawater (Quinby-Hunt and Turekian, 1983). The free fraction of Tl^+ in seawater was estimated at 53-61% by Turner et al. (1981) and Byrne et al. (1988), which agrees with the computation results of Kaplan and Mattigod (1998). The experimentally derived value of the overall free Tl^+ fraction in seawater is approximately 40%, also supporting the previous results of thermodynamically calculated speciation (Savenko, 2001). Savenko (2001) also demonstrated that most of Tl^{3+} in seawater exists in the neutral hydroxo complex $Tl(OH)_3^0$.

This character of Tl^{3+} may greatly contribute to the extremely high accumulation of thallium in the Fe-Mn concretions in the deep sea (Ahrens et al., 1967; Iskowitz et al., 1982). $Tl(OH)_3$ has a very low solubility constant ($10^{-45.2}$) (Dean, 1999), thus the formation of solid $Tl(OH)_3$ under oxidizing conditions may constrain the total level of Tl in aqueous environments, whereas the solubility of Tl^+ hydroxide $Tl(OH)_{(solid)}$ is up to 350 μg/l (Dean, 1999) and thus is unlikely to be precipitated under normal environmental conditions. Tl^{3+} can also be stabilized in solution by the formation of successive complexes with chloride up to $TlCl_6^{3-}$ and $TlCl_2^-$, and with other ligands (Blix et al., 1989; Blix et al., 1995).

Contrary to the thermodynamic prediction that Tl^+ is favoured in natural waters, Tl^{3+} may be dominant over Tl^+ in some natural waters. This unexpected finding was obtained from the study of Lin and Nriagu (1999). They showed that Tl^{3+} is the predominant form of dissolved thallium in the Great Lakes water in north America accounting for 68±6% of the dissolved phase. They attributed the majority of Tl^{3+} to existence of colloids in the lake water. The hydrolysis behaviour of Tl in dilute aqueous systems deviates significantly from what one would predict using available thermodynamic data. The distribution of Tl species can be influenced by complex agents, particulates, and colloids in water. These factors are therefore responsible for the unexpected Tl^{3+}/ Tl^+ ratios (Lin and Nriagu, 1999). The high portion of Tl^{3+} in seawater was also observed by Batley and Florence (1975), and they reported that 80% of the thallium in Pacific Ocean was found to occur in form Tl^{3+} and only 20% occurs as Tl^+ and alkyl-thallium compounds. Thermodynamic calculations also show that Tl in the Rocaamonfina groundwater mostly

occurs as $Tl(OH)_2aq$. This is due to the oxidation of Tl^+ that occurs in the igneous rocks after introduction to the hydrosphere (Calderoni et al., 1985a).

The solubility of Tl^+ compounds, like those for alkali metals, is quite high (Zitko, 1975a; Sager, 1994). This suggests that Tl^+ would not precipitate from solution in most aqueous environments. However, in the rare instance when Tl^{3+} exists, thallium may form precipitates from solution.

In addition to dissolved species and solid phases, the adsorbed forms represent another important thallium component in natural waters. According to Lin and Nriagu (1998), the suspended particulates consisting of a mixture of inorganic and organic chelating ligands in natural waters have a strong control on the speciation of thallium. The study by Muller and Sigg (1990) showed that the adsorption of trace metals on natural particle surfaces are much stronger than those on a hydrous ferric oxide surface. A study by Bidoglio et al. (1993) suggested that thallium is accumulated by mineral oxides (e.g. manganese nodules) as a result of Tl^+ sorption followed by oxidation at the mineral surfaces. However, the study of Kaplan and Mattigod (1998) showed that the dominant mechanism of thallium adsorption appears to be cation exchange rather than precipitation, coprecipitation or absorption into the structure of a solid phase. Cation exchange is a process that does not bond Tl^+ very tenaciously. Thus, thallium would be expected to move rather readily with groundwater flow, that is, its attenuation by sediments would be rather limited (Kaplan and Mattigod, 1998).

As for the determination of thallium and its speciation (Tl^{+} and Tl^{3+}) in natural waters, Chou and Moffatt (1998) presented a good review of several effective analytical methods and offered detailed information regarding analytical methods.

4.2.2 Distributions of thallium in natural waters

Thallium is widely distributed in natural waters, but its concentration is generally low. The concentration of thallium in various natural waters is presented in Table 4-15. The distribution of thallium in seawater is low, but relatively constant, ranging from 9.4–17.5 ng/l (Table 4-15). Its distribution in the world oceans appears to be similar to that of the alkali metals, which are its principal biogeochemical analogues (Flegal and Patterson, 1985). Thallium in groundwater generally shows a low concentration ranging from 0.001–1.264 μg/l (Table 4-15). However, the concentrations of thallium in groundwater related to the ore/oil mineralization or mining are elevated greatly, up to 2.1–810 μg/l (Table 4-15). Waste water from metal smelters also contains high thallium. In fresh surface water (e.g., lake water, river water and stream water), thallium concentration varies in different localities. What is more interesting is that river water running through mining areas contains higher thallium concentration (Zitko et al., 1975), whereas high thallium in lake waters is due to the precipitates of thallium-bearing coal dust (Cheam et al., 1995). The waters in the Garfagnana area (Italy) shows different Tl contents as a function of the kind of rocks they interact with. Waters interacting with limestones and sandstones show Tl levels of 1–6 ng/l and 100–500 ng/l, respectively (Mario et al., 1994). However, the

distribution of thallium in groundwaters is not clearly related to lithology in the crystalline bedrock areas of Norway (Frengstad et al., 2000).

4.2.3 Summary

Thallium is widely distributed in natural waters, but its concentration is generally low and varies in different natural water bodies from different regions. Tl^{+} is generally the predominant species of the dissolved thallium and has a rather mobile behavior in aqueous environment. In some natural waters having an abundance of complex ligands, Tl^{3+} may replace Tl^{+} to become the predominant thallium species. The complexes of Tl^{+} are usually easily soluble, whereas the Tl^{3+} compounds are more stable.

In an environmental perspective, the groundwater and surface water related to ore mineralization and mining containing higher concentrations of thallium are of greater significance.

4.3 Soil

4.3.1.Soil geochemistry of Tl

The geochemistry of thallium in soils inherits its chemical composition from parent materials involved in the weathering processes from which these soils are produced. During weathering of thallium-bearing ores or minerals, thallium is readily mobilized and transported together with alkaline metals. However, Tl is most often fixed *in situ* by clays and gels of Mn and Fe oxides. The adsorption of Tl by organic matter, especially under reducing conditions, is also known.

Thallium from anthropogenic sources is often released from flue dust depositions from the cement industry, coal combustion, and the smelting and refining of sulfide ores, etc. Thallium from these anthropogenic sources is mostly soluble in water, but when it enters in soils it becomes immobile. For instance, after injection of 2.5 ppm thallium into soil in easily soluble form, only 40% could be determined to be still in this form after 13 days (Cataldo and Wildung, 1978).

Thallium from natural sources, i.e. the weathering of thallium-bearing ores and minerals, tends to be in a form that is less toxic than anthropogenic sources. The reason is that the thallium from the natural sources readily exists in the mineral lattices and is not easily substituted by other constituents, while thallium from anthropogenic sources is easily adsorbed on the surfaces of soil minerals at sites where Tl may be easily replaced. The natural processes of ore/rock weathering contribute greatly to introduce thallium into the soils and the (sub)surface waters.

As for the species of thallium in soils, many studies have been carried out to determine its various species. Studies show that most of the thallium in uncontaminated soils is bound in the residual silicate fraction, the oxalate leachable fraction (Fe-hydroxides) and in the organic fraction, while thallium in contaminated soils is almost all in the exchangeable form (>95%) (Lehn and Schoer, 1987; Sager, 1992). This indicates that the labile fraction of thallium in soils can be desorbed to soil water to further migrate under suitable conditions, or can be readily absorbed by plants growing in the soils. According to Schoer (1984), thallium related to the flue deposition in soils appears to occur in a chemical form that does not allow a rapid "wash-out", since results of analysis showed that the

concentrations of thallium is substantially higher in topsoil than that in subsoil (<35 cm) around a cement plant in Germany.

It is generally believed that Tl is present as Tl^{+}, and is transferred to solution in this form (Edwards et al., 1995). It becomes enriched in sediments, especially in strongly reducing environments where organic matter is accumulating under anaerobic conditions. In strong oxidizing conditions, Tl^{+} will be removed from solution as Tl^{3+} by precipitation with Mn or Fe (Smith and Crason, 1977).

The chemical leaching sequences show that thallium in most soils is found largely in the nitric-acid leachable, and the oxalate-extractable fractions (Sager, 1992), which indicates preferential affinities toward Fe hydroxides, sulfides and silicates. The exchangeable proportion of thallium strongly increased with decreasing grain size, thus demonstrating the effect of active surfaces (Lehn and Schoer, 1987).

Like other metals, the behaviour of thallium in soils is geochemically constrained by soil origin, pH, Eh, ionic strength of soil solution, the type and concentration of electrolyte, organic matter, clay mineral and Fe/Mn oxides (Kabata-Pendias and Pendias, 1992). The labile fraction of thallium in soils directly contributes to the bioavailability of thallium corresponding to uptake of plants. The larger the fraction of thallium in soil, the more thallium can be taken up by the plants. Anthropogenic thallium in soils seems to be easily soluble and thus readily available to plants.

4.3.2.Distribution of thallium in soils

Thallium is also widely distributed in soils but varies greatly in different soils. Both the geographical-geological conditions and the parent materials affect its distribution.

Since Tl is concentrated with K-minerals, clay minerals and Fe-Mn oxides, it may be expected that Tl in soils will depend on their abundance in the parent materials of soils. This means that granitoid and argillaceous rocks will form soils containing a higher amount of Tl in relation to mafic and carbonate rocks. Thallium exists at higher concentrations in soils with high organic matter. In addition, the sulfide ores of Pb, Zn, Cu, Sb, Hg and As, etc. usually contain quite a high concentration of thallium. Thus, the weathering of these sulfide ores can release significant amounts of thallium into the weathering products to enhance the levels of thallium in soils overlying outcropping ore bodies, or containing slag and/or waste material or lying within the flooding area of a stream cutting through the mining area.

However, the distribution of thallium in uncontaminated soils worldwide generally presents the same range of concentration. Table 4-16 gives the distribution of thallium in various soils worldwide. According to this table, the concentration of thallium in uncontaminated soils is generally low, ranging from 0.01–3 ppm, but most soils contain under 1 ppm. In upper Austria, the higher thallium in soils is related to the crystalline rocks, probably due to enrichment in K-feldspars. No significant correlation between pH, clay size fraction, humus and thallium were found (Sager, 1998). However, the thallium in soils in China shows one of the most positive correlations with organic matter content (Qi et al., 1992). Also, the higher thallium contents in Chinese soils are related to the weathering of

limestones (Qi et al., 1992). According to Mermut et al. (1996), the total content of thallium in soils positively correlates to the percent of clay content, which suggests that most of the thallium is associated with the silicate clay minerals in soils.

On the contrary, in contaminated soils or in soils related to sulfide mineralization or old mine sites or cement factories, etc., the contents of thallium are pronouncedly enhanced, up to 5–55 ppm. Similarly, the higher contents of thallium in soils derived from the highly mineralized parent rocks were also observed in France by Tremel et al. (1997). The content of thallium in such soils range from 1.54 to 55 ppm (Tremel et al., 1997). According to Tremel et al. (1997), high thallium concentrations are common in limestone, marl or granite derived soils, and the Tl in limestones or marls is probably concentrated in the sulfides occurring in these rocks because of the high affinity of Tl to S, or in the clay minerals, Fe/Mn oxides and micas. Furthermore, thallium was observed to be positively correlated with Ba, V, Pb, Fe, Ni, Cd, Zn, Co, As and especially Mn (Tremel et al., 1997).

Higher thallium content in soils may also originate from the use of thallium-bearing fertilizers. Smith and Carson (1977) assumed that the K/P-rich fertilizers containing significant amounts of thallium may represent a potential source of thallium contamination in soils. Lottermoser and Schomberg (1993) found thallium content in various European fertilizers ranging from <0.1 to 2.7 ppm. The thallium in the Canadian fertilizers was also investigated by Mermut et al. (1996), and they observed a range of <0.05–0.48 ppm. The contents of thallium in both European and Canadian fertilizers are within the general range of thallium in uncontaminated soils around the world, but the

increasing use of a great amount of fertilizers worldwide over the years will increase contents of thallium in arable soils.

4.3.3.Summary

The concentration of thallium in uncontaminated soils worldwide is generally low (most <1 ppm), but can be readily enhanced to higher contents in soils associated with sulfide mineralization, enrichment of K-feldspars and micas, old mine sites and cement/metal smelting and refining factories (1–60 ppm). Based on the thallium regulation in Germany that 1 ppm thallium in soil is regarded as the maximum tolerance level for agricultural crops (Sager, 1998), the soils containing thallium at more than 1 ppm can pose a thallium risk to the food chain especially in highly mineralized areas. The natural soil erosion by water can also facilitate the mobility of soil thallium into the soil water or (sub)surface water to increase the thallium level in water systems. The use of thallium-bearing fertilizers may also introduce appreciable amounts of thallium into arable soils to produce additional thallium soil contamination.

4.4 Thallium in the biosphere

4.4.1.Biogeochemistry of Tl

Thallium is a non-essential trace element for organisms, and can cause toxicity in plants, animals and human beings when entering the biosphere, thus, thallium is regarded as one of the most toxic metals. The toxicity of thallium on organisms was widely studied and reviewed (Bank et al., 1972; Zitko, 1975b; Siegel and Siegel; 1976; Davis et al., 1978;

Davis et al., 1981; Leblanc and Dean, 1984; Marcus, 1985; Allus et al., 1987; Al-Attar et al., 1988; Thompson et al., 1988; Douglas et al., 1990; Kaplan et al., 1990; Mulkey and Oehme, 1993; Moore et al., 1993; Tabandeh et al., 1994; Repeto et al., 1998; Gregotti and Faustman, 1998; Tabandeh, 1998).

Since Tl and potassium have the same charge and similar ionic radius, Tl follows K distribution pathways and inhibits a number of K-dependent processes. Various K^+–dependent proteins are known to posses a higher affinity for Tl^+ than K^+ (Britten and Blank, 1968). Possible toxic mechanisms of Tl include ligand formation of thallium with protein sulfhydryl groups, inhibition of cellular respiration, interaction with riboflavin and riboflavin-based cofactors, and disruption of calcium homeostasis (Douglas et al., 1990; Mulkey and Oehme, 1993). Tl^{3+} compounds are somewhat less toxic than are Tl^+ compounds for different animals. In fact, Tl^{3+} will always be reduced to Tl^+ because of the poor stability of Tl^{3+} in biological systems (Repetto et al., 1998).

The combination of rapid, diffuse alopecia, and neurologic and gastrointestinal disturbance is pathognomonic for thallium toxicity (Feldman and Levisohn, 1993; Mulkey and Oehme, 1993). The hair mount, showing a tapered or bayonet anagen hair with black pigmentation at the base, may be highly diagnostic before the onset of Alopecia. Thus, acute hair-loss is regarded as a clue to thallotoxicosis (Feldman and Levisohn, 1993; Meggs et al., 1994). The high levels of thallium in urine, hair, blood and nails were also determined in relation to thallium poisoning (Wainwright et al., 1988; Gassner et al., 2000).

The presence of elevated Tl levels in the urine or other biological materials confirms the diagnosis of Tl poisoning. Treatment with Prussian blue (or activated

charcoal) will interrupt the enterohepatic cycling of Tl, thus enhancing fecal elimination of the metal. Forced diuresis with potassium loading will increase the renal clearance of Tl, but should be used cautiously because neurologic and cardiovascular symptom may be exacerbated (Mulkey and Oehme, 1993). A further review of the toxicity of thallium poisoning on humans is beyond the scope of this study.

The uptake of thallium by plants and its toxicity to plants are of much interest for potential risk of thallium poisoning. It is through the uptake of plants that thallium from rocks/ores, soils and waters in the geosphere enters the food chain. The uptake of thallium can impair the growth of plants, but on the other hand, the readily high uptake of thallium by many plants has been observed.

The studies of Davis et al. (1978) and Al-Attar et al. (1988) showed that thallium is among the more toxic metals to plant growth. The hydroponic, rhizotron and field studies from Kaplan et al. (1990) indicated that Tl significantly reduced the biomass and drastically altered nutrient concentration in soybean. According to these studies, it appears that thallium exerts its toxic effect by interfering with root cell metabolism, which disturbs both macro- and micronutrient balances in the plant tissue (Kaplan et al., 1990). Schoer (1984) established that sufficient thallium can cause the following symptoms in plants: reduction of chlorophyll synthesis, decreasing of transpiration, decreasing of seed germination, reduction in plant growth and root development and chlorosis of leaves.

Other studies on Tl uptake by plants indicate that thallium is a mobile element with rapid movement from root to shoot and that the uptake of thallium is highly controlled by the presence of potassium (Lehn and Schoer, 1985; Logan et al., 1984; Jovic, 1993).

Some differences in the uptake of Tl^+ and Tl^{3+} by roots were observed by Logan et al. (1984). The uptake of Tl^+ is metabolically controlled and depends on the temperature and metabolic inhibitors, while the ion Tl^{3+} is absorbed passively, probably by cation exchange and diffusion in the same system. The system of (Na^+–K^+)-activated ATPase is thought to contribute to the uptake of Tl^+ (Britten and Blank, 1968). Logan et al. (1984) also concluded that Tl^{3+} was reduced to Tl^+ before uptake by plants in the nutrient solution or in the root system from the study of the whole maize plant (Britten and Blank, 1968).

Concentration of thallium correlates well with concentration of K in plants (Kaplan et al., 1990). The influence of K^+ over Tl^+ uptake is not surprising. Both elements have similar ionic radii, and Tl^+ can substitute K^+ in several enzyme systems, notably (Na^+–K^+)-activated ATPase. Tl^+ appears to be absorbed by roots via the K^+ system, but Tl has a lower affinity for this carrier than K (Edwards et al., 1995). The biological significance of the K-Tl interaction was demonstrated by Siegel and Siegel (1976), that is K-deficient cucumber seedlings are more sensitive to thallium than those provided with an adequate supply of K. According to this study, it seems evident that K can mitigate Tl toxicity and that when K is deficient, the presence of relatively high levels of Tl will bring about the impairing symptoms of overt K deficiency.

4.4.2. Distribution of thallium in plants

Concentrations of thallium in various plants are listed in Table 4-17. According to this table, it can be inferred that the concentration of thallium in plants is species-specific and varies with the concentration of thallium in soils where the plants grow.

According to the data published for thallium in various plants by Bowen (1979), Schoer (1984), Fergusson (1990) and Sager (1998), the concentrations of thallium (based on dry weight (DW)) in plants growing in non-contaminated soils are generally low, ranging from 0.02–0.125 ppm, but thallium in kale and cabbage is relatively enriched. However, thallium increases greatly in plants growing in soils which contain thallium near cement works, old mine workings and some mineralized areas. The data cited by Allus et al. (1987) showed that cereal grains and cabbages near a German cement factory contained higher thallium with the range of 9.5–45 ppm (DW). Zhang et al. (1998) studied the thallium in various plants in the As-Tl mineralized area and targeted high thallium in cabbages and fern, radish leaves and ferns. The study from Leblance et al. (1999) showed that wild plants growing on the Pb/Zn mine tailings and plants from pot trials in France contain extremely high thallium, ranging from 34–3070 ppm. Certain plants in some gold mineralized areas have also been analyzed for their thallium content and then used as pathfinders for gold exploration. Warren and Horsky (1986) obtained a thallium concentration of 0.071 ppm (DW) in firs, spruce and pine from a gold mineralized fault zone in British Columbia, Canada. Similarly, Chen et al. (1999) observed 57.2 ppm (AW) of Tl in ferns, 0.11–0.42 ppm (AW) in mosses and 0.264 ppm (AW) in birch in the Au-Hg-Tl mineralized area in Southwest Guizhou, China. Both of these studies showed thallium in certain plants is an ideal indicator for gold exploration.

According to Edwards et al. (1995) and Sager (1998), green cabbage, turnip-rooted cabbage (kohlrabi) and rape accumulated significant amounts of Tl even from soils with low Tl status, whereas the Tl contents of bush beans and rye grass increased only

marginally. For all vegetables investigated, leaves contained much thallium than the roots. The high accumulation of thallium by food crops, particularly brassicaceous plants, was also observed by Kurz et al., 1997. Therefore, rape and cabbage with a high Tl-accumulating ability are not recommended to be planted within a Tl-polluted area. In Germany, a soil Tl content of 1 ppm (DW) was recommended as the tolerable margin, while in Switzerland, this was doubled to 2 ppm total Tl as the recommended maximum for agricultural soils. As for the fresh fruits and vegetables, a Tl tolerance level of 0.1 ppm (fresh weight) was also suggested in Germany. In vegetables tested for several years on the same polluted soils, Tl contents declined from year to year, probably due to the decline of the Tl mobility in the soils. On the other hand, even for strongly accumulating green plants, depletion of the soil by plant growth is too low to achieve sanitation of heavily polluted sites (Sager, 1998).

High accumulation of thallium in some specific plants has interested many scientists. Brooks and Robinson (1998) defined such specific plants as hyperaccumulators. Both *Biscutella laevigata* and *Iberis intermedia* from Les Malines in southern France containing very high levels of Tl up to 1.4% (DW) in *Biscutella* and 0.4% (DW) in *Iberis* are suggested as the typical accumulators of thallium (Anderson et al., 1999; Leblanc et al., 1999; Brooks et al., 1998). These authors also suggested that these thallium accumulators can be used for phytomining for thallium in thallium-rich soils and mine tailings as well as for the soil remediation. The specific food crops with high thallium-accumulation properties such as green cabbage and rape (Lehn and Schoer, 1987; Kurz et al., 1997, Edwards et al., 1995; Sager, 1998) may also be regarded as high accumulators of thallium

in food crops. It is important to identify the thallium accumulators in food crops, because the high thallium in such accumulators can easily enter the food chain and introduce toxicity to human health.

4.4.3. Summary

Thallium is one of the most toxic metals and can cause toxicity to organisms.

Tl follows K distribution pathways and inhibits a number of K-dependent processes. Various K^+–dependent proteins are well known to posses a higher affinity for Tl^+ than K^+. The combination of rapid, diffuse alopecia, and neurologic and gastrointestinal disturbance is pathognomonic for most thallium toxicity. The presence of elevated Tl levels in the urine or other biologic materials confirms the diagnosis of Tl poisoning.

Thallium is widely distributed in plants but depends on the species-specific plants and the concentrations of thallium in soils where the plants are growing. Plants contain higher thallium from thallium-rich soils. However, some specific plants pronouncedly accumulate more thallium than others. Some thallium hyperaccumulators may accumulate extremely high level of thallium (1% DW), and can be used for phytomining and soil reclamation. The high thallium-accumulating plants in food crops, such as green cabbage and rape, have an important environmental significance, since thallium can be transferred from the food chain to affect the health of humans.

Table 4-1 Ionic radii of thallium and some other metals

Ions	Radii (A)		
	Coordinated number		
	6	8	12
Tl^{3+}	0.885	0.98	
Tl^{+}	1.5	1.59	1.7
K^{+}	1.38	1.51	1.64
Rb^{+}	1.52	1.61	1.72
Na^{+}	1.02	1.18	1.39
Ba^{2+}	1.35	1.42	1.61
Sr^{2+}	1.18	1.26	1.44
Ca^{2+}	1	1.12	1.34
Zn^{2+}	0.74	0.9	
Ag^{+}	1.15	1.28	
As^{3+}	0.46		
As^{5+}	0.46		
Hg^{+}	1.02	1.19	
Hg^{2+}	1.02	1.14	
Pb^{2+}	1.19	1.29	1.49
Ce^{3+}	1.01	1.143	1.34
Ce^{4+}	0.87	0.97	1.14
Bi^{3+}	1.03	1.17	

Source: Shannon, 1976

Table 4-2 Average thallium content (ppm) in common igneous rocks

Ultramafic rocks	Mafic rocks	Intermediate rocks	Granitic rhyolitic rocks	Syenite	Alkalic rocks	Reference
0.06	0.12	0.15	3.2	1.4	–	Shaw (1952, 1957)
0.06	0.21	–	0.72 (high-Ca)	1.4	–	Turekian and Wedepohl (1961)
–	–	–	2.3 (low-Ca)			Turekian and Wedepohl (1961)
–	0.11	–	0.73	–	–	Brooks and Ahrens (1961)
0.05	0.1		0.75	0.3	–	Taylor (1964, 1966)
0.05	0.18	0.55	1.7	–	1.2	De Albuquerque and Shaw (1971)

Table 4-3 Abundance of Tl in selected metamorphic rocks

Rocks	**Locality**	**Tl (ppm)**	**Reference**
Phyllite	Clove Quadr., New York	0.56-0.66	Shaw (1952)
Phyllite	Swiss Alps	0.8	Heinrichs et al., 1980
Schist	Sayan Mountains, U.S.S.R.	2	Slepnev (1961)
Quartz-sericite schist	Maykan, North Kazakhstan	0.16	Kurbanayev (1966)
Garnet schist	Clove Quadr., New York	0.61-1.3	Shaw (1952)
Mica schist	Swiss Alps, France and Namibia	0.74	Heinrichs et al., 1980
Aluminous silicates rocks (schists, slates, etc.)	Canadian Shield	0.48	Heinrichs et al., 1980
Gneiss	Oki Island, Japan	0.6-0.9	De Albuquerque and Shaw, 1971
Gneiss	Norway,Austria, France, Switzerland, Germany and Guyana	0.74	Heinrichs et al., 1980
Dioritic gneiss	Albany Co., Wyoming	0.42	Shaw (1952)
Granet gneiss	N. Isortog, Greenland	0.25	Shaw (1952)
Amphibolite	Impilahti, K.F.S.S.R.	0.4	Shaw (1952)
Eclogite	Nodule, Kimberley, South Africa	0.56	Brooks and Ahrens (1961)
Granulites, charnockites (salic)	Norway,U.S.A., Tanzania, Canada, India and Guyana	0.38	Heinrichs et al., 1980
Granulites, charnockites (intermediate mafic)	Austria, Norway, India, Tanzania, Guyana and U.S.A.	0.08	Heinrichs et al., 1980

Table 4-4 Abundance of thallium in common sedimentary rocks

Rocks	Locality	Tl (ppm)	Reference
Sandstone	Huvitas, Finland	1.3	Shaw, 1952
Sandstone	Germany and France	0.21	Heinrichs et al., 1980
Siltstone	Caucasus, U.S.S.R.	0.68	Voskresenskaya et al., 1962
Siltstone	Germany, France and Japan	0.42	Heinrichs et al., 1980
Siltstone	Southwest Guizhou, China	0.68-1.55	Chen et al., 1996
Graywacke	North America	0.13-0.21	Shaw, 1952
Graywacke	Germany and France	0.205	Heinrichs et al., 1980
Clay	Finland, U.S.S.R. and U.S.A.	0.24-0.70	Shaw, 1952
Clay	Yashma-More Region, U.S.S.R.	2.0-3.0	Nuriyev and Dzhabbarova, 1973
Sandy clay	Yashma-More Region, U.S.S.R.	1.0-1.6	Nuriyev and Dzhabbarova, 1973
Argillite	Michigan, U.S.A.	1.4	Shaw, 1952
Slate	Bagle Bridge, New York	0.81	Shaw, 1952
Shale	South Africa and New York	0.12-0.50	Shaw, 1952; Brooks et al., 1960; Brook and Ahrens, 1961
Shale	Grermany, France and Portugal	0.68	Heinrichs et al., 1980
Shales, black	Germany	2.54	Heinrichs et al., 1980
Shales, dark	Germany, Spain and Poland	0.84	Heinrichs et al., 1980
Anthraxolite	Ontario	2.8	Shaw, 1952
Argillaceous limestone	Caucasus, U.S.S.R.	0.7	Voskresenskaya et al., 1962
Loess	Illinois, U.S.A.	0.31	Shaw, 1952
Calcareous rocks	Canadian Shield	0.1	Heinrichs et al., 1980
Limestone, argillaceous	Germany and U.S.A.	0.195	Heinrichs et al., 1980
Limestone	Germany and France	0.05	Heinrichs et al., 1980
Limestone	Gissar range	0.44-0.63	Valiyev et al., 1984
Limestone	Southwest Guizhou, China	0.50-0.70	Chen et al., 1996
Dolomite	Lengenbach, Switzerland	0.45	Hoffmann and Knill, 1996

Table 4-5 Significant correlations of Tl, Pb, Bi and Rb in common rocks (Heinrichs et al., 1980)

		Tl	Rb	Pb	Bi
(a) Ultramafic and mafic rocks					
	*1	Pb	K	Tl	Pb
	2	Bi	Pb	K	Tl
	3	K		Bi	
				Rb	
(b) Granitic and gneissic rocks					
	1	Pb	Pb	Rb	Tl
	2	Bi	K	Tl	
	3	Rb	Tl	K	
(c) Sedimentary rocks					
	1	K	K	Bi	K
	2	Illite	Illite	Zn	Rb
	3	Bi	Tl	Illite	Illite
	4	Rb	Bi	Chlorite	Tl
	5			K	Zn
	6				Pb

*Increasing numbers indicating the order of decreasing coefficients of correlation; level of confidence 95%

Table 4-6 abundance of thallium in deep ocean sediments

Rocks	Locality	Tl (ppm)	Reference
Pelagic clay	Atlantic Ocean	1.07	Heinrichs et al., 1980
Pelagic clay	Pacific Ocean	1.3	Heinrichs et al., 1980
Pelagic clay	Pacific Ocean	0.96	Marowsky and Wedepohl, 1971
Calcareous ooze	Atlantic Ocean	0.43	Heinrichs et al., 1980
Calcareous ooze	Pacific Ocean	0.15	Heinrichs et al., 1980
Fe-Mn-rich ooze	Pacific Ocean	0.3	Shaw, 1952
Ridge and basal sediments	Atlantic Ocean	0.5	Heinrichs et al., 1980
Mn nodules	Atlantic Ocean	140	Ahrens et al., 1967
Fe-Mn nodules	Pacific Ocean	123	Iskowitz et al., 1982
Fe-Mn nodules	Atlantic Ocean	106	Iskowitz et al., 1982
Fe-Mn nodules	Indian Ocean	82	Iskowitz et al., 1982

Table 4-7 Average abundance of Tl, K and Rb in crustal units and the upper mantle (Heinrichs et al., 1980)

	K(%)	Rb (ppm)	Tl (ppb)	K/Rb	K/Tl ($x10^4$)
Sedimentary rocks	1.77	100 (90-110)	413 (370-480)	177	4.28
Magmatic rocks in upper continental crust	3.07	197	980	156	3.14
Metamorphic rocks in upper continental crust	2.13	97	592	220	3.6
Upper continental crust	2.52	142	749	177	3.36
Lower continental crust	1.85	54	232	342	7.96
Continental crust (average)	2.19	98	491	223	4.46
Canadian shield (Shaw et al., 1967,1976)	2.57	110	520		
Continental crust (Taylor, 1964)	2.09	90	450		
Upper mantle	0.04	1.2	11	298	3.25

Table 4-8 Concentration of thallium in ores from mineral deposits

Sulfides	Deposit	Tl (ppm)	Reference
Galena	Zolotoi Kurgan polymetallic deposit, Caucasus	74-112	Voskresenskaya, 1961
Galena	Polymetallic deposits, E. Transbaikaliya, U.S.S.R.	10-50000	De Albuquerque and Shaw, 1971
Sphalerite	Belgium, Westphalia, Silesia	100-1000	Shaw, 1957
Realgar	Lojane, Yugoslavia	100-1000	Jankovic, 1989
Realgar	Allchar, Yugoslavia	300->1%	Jankovic, 1989
Realgar	Smrdlive, Yugoslavia	10-250	Jankovic, 1989
Realgar	Nanhua, China	90-1800	Zhang et al., 1996
Realgar	Yata, China	1.16	Zhang et al., 1996
Pyrite	Sukhumi, Caucasus	210	De Albuquerque and Shaw, 1971
Hydrothermal pyrite	Latium, Italy	0.2-7.3	Calderoni et al., 1985b
Volcanic pyrite	Latium, Italy	9.0-28.0	Calderoni et al., 1985b
Mean for pyrite-marcasite from Dicthyonema shales	Russian platform	5.0-30.0	Voskresenskaya, 1969
Mean for pyrite from limestones and dolomitic marls	Russian platform	0.0-10.0	Voskresenskaya, 1969
Mean for pyrite from marls	Crimea	0-2.5	Voskresenskaya, 1969
Mean for sulfides from carbonate rocks in tectonic zones	Russian platform	4.0-160.0	Voskresenskaya, 1969
Mean for marcasite from black clays	Russian platform	0.0-5.0	Voskresenskaya, 1969
Weighted mean for pyrite from clay rocks	Caucasus	0.0-11.0	Voskresenskaya, 1969
Weighted mean for pyrite from sandstones	Caucasus	0.6-2.2	Voskresenskaya, 1969
Marcasite	Hanaoka, Japan	1250	De Albuquerque and Shaw, 1971
Marcasite	Verkhnyaya Kvaisa, Caucasus	56-64	Voskresenskaya and Karpova, 1958
Chalcopyrite	Sadon polymetallic deposit, Caucasus, U.S.S.R.	0.8	Voskresenskaya, 1961
Cinnabar	Mercury-arsenic deposit, Caucasus	0.4	Voskresenskaya, 1961
Stibnite	Ferberite-stibnite deposit, Caucasus	0.2-0.3	Voskresenskaya, 1961
Berthierite	Ferberite-stibnite deposit, Caucasus	10	Voskresenskaya, 1961
Enargite	Shimokita, Japan	560	De Albuquerque and Shaw, 1971

Table 4-8 (continued)

Sulfides	Deposit	Tl ppm)	Reference
Boulangerite	Eastern Transbaikaliya, U.S.S.R.	10-1000	De Albuquerque and Shaw, 1971
Jamesonite	Eastern Transbaikaliya, U.S.S.R.	10-100	De Albuquerque and Shaw, 1971
Thallium-jordanite	Eastern Transbaikaliya, U.S.S.R.	0.0156	De Albuquerque and Shaw, 1971
Pyrolusite	Eastern Kradzhal, U.S.S.R.	2.4-5.0	De Albuquerque and Shaw, 1971
Psilomelane	Dzhesda deposit, Central Kazakhstan	20-300	De Albuquerque and Shaw, 1971
Psilomelane	Eastern Transbaikaliya, U.S.S.R.	320-1000	De Albuquerque and Shaw, 1971
Geothite	Daraiso Pb-Zn deposit, U.S.S.R.	100	De Albuquerque and Shaw, 1971
Hydrogoethite	Sarykan deposit, U.S.S.R.	5-14	De Albuquerque and Shaw, 1971
Hydrous iron oxides	Kurgashinkan deposit,E. Transbaikaliya, U.S.S.R.	3-85	De Albuquerque and Shaw, 1971
Mn-rich limonite	Polymetallic deposit, E. Transbaikaliya, U.S.S.R.	10-50	De Albuquerque and Shaw, 1971
Mn-hydroxides	Lachin-Khana polymetallic deposit, U.S.S.R.	40-95	De Albuquerque and Shaw, 1971
Thallium-jarosite	Daraiso Pb-Zn deposit, U.S.S.R.	1.75-2.04%	De Albuquerque and Shaw, 1971
Plumbojarosite	Kurgashinkan deposit,E. Transbaikaliya, U.S.S.R.	3.7-4.7	De Albuquerque and Shaw, 1971
Jarosite	Lachin-Khana polymetallic deposit, U.S.S.R.	1-40	De Albuquerque and Shaw, 1971
Blac cerussite	kummyshtan Pb-Zn deposit, U.S.S.R.	10-20	De Albuquerque and Shaw, 1971
Chalcanthite	Lachin-Khana polymetallic deposit, U.S.S.R.	2	De Albuquerque and Shaw, 1971
Cuprohalloysite	Lachin-Khana polymetallic deposit, U.S.S.R.	12	De Albuquerque and Shaw, 1971
Hydrothermal precipitates	Rotokawa, New Zealand	200-5000	Krupp and Seward, 1987
Red amorphous sulfides	Rotokawa, New Zealand	80-90	Krupp and Sweard, 1987
Hydrothermal precipitates	Rotokawa, New Zealand	200-5000	Krupp and Seward, 1987
Red amorphous sulfides	Rotokawa, New Zealand	80-90	Krupp and Seward, 1987

Table 4-9 List of known thallium minerals

Thallium minerals	Formula	Rfs.	Thallium minerals	Formula	Rfs
Avicennite	Tl_2O_3	1	Lorandite	$TlAsS_2$	1
Berardite	$Tl(As,Sb)_5S_8$	2	Monsmedite	$H_8K_2Tl_2(SO4)_8{\cdot}11H_2O$	1
Bukovite	$Tl(Cu,Fe)_2Se_2$	1	Parapierrotite	$TlSb_5S_8$	1
Carlinite	Tl_2S	1	Perlialite	$K_8TlAl_{12}Si_{24}O_{72}{\cdot}20(H_2O)$	11
Chabourneite	$(Tl,Pb)_5(Sb,As)_{21}S_{34}$	1	Picotpaulite	$TlFe_2S_3$	1
Chalcothallite	$Tl_2(Cu,Fe)_6SbS_4$	1	Pierrotite	$Tl_2As_4Sb_6S_{16}$	1
Criddleite	$TlAg_2Au_3Sb_{10}S_{10}$	2	Raguinite	$TlFeS_2$	1
Christite	$TlHgAsS_3$	1	Rathite	$(Pb,Tl)_3As_5S_{10}$	1
Crookesite	$(Cu,Tl,Ag)_2Se$	1	Rayite	$Pb_8(Ag,Tl)_2Sb_8S_{21}$	1
Cuprostibite	$Cu_2(Tl,Sb)$	1	Rebulite	$Tl_5As_8Sb_5S_{22}$	1
Dorallcharite	$(Tl,K)Fe_3^{3+}(SO_4)_2(OH)_6$	3	Rohaite	$TlCu_5SbS_2$	1
Dufrenoysite	$(Pb,Tl)As_5S_5$	4	Routhierite	$TlHgAsS_3$	1
Edenharterite	$TlPbAs_3S_8$	5	Sabatierite	Cu_6TlSe_4	1
Ellisite	Tl_3AsS_3	1	Scleroclase	$(Pb,Tl)As_2S_4$	4
Erniggliite	$Tl_2SnAs_2S_6$	6	Simonite	$TlHgAs_3S_6$	1
Fangite	Tl_3AsS_4	7	Stalderite	$(Tl,Cu)(Zn,Fe,Hg)AsS_3$	12
Galkhaite	$(Hg,Cu,Zn,Tl)(As,Sb)S_2$	1	Thalcusite	$Tl_2Cu_3FeS_4$	1
Gillulyite	$Tl_2(As,Sb)_8S_{13}$	8	Thalfenisite	$Tl_6(Fe,Ni,Cu)_{25}S_{26}Cl$	1
Hatchite	$PbAgTlAs_5S_9$	1	Vaughanite	$TlHgSb_4S_7$	2
Hutchinsonite	$PbTlAs_5S_9$	1	Vrbaite	$Tl_4Hg_3Sb_2As_8S_{20}$	1
Imhofite	$Tl_{5.6}As_{15}S_{25.3}$	1	Wallisite	$(Cu,Ag)PbTlAs_2S_5$	1
Jankovicite,	$Tl_5Sb_9(As,Sb)_4S_{22}$	9	Weissbergite	$TlSbS_2$	1
Jentschite	$TlPbAsSbS_6$	10			

References: 1.Sobbot et al., 1987; 2. Nriagu, 1998; 3. Balic Zunic et al., 1994; 4. Jankovic, 1989; 5. Graeser et al., 1992a; 6. Graeser et al., 1992b; 7. Wilson et al., 1993; 8. Wilson et al., 1991; 9. Cvetkovic et al., 1995; 10. Jambor et al., 1997; 11. Artioli and Kvick, 1990; 12. Jambor and Burke, 1993

Table 4-10 List of famous thallium deposits in the world

Deposit	Locality	Occurring Tl minerals	Paragenous association of sulfides	References
Allchar	Macedonia, Yugoslavia	parapierrotite, lorandite, vrbaite, rebulite, simonite	pyrite, marcasite, arsenopyrite, stibnite, realgar, orpiment	Sobott et al., 1987; Jankovic, 1989; Rieck, 1993; Percival and Radtke, 1994
Lengenbach	Wallis, Switzland	hutchinsonite, imhofite, lorandite, wallisite, hatchite, rathite	pyrite, sphalerite, galena, arsenopyrite, realgar, orpiment	Sobott et al., 1987; Hofmann, 1994; Hofmann and Knill, 1996;
Carlin	Nevada, USA	lorandite, ellisite, christite, galkhaite	realgar, orpiment, cinnabar	Radtke et al., 1977; Ikramuddin et al., 1986; Sobott et al., 1987; Percival and Radtke, 1993;
Jas Roux	France	pierrotite, parapierrotite, routhierite, chabourneite	pyrite, sphalerite, stibnite, realgar, orpiment	Johan and Mantienne, 1976; Johan et al., 1981; Sobott et al., 1987
Verkhnyaya Kvaisa	Caucasus, USSR	hutchinsonite	pyrite, sphalerite, galena, orpiment	Voskrenskaya and Karpova, 1958; Voskresenskaya ; 1961; Sobott et al., 1987;
Lanmuchang	Guizhou, China	Lorandite, christite	pyrite, cinnabar, realgar, orpiment	Chen, 1989a,b; Li, 1996

Table 4-11 Distribution of thallium in coals

Coal	**Locality**	**Tl (ppm)**	**Reference**
Coal	Central Asia	0.3-1.5	De Albuquerequeand Shaw, 1971
Coal	Worldwide	<0.2-1	Swaine, 1990
Pyrites in Coal	Central Asia	34	Bouska, 1981
Pyrites in Coal	Moscow Basin	3.3	Bouska, 1981
Pyrites in Coal	Transcarpathian Basin	11	Bouska, 1981
Coal	Virginia	0.51-2.8	Henderson et al., 1985
Coal	Illinois Basin	0.12-1.3	Gluskoter et al., 1977
Coal	Eastern U.S.A.	<0.3-2.2	Zubovic et al., 1980
Coal	Switzerland	<0.2-3	Hugi et al., 1993
Coal	United Kingdom	0.6-1.7	Swaine, 1990
Coal	Australia	<0.6-3	Swaine, 1990
Coal	Germany	0.01-0.60	Swaine, 1990
Coal	Coal New-Zealand	0.6-6.7	Swaine, 1990
Coal	Guizhou, China	0.10-0.73	Feng et al., 1999
Coal	Liupanshui, China	0.12-0.62	Zhuang et al., 1999
Coal	Datong, China	0.15-0.54	Zhuang et al., 1999
Coal	Pingsuo, China	0.28-0.88	Zhuang et al., 1999

Table 4-12 Electrochemical properties of thallium (Downs, 1993b)

Reaction	Standard electrode potential (V, 25° C)
$Tl^{+} + e = Tl$	−0.336
$Tl^{3+} + 2e = Tl^{+}$	+1.25
$Tl(OH)_3 + 2e = TlOH + 2OH^{-}$	−0.05

Table 4-13 Estimated mean composition (mg/l) of some selected natural water bodies*

Dissolved constituent	Groundwater	River water	Eutrophic lake water	Bog water	Seawater
Ca	59	15	40	0.2	422
Mg	26	4.1	10	0.19	1322
Na	22	6.3	9	1.5	11020
K	4	2.3	2	0.31	408
Tl^+	0.00725	0.00002	0.00002	0.00002	0.000013
CO_3	266	57	122	0.06	145
SO_4	108	11	24	0.53	2775
Cl	11	7.8	9	0.99	19805
F	0.1	1	1	0.1	1.4
NO_3	39	1	3.4	1	0.3
PO_4	0.1	0.0767	0.6	0.0767	0.0614
H_4SiO_4	48	20.8	2	20.8	4.4
Organic carbon	0.7	5.0	10.0	30.0	0.5
pH	7.14	8.01	7.70	3.60	8.22

*Data from Kaplan and Mattigod, 1998

Table 4-14 Distribution of Tl^+ species (% of total) in selected natural water bodies*

Aqueous species	Groundwater	River water	Eutrophic lake water	Bog water	Seawater
Tl^+	90.4	82.7	76.8	32.4	51.9
$TlHCO_3^0$	4.4	1.2	2.0	–	0.5
$TlCO_3^-$	–	–	–	–	0.1
$TlSO_4^-$	3.6	0.4	0.8	–	11.2
$TlCl^0$	0.1	0.1	0.1	–	30.7
$Tl(Cl)_2^-$	–	–	–	–	5.4
Tl–Fulvate^0	1.4	15.6	20.3	67.6	0.2

* Concentrations of $TlOH^0$, TlF^0, $TlNO_3^0$, $TlH_2PO_4^-$, $TlHPO_4^-$ and $TlPO_4^{2-}$ species were negligible in all system; source: Kaplan and Mattigod, 1998

Table 4-15 Concentration of thallium in natural waters

Water	Concentrations (µg/l)	Reference
Seawater	0.012-0.016	Flegal and Patterson, 1985
Seawater	0.0094-0.0164	Matthews and Riley, 1970
Pacific Ocean surface	0.013	Batley and Florence, 1975
Groundwater	0.001-0.250	Banks et al., 1995; Frengstad et al., 2000
Groundwater	0.003-0.006	Calderon et al., 1985a
Groundwater in petroleum deposits	0.7-2.1	Nuriyev and Dzhabbarova, 1973
Great Lake water	0.001-0.036	Cheam et al., 1995; Lin and Nriagu, 1999
Lake water	2.1-23.1	Mathis and Kevern, 1975
River water	1-80	Zitko et al., 1975
Tap water	0.12-0.18	De Ruck et al., 1988
Groundwater	0.0175	De Ruck et al., 1988
Spring water	0.064-0.155	
Ottawa River water	0.006	Hall et al., 1996
Groundwater	0.28-0.4	Stetzenbach et al., 1994
Seawater	0.0148-0.0175	Riley and Siddiqui, 1986
Arctic snow	0.0000003-0.0000009	Cheam et al., 1996
Rhine River water	0.715	Cleven and Fokkert, 1994
Several German rivers	0.002-0.040	Schoer, 1984
Tap water (Poland)	0.0051-0.0238	Lukaszewski et al., 1996
River water	0.0051-0.071	Lukaszewski et al., 1996
Lake water	0.0085	Lukaszewski et al., 1996
Baltic Sea	0.612	Lukaszewski et al., 1996
Stream water	0.11	Magorian et al., 1974
Thermal and stream water (Italy)	0.001-0.006	Dall'Aglio et al., 1994
Thermal and stream water (Italy)	0.102-0.550	Dall'Aglio et al., 1994
Groundwater in Volcano Island	1.264	Dall'Aglio et al., 1994
Hot springs (New Zealand)	7	Weissberg, 1969
Mining waste water	23	Schoer, 1984
Mining waste water	88.3	Zitko et al., 1975
Smelting waste water	800	Schoer, 1984
Oil drill, waste water	672	Schoer, 1984
Groundwater of zinc smelter	810	Schoer, 1984

Table 4-16 Distribution of thallium in various soils

Soil	Locality	Thallium (µg/g)	References
Surface Soils	United States	0.02-2.8	Smith and Carson, 1977
Soils (over sphalerite veins)	United States	5	Smith and Carson, 1977
Garden soils	Holland Marsh, Canada	0.17-0.22	Chattopadhyay and Jervis, 1974
Topsoil	Poland	0.014-0.405	Kabata-Pendias and Pendias, 1992
Soil	Austria	0.076-0.91	Sager, 1998
Soil	China	0.292-1.172	Qi et al., 1992
Soil (uncontaminated)	Baden, Germany	0.1-2.2	Sager, 1998
Soil (near old mines and cement factory)	Baden, Germany	0.1-73	Sager, 1998
Soil	Saskatchewan, Canada	0.25-0.71	Mermut et al., 1996
Soil	Scotland	0.1-0.8	Ferguson, 1990
Soil	Russia	1.5-3.0	Il'in et al., 2000
Soil	Great Britain	0.03-0.99	Fergusson, 1990
Arable Soil	France	0.13-1.54	Tremel et al., 1997
Soil in rural areas	France	1.54-55	Tremel et al., 1997
Soil (within a As-Tl mineralized area)	Yunnan, China	0.08-3.6	Zhang et al., 1998
Soil	Switzerland	0.121	Tremel et al., 1997
Soil	World	0.200	Bowen, 1979

Table 4-17 Distribution of thallium in various plants

Plants	Locality	Thallium (ppm)*	Reference
Carrot	Non-contaminated area, Germany	0.02-0.25	Schoer, 1984
Red cabbage	Non-contaminated area, Germany	0.04	Cited from Schoer, 1984
Lettuce	Non-contaminated area, Germany	0.021	Schoer, 1984
Kale	Non-contaminated area, Germany	0.125	Cited from Schoer, 1984
Plants	World	0.03-0.3	Bowen, 1979
Cabbage	Near a cement factory, Germany	45	Allus et al.,1987
Cereal grain	Near a cement factory, Germany	9.5	Allus et al.,1987
Hay		0.02-0.025	Smith and Carson, 1977
Cabbage		0.04-0.125	Ferguson, 1990
Potato		0.025-0.03	Ferguson, 1990
Pine		2-100 (AW)	Ferguson, 1990
Grasses	Russian	0.02-1.0	Dvornikov et al., 1976
Edible plants		0.02-0.125	Smith and Carson, 1977
Linaria triphylla	Alsar deposits, Yugoslavia	3000-3800 (AW)	Zyka, 1971
Green plants	Baden, Germany (Near a cement factory)	0.02-0.08	Sager, 1998
Green plants	Old mining sites	0.1-3.5	Sager, 1998
Mushroom	Europe	<0.25-5.5	Sager, 1998
Mushroom	Japan	0.001-0.34	Sager, 1998

Table 4-17 (continued)

Plants	Locality	Thallium (ppm)*	Reference
Cabbage	Nanhua, China (As-Tl mineralized area)	1.026	Zhang et al., 1998
Fern	Nanhua, China (As-Tl mineralized area)	2.526-4.641	Zhang et al., 1998
Moss	Lanmuchang, China	0.11-0.42 (AW)	Chen et al., 1999
Fern	Yanjiawan-Lanmuchang, China	57.2 (AW)	Chen et al., 1999
Birch	Lanmuchang, China	0.264 (AW)	Chen et al., 1999
Fir,spruce, pine	Highland Valley, British Columbia	0.071 (AW)	Warren and Horsky, 1986
Biscutella laevigata (leaves)	Les Avinières, France	244-308	Leblanc et al., 1999
Iberis intermedia (leaves)	Les Avinières, France	47-3070	Leblanc et al., 1999
Silence cucubalus	Les Avinières, France	34	Leblanc et al., 1999
Brassica napus	Carnoulès, France	1197	Leblanc et al., 1999

* All concentrations are DW except where indicated (DW= Dry Weight; AW=Ash weight)

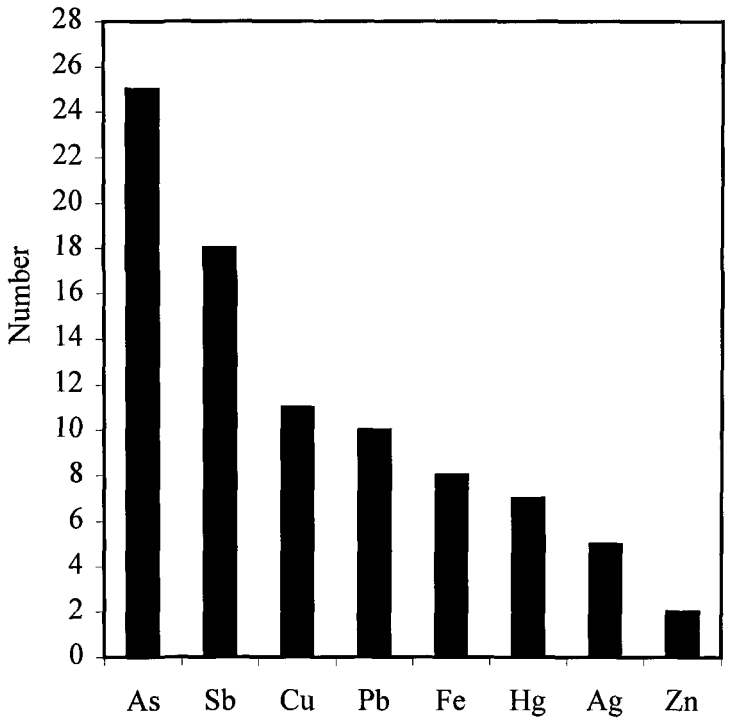

Fig. 4-1 Frequency distribution of metals associated with Tl in Tl-bearing minerals (number of counted minerals: 45; see Table 4-9)

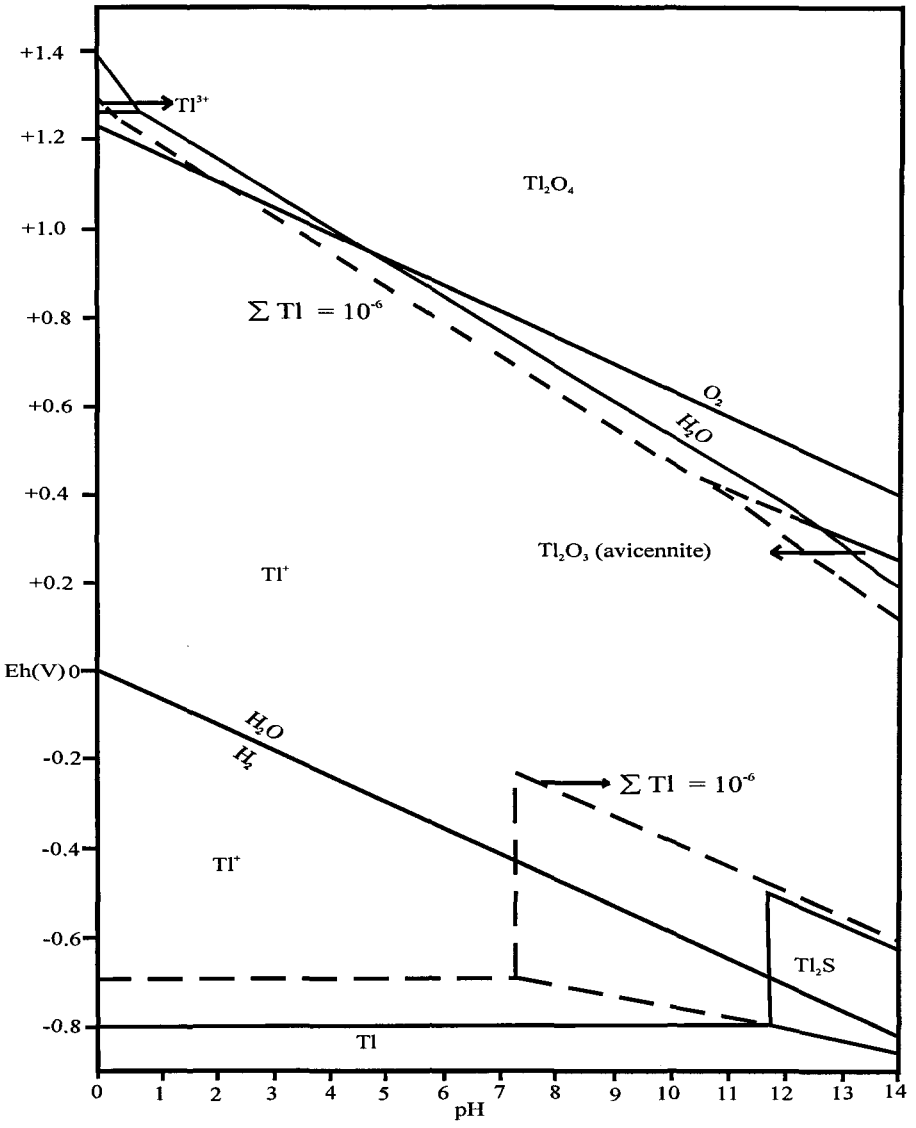

Fig. 4-2 Eh-pH diagram for the system Tl-S-O-H— "normal area".
(Activity for total dissolved thallium species: 10^{-8} M (contoured for 10^{-6} M).
Activity of total dissolved sulfur species 10^{-3} M (after Vink, 1993))

CHAPTER 5

OCCURRENCE OF THALLIUM IN THE LANMUCHANG AREA

5.1 Sampling patterns

Field work was undertaken between October 1998 and November 1999. The samples collected in the Lanmuchang area and the background area (see section 1.2) include rocks, soils, sediments, waters, vegetables and cereals. The overall strategy of the sampling was to quantify the occurrence and spatial distribution of thallium and other toxic metals in various materials in the ecosystem. The objective was to track the dispersion of thallium through both the natural geochemical, and biogeochemical processes and anthropogenic activities, affecting the environmental behavior of toxic metals derived from the mineral deposit and its mining wastes.

Water sampling was carried out using the Geological Survey of Canada-approved protocols. Onsite measurements comprised pH, electric conductance (a measure of the total dissolved solids), temperature, and dissolved oxygen. Solid sampling includes country rocks, ores, precipitates on adit walls, waste piles and outcrops, soils, sediments, vegetables, cereals and some wild cabbages and fern. Laboratory analyses were carried out using a variety of techniques to determine mineralogical and chemical compositions of sampled materials.

The sampling patterns for rocks, soils, sediments, waters and vegetations in the Lanmuchang area are represented by plotting the sampling sites on topographical maps. All the samples were collected in different locations within the Hg-Tl mineralized area, that is within, close to and outside the mineralized area. The samples associated with mining or not were also discriminated when sampling in the field. The sampling pattern reflects the topographical and hydrological characteristics (e.g. hill top versus low area versus slope, upstream versus downstream, and dry season versus rainy season, etc.) related to the thallium-mineralization, either in a sequential or random pattern.

The detailed information on sampling protocols, treatment and analytical methods for the rocks, soils, sediments, waters and vegetations are described in the Appendix.

5.2 Lithological distribution of thallium

5.2.1 Bulk-rock geochemistry and trace element features

41 samples of sedimentary rocks, Tl-As-Hg ores and coals were collected from outcrops and underground sites in the Lanmuchang area to document the geochemical affinities of host rocks and ores, and to delineate the variations in major elements with respect to thallium mineralization and the dispersion characteristics of thallium and other trace metals in the study area (Fig. 5-1). Note that the host rocks in the Lanmuchang mineralized area are all hydrothermally altered and are defined in this study as altered host rocks and, for those exposed to the surface, as outcropped host rocks. The rocks from the background area are unaltered country rocks.

The results of major element analysis are listed in Table 5-1. Based on the comparison with the North American Shale Composition (Gromet et al., 1984) and the average composition of upper crust (Condie, 1993), the non-carbonate host rocks and ores in the Lanmuchang Hg-Tl mineralized area are depleted in alkali metals, MnO, CaO and MgO. The depletion of alkali metals is a reflection of the paucity of silicates in the study area, but the K_2O is slightly higher than Na_2O due to the occurrence of K-rich clay minerals as a result of kaolinization. The CaO and MgO are much higher in unaltered country rocks than in altered host rocks and ores, and the CaO dominates the MgO in unaltered country rocks, but is slightly lower than MgO in altered host rocks and ores. This is probably due to intensive decalcification, as the carbonate rocks (mainly limestones) are one of the main host rocks.

As for the total Fe, it is relatively rich in claystone and siltstone, and much richer in thallium ores than in mercury and arsenic ore. This may imply that pyritization also follows thallium mineralization. The Al_2O_3 shows the same distribution as total Fe, but it is relatively enriched in mercury ores. The variation of TiO_2 and P_2O_5 are not obvious. The SiO_2 content is high in the host rocks and ores, indicating silicification during thallium mineralization.

The host rocks and ores in the Lanmuchang Hg-Tl mineralized area have relatively high values for loss on ignition (LOI) and sulfur. The high LOI characterizes the limestone rocks containing high carbonate C, sulfide ores containing high sulfur, and coals and sulfide ores containing high organic C. Especially in the ores and altered host rocks, the

LOIs are probably due to organic matter, since the ores and host rocks are dark gray to black in color. The high sulfur results from the abundance of sulfide minerals.

The results of trace elements analysis are listed in Table 5-2. Based on the comparison to the shale, the average composition of upper crust or crust (Gromet et al., 1984; Condie, 1993; Taylor, 1964; Turekian and Wedepohl, 1961) and the background values (this study), the elements Tl, Hg, As, W and Ba are enriched, while Cu, Pb, Zn, Sb, Cd, Co, Ni, Cr, Sn, V and Mo show similar concentrations. The concentrations of the above metals indicate that Tl, Hg and As are the main components of mineralization and the base metals are poorly represented in the mineralized area. This is also in accordance with the abundance of sulfide minerals such as lorandite, realgar, orpiment and cinnabar and sparse base metal sulfides. Ba is highly enriched in the altered host rocks and ore relative to the unaltered country rocks, indicating an association of barite with mineralization. Compared with the unmineralized country rocks in the background area, the host rocks/ores and secondary minerals in the Lanmuchang area show high enrichments of Tl, Hg and As. The enrichment in ores are 22763-fold for Tl, 7387-fold for Hg, 10211-fold for As, 300-fold for W and 100-fold for Ba. Tl, Hg and As are the elements with potential for negatively affecting the environment and hence require particular attention (Fergusson, 1990).

5.2.2 Distribution of Tl in rocks and ores

The average distribution of thallium, mercury and arsenic in various rocks and ores are listed in Table 5-3.

According to the distribution patterns, the sulfide assemblage of thallium, mercury and arsenic is the carrier of thallium in the primary ores. The average thallium concentration is up to 1.34% in thallium ores, the maximum being 3.5%. The principal ore mineral in Tl ore is lorandite, although other ore minerals such as As sulfides (realgar and orpiment) often are represented in various amounts. The mercury ore and arsenic ore also contain thallium up to 208 ppm and 650.5 ppm, respectively. Coal occurring in the Hg-Tl mineralized area is also highly rich in thallium. Thallium in coals is enriched up to 29 ppm, clearly much higher than in coals of China and worldwide as listed in Table 4-11. The secondary minerals contain pronouncedly high contents of thallium with an average of 405 ppm. The highest value 1100 ppm was determined from the mineral association quartz, pyrite, marcasite and realgar (sample R198). In the altered host rocks, the concentration of thallium is up to 152 ppm, quite similar to the thallium average level of 110 ppm in mercury ores determined in the regional geological survey (Guizhou Geological Bureau, 1960). The host rocks collected from the outcrops in the Lanmuchang mineralized area, contain 6-330 ppm of thallium, and the high value is related to the occurrence of secondary minerals in fractures. As for mine tailings on the ground surface resulting from underground mining, they also contain very high concentration of thallium, ranging from 32-2600 ppm. The high values of thallium in tailings are up to ore-grade, but the thallium minerals occur as fine particles and the local miners abandoned them as tailings or mine wastes. As for the unaltered country rocks outside the Lanmuchang mineralized area, thallium occurs at very low levels, down to 0.1 ppm on average.

Therefore, the dispersion of thallium in various rocks decreases in concentration as follows: thallium ore > arsenic ore > secondary mineral > mercury ore > altered host rock (except for outcropped host rocks)> outcropped host rocks > coal > unaltered country rocks (Fig. 5-2).

Mercury and arsenic both show similar distribution to thallium in host rocks and ores (Fig. 5-2). They have high concentrations in sulfide ores and their accessory minerals. The highest values are 9.4% for Hg and 44.2% for As, respectively. In coals, the concentration of Hg is 3 ppm and As 99 ppm. In altered host rocks, these two metals are both enriched, while they are quite low in the unaltered country rocks outside the Lanmuchang area.

5.3 Pedological distribution of thallium

5.3.1 Bulk geochemistry and trace element features

The different horizons of soils in Lanmuchang are not well developed. Most of soils in the study area are intensively disturbed by farming. The arable soils were sampled from the farmland within the Lanmuchang Hg-Tl mineralized area and vegetable gardens along the Qingshui Stream. Some undisturbed natural soils, slope wash materials overlying the bedrocks, and alluvial deposits were also collected. The surficial processes producing these materials involve the weathering of bedrock exposures at high elevations, transport of a surface mantle of weathered debris downslope to the stream drainage, and reworking of the transported debris by streams. These unconsolidated deposits are widespread at lower elevations of the study area.

The mine debris was not homogeneously dispersed during the residential activity in the community area. Most of the Lanmuchang area has been developed for agricultural and residential purposes. The related disturbances, including farming, surface grading and excavations for foundations and septic systems, are very common. Some local areas have had fill materials comprised mostly local soils, some mine debris or waste and coal ashes, whereas the farming and residential areas are largely made up of reworked original surficial materials including alluvial deposits and colluviums.

45 samples of arable soils and undisturbed natural soils were collected within and around (background area) the Lanmuchang area to document the geochemical characteristics of soils associated with the natural pedogenesis and mining-related disturbance, and to delineate the variations in major elements with thallium mineralization and the dispersion characteristics of thallium and other trace metals in the study area.

The methods of analysis are described in Appendix A3.2. The sampling sites are illustrated in Fig. 5-3. Some parameters relating to soil properties are listed in Table 5-4. The results of major elements and trace elements analysis are listed in Table 5–5 and Table 5-6, respectively.

The soils in Lanmuchang are characterized by low cation exchange capacity (CEC), ranging from 3.33 to 28.3 meq/100 g. Among the exchangeable cations, calcium is dominant and represents 90%. The base saturation varies greatly, from a very high value (335 %) to a very low value (7%). The soil pH values range from 3.3 to 7.3, running from a normal, near-neutral, Ca-rich limestone-derived soil to acidic, sulfide-rich materials in the mining area.

The major-element chemistry of the soils reflects the clay mineralogy. In the soils of the Lanmuchang Hg-Tl mineralized area, > 70% (wt) of the major element components are accounted for by a SiO_2–Al_2O_3–Fe_2O_3 assemblage, with minor TiO_2 and K_2O. Based on a comparison to the North American Shale Composition (Gromet et al., 1984) and the average composition of the upper crust (Condie, 1993), these soils are more ferruginous and titaniferous, with considerably lower levels of Na_2O, MgO and CaO.

These soils are highly concentrated in sulfur, ranging from 0.02–2.90 % (wt). The high sulfur content results from the abundances of sulfide minerals. These soils are also enriched in organic carbon, ranging from 0.3–18.3 (wt%), which implies an organic matter mixture in topsoils from farmland.

The results of trace elements determination are listed in Table 5-6. Based on a comparison to shale, the average composition of upper crust or crust (Gromet et al., 1984; Condie, 1993; Taylor, 1964; Turekian and Wedepohl, 1961) and background values (this study), Tl, Hg, As, Ba, and Sr are enriched, while Cu, Pb, Zn, Sb, Cd, Co, Ni, Cr, Sb, Sn, V and Mo show comparable concentrations. The concentrations of the above metals indicate that Tl, Hg and As are the main toxic metals in soils, and the base metals and other metals are not profoundly concentrated in soils in the study area. This agrees with the intensive mineralization of Tl, Hg and As and the poor mineralization of base metals in bedrocks. Compared with the background soils, the soils in Lanmuchang show high enrichments in Tl, Hg, As, Ba and S. The enrichment factors are 100-fold for Tl, 30-fold for As, 300-fold for Hg, 15-fold for Ba, and 25-fold S. Among them, Tl, Hg and As are three specific toxic

metals, and their high enrichment in soils could have negative environmental impacts on the local ecosystem.

5.3.2 Distribution of Tl, Hg and As in soils

The average concentrations of thallium, mercury and arsenic in various soils are listed in Table 5-7. Concentrations of Tl, Hg and As differ from each other in various soils, i.e. soils from the mine area, slope wash materials, alluvial deposits and/or foundation soil, undisturbed natural soil and background soil. In general, Hg and As show much higher levels than Tl in soils.

Tl is found at high concentrations in soils within the mine area, ranging from 53 to 282 ppm. In slope wash materials, Tl ranges from 40-46 ppm with an average of 43 ppm. In alluvial and/or foundation soils along the Qingshui Stream, Tl ranges from 21 to 100 ppm with an average of 54 ppm. Comparably, the undisturbed natural soils within and around the mine area show a lower concentration of thallium, ranging from 2.2 to 29 ppm with an average of 10.8 ppm. Among them, samples S108 and S142 are from the mine area, and their Tl concentrations are 12 ppm and 29 ppm, respectively, higher than other natural soils from around the mine area. However, background soils have very low Tl contents ranging from 0.47 to 0.97 ppm with an average of 0.7 ppm.

Mercury in soils from mine areas, slope wash materials and alluvium and/or foundation soils along the stream occurs over a wide range of concentrations from 40 to 950 ppm, and the highest level of 950 ppm was found in the topsoil (sample S101) of a rice field besides a midstream bank. In undisturbed natural soils within and around the mine

area, Hg shows much lower levels 0.8-61.8 ppm, and the maximum value came from sample S142. The background level of Hg is pretty low, down to 0.53 ppm.

Arsenic almost shows the same dispersion pattern as Hg in soils in mine areas, slope wash materials and alluvial and/or foundation soils along the stream. The concentration of As ranges from 54 to 586 ppm, and the highest value (sample S102) came from the subsoil of the rice field where the topsoil (sample S101) had the highest Hg level of 950 ppm. In undisturbed natural soils within and around the mine area, As shows slightly lower levels 37.1-89 ppm, with the average 58.6 ppm. The background level of As is pretty low, down to 5.5 ppm.

The relationships of Hg vs Tl and As vs Tl are shown in Fig. 5-4 and Fig. 5-5. Except for a few scattered data, Hg and As generally have higher concentration with respect to increasing concentration of Tl in soils. Their correlations follow the power law distribution (R^2 =0.71 for Hg, and R^2 = 0.80 for As, respectively).

In some sites, the topsoil (0-20 cm) and subsoil (20-50 cm) were both sampled. The topsoil layer is often disturbed by farming activity while the subsoil layer is relatively undisturbed. Tl in the subsoil generally shows slightly higher contents than in topsoil (Fig. 5-6a), but the As and Hg vary considerably in the two soil layers (Fig. 5-6b,c).

In one garden soil profile, variations of Tl, Hg and As are illustrated in Fig. 5-7. This profile shows marked concentration increases in Tl, Hg and As at the depth of 40-60 cm, whereas the surface soil and deeper soils show similar contents.

In general, Tl concentration in soils increases corresponding to slight decrease of pH values except for a few scattered data (Fig. 5-8). However, in the undisturbed natural

soils within and around the mine area, pH values slightly increase followed by increases in Tl. In background soils, low Tl levels are also correlated to low pH values. All the soils are generally acidic, and 75% of pH values fall within the range of pH = 3.0–6.0, and the other 25 % samples have higher pH values, ranging from 6.4 to 7.3.

5.4. Hydrogeological distribution of thallium

Sites selected for water and sediment samples are plotted in Fig. 5-9 and Fig. 5-10, respectively. Waters can be categorized in the following manner: deep (mine) groundwater, shallow groundwater, well water and stream water, and sediments are mainly stream sediments.

5.4.1 Hydrogeochemistry of major elements

Results of major ions determination in waters are listed in Table 5-8. The observed ionic balance is better than ±15%. The waters generally show a weak alkalinity with a pH range of 7.17–8.33, except for the deep mine groundwater which has low pH values (2.61–6.62). The electrical conductivity is generally stable, mostly in the 200–400 μS/cm range, except for extremely high values in deep mine groundwater. The observed water temperature varied from 14 to 23°C, and the hotter waters were collected during the rainy summer period.

A piper plot of major elements (Fig. 5-11), allows for the recognition of the chemical types of groundwater. This plot indicates that calcium is the major cation present while the sulfate and bicarbonate dominate the anion chemical component. The deep mine

groundwater is characterized by high contents of Ca, Mg and SO_4, and the shallow groundwater is chemically dominated by enrichment of Ca, Mg and HCO_3. In all waters, sulfate is substantially higher than chloride. The high calcium and sulfate indicate a major contribution from the oxidation of sulfide minerals and reaction with carbonate, and/or dissolution of gypsum. The water type of SO_4/HCO_3 –Ca-Mg and /or SO_4–Ca is consistent with the water types found for deep groundwater from the borehole at the study area in early 1980's (Guizhou Hydrogeological Survey, 1985). The cations sodium and potassium show insignificant concentrations and are less than 10% of the major cations. This is in accord with the regional geological context that shows a paucity of silicate rocks.

5.4.2. Distribution of thallium and other trace elements in (sub)surface water

The water analysis results for trace metals are listed in Table 5-9. The distribution of Tl in groundwater shows three distinct patterns (Fig. 5-12). First, the concentration of Tl in the deep mine groundwaters (group A), at sites 1003, 1072, 1094, 1097 and 1104, range between 13.4 μg/l to 1102 μg/l representing the highest enrichment in the water system. The average is 340 μg/l, 4 orders of magnitude higher than the background values in water. Secondly, at a location slightly away from the Tl mineralized area, the shallow groundwater (group B) from the Tl-Hg-coal-hosted strata of P_2c and P_2l, at sites 1001, 1004, 1006 and 1012, shows an average concentration of 0.35 μg/l. The water at site 1012, taken from a domestic well, shows a slightly higher Tl content of 0.377 μg/l. Finally, the shallow groundwater (group C) from outside of the Tl mineralized area gave lower Tl levels with an

average of 0.024 μg/l (at sites 1008, 1009, 1010, 1013, 1015, 1051, 1091, 1092, 1096, 1071, 1047, 1057).

The Tl-rich deep mine groundwater is characterized by lower pH, lower dissolved oxygen (DO), and higher electrical conductivity (EC) (Fig. 5-13). The pH is strongly acidic with values down to 3.0, and the DO is very low down to 0.79 mg/l. Away from the Tl mineralized area, these parameters change with increasing pH and DO values and decreasing EC values.

The Tl average concentration in stream water is up to 9.7 μg/l during the dry season (base-flow regime), and 1.9 μg/l during the rainy season (flood-flow regime). The dispersion patterns of Tl along the stream in both sampling seasons are illustrated in Fig. 5-14. The pattern in base-flow is characterized as follows. First, Tl content of groundwater upstream (at sites 1008 and 1009) is very low (0.005 μg/l), but at site 1098 (Creek A) it increases up to 0.09 μg/l. At site 1001, Tl is only 0.12 μg/l, but at site 1100 (Creek B), it increases to a high level of 4.8 μg/l within a distance of less than 500 meters. At site 1099, where water from Creeks A and B merge, Tl concentration decreases to 0.76 μg/l. Secondly, mid-stream, Tl values are up to 0.99–2.1 μg/l, and at site 1016 it decreases to 0.8 μg/l. In Creek C, the Tl level is 0.12 μg/l at site 1045. Thirdly, in the downstream section, the Tl level clearly increases from 3.1 μg/l (site 1035) to the highest level 31–33 μg/l, at sites 1065 and 1070. At the sinkhole site 1002 the Tl content is 19.3 μg/l. The water seeps slowly through the sinkhole to the underground.

The content of Tl in stream water in the flooding regime shows very similar dispersion to that of base-flow (Fig. 5-14), although the average level of Tl decreases to 1.9

μg/l due to water dilution. However, in mid-stream, the concentrations of Tl are a little higher than in base-flow, with an average 1.6 μg/l against 1.49 μg/l during dry season. Much higher concentrations of Tl also occur downstream, ranging from 3 μg/l to 4.5 μg/l. Sample 1142, collected from the inundated sinkhole area and representing the inundated water in the sinkhole and its surrounding area in the flood condition, contains 4.5 μg/l of Tl.

Two other toxic metals of interest are mercury and arsenic which also show high concentrations in the water system. The average level of arsenic in deep mine groundwater, shallow groundwater and surface stream water are 211 μg/l, 0.4 μg/l and 12.2 μg/l, respectively. The dispersion patterns of arsenic in both groundwater and stream water are similar to Tl, particularly in downstream stream water, it shows an increase in arsenic during both sampling conditions (Fig. 5-14; Fig. 5-15). As for mercury, the enrichment compared to the background level is not as strong as its counterpart thallium and arsenic, and its dispersion pattern is rather irregular (Fig. 5-15). The average levels of Hg in deep mine groundwater and shallow groundwater are 0.56 μg/l and 0.43 μg/l, respectively. The mercury in stream water is low to 0.2 μg/l, very close to the background level 0.15 μg/l.

Concentrations of the trace elements Rb, Sr, Li and B go from high to low in the sequence of mine groundwater > stream water > shallow groundwater, showing a spatial dispersion similar to thallium and arsenic. The concentrations of Rb, Sr, Li and B in stream water were slightly diluted during the flooding regimes.

5.4.3 Geochemical composition of sediments and Tl distribution

Concentration for trace elements in stream and well sediments are listed in Table 5-10. The results show that targeted toxic metals Tl and As are enriched in sediments. Cr, Cu, Zn, V and Sr also show high concentrations. Mercury has been determined semi-quantitatively and shows low concentrations (thus it is not proper to use the semi-quantitative data for an exact comparison). Other metals including Pb, Co, Mo, Sb and Rb generally do not show abnormal concentrations, presenting the same distribution as in soils and bedrocks.

Thallium exhibits various concentrations in groundwater sediments collected in the mine adits and well bottoms within and outside the Lanmuchang Hg-Tl mineralized area. In the Hg-Tl mine adits, the silty sediments on the adit surface or conduit (at sites SD1040, SD1086 and SD1094) contain from 75 to 3800 ppm of thallium, and from 345 to 3238 ppm of As. In the sediments from a coal adit mined at Xialongdong, Tl and As values are 53 ppm and 268 ppm, respectively. In the well bottom sediments collected at site SD1012, Tl is 62 ppm and As is 237 ppm, while the well sediment at site 1091 outside the Lanmuchang area containes Tl at 1.3 ppm and As at 14 ppm, respectively. This indicates a distinct Tl dispersion pattern in groundwater sediments: concentrations tend to decrease away from the center of Hg-Tl mineralized area till with very low values outside the Lanmuchang mineralized area. Arsenic presents very similar distribution patterns in sediment to that of Tl.

Thallium distribution patterns in stream sediments in both the base-flow and flood-flow conditions are illustrated in Fig. 5-16. Thallium shows a very similar concentration

distribution pattern in both the base-flow condition (dry season) and flood flow condition (rainy season) in the stream sediments running through the Lanmuchang area, although concentrations for the former are slightly higher than the latter.

In base-flow condition, Tl in stream sediments ranges from 7.6 to 51 ppm, with an average of 25 ppm. Stream sediment from Creek A contains only 7.6 ppm of Tl, and 1.8 ppm from Creek D which is slightly away from the Lanmuchang area. However, sediments from Creek B and the main Qingshui Stream are much richer in Tl, ranging from 22 to 51 ppm. The highest level is from the Creek B, the main water source discharging from the Lanmuchang mineralized area. Tl in sediments from the Qingshui Stream from upstream to downstream shows more stable concentration (20-23 ppm), except for a higher value of 35 ppm at site 1065 downstream. Note that the sinkhole sediment (site SD1112) downstream has a very similar Tl level as the bank sediment (site SD 1113) of the sinkhole. They are 20 ppm and 23 ppm, respectively.

In flood-flow condition, Tl is slightly depleted in the streambed sediments of the Qingshui stream, probably due to the sediment "dilution" by increased runoff. The Tl concentrations range from 6 to 21 ppm, with an average of 13 ppm. Stream sediment from Creek A contains 6 ppm of Tl, almost the same as it is in base-flow condition (7.6 ppm). However, sediments of Creek B contain more elevated Tl concentrations, even much higher than they are in base-flow condition. The newly formed fine sediments leached from the mine waste piles and the outlet of coal adit at Xialongdong after the rains contain much higher contents of thallium. They are in the range of 49-63 ppm, much higher than concentrations in the Qingshui Stream sediments. Very high Tl in the newly formed fine

sediments leached from the mine wastes at Hangnijiang mining site was also examined and found to contain about 340 ppm of thallium.

5.5 Bio-distribution of thallium

Various plants and agricultural products were collected and the sampling sites are plotted in Fig. 5-17. The sampled materials were green cabbage, Chinese cabbage, corn, rice and chili. Some wild grasses and ferns were also collected in the mine area. The sampling sites for vegetation correspond to the locations of soil samples, that is, around crops, the soils on which the crops were growing were also collected.

5.5.1 Distribution of major and trace elements in vegetation

The analysis results of major and trace elements of various vegetation are listed in Table 5-11 and Table 5-12. Note that the data for the selected elements (except for Hg) are the original analyzed data based on ash weight (AW). Mercury is directly determined by cold vapor ICP-MS, and the results are based on DW. Concentrations of major and trace elements based on dry weight (except for Hg) were obtained by multiplying the original data (AW) to the ash yield factor (wt %) which were determined by the division of ash weight to dry weight (DW) of the air-dried samples, and are listed in. Table 5-13 and Table 5-14. The following discussion relating to elements in crops and vegetation are all based on their dry weights.

The major elements Na, Mg, Ca, Si, Fe, Mn and Al are more enriched in Chinese cabbage, green cabbage and carrot than in chili, corn and rice. Wild cabbage and fern are

also rich in the above major components. On the contrary, chili, corn and rice are much depleted in the above chemical constituents, some are even lower by 3 orders of magnitude. Corn shows the lowest elemental content, particularly for Na and Al.

The trace elements also generally show higher concentrations in Chinese cabbage, green cabbage and carrot than in chili, corn and rice, except for Cu and Ni. Cu and Ni show almost the same range of concentration as for other vegetables.

Some metals in vegetations from the Lanmuchang area show higher contents than the average concentrations found in land and edible plants worldwide as cited in Table 5-15. These metals include Tl, Hg, As, Fe and Sr, and because of their potential health impacts, only Tl, Hg and As will be discussed.

5.5.2 Distribution of Tl, Hg and As in various crops and vegetation

The average concentrations of Tl, Hg and As in various crops and vegetation are listed in Table 5-16.

Thallium occurs at the highest concentration in green cabbage, ranging from 120 to 494 ppm with an average of 338 ppm, while outside the Lanmuchang Hg-Tl mineralized area it is only 0.39 ppm. Thallium shows the secondary highest contents in chili, ranging from 2.9-5.3 ppm, and 4.1 ppm on average. Chili outside the Lanmuchang area contains only 0.27 ppm Tl on average. The widely planted Chinese cabbage contains 0.7-5.4 ppm of thallium, with an average of 2.2 ppm. Chinese cabbage outside the Lanmuchang is depleted in thallium with an average of 0.26 ppm. The shelled rice contains thallium from 0.99 to 5.2 ppm, and 2.4 ppm on average, whereas corn from outside the Lanmuchang mineralized

area shows an average of 0.25 ppm of thallium. Thallium in granular corns shows lower concentration, ranging from 0.78-3.1 ppm and 1.4 ppm on the average, while corn from outside the Lanmuchang mineralized area shows a thallium concentration of 0.07 ppm on average.

One carrot root sample, two wild cabbage samples and one fern sample were also collected in the Lanmuchang area. Thallium in the carrot root was high at 22 ppm. Although this value is relatively high, carrot is not a common crop plant in the Lanmuchang area. Whole wild cabbage also shows a higher average thallium concentration of 36 ppm. The fern, widely growing on the mountain surface in the Lanmuchang mineralized area, shows a concentration of 14.5 ppm of thallium. The concentrations of Hg and As are much lower than Tl in vegetation.

Hg shows slightly higher concentrations in green cabbage, Chinese cabbage and carrot, generally ranging from 0.48 to 0.63 ppm, but presents very low levels in rice and corn. Hg shows the highest value of 0.63 ppm on average in green cabbage, and in Chinese cabbage and carrot, the average values are 0.48 ppm and 0.55 ppm, respectively. Concentrations of Hg outside the Lanmuchang area are 0.33 ppm for green cabbage and 0.28 ppm for Chinese cabbage, respectively. On the contrary, Hg in chili, rice and corn is more depleted. Chili and rice almost contain the same concentrations (0.03 ppm on average), as from outside the Lanmuchang area (0.02 ppm for chili and 0.02 ppm for shelled rice). Hg in corn is the most depleted of all elements from corn samples, from both within and outside the Lanmuchang area, and is below the detection limit (0.005 ppm). However, Hg shows the highest content in wild cabbage grown on the Tl-contaminated

arable soils, up to 4.2 to 12.5 ppm, nearly 20-fold the content in the crops. In fern, Hg shows an average concentration of 0.45 ppm.

Arsenic also shows its highest concentration level in wild cabbage (up to 13 ppm) and then in the fern leaves (2.3 ppm). In the crops, arsenic presents slightly higher levels than Hg, but much lower than Tl. Arsenic in green cabbage, Chinese cabbage and carrot are much higher than in corn and rice, generally ranging from 0.7 to 1.3 ppm. In corn and rice, arsenic contents are relatively low, down to from 0.02 to 0.15 ppm. Arsenic shows its highest value in carrot, up to 1.3 ppm. The average content of As in crop plants from outside the Lanmuchang Hg-Tl mineralized area are low (0.02 ppm for corn, 0.09 ppm for rice, 0.2 ppm for chili, 0.3 ppm for green cabbage, and 0.7 ppm for Chinese cabbage).

The above presence and distribution of Tl, Hg and As in crops and vegetation are either related to the Hg-Tl mineralization and mining disturbance within the Lanmuchang area, or to outside the Lanmuchang area without Hg-Tl mineralization. However, some crops were also collected at locations slightly away from the Lanmuchang Hg-Tl mineralized area, where the soils supporting crop growth are slightly affected by the primary dispersion of Hg-Tl mineralization. These samples are B148, B135, B305, B410, B406 and B509. Thallium concentrations in crops growing in these sample locations are slightly higher than for the same crops grown from the background area, but much lower than those growing within the Lanmuchang mineralized area. Concentrations of Hg and As showed a similar dispersion as did Tl. These results also reflect the impact of metal mineralization of bedrock on the dispersion of toxic metals in crops.

Table 5-1 Compositions of major elements in rocks (unit in wt%)

Sample	Rock unit	SiO_2	TiO_2	Al_2O_3	Fe_2O_{3t}	MnO	MgO	CaO	Na_2O	K_2O	P_2O_5	S_t	Total	LOI
Unaltered country rocks from the background area														
R180	Limestone	4.10	0.06	0.30	0.41	0.03	1.90	50.90	nd	0.05	nd	0.04	57.79	31.5
R184	Siltstone	27.40	1.83	6.60	6.80	0.06	3.36	28.17	nd	1.12	0.21	0.02	75.57	21.6
R185	Limestone	2.10	0.03	0.30	0.32	0.02	0.60	52.50	nd	0.13	nd	0.08	56.08	30.1
R186	Clay stone	58.10	2.98	14.20	10.70	0.45	3.04	0.52	2.70	1.65	0.17	nd	94.49	nd
R187	Argillite	29.20	2.74	11.10	7.20	0.07	3.82	23.67	0.00	0.47	0.33	0.06	78.66	18.9
Outcropped host rocks														
R205	Limestone	1.90	0.13	0.00	0.30	0.07	1.45	54.89	nd	0.01	nd	0.07	58.82	29.6
R146	Siltstone	76.90	2.63	7.00	1.80	nd	0.11	0.05	nd	0.25	0.48	1.29	90.51	8.6
R199	Siltstone	79.70	1.88	10.40	0.60	nd	0.36	0.04	nd	0.84	0.28	0.32	94.42	nd
R332	Clay stone	82.90	1.49	4.60	5.80	nd	0.10	0.66	0.10	0.13	0.16	0.30	96.24	nd
R107	Argillite	76.90	2.79	9.40	0.90	nd	0.18	0.07	nd	0.48	0.69	2.07	93.48	6.3
R169	Argillite	69.30	3.61	14.80	2.20	nd	0.20	0.04	nd	0.47	0.34	0.73	91.69	nd
Secondary minerals														
R126	Halotrichite	27.00	0.17	5.90	15.40	0.03	0.19	0.16	nd	0.10	0.03	11.30	60.28	50.7
R139	Kalinite	41.30	2.17	11.80	9.37	nd	0.49	0.15	nd	1.33	0.42	7.24	74.27	32.1
R198	Jarosite	41.10	0.28	1.20	3.48	nd	0.07	0.12	nd	0.21	0.06	19.50	66.02	48.7
Altered host rocks														
R103	Argillite	45.20	2.47	13.60	10.00	nd	0.54	0.13	nd	1.68	0.36	8.28	82.26	25.6
R108	Argillite	63.50	2.74	13.10	7.55	nd	0.47	0.10	nd	1.42	0.34	5.90	95.12	11.9
R109	Siltstone	81.30	1.25	6.50	1.50	nd	0.14	0.04	nd	0.23	0.11	1.39	92.46	7.6
R117	Argillite	44.20	2.60	13.80	14.50	nd	0.56	0.10	nd	1.62	0.40	11.80	89.58	22.5
R118	Argillite	84.40	0.47	2.70	1.20	nd	0.10	0.36	nd	0.10	0.15	1.77	91.25	8.4
R128	Argillite	85.80	0.30	1.10	4.60	nd	0.07	0.04	0.10	0.06	0.06	4.42	96.55	5.6
R174	Siltstone	54.40	2.30	15.30	8.62	nd	0.48	0.09	nd	1.32	0.58	6.64	89.73	18.4

Table 5-1 (continued)

Sample	Rock unit	SiO_2	TiO_2	Al_2O_3	Fe_2O_{3t}	MnO	MgO	CaO	Na_2O	K_2O	P_2O_5	S_t	Total	LOI
Ores														
R173	Coal	11.30	0.24	2.10	3.49	0.01	0.89	3.83	nd	0.27	nd	3.02	25.12	76.9
R208	Coal	10.20	0.06	10.80	0.88	nd	0.07	0.68	nd	0.16	1.18	1.98	26.01	71.8
R113	As ore	13.90	0.12	0.60	1.47	nd	0.04	0.11	nd	nd	0.03	25.60	41.87	82.9
R197	As ore	46.90	0.09	0.60	0.48	nd	0.04	0.21	nd	0.09	0.01	20.60	69.02	51.9
R181	Hg ore	72.30	2.16	12.00	1.75	nd	0.22	0.08	nd	0.87	0.33	2.59	92.30	10.6
R330	Hg-Tl ore	73.80	2.43	13.40	1.59	nd	0.10	0.09	nd	0.31	0.16	1.87	93.75	8.9
R115	Hg ore	51.70	2.34	11.10	14.20	nd	0.34	0.08	nd	1.01	0.29	12.20	93.26	18.3
R119	Tl ore	19.60	0.82	7.80	13.20	nd	0.20	0.10	nd	0.37	0.13	12.10	54.32	53.4
R190	Tl-As ore	56.00	2.59	11.70	12.00	nd	0.30	0.09	nd	0.87	0.21	10.20	93.96	16.5
R191	Tl-As ore	60.80	0.53	3.80	4.64	nd	0.10	0.26	nd	0.26	0.14	12.20	82.73	27.5
R192	Tl ore	50.90	2.85	13.70	11.60	nd	0.32	0.10	nd	0.99	0.51	11.10	92.07	15.5
R193	Tl ore	41.90	1.97	8.20	16.20	nd	0.29	0.13	nd	0.97	0.34	15.20	85.20	24.0
R195	Tl-As ore	50.70	2.29	11.70	17.30	nd	0.27	0.09	nd	0.71	0.33	13.90	97.29	17.2
R196	Tl ore	48.60	0.19	6.10	7.28	nd	0.08	0.35	nd	0.05	0.21	11.00	73.86	38.9
R333	Tl-As	56.80	2.57	14.80	9.70	0.01	0.58	0.20	nd	1.50	0.31	8.03	94.50	14.2
R334	As ore	55.30	0.76	5.60	8.56	0.01	0.21	0.15	nd	0.60	0.37	13.00	84.56	23.1
Mine wastes														
R206	Fault gouge	64.00	2.84	12.30	5.59	nd	0.35	0.09	nd	1.11	0.39	3.59	90.26	14.3
R207	Fault gouge	65.70	1.28	10.90	7.19	0.01	0.39	0.14	nd	1.11	0.32	6.34	93.38	12.5
S111	Argillite	59.80	3.14	14.30	3.60	nd	0.65	0.01	0.10	1.73	0.31	3.27	86.91	13.0
S162	Argillite	44.80	2.44	11.70	9.40	0.01	0.45	1.42	0.10	1.50	0.21	2.56	74.59	25.3
NASC [1]		64.80	0.70	16.90	5.70	0.06	2.85	3.63	1.13	3.97	0.15			
Upper Crust [2]		66.33	0.54	14.87	4.68		2.46	3.55	3.43	2.85	0.12			

Fe_2O_{3t} as total Fe; S_t as total sulfur; LOI as total loss on ignition, not included in the Totals; "nd" means not detectable;
Reference: 1. Gromet et al., 1984; 2.Condie, 1993

Table 5-2 Concentrations of selected trace elements in rocks/ores (unit in ppm)*

Sample	Rock unit	Tl	Hg	As	W	Ba	Cd	Co	Cr	Sb	Cu	Pb	Zn	V	Mo	Sn	Ni	Rb	Cs	Sr
Unaltered country rocks from the background area																				
R180	Limestone	nd	na	na	na	nd	nd	nd	11	0.5	nd	nd	58	9	nd	nd	nd	2.4	0.16	462
R184	Siltstone	0.06	na	na	na	190	nd	23	194	1.9	32	5	81	149	0.2	1.5	52	26	5.50	640
R185	Limestone	nd	0.062	2.6	nd	nd	nd	nd	nd	nd	nd	nd	58	5	nd	nd	nd	1.6	0.02	1122
R186	Clay stone	0.2	na	na	na	190	nd	40	281	nd	92	13	137	196	0.6	2.7	118	52	1.9	87
R187	Argillite	0.86	na	na	na	nd	nd	29	257	2.4	58	4	130	194	0.3	2.7	68	23	4.1	470
Outcropped host rocks																				
R205	Limestone	8.3	0.14	2.8	nd	nd	nd	nd	23	nd	nd	nd	58	13	0.3	nd	nd	0.25	0.03	980
R146	Siltstone	330	130	240	260	1700	nd	10	90	0.5	21	11	7	169	0.6	4.0	13	14	4.4	2200
R199	Siltstone	25	21	16.3	210	390	0.3	nd	73	5.0	nd	7	56	133	0.9	3.3	nd	31	1.7	1800
R332	Clay stone	6	9	50	120	7000	nd	nd	89	0.6	29	5	7	98	0.5	1.6	nd	7.6	3.1	770
R107	Argillite	53	400	15.1	96	360	nd	8	78	0.7	nd	15	6	167	1.3	4.8	nd	25	1.5	4700
R169	limestone	71	120	311	74	1600	nd	10	110	0.7	23	9	11	209	2.2	3.9	nd	25	2.3	810
Secondary minerals																				
R126	Halotrichite	25	39	331	170	242	0.9	43	80	4.2	86	2	84	55	6.4	0.6	124	2.6	0.76	231
R139	Kalinite	89	30	416	80	354	0.3	42	127	0.4	64	11	141	232	1.1	4.4	126	60	5.8	1668
R198	Jarosite	1100	370	217000	nd	1880	nd	nd	38	1.5	28	2	8	26	3.4	17.0	17	8.8	1.4	248
Altered host rocks																				
R103	Argillite	200	65	786	140	1060	0.5	38	98	0.7	101	14	164	200	1.2	4.3	115	76	6.0	2405
R108	limestone	210	34	185	400	1970	0.4	36	113	0.5	89	11	74	220	0.9	3.8	69	74	5.9	1108
R109	limestone	47	na	na	na	140	nd	12	89	0.3	28	4	50	57	1.3	2.9	49	11	2.9	500
R117	limestone	490	68	755	67	445	0.6	49	126	0.7	69	11	205	213	4.6	4.0	128	70	4.6	2637
R118	Argillite	48	na	na	na	860	0.4	nd	72	12.0	18	2	17	70	2.6	1.3	19	4.6	1.2	950
R128	Argillite	33	na	na	na	4300	nd	nd	62	4.0	27	1	16	29	5.8	0.8	22	2.8	2.4	450
R174	Siltstone	39	na	na	na	6420	nd	38	94	18.0	126	7	39	178	1.2	3.4	82	69	6.8	2124

Table 5-2 (continued)

Sample	Rock unit	Tl	Hg	As	W	Ba	Cd	Co	Cr	Sb	Cu	Pb	Zn	V	Mo	Sn	Ni	Rb	Cs	Sr
Ores																				
R173	Coal	12	1.88	15.4	nd	2970	0.5	nd	nd	1.3	28	6	40	98	13.0	1.3	nd	6.8	1.4	nd
R208	Coal	46	3.9	183	19400	1260	0.6	18	18	1.3	36	4	227	261	6.8	1.4	45	4.5	1.5	22
R113	As ore	1300	280	442000	nd	4420	nd	5	27	2.0	18	nd	16	7	nd	5.0	24	2.6	0.73	164
R197	As ore	1	3	267000	nd	80	nd	nd	31	2826	14	2	6	6	nd	7.3	nd	3.1	0.35	183
R181	Hg ore	490	12000	735	173	2810	nd	10	61	4.4	nd	26	nd	144	1.0	5.2	nd	46	4.8	659
R196	Hg-Tl ore	100	94000	996	27	1970	nd	nd	28	12.0	20	46	36	23	5.7	1.0	20	0.86	0.49	1030
R330	Hg ore	33	na	na	na	13400	nd	11	82	0.6	18	6	5	130	0.2	2.9	14	18	1.8	724
R115	Tl ore	4300	na	na	na	4900	nd	41	107	2.5	71	11	202	165	1.4	4.7	100	46	5.3	957
R119	Tl-As ore	35000	120	11500	85	5460	0.4	55	88	0.7	113	4	234	53	0.5	7.0	137	18	3.6	611
R190	Tl-As ore	4400	120	3600	96	2240	nd	38	112	1.3	96	8	156	169	0.9	5.9	98	37	3.4	622
R191	Tl ore	2300	na	na	na	21000	nd	18	57	1.4	53	6	87	40	0.6	8.0	82	11	1.9	802
R192	Tl ore	31000	95	11300	325	6490	nd	35	102	0.8	91	10	156	199	5.0	5.9	98	42	4	2884
R193	Tl-As ore	25000	na	na	na	21300	nd	25	111	3.2	112	9	150	166	1.4	11.0	78	38	5	1340
R195	Tl ore	1000	na	na	na	732	0.3	24	92	0.5	67	8	157	168	6.4	4.6	60	32	7	1672
R333	Tl-As	18000	1500	79800	466	8950	0.6	21	75	1.5	133	12	107	79	28.0	25.0	67	27	3.2	2054
R334	As ore	130	na	na	na	383	nd	40	105	10.0	139	12	104	222	1.9	4.7	80	53	14	1870
Mine wastes																				
R206	Fault gouge	2600	87	1290	62	1520	nd	33	106	0.6	63	9	125	183	0.9	4.0	41	47	3.4	2570
R207	Fault gouge	1600	na	na	na	1710	0.6	32	102	1.1	49	8	98	150	0.7	3.6	73	51	4.4	1820
S111	Argillite	32	63.7	56.4	na	5700	nd	13	103	1.4	33	14	19	221	2.6	5.4	26	97	9.9	1000
S162	Argillite	136	188	261	na	3800	0.2	11	117	14.0	56	22	42	210	7.4	4.2	26	53	7	650
NASC [1]						636		26	125	2.1							58	125	5.16	142
Upper Crust [2]						626		18	112			18		86			60	87		269
Continent Crust [3]		0.45				425	0.2	25	100	0.2	55	13	70	135	1.5	2.0	75	90		375
Shale [4]		1.40				580	0.3	19	90	1.5	45	20	95	130	2.6	6.0	68	140	5	300
Carbonate [4]		0.0x				10	0.0	0.1	11	0.2	4	9	20	20	0.4	0.x	20	3	0.x	610

Reference: 1. Gromet et al., 1984; 2.Condie, 1993; 3. Taylor, 1964; 4. Turekian and Wedepohl, 1961; * Hg, As and W are determined by INAA, and the others by ICP-MS; na: not analyzed; nd: not detectable

Table 5-3 Distribution of thallium in various rocks/ores in the Lanmuchang Hg-Tl mineralized area (unit in ppm)*

Rocks/ores	Number of samples	Tl		Hg		As	
		Range	Average	Range	Average	Range	Average
Tl ores	9	130-35000	13459	95-1500	729	3600-79800	26550
As ores	2	1-1300	650.5	3-280	142	267000-442000	354500
Hg ores	3	33-490	208	12000-94000	53000	735-996	866
Coals	2	12-46	29	1.88-3.9	3	15.4-183	99
Mine wastes	4	32-2600	1092	63.7-188	112.9	56.4-1290	535.8
Altered host rocks	7	33-490	152	34-68	56	185-786	575
Outcropped host rocks	6	6-330	82	0.14-400	113	2.8-311	106
Secondary minerals	3	25-1100	405	30-370	205	331-217000	72582
Unaltered country rocks	5	<0.02-0.86	0.1	0.06	0.06	2.6	2.6

* Tl was determined by ICP-MS, Hg by cold vapor ICP-MS, and As by INAA

Table 5-4 Composition and characteristics of soils

Sample	Ca (meq/100g)	Mg (meq/100g)	Na (meq/100g)	K (meq/100g)	TEC[a] (meq/100g)	CEC[b] (meq/100g)	ESP[c] (%)	Base saturation[d] (%)	pH
Soils in mine area									
99S-112	13.2	0.5	0	0	14	22.6	0.17	62	5.1
99S-113	63.5	0.7	0	0	64.4	21.2	0.23	304	7.2
99S-114	23.3	2.2	0.4	1	26.5	17.8	1.99	149	6.6
99S-115	18.4	1.8	0.1	0	20.5	20.1	0.46	102	6.4
99S-116	20.8	1.4	0.2	0	22.7	18.3	1.06	124	6.6
99S-117	18	1.6	0.1	0	20	19.0	0.76	105	6
99S-145	2.5	0.4	0.4	0	3.4	13.6	2.74	25	3.5
99S-151	6.4	1	0	0	7.8	21.1	0.22	37	4.5
99S-153	35.6	1.9	0.5	0	38.5	18.2	2.95	212	7.2
99S-154	24	0.8	0.4	0	25.5	20.4	1.83	125	7
99S-159	3.2	0.2	0.1	0	3.7	23.1	0.25	16	4
99S-160	32.4	0.1	0.1	0	32.9	23.3	0.25	141	4
99S-163	6	0.7	0.3	0	7.2	17.6	1.88	41	4.5
99S-164	2.4	0.4	0.2	0	3.2	14.5	1.65	22	3.7
99S-165	7.7	0.5	0.1	0	8.5	27.4	0.37	31	4.5
99S-166	4.3	0.3	0.1	0	4.8	15.0	0.64	32	4.5
Alluvial deposits or foundation soils									
99S-101	38.5	1.6	0.3	0	40.9	19.7	1.55	208	7
99S-102	20	1.1	0.2	0	21.6	16.7	1.19	129	6.8
99S-121	25.1	1.3	0.3	1	27.2	28.3	0.97	96	6.5
99S-122	9.7	0.5	0.2	0	10.6	20.4	0.92	52	4.5
99S-128	9.9	1.2	0.3	0	11.6	20.7	1.54	56	4.6
99S-129	11	1.6	0.4	0	13.2	21.6	1.64	61	5.1
99S-130	15	1.9	0.2	0	17.5	20.3	1.15	86	5.3
99S-131	18.8	2.3	0.2	0	21.8	21.0	1.01	104	5.6
99S-133	5.4	0.5	0.2	0	6.3	23.3	0.92	27	4.3
99S-135	11	0.9	0.4	0	12.6	19.4	2.25	65	4.9
99S-137	7.4	0.7	0.2	0	8.5	22.4	0.74	38	4.6
99S-141	5.7	0.4	0.1	0	6.7	25.8	0.46	26	4.4
99S-144	25.8	1.9	0.5	1	28.6	24.7	1.95	116	6.7
99S-150	3.8	0.5	0	0	4.5	17.3	0.27	26	4
99S-203	27.1	1.6	0.2	0	29.3	17.4	0.89	168	7.3
99S-204	31.3	1.5	0.3	0	33.3	21.5	1.46	155	7
Undisturbed natural soils									
99S-108	0.4	0.1	0	0	0.5	3.3	0.79	15	4.2
99S-120	11.3	1.2	0.3	0	13.2	21.3	1.47	62	5.3
99S-142	9.6	1.5	0.6	1	12.6	26.8	2.23	47	4.7
99S-148	0.8	0.2	0	0	1.1	12.2	0.25	9	3.9
99S-149	0.4	0.1	0	0	0.6	8.6	0.45	7	4

Table 5-4 (continued)

Sample	Ca (meq/100g)	Mg (meq/100g)	Na (meq/100g)	K (meq/100g)	TEC[a] (meq/100g)	CEC[b] (meq/100g)	ESP[c] (%)	Base saturation[d] (%)	pH
Undisturbed natural soils									
99S-172	1.2	0.4	0	0	1.8	12.0	0.21	15	3.3
99S-173	71.3	0.2	0	0	71.6	21.4	0.12	335	5.1
99S-136	12.4	0.9	0.6	0	14.3	22.7	2.58	63	5.2
Slope materials									
99S-140	16.9	1.5	0.5	0	19.2	23.7	2.05	81	5.4
99S-167	19.5	1.3	0	0	21.1	22.4	0.16	94	6.2
Background soils									
99S-168	8.8	3.7	0	0	12.6	16.6	0.27	76	4.8
99S-169	2.2	0.5	0.1	0	2.9	14.5	1.01	20	4.3
99S-170	5.7	0.9	0.1	0	6.8	20.6	0.28	33	4.1

a. TEC: Total exchangeable cations; b. CEC: Cation exchangeable capacity;

c. ESP : Exchangeable sodium percentage (100 × Na/CEC); d. Base saturation = 100 × TEC/CEC

Table 5-5 Concentration of major elements in soils (unit in wt%)

Sample	SiO_2	TiO_2	Al_2O_3	Fe_2O_{3t}	MnO	MgO	CaO	Na_2O	K_2O	P_2O_5	CO_{2total}	CO_2	C	S_t	Total*	LOI
Soils in mine area																
99S-112	44.8	1.96	11.2	13.0	0.07	0.51	0.64	0.2	1.31	0.40	21.8	0.2	5.9	2.08	82.1	15.3
99S-113	49.2	1.98	12.2	12.0	0.13	0.64	2.97	0.1	1.51	0.39	22.2	1.6	5.6	0.76	89.1	15.6
99S-114	43.3	2.06	11.6	12.7	0.11	0.92	1.02	0.2	1.36	0.45	23.8	0.4	6.4	1.80	82.4	16.5
99S-115	41.3	1.91	10.6	12.3	0.16	0.84	0.80	0.2	1.24	0.34	15.0	0.2	4.0	2.90	76.8	12.8
99S-116	49.6	2.88	14.9	11.4	0.11	0.99	0.81	0.1	1.55	0.44	18.1	0.2	4.9	0.38	88.3	15.3
99S-117	53.0	2.98	14.0	10.2	0.10	0.93	0.66	0.1	1.56	0.36	13.6	0.1	3.7	0.58	88.2	13.5
99S-145	50.7	2.59	12.3	9.9	0.01	0.47	0.20	0.1	1.40	0.31	36.7	<0.1	10.0	1.05	89.0	20.2
99S-151	46.7	3.34	16.3	13.4	0.13	1.16	0.26	0.2	1.24	0.43	11.2	0.1	3.0	0.23	86.5	14.6
99S-153	44.4	2.44	13.3	13.0	0.14	0.69	2.26	0.2	1.09	0.67	34.3	1.0	9.1	0.49	88.8	19.5
99S-154	46.1	2.48	13.2	14.1	0.09	0.53	1.25	0.1	0.97	0.64	29.1	0.3	7.9	0.57	88.3	18.2
99S-159	44.5	2.08	12.9	12.4	0.04	0.52	0.35	0.1	1.27	0.46	47.3	<0.1	12.9	0.70	88.2	24.2
99S-160	36.9	1.33	14.2	11.8	0.04	0.50	1.43	0.1	1.44	0.24	67.0	<0.1	18.3	1.27	87.6	30.5
99S-163	54.3	2.18	12.4	10.7	0.08	0.67	0.37	0.1	1.44	0.54	27.3	<0.1	7.5	0.29	90.6	16.6
99S-164	54.3	3.04	13.4	12.0	0.02	0.71	0.15	0.1	2.15	0.56	13.8	<0.1	3.8	0.69	90.9	13.2
99S-165	53.8	2.35	12.7	11.7	0.05	0.51	0.33	0.1	1.41	0.38	22.9	0.1	6.2	0.59	90.2	15.7
99S-166	54.7	2.23	12.1	12.8	0.04	0.55	0.28	0.1	1.48	0.37	17.7	<0.1	4.8	0.82	90.3	13.2
Alluvial deposits or foundation soils																
99S-101	42.9	3.06	13.7	14.6	0.11	0.78	2.28	0.1	1.02	0.38	31.6	1.2	8.3	0.70	89.1	17.4
99S-102	45.2	2.61	11.3	14.5	0.07	0.60	1.20	0.1	1.33	0.28	23.0	0.6	6.1	1.81	85.7	15.0
99S-121	47.1	2.96	15.0	13.0	0.11	0.74	0.97	0.1	1.08	0.63	24.2	0.3	6.5	0.25	88.8	16.9
99S-122	46.7	2.57	12.8	13.4	0.05	0.56	0.53	0.1	1.27	0.40	38.0	0.1	10.3	0.64	89.5	19.8
99S-128	48.9	3.42	14.6	12.5	0.13	0.95	0.44	0.1	1.16	0.53	17.1	0.2	4.6	0.26	87.7	15.4
99S-129	49.7	3.29	15.2	13.2	0.12	0.93	0.56	0.1	1.16	0.43	17.0	0.1	4.6	0.18	89.5	14.6
99S-130	53.5	3.04	14.1	10.6	0.1	0.71	0.55	0.1	1.31	0.36	15.8	0.2	4.3	0.45	89.3	13.1
99S-131	50.5	3.22	15.6	13.8	0.11	0.72	0.68	0.1	1.01	0.33	13.7	<0.1	3.7	0.23	90.0	12.8
99S-133	47.7	2.53	13.1	14.7	0.06	0.55	0.43	0.1	1.22	0.59	30.2	0.1	8.2	0.73	90.0	17.9
99S-135	47.9	3.00	13.6	13.2	0.12	0.77	0.52	0.1	1.04	0.49	26.1	<0.1	7.1	0.38	88.3	17.2

Table 5-5 (continued)

Sample	SiO_2	TiO_2	Al_2O_3	Fe_2O_{3t}	MnO	MgO	CaO	Na_2O	K_2O	P_2O_5	CO_{2t}	CO_2	C	S_t	Total*	LOI
99S-137	47.0	3.17	15.7	13.3	0.08	1.05	0.43	0.1	1.26	0.52	18.5	<0.1	5.0	0.24	87.9	16.4
99S-141	43.2	1.73	14.3	10.7	0.12	0.59	0.68	0.1	1.44	0.56	50.5	<0.1	13.8	0.43	87.7	24.9
99S-144	44.8	2.59	15.1	12.6	0.13	0.83	1.33	0.1	1.39	0.58	27.6	<0.1	7.5	0.31	87.2	18.6
99S-150	50.2	2.85	14.5	12.5	0.08	0.93	0.22	0.1	1.24	0.49	16.7	<0.1	4.6	0.51	88.2	15.1
99S-203	44.3	2.92	15.0	15.6	0.12	1.11	2.06	0.1	1.21	0.46	21.0	1.0	5.5	0.34	89.8	16.5
99S-204	43.5	3.62	17.0	14.4	0.16	1.17	1.10	0.1	1.12	0.37	14.5	0.2	3.9	0.17	86.9	16.4
Natural soils																
99S-108	75.4	2.89	10.8	2.4	0.00	0.16	0.07	0.1	0.29	0.39	1.5	<0.1	0.4	0.39	98.7	nd
99S-120	49.1	2.64	15.4	12.4	0.23	1.01	0.50	0.1	1.51	0.61	18.2	0.2	4.9	0.11	88.6	15.4
99S-142	46.3	3.37	15.6	13.7	0.13	1.23	0.46	0.2	1.28	0.57	17.3	<0.1	4.7	0.13	87.7	15.9
99S-148	44.3	3.99	18.8	15.8	0.18	0.59	0.06	0.0	0.74	0.41	9.3	0.2	2.5	0.06	99.7	12.0
99S-149	48.8	4.27	19.1	15.3	0.14	0.48	0.05	0.0	0.69	0.45	3.3	<0.1	0.9	0.06	100.1	9.8
99S-172	50.1	2.20	14.7	3.9	0.00	0.56	1.62	0.1	2.13	0.13	46.1	<0.1	12.6	1.28	89.4	21.8
99S-173	47.2	3.03	15.3	12.4	0.07	0.88	0.48	0.1	1.25	0.36	24.6	<0.1	6.7	0.14	87.9	18.2
Slope materials																
99S-136	45.1	3.28	15.9	13.8	0.13	1.01	0.57	0.1	1.17	0.51	19.5	0.1	5.3	0.23	87.2	17.3
99S-140	44.3	2.86	14.6	13.0	0.12	0.80	0.91	0.1	1.13	0.62	31.8	<0.1	8.7	0.31	87.5	19.9
Background																
99S-167	55.6	3.86	13.7	11.7	0.17	1.35	0.67	0.2	1.20	0.15	8.4	0.2	2.2	<0.02	100.9	9.8
99S-168	46.6	4.34	17.3	16.3	0.15	1.84	0.29	0.1	1.53	0.19	5.5	0.1	1.5	0.02	101.1	11.0
99S-169	37.6	4.94	22.6	21.2	0.25	0.93	0.06	0.0	0.53	0.29	1.4	0.2	0.3	0.02	101.6	12.5
99S-170	43.7	3.91	20.1	16.9	0.23	1.15	0.06	0.1	1.40	0.23	3.9	0.2	1.0	0.03	101.2	12.1

*: LOI: Loss of ignition; *: Totals do not include LOIs; Fe_2O_{3t} as total Fe; CO_{2t} as total C; S_t as total S.

Table 5-6 Concentration of trace elements in soils (unit in ppm)

Sample	Ba	Cd	Co	Cr	CS	Cu	Mo	Ni	Pb	Rb	Sb	Sr	Tl	V	Zn	Tl*	Hg*	As*
Soils in mine area																		
99S-112	56000	nd	18	107	8.1	96	10.0	43	89	53	17.0	810	110	181	82	78.2	243	298
99S-113	7600	0.3	24	110	9.1	92	8.8	61	34	60	7.8	780	98	182	105	62.9	264	326
99S-114	54000	0.2	24	107	7.3	85	7.8	59	44	53	7.1	630	87	185	110	69.3	421	212
99S-115	99000	nd	28	100	6.8	81	6.5	58	51	47	7.9	750	170	169	148	136	176	230
99S-116	6300	0.2	36	146	8.3	96	7.7	72	31	68	14.0	600	53	238	123	35.2	353	194
99S-117	4200	nd	28	156	7.6	87	6.8	62	23	65	12.0	730	61	240	96	43.4	505	319
99S-145	6300	nd	8	132	8.2	53	8.6	27	15	54	8.4	930	130	225	46	81.4	410	504
99S-151	1700	0.3	40	142	13.0	127	7.8	70	22	73	3.8	550	150	261	133	97.6	148	262
99S-153	4900	0.6	28	184	7.8	117	18.0	65	41	55	70.0	760	94	219	411	43	122	176
99S-154	7000	0.5	33	193	7.9	128	17.0	69	77	51	77.0	840	110	217	193	63.2	207	185
99S-159	4800	0.4	18	111	11.0	117	14.0	37	100	63	11.0	590	210	180	81	124	243	201
99S-160	1300	0.6	17	82	9.9	98	15.0	38	33	48	8.4	360	282	141	64	165	1.9	153
99S-163	1900	0.3	22	123	7.2	81	9.7	55	30	61	26.0	450	67	195	131	40.4	130	157
99S-164	3900	nd	9	133	9.3	64	6.6	27	30	97	11.0	930	97	244	55	54.4	197	232
99S-165	4400	0.2	18	127	6.6	81	7.8	52	26	58	28.0	970	88	220	109	46.6	192	202
99S-166	12000	nd	14	131	8.2	74	9.1	44	30	65	17.0	890	107	218	93	61.5	186	301
Alluvium deposits or foundation soils																		
99S-101	11000	0.3	33	267	8.3	104	15.0	80	32	48	86.0	590	56	262	249	46.1	950	257
99S-102	36000	nd	23	214	9.3	83	9.9	47	73	51	36.0	780	91	217	80	77.7	225	586
99S-121	2200	0.2	45	268	10.0	236	11.0	86	55	52	27.0	500	21	260	186	13.5	72	115
99S-122	4600	nd	22	197	9.4	115	21.0	60	35	52	24.0	590	61	251	96	45	184	269
99S-128	2300	0.2	43	295	8.0	110	8.0	87	33	63	15.0	510	50	270	163	30.9	135	140
99S-129	2300	0.2	47	298	9.3	119	12.0	91	33	58	21.0	490	40	277	190	24.3	293	137
99S-130	4700	nd	29	203	8.2	86	8.2	53	25	56	13.0	860	87	256	144	72.1	263	308
99S-131	2100	nd	43	294	12.0	123	11.0	79	35	46	29.0	590	48	280	168	39.6	116	158
99S-133	4700	nd	25	206	10.0	117	17.0	52	46	47	34.0	690	50	235	178	31.3	659	424

Table 5-6 (continued)

Sample	Ba	Cd	Co	Cr	CS	Cu	Mo	Ni	Pb	Rb	Sb	Sr	Tl	V	Zn	Tl*	Hg*	As*
99S-135	5700	0.3	40	283	5.8	113	17.0	78	30	47	41.0	660	56	256	143	35.1	137	117
99S-137	2200	0.3	35	265	7.7	133	6.5	86	29	58	24.0	510	40	258	154	26.5	72	106
99S-141	4200	0.5	34	135	11.0	98	10.0	59	33	52	21.0	520	42	161	146	23	375	54
99S-144	2400	0.3	34	135	9.1	122	7.5	66	28	66	12.0	530	51	224	159	29	136	179
99S-150	6600	0.2	24	138	11.0	110	6.5	63	21	56	7.1	730	100	236	119	62	374	338
99S-203	3000	0.4	51	285	7.5	135	9.0	101	33	54	29.0	500	51	272	291	39.1	109	146
99S-204	1000	0.7	55	286	6.4	131	4.7	110	26	55	13.0	300	22	291	180	13.3	40	65
Natural soils																		
99S-108	14000	nd	5	102	2.7	28	2.4	nd	11	16	0.7	1500	12	174	14	2.87	19	59
99S-120	870	0.4	41	140	6.8	108	6.5	90	26	68	13.0	220	10	229	181	6.88	28	89
99S-142	1500	0.3	42	284	6.4	114	5.4	88	27	63	13.0	390	29	278	154	16	62	70
99S-148	290	0.2	76	287	6.5	146	13.0	94	19	47	23.0	1900	7.4	351	118	4.22	13	37
99S-149	290	nd	76	348	5.2	150	30.0	102	16	40	21.0	2400	5.5	374	111	4.48	10	47
99S-172	350	nd	10	101	6.9	25	15.0	16	22	63	16.0	290	2.2	176	50	1.5	0.8	50
99S-173	510	0.4	34	205	7.0	95	6.8	76	25	66	62.0	250	9.4	247	130	6.3	17	319
Slope materials																		
99S-136	2000	0.3	46	275	7.1	117	6.8	90	34	59	22.0	460	46	267	179	27.9	82	96
99S-140	3200	0.5	39	240	6.8	118	10.0	79	31	51	22.0	630	40	253	190	20.2	64	109
Background soils																		
99S-168	310	0.3	60	424	6.8	117	1.5	125	18	80	1.9	98	0.97	344	154	0.33	0.9	4.7
99S-169	150	0.3	64	429	1.4	143	0.8	128	17	33	0.4	16	0.47	391	112	nd	0.3	4.4
99S-170	120	nd	51	367	5.1	96	2.2	98	33	65	1.0	19	0.64	328	100	0.52	0.5	7.5

*: Strong acid extraction; nd as not detectable.

Table 5-7 Distributions of Tl, Hg and As in various soils (unit in ppm)

Soils	Tl[a]		Hg[b]		As[b]	
	Range	Average	Range	Average	Range	Average
Soils in mine area	53-282	120	122-505	249	153-504	247
Slope wash materials	40-46	43	64.4-81.5	73	95.7-109	102.4
Alluvial deposits or foundation soils	21-100	54	40.2-950	258.8	54.4-586	212.4
Undisturbed natural soils	2.2-29	10.8	0.8-61.8	21.3	37.1-89.1	58.6
Background soils	0.47-0.97	0.7	0.26-0.87	0.5	4.4-7.46	5.5

a. Total concentration; b. partial extraction by strong acid.

Table 5-8 Major ions and field parameters of waters in the Lanmuchang area

Sample	Ca (mg/l)	Mg (mg/l)	Na (mg/l)	K (mg/l)	SiO_2 (mg/l)	SO_4 (mg/l)	Cl (mg/l)	HCO_3 (mg/l)	TDS (mg/l)	EC (μS/cm)	pH	T °C	DO (mg/l)
Shallow groundwater													
W1004	48	5.5	0.95	0.84	3.9	25.8	0.33	97.9	183	241	8.01	15.9	7.4
W1001	59	9.1	2.9	0.88	5.5	55.8	0.93	114	249	326	7.74	17	7.94
W1006	200	34	5.3	2	6	354	2.57	199	804	929	6.64	16.8	1.61
W1008	49	2.8	1.2	0.64	3.3	11.1	0.77	108	177	227	8.33	16.2	8.3
W1009	47	3.1	1.3	0.86	4.8	9.33	0.56	113	180	222	8.27	16.2	8.31
W1010	56	1.5	0.53	0.47	2.3	11.1	0.6	125	197	263	7.53	16.4	4.01
W1092	71	5.7	1.6	0.68	2.7	40.9	1.45	134	258	329	7.61	16.5	4.37
W1071	58	4.3	1.2	0.98	5.4	3.39	0.49	143	218	255	7.71	16.5	5.04
W1012	104	6	7.3	6.4	10	111	12.7	143	401	628	7.05	16.3	3.49
W1013	35	3.1	2.6	0.79	6.2	8.07	0.37	93	149	181	8.01	16.7	7.99
W1015	47	3.7	2.2	0.47	4.8	12	0.22	110	180	229	7.19	16.3	7.9
W1051	52	3.9	2.2	0.97	4.7	7.25	1.19	145	217	294	7.33	16.5	5.96
W1096	45	3.4	0.53	0.45	3	2.44	0.42	127	182	238	8.28	10.6	8.66
Deep mine groundwater													
W1003	300	34	1.6	3.6	2.4	612	0.74	151	1106	1305	6.62	18.5	1.79
W1094	290	2.4	0.92	0.81	7.5	225	0.63	nd	527	>2000	3.56	17.8	1.31
W1072	240	21	5.9	0.8	10	806	1.79	nd	1086	>2000	2.61	16.3	0.69
W1097	480	54	3.3	0.88	29	1801	7.7	nd	2376	>2000	2.91	16	0.81
W1104	290	31	2.3	na	59	867	12.9	nd	1262	>2000	2.88	21.5	0.59
Background groundwater													
W1047	76	3.6	1.6	0.68	3	23.8	0.98	170	280	395	7.24	16.4	5.55
W1057	43	3.4	1.9	0.53	5	17.1	0.31	118	190	252	7.31	17.3	6.97
Stream water in base-flow													
W1100	110	15	3.3	2.3	9.4	164	1.33	124	429	319	7.63	16.6	6.8
W1099	62	6	2	1.4	5.3	41	0.93	118	236	313	7.64	16.7	6.9
W1102	64	6.5	2.2	1.5	5.6	48.4	0.99	120	249	318	7.64	16.8	6.31

Table 5-8 (continued)

Sample	Ca (mg/l)	Mg (mg/l)	Na (mg/l)	K (mg/l)	SiO_2 (mg/l)	SO_4 (mg/l)	Cl (mg/l)	HCO_3 (mg/l)	TDS (mg/l)	EC (µS/cm)	pH	T °C	DO (mg/l)
Stream water in base-flow													
W1103	67	6.9	2.7	1.9	6	53.9	1.4	121	261	336	7.36	16.7	5.27
W1061	77	7.4	8.4	3	6.9	70.1	3.03	135	311	402	7.1	16.4	7.5
W1016	55	5	3.4	1.4	3.2	28.7	1.48	119	217	283	7.9	16.5	5.51
W1035	50	5.7	4	2	4.4	39.5	1.97	133	240	325	7.64	13.3	8.19
W1065	65	5.9	4.2	2.8	9	69.7	2.04	137	296	333	6.24	14.5	6.94
W1070	67	6.2	3.8	3.3	9.4	90	2.53	78	260	355	7.05	14.6	8.48
W1002	65	5.5	3.6	3	7.8	68.4	2.53	97	252	331	7.71	14	8.18
W1098	55	4.5	2.1	1.3	4.7	22.6	0.91	123	215	276	7.94	17	7.32
W1045	46	4	2.5	0.87	1.9	10.2	1.09	109	176	331	8.6	16.6	9.24
Stream water in flood-flow													
W1124	65	10	3.2	0.9	5.5	na	na	na		346	5.8	17.1	4
W1125	100	16	3.3	1.3	6.4	na	na	na		610	6.3	17.7	4.8
W1126	47	4.2	2	1.3	4.2	na	na	na		232	7.01	17.4	na
W1127	56	6.2	2.4	1.3	4.6	na	na	na		274	6.92	17.5	2.7
W1128	62	7.1	2.5	1.5	4.8	na	na	na		305	6.2	19.2	4.54
W1131	63	7.1	2.9	1.9	5.1	na	na	na		342	7.4	17.8	na
W1135	65	7	3.2	2.1	5.2	na	na	na		347	6.8	18.3	na
W1137	53	4.8	2.2	1.4	4.3	na	na	na		288	7.7	18.7	na
W1139	56	5.3	2.6	1.7	4.6	na	na	na		312	6.7	20.1	na
W1140	57	5.3	2.6	1.8	4.9	na	na	na		298	6.24	20.4	na
W1141	57	5.3	2.7	1.9	5	na	na	na		301	6.39	22.5	na
W1142	57	5.2	2.8	27	5	na	na	na		290	6.42	23	na
W1136	48	3.6	1.8	1.1	3.9	na	na	na		235	7.5	19.8	na
W1132	110	4.2	5.5	4.5	5.4	na	na	na		502	7.19	16.6	1.78
Acid mine drainage													
W1143	400	39	na.	na	24	na	na	na		869	3.81	21.1	1.47

na= not analyzed; nd= not detectable.

Table 5-9 Concentration of trace elements in groundwaters and stream waters (in µg/l)

Sample	Al	Fe	Mn	Li	B	Rb	Sr	Sb	As	Tl	Hg
Shallow groundwater											
W1004	1.5	7	0.30	1.48	2.8	1.50	220	<0.05	0.2	0.752	0.171
W1001	32.0	43	9.50	3.94	5.2	0.82	1500	0.07	<0.2	0.123	1.305
W1006	3.0	420	320	9.71	15.4	2.20	4100	0.27	1.4	0.182	0.363
W1008	6.8	<3	0.25	0.04	1.7	0.52	380	0.08	0.3	<0.005	0.491
W1009	7.6	6	0.37	0.39	1.2	1.40	340	0.27	0.3	<0.005	0.644
W1010	6.4	8	8.20	0.18	<0.5	0.68	280	0.32	0.3	0.037	0.188
W1092	6.7	12	1.30	0.36	1.3	1.10	430	0.13	0.7	0.026	0.106
W1071	3.3	<3	0.16	0.99	1.0	1.80	360	0.18	0.6	0.008	0.344
W1012	5.0	40	32.10	0.47	12.3	2.63	522	0.44	2.3	0.377	0.248
W1013	2.8	3	0.18	1.48	1.6	0.69	230	<0.05	<0.2	0.006	0.509
W1015	3.1	10	12.00	0.62	1.7	0.80	250	0.12	<0.2	0.006	0.778
W1051	5.2	33	0.49	0.15	1.7	1.00	550	<0.05	0.2	0.036	0.280
W1096	26	33	3.00	0.33	<0.5	0.76	190	<0.05	0.2	0.088	0.198
Deep mine groundwater											
W1003	55	72382	1870	16.72	5.2	4.69	12380	0.13	540.0	13.4	0.898
W1094	20351	7956	275	10.17	3.2	3.81	81	0.01	43.9	62.3	0.199
W1072	37000	130000	2100	25.11	15.7	10.00	610	1.30	250.0	1102	1.270
W1097	300000	420000	4600	248.81	232.0	18.00	880	3.00	200.0	54.4	0.240
W1104	460000	450000	7300	253.64	230.8	38.00	450	0.06	23.0	470	0.196
Background groundwater											
W1047	7.6	10	28.00	0.10	1.5	0.56	510	<0.05	0.6	<0.005	0.163
W1057	7.2	<3	1.00	1.19	1.4	0.64	380	<0.05	<0.2	<0.005	0.135

Table 5-9 (continued)

Sample	Al	Fe	Mn	Li	B	Rb	Sr	Sb	As	Tl	Hg
Stream water in base-flow											
W1100	8.0	720	100	4.57	9.3	2.9	1900	0.10	18.0	4.8	0.097
W1099	14.0	130	38	1.09	5.3	2	670	0.34	4.1	0.76	0.075
W1102	9.6	33	19	1.32	4.9	2.1	740	0.34	3.8	0.99	0.056
W1103	12.0	210	47	1.56	5.3	2.7	780	0.39	14.0	1.42	0.059
W1061	15.0	240	150	2.09	7.2	3.9	830	0.56	20.0	2.07	0.173
W1016	26.0	74	48	0.79	3.1	1.8	440	0.55	5.6	0.8	0.634
W1035	22.0	140	51	1.15	4.2	2.3	510	0.50	7.9	3.09	0.198
W1065	4.0	<3	270	3.47	13.9	5	530	0.37	10.0	33	0.212
W1070	53.0	780	450	2.46	12.7	5.5	500	0.28	25.0	30.8	0.212
W1002	18.0	100	270	1.93	10.4	4.7	450	0.24	14.0	19.3	0.241
W1098	26.0	210	28	0.48	8.1	1.9	460	0.41	1.6	0.09	0.079
W1045	31.0	64	19	0.16	1.4	1.2	330	0.56	1.0	0.12	0.221
Stream water in flood-flow											
W1124	16	1100	19	3.24	4.6	0.83	1600	0.10	0.1	0.3	<0.003
W1125	28.0	2100	290	6.02	6.8	1.5	1900	0.08	1.9	3.3	0.073
W1126	32.0	33	31	0.46	3.5	1.5	380	0.16	0.8	0.19	0.042
W1127	54.0	300	78	1.42	4.1	1.6	620	0.16	0.9	0.73	0.042
W1128	11.0	6	0.21	1.62	5.0	1.8	750	0.28	0.3	1.1	0.083
W1131	12.0	10	0.27	1.68	5.8	2.1	740	0.30	1.3	1.6	0.083
W1135	13.0	12	0.18	1.71	6.5	2.3	730	0.49	2.1	2.1	0.006
W1137	12.0	7	0.1	0.61	3.5	1.7	460	0.34	1.3	0.67	0.052
W1139	13.0	12	0.11	0.88	4.4	2.1	510	0.38	2.3	1.4	0.004
W1140	9.8	9	0.27	0.87	4.5	2.2	500	0.32	1.8	3	<0.003
W1141	7.8	4	0.13	0.90	5.0	2.5	500	0.35	3.0	4.2	<0.003
W1142	25.0	210	2.9	1.05	5.3	3.9	480	0.42	6.5	4.5	<0.003
W1136	8.9	<3	0.14	0.15	1.6	1.4	310	0.37	0.4	0.07	<0.003
W1132	2.7	<3	2.7	0.27	8.1	1.8	440	0.35	0.5	0.22	0.004
Acid mine drainage											
W1143	220.0	150	2.9	200.00	188.4	17	1100	0.06	48.0	59	0.010

Table 5-10 Concentration of trace elements in sediments (ppm)*

Sample	Ba	Co	Cr	Cu	Mn	Ni	Pb	Rb	Sb	Sr	Tl	V	Zn	Tl*	As*	W*	Hg*
SD1122	11000	9	103	52	4.4	23	18	79	3.5	907	63	217	54	54.5	643	23.1	0.100
SD1121	7300	14	125	103	9.4	35	29	65	4.6	520	49	240	110	25.0	92.4	18.3	0.097
SD1123	8100	10	110	51	5.9	24	18	78	3.0	794	61	223	57	44.6	506	19.0	0.062
SD1125	8300	42	117	144	7.5	70	24	62	6.9	715	54	212	132	27.3	186	17.1	0.057
SD1126	1400	71	456	116	3.4	110	23	57	13.0	196	6	320	202	1.9	33.3	4.3	0.023
SD1127	3700	69	368	121	4.4	109	23	56	15.0	283	11	300	190	4.2	53.9	6.7	0.023
SD1137	1700	57	409	113	3.1	102	28	55	16.0	256	10	317	177	4.2	25.7	4.5	0.019
SD1139	2800	55	443	111	3.5	100	23	54	16.0	282	16	318	174	7.0	36.4	6.4	0.024
SD1140	2300	57	419	111	4.0	101	21	54	15.0	378	21	317	165	9.0	41.7	6.6	0.023
SD1142	1500	56	436	110	3.0	102	19	53	13.0	365	16	317	154	6.3	43.0	4.5	0.015
SD1098	1100	60	424	112	4.4	104	25	55	12.0	225	8	299	214	2.2	49.3	27.8	0.029
SD1099	3500	57	264	124	5.3	97	28	54	11.0	386	22	257	204	6.7	224	17.9	0.035
SD1100	7800	40	144	124	9.0	77	25	56	13.0	596	51	224	176	33.6	543	28.2	0.068
SD1035	1400	51	307	107	3.3	94	29	53	17.0	350	21	285	211	8.0	96.2	14.1	0.038
SD1065	1300	51	333	110	3.3	99	24	53	12.0	329	35	305	204	24.4	95.1	5.5	0.026
SD1066	490	50	326	96	2.0	95	19	69	23.0	330	2	291	189	0.5	9.4	0.3	0.009
SD1002	660	57	353	107	2.4	104	20	60	9.0	249	21	303	163	8.7	63.6	4.1	0.019
SD1112	540	61	372	115	2.2	111	19	59	9.0	260	20	317	166	8.5	38.7	4.4	0.013
SD1113	790	45	409	112	2.5	101	20	57	8.3	287	23	314	148	7.8	33.8	6.3	0.047
SD1012	2400	27	212	100	8.0	71	35	57	42.0	512	62	248	293	42.5	237	30.5	0.102
SD1086	3800	10	140	47	5.3	22	12	62	31.0	1117	75	245	44	73.5	345	35.4	0.052
SD1091	330	78	512	108	2.0	105	23	62	4.1	526	1	317	190	0.4	14.2	0.3	0.009
SD1094	2600	6	122	25	52.0	-10	10	32	0.6	495	190	354	16	115	2068	5039	1.093
SD1040	9600	12	120	50	14.0	38	17	97	7.5	2028	3800	202	54	3091	3238	205	0.110
SD1138	1200	44	148	126	4.5	75	20	68	20.0	840	340	278	124	276.3	434	22.1	0.072

*: Data are determined by disc fusion ICP-MS except for As, W and Hg by enzyme leaching; Tl is by both methods and Hg is of semi-quantitative determination

Table 5-11 Concentration of major elements in ash of crops and vegetation
(unit in ppm unless otherwise indicated)

Sample	Ash yield(%)	Na%	K%	Mg%	Ca%	Fe%	Mn	Al	Si
Chinese cabbage									
B109	26.2	2.95	nd	1.32	15.5	0.12	212	469	682
B116	25.2	2.69	nd	1.06	12.6	0.11	109	525	970
B118	25.9	1.87	nd	1.52	17.6	0.19	188	525	904
B134	24.7	3.82	nd	1.04	13.9	0.14	215	619	900
B138	24.6	4.08	nd	1.20	14.9	0.15	201	713	1240
B148	24.7	3.75	nd	0.914	15.3	0.13	105	605	885
B151	25.8	nd	nd	1.12	12.9	0.14	492	774	1410
B158	23.1	2.40	nd	1.34	13.8	0.15	336	929	1060
B162	26.9	1.95	nd	1.14	13.0	0.12	209	520	442
B210	24.3	1.63	nd	1.76	24.8	0.19	353	1060	658
B211	15.6	0.92	nd	2.39	7.60	0.10	507	197	298
B101	26.3	3.44	nd	0.99	12.0	0.09	204	294	460
B128	16.4	4.52	nd	1.36	14.9	0.16	203	715	1080
Green cabbage									
B111	16.4	0.84	nd	1.74	17.5	0.13	242	389	1210
B200	24.4	4.04	nd	2.23	20.9	0.15	928	449	726
B201	25.4	1.48	nd	1.97	23.0	0.16	347	544	661
B205	23.3	1.61	nd	1.71	28.6	0.16	311	403	535
B212	20.8	2.31	nd	1.74	24.3	0.26	732	1390	1330
Chili									
B303	9.4	0.03	nd	1.71	1.68	0.18	247	471	443
B304	11.7	0.05	nd	1.58	0.56	0.14	433	242	313
B305	6.7	0.05	nd	2.31	1.03	0.32	310	844	608
B306	10.7	0.03	nd	1.44	0.57	0.15	169	354	390
B307	12.8	0.04	nd	2.26	0.53	0.11	147	155	191
Corn									
B403	1.48	nd	nd	8.21	0.57	0.12	588	178	261
B404	1.28	0.02	nd	8.95	0.55	0.15	353	254	351
B405	1.26	0.05	nd	7.40	0.33	0.12	470	1870	550
B406	1.55	nd	nd	6.05	0.49	0.14	535	121	269
B407	1.35	0.02	nd	9.59	0.33	0.16	401	153	254
B408	1.46	0.03	nd	7.60	0.61	0.14	518	140	253
B409	1.55	nd	nd	8.14	0.27	0.11	456	122	207
B410	1.15	0.02	nd	7.84	0.57	0.29	704	157	422
B411	1.14	nd	nd	7.61	0.52	0.24	463	313	225
B412	1.43	nd	nd	8.87	0.32	0.14	469	129	144
B413	1.26	0.02	nd	9.35	0.44	0.23	537	205	191
B414	1.26	nd	nd	8.66	0.40	0.23	431	122	159
B415	1.36	0.01	nd	6.95	0.43	0.16	505	128	187

Table 5-11 (continued)

Sample	Ash yield(%)	Na%	K%	Mg%	Ca%	Fe%	Mn	Al	Si
Rice									
B504	1.59	0.03	nd	7.08	0.81	0.116	1650	494	504
B505	1.67	0.04	nd	6.70	0.72	0.103	1590	436	572
B506	1.73	0.05	nd	6.82	0.74	0.128	1370	559	581
B507	1.48	0.09	nd	8.01	0.71	0.090	1070	543	587
B508	1.51	0.05	nd	8.39	0.70	0.100	1280	398	494
B509	1.54	0.16	nd	7.76	0.76	0.138	1070	1240	633
B510	1.52	0.05	nd	7.84	0.73	0.101	1920	531	506
B511	1.52	0.12	nd	8.20	0.70	0.083	1760	623	596
Carrot root									
B156	23.5	0.26	nd	1.81	16.5	0.281	4510	2150	2420
Fern leaf									
B203	14.3	0.19	nd	2.77	14.8	2.38	2400	10600	1950
Wild cabbage									
B204	11.3	0.17	nd	3.28	14.3	3.65	2840	7180	2040
B206	6.57	0.02	nd	2.59	4.34	0.81	8930	43000	2450

Table 5-12 Concentration of trace elements in ash of crops and vegetation (Hg is based on dry weigh, unit all in ppm)

Sample	Ash yield(%)	Tl	As	Ni	Cu	Zn	Rb	Sr	Mo	Cd	Ba	Sb	W	Pb	Hg
Chinese cabbage															
B109	26.17	3.78	3.0	6.32	26.3	183	323	1000	7.93	1.42	424	0.59	1.8	8.67	0.448
B116	25.24	3.46	2.8	7.10	21.9	173	255	1080	7.17	0.70	160	0.51	0.8	9.72	0.529
B118	25.92	4.06	3.4	10.7	23.2	217	443	1770	7.89	1.65	381	0.63	0.4	7.95	0.257
B134	24.73	2.84	2.5	8.45	37.3	284	266	709	3.46	1.23	143	0.76	0.4	10.8	0.377
B138	24.58	4.82	3.9	7.29	22.4	198	367	821	15.2	1.26	200	1.02	0.7	48.9	0.299
B148	24.72	1.24	3.7	3.39	20.8	188	280	680	7.45	0.63	165	0.82	4.0	6.25	0.571
B151	25.81	21.1	4.8	12.6	21.6	356	304	597	1.78	0.98	212	0.76	1.2	5.49	0.701
B158	23.09	16.4	4.0	7.57	41.7	160	444	720	1.24	0.65	323	0.54	1.3	5.77	0.673
B162	26.95	54.2	2.6	13.8	29.3	213	352	632	2.19	1.30	333	0.54	0.2	7.86	0.377
B210	24.25	21.9	3.0	3.95	14.4	123	465	935	2.30	0.62	97.3	0.70	0.1	4.00	0.153
B211	15.57	8.29	1.1	14.7	36.0	286	806	378	1.36	1.15	198	0.22	0.1	2.73	0.089
B101	26.27	0.82	2.2	9.89	28.5	195	318	747	5.06	0.68	239	0.47	0.2	5.15	0.261
B128	16.39	1.90	2.3	13.1	39.9	240	509	680	5.37	3.83	224	0.96	0.3	13.5	0.3
Green cabbage															
B111	16.41	2.36	1.9	11.1	21.2	206	277	1110	6.69	0.58	316	0.49	0.9	4.47	0.329
B200	24.37	492	3.7	10.9	12.7	376	245	1220	3.80	1.43	336	0.28	1.7	2.77	0.718
B201	25.40	1570	3.3	6.12	11.4	131	215	1840	5.55	0.67	244	0.25	6.4	2.79	0.706
B205	23.32	2120	1.6	2.64	11.4	137	561	1480	5.14	1.19	198	0.26	0.4	1.97	0.452
B212	20.81	152	4.7	13.1	18.0	220	308	1170	6.26	1.83	268	0.85	1.9	4.80	1.26
Chili															
B303	9.38	31.0	3.1	26.9	76.0	146	187	67.7	1.21	0.47	42.7	0.27	0.2	2.46	0.041
B304	11.7	3.02	2.1	59.0	64.9	135	250	17.6	0.431	0.85	14.4	0.18	0.1	1.79	0.019
B305	6.74	11.4	2.2	37.32	117	360	642	30.4	0.665	1.68	22.1	0.36	0.1	4.20	0.008
B306	10.67	1.80	1.3	17.1	61.0	104	229	14.0	1.41	0.49	7.9	0.16	0.2	1.87	0.008
B307	12.83	41.4	1.9	9.24	67.0	158	115	19.9	5.14	0.36	11.1	0.11	0.6	1.39	0.013
Corn															
B403	1.48	90.9	1.3	29.3	153	1360	431	26.6	2.25	0.38	30.8	0.10	-0.1	4.17	-0.005

Table 5-12 (continued)

Sample	Ash yield(%)	Tl	As	Ni	Cu	Zn	Rb	Sr	Mo	Cd	Ba	Sb	W	Pb	Hg
B404	1.28	60.7	1.3	11.9	111	1340	237	24.7	20.8	1.26	18.2	0.26	0.4	3.41	-0.005
B405	1.26	151	1.3	27.9	81.3	1350	583	26.8	6.47	3.40	12.9	0.14	0.1	2.57	-0.005
B406	1.55	15.6	0.7	14.9	83.2	840	526	15.2	0.66	1.65	7.2	0.18	-0.1	1.61	-0.005
B407	1.35	121	1.6	18.2	93.8	1440	220	25.8	7.30	0.44	3.4	0.13	-0.1	1.92	-0.005
B408	1.46	211	1.7	10.6	209	1300	571	42.0	13.3	0.89	55.5	0.19	0.2	2.39	-0.005
B409	1.55	5.52	1.6	8.19	59.6	1110	418	15.0	28.4	3.92	7.7	0.27	-0.1	2.55	-0.005
B410	1.15	22.4	3.2	18.6	115	2170	365	31.4	35.4	4.20	27.1	0.19	0.5	8.81	0.007
B411	1.14	91.9	2.8	18.7	154	1500	611	23.5	3.41	2.57	45.4	0.32	0.2	3.45	-0.005
B412	1.43	54.8	1.4	7.18	96.9	1640	436	16.6	16.3	1.10	12.6	0.19	-0.1	2.65	-0.005
B413	1.26	114	1.5	20.5	100	1650	371	21.6	37.7	12.5	7.1	0.43	0.1	9.02	-0.005
B414	1.26	113	0.8	7.77	110	1400	231	12.5	3.06	0.71	3.2	0.19	0.2	2.66	-0.005
B415	1.36	3.80	1.7	15.7	96.8	1940	431	20.0	9.81	6.56	19.5	0.21	0.2	7.41	-0.005
Rice															
B504	1.59	146	6.5	6.44	47.5	1530	883	38.6	13.5	0.95	123	0.17	0.1	3.94	0.022
B505	1.67	59.8	9.7	8.53	26.0	1040	360	48.8	17.0	1.57	36.6	0.22	0.2	2.05	0.03
B506	1.73	18.0	7.4	7.63	13.5	1060	621	52.0	14.5	0.50	47.7	0.20	0.2	3.12	0.022
B507	1.48	353	11.8	10.3	9.82	1140	301	70.3	11.0	1.88	40.0	0.22	-0.1	2.68	0.019
B508	1.51	11.1	21.2	5.02	46.7	1280	1120	31.4	14.6	1.56	50.0	0.22	-0.1	2.72	0.009
B509	1.54	21.0	13.4	3.34	47.0	903	863	84.2	20.5	0.56	80.6	0.38	0.8	3.66	0.042
B510	1.52	71.4	9.4	5.65	103	1160	473	58.0	12.1	1.23	53.4	0.57	0.1	3.25	0.035
B511	1.52	17.8	4.0	4.59	70.4	1330	1730	35.2	11.5	0.96	25.1	0.18	-0.1	2.55	0.013
Carrot root															
B156	23.49	91.8	5.4	71.9	21800	457	483	1030	2.66	3.62	254	1.07	1.2	8.23	0.549
Fern leaf															
B203	14.27	330	120	45.7	125	386	196	927	4.17	4.26	439	0.503	11.8	14.2	12.5
Wild cabbage															
B204	11.31	221	77.9	35.1	141	717	244	919	7.00	3.95	305	1.297	25.0	23.2	4.19
B206	6.57	220.8	35.4	21.7	47.3	338.1	425.1	498.0	2.6	3.45	285	0.658	1.13	110	0.45

Table 5-13 Concentration of major elements in crops and vegetation in dry weight (ppm)

Sample	Na	K	Mg	Ca	Fe	Mn	Al	Si
Chinese cabbage								
B109	7720	nd	3460	40654	316	565	123	179
B116	6779	nd	2666	31912	280	27	133	245
B118	4853	nd	3934	45629	488	49	136	234
B134	9445	nd	25709	34267	340	53	153	223
B138	10030	nd	2943	36510	374	49	175	305
B148	9279	nd	2259	379011	318	26	150	219
B151	nd	nd	2880	33309	369	127	200	364
B158	5552	nd	3100	31968	345	78	215	245
B162	5255	nd	3063	35073	333	56	140	119
B210	3960	nd	4266	60249	452	86	257	159
B211	1438	nd	3720	11834	161	79	316	46
B101	9045	nd	2590	31427	239	54	77	121
B128	7402	nd	2223	24457	257	33	117	177
Green cabbage								
B111	1374	nd	2856	28756	215	40	64	199
B200	9836	nd	5443	50847	373	226	109	177
B201	3758	nd	5017	58498	398	88	138	168
B205	3766	nd	3990	66690	361	73	94	125
B212	4801	nd	3627	50546	546	152	289	277
Chili								
B303	29.8	nd	1608	1572	156	23	44	42
B304	52.8	nd	1843	649	167	51	28	37
B305	37.0	nd	1556	693	213	21	57	41
B306	36.1	nd	1534	613	160	18	38	42
B307	46.6	nd	2896	683	146	19	20	25
Corn								
B403	nd	nd	1212	85	18	9	3	4
B404	2	nd	1149	71	20	5	3	5
B405	7	nd	934	41	15	6	24	7
B406	nd	nd	940	76	22	8	2	4
B407	2	nd	1294	45	21	5	2	3
B408	4	nd	1111	89	21	8	2	4
B409	nd	nd	1262	42	17	7	2	3
B410	2	nd	901	65	33	8	2	5
B411	nd	nd	868	59	28	5	4	3
B412	nd	nd	1270	46	19	7	2	2
B413	2	nd	1173	55	29	7	3	2
B414	nd	nd	1091	51	29	5	2	2
B415	2	nd	945	58	22	7	2	3

Table 5-13 (continued)

Sample	Na	K	Mg	Ca	Fe	Mn	Al	Si
Rice								
B504	5	nd	1126	129	19	26	8	8
B505	7	nd	1118	121	17	27	7	10
B506	9	nd	1180	129	22	24	10	10
B507	13	nd	1185	105	13	16	8	9
B508	7	nd	1266	106	15	19	6	8
B509	24	nd	1195	117	21	17	19	10
B510	8	nd	1191	110	15	29	8	8
B511	18	nd	1247	106	13	27	10	9
Carrot root								
B156	612	nd	4261	38785	660	1060	505	569
Fern leaf								
B203	270	nd	3950	21138	3398	343	1513	278
Wild cabbage								
B204	189	nd	3709	16121	4124	321	812	231
B206	13	nd	1703	2854	532	587	2825	161

*: Converted from source data in Table 5-10

Table 5-14 Concentration of trace elements in crops and vegetation in dry weight (unit in ppm)*

Sample	Tl	As	Ni	Cu	Zn	Rb	Sr	Mo	Cd	Ba	Sb	W	Pb	Hg
Chinese cabbage														
B109	0.99	0.78	1.7	6.9	48	84	262	2.1	0.37	111	0.15	0.47	2.3	0.45
B116	0.87	0.71	1.8	5.5	44	64	273	1.8	0.18	40	0.13	0.19	2.5	0.53
B118	1.05	0.87	2.8	6.0	56	115	459	2.1	0.43	99	0.16	0.09	2.1	0.26
B134	0.70	0.61	2.1	9.2	70	66	175	0.9	0.3	35	0.19	0.1	2.7	0.38
B138	1.19	0.96	1.8	5.5	49	90	202	3.8	0.31	49	0.25	0.18	12.0	0.30
B148	0.31	0.91	0.8	5.2	47	69	168	1.8	0.16	41	0.20	0.99	1.5	0.57
B151	5.44	1.25	3.3	5.6	92	78	154	0.5	0.25	55	0.20	0.3	1.4	0.70
B158	3.79	0.91	1.8	9.6	37	103	166	0.3	0.15	75	0.12	0.3	1.3	0.67
B162	14.60	0.70	3.7	7.9	57	95	170	0.6	0.35	90	0.15	0.06	2.1	0.38
B210	5.30	0.73	1.0	3.5	30	113	227	0.6	0.15	24	0.17	0.03	1.0	0.15
B211	1.30	0.17	2.3	5.6	44	126	59	0.2	0.18	31	0.03	0.02	0.4	0.09
B101	0.22	0.57	2.6	7.5	51	84	196	1.3	0.18	63	0.12	0.04	1.4	0.26
B128	0.31	0.37	2.2	6.5	39	83	111	0.9	0.63	37	0.16	0.05	2.2	0.30
Green cabbage														
B111	0.4	0.32	1.8	3.5	34	46	182	1.1	0.1	52	0.08	0.14	0.7	0.33
B200	119.8	0.89	2.7	3.1	92	60	297	0.9	0.35	82	0.07	0.42	0.7	0.72
B201	398.8	0.84	1.6	2.9	33	55	467	1.4	0.17	62	0.06	1.63	0.7	0.71
B205	494.4	0.38	0.6	2.7	32	131	345	1.2	0.28	46	0.06	0.09	0.5	0.45
B212	31.7	0.98	2.7	3.8	46	64	243	1.3	0.38	56	0.18	0.41	1.0	1.26
Chili														
B303	2.91	0.29	2.5	7.1	14	18	6.4	0.1	0.04	4.0	0.02	0.02	0.23	0.04
B304	0.35	0.24	6.9	7.6	16	29	2.1	0.1	0.1	1.7	0.02	0.01	0.21	0.02
B305	0.77	0.15	2.5	7.9	24	43	2.1	0.0	0.11	1.5	0.02	0.01	0.28	0.01
B306	0.19	0.14	1.8	6.5	11	24	1.5	0.2	0.05	0.8	0.02	0.03	0.2	0.01
B307	5.31	0.24	1.2	8.6	20	15	2.6	0.7	0.05	1.4	0.01	0.08	0.18	0.01
Corn														
B403	1.34	0.02	0.4	2.3	20	6	0.4	0.03	0.01	0.45	0	0	0.06	-0.005

Table 5-14 (continued)

Sample	Tl	As	Ni	Cu	Zn	Rb	Sr	Mo	Cd	Ba	Sb	W	Pb	Hg
B404	0.78	0.02	0.2	1.4	17	3	0.3	0.3	0.02	0.2	0	0	0.04	-0.005
B405	1.90	0.02	0.4	1.0	17	7	0.3	0.1	0.04	0.2	0	0	0.03	-0.005
B406	0.24	0.01	0.2	1.3	13	8	0.2	0.0	0.03	0.1	0	0	0.03	-0.005
B407	1.64	0.02	0.3	1.3	19	3	0.4	0.1	0.01	0.1	0	0	0.03	-0.005
B408	3.08	0.02	0.2	3.1	19	8	0.6	0.2	0.01	0.8	0	0	0.03	-0.005
B409	0.09	0.03	0.1	0.9	17	6	0.2	0.4	0.06	0.1	0	0	0.04	-0.005
B410	0.26	0.04	0.2	1.3	25	4	0.4	0.4	0.05	0.3	0	0.01	0.1	0.007
B411	1.05	0.03	0.2	1.8	17	7	0.3	0.0	0.03	0.5	0	0	0.04	-0.005
B412	0.78	0.02	0.1	1.4	23	6	0.2	0.2	0.02	0.2	0	0	0.04	-0.005
B413	1.43	0.02	0.3	1.3	21	5	0.3	0.5	0.16	0.1	0.01	0	0.11	-0.005
B414	1.42	0.01	0.1	1.4	18	3	0.2	0.0	0.01	0.0	0	0	0.03	-0.005
B415	0.05	0.02	0.2	1.3	26	6	0.3	0.1	0.09	0.3	0	0	0.1	-0.005
Rice														
B504	2.32	0.10	0.1	0.8	24	14	0.6	0.2	0.02	2.0	0	0	0.06	0.02
B505	1.00	0.16	0.1	0.4	17	6	0.8	0.3	0.03	0.6	0	0	0.03	0.03
B506	0.31	0.13	0.1	0.2	18	11	0.9	0.3	0.01	0.8	0	0	0.05	0.02
B507	5.22	0.18	0.2	0.2	17	4	1.0	0.2	0.03	0.6	0	0	0.04	0.02
B508	0.17	0.32	0.1	0.7	19	17	0.5	0.2	0.02	0.8	0	0	0.04	0.01
B509	0.32	0.21	0.1	0.7	14	13	1.3	0.3	0.01	1.2	0.01	0.01	0.06	0.04
B510	1.09	0.14	0.1	1.6	18	7	0.9	0.2	0.02	0.8	0.01	0	0.05	0.04
B511	0.27	0.06	0.1	1.1	20	26	0.5	0.2	0.01	0.4	0	0	0.04	0.01
Carrot root														
B156	21.6	1.26	16.9	5121	107	113	242	0.6	0.85	59.7	0.25	0.28	1.93	0.55
Fern leaf														
B203	47.1	17.1	6.5	17.9	55	28	132	0.6	0.61	62.7	0.07	1.69	2.02	12.5
Wild cabbage														
B204	24.9	8.8	4.0	16.0	81	28	103.9	0.8	0.45	34.5	0.15	2.82	2.63	4.19
B206	14.5	2.3	1.4	3.1	22	28	32.7	0.2	0.23	18.7	0.04	0.07	7.26	0.45

*: Converted from source data (except for Hg) in Table 5-12

Table 5-15 Average level of the heavy metals in plants*

Metals	Land plants (ppm)	Edible plants (ppm)
Tl	0.008-1.0	0.03-0.3
Hg	0.005-0.02	0.013-0.17
As	0.02-7	0.01-1.5
Cd	0.1-2.4	0.05-2.0
Sb	0.002-0.06	0.001-0.2
Cu	1.8-16.2	1.1-8.8
Zn	12-47	10-44
Mo	0.33-2.3	0.07-1.75
W	0.0-0.15	0.01-0.15
Ni	0.13-2.6	1.2-3.6
Ba	142-198	2-160
Sr	6-850	2.6-74
Rb	44-130	3-220
Fe	18-1000	25-130
Mn	17-334	1.3-113
Al	25-3410	2.6-135
Si	3000-12000	/

*: Concentrations on a dry weight basis. Sources: Bowen (1979), and Kabata-Pendias and Pendias (1992)

Table 5-16 Concentration distribution of Tl, As and Hg in various crops and vegetation (dry weight, unit in ppm)

Vegetation	Locality	Tl		Hg		As	
		Range	Average	Range	Average	Range	Average
Chinese cabbage	Lanmuchang MA*	0.7-5.4	2.34	0.15-0.86	0.48	0.6-2	0.98
	Outside Lanmuchang MA	0.31-0.22	0.26	0.26-0.57	0.42	0.53-0.91	0.7
Green cabbage	Lanmuchang MA	120-494	338	0.452-0.718	0.63	0.38-0.89	0.7
	Outside Lanmuchang MA	0.39	0.39	0.33	0.33	0.32	0.32
Chili	Lanmuchang MA	2.9-5.3	4.1	0.013-0.041	0.03	0.24-0.29	0.27
	Outside Lanmuchang MA	0.19-0.36	0.27	0.008-0.02	0.01	0.14-0.24	0.19
Corn	Lanmuchang MA	0.26-3.1	1.4	<0.005-0.007	<0.005	0.01-0.04	0.02
	Outside Lanmuchang MA	0.05-0.09	0.07	<0.005	<0.005	0.024-0.025	0.024
Rice	Lanmuchang MA	1-5.2	2.4	0.02-0.04	0.03	0.1-0.18	0.15
	Outside Lanmuchang MA	0.17-0.3	0.25	0.009-0.022	0.015	0.06-0.13	0.09
Carrot	Lanmuchang MA	21.6	21.6	0.55	0.55	1.3	1.3
Wild grass	Lanmuchang MA	25-47	36	4.2-12.5	8.2	8.5-17	13
Fern	Lanmuchang MA	14.5	14.5	0.45	0.45	2.3	2.3

MA = mineralized area

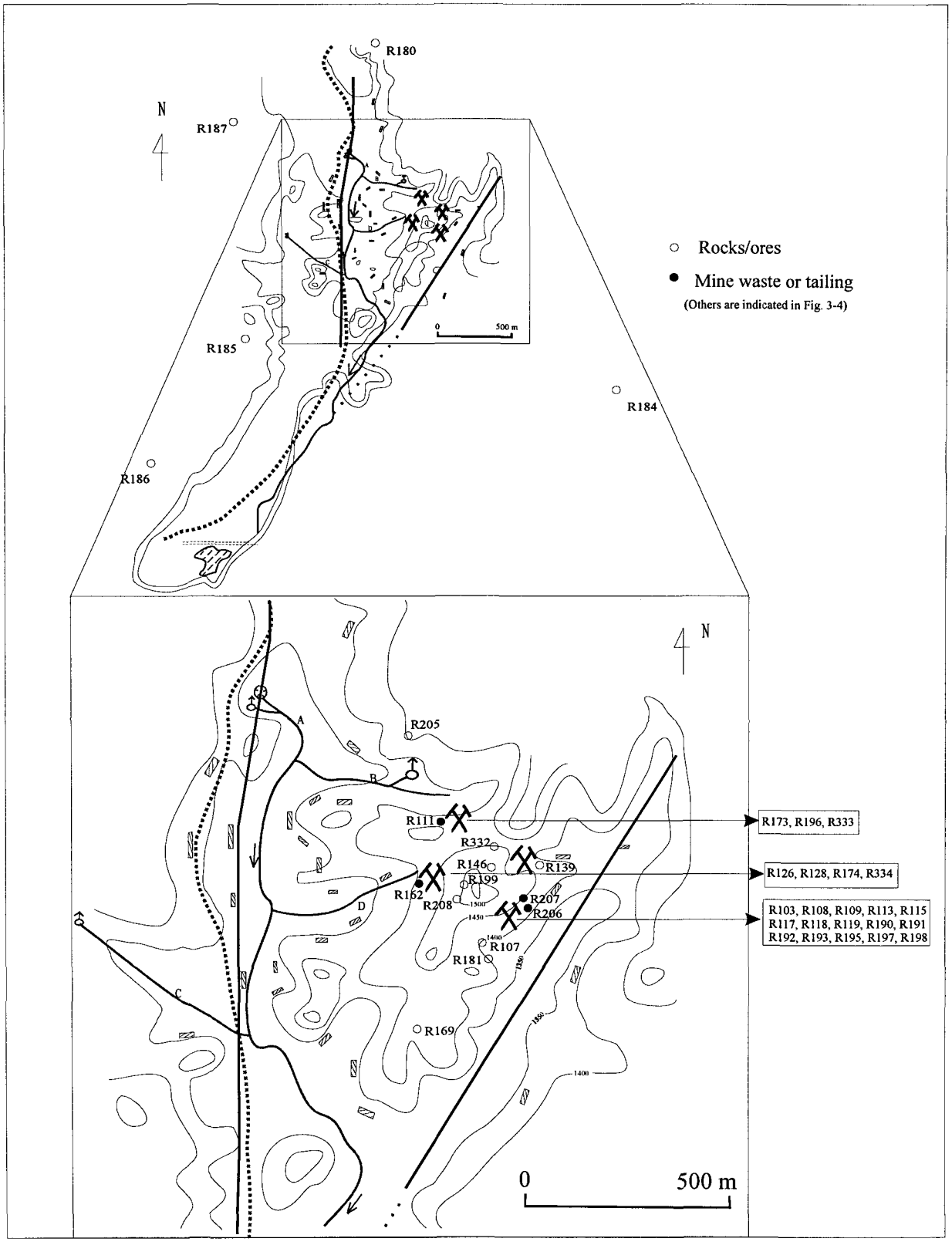

Fig. 5-1 Location of sampling sites of rocks

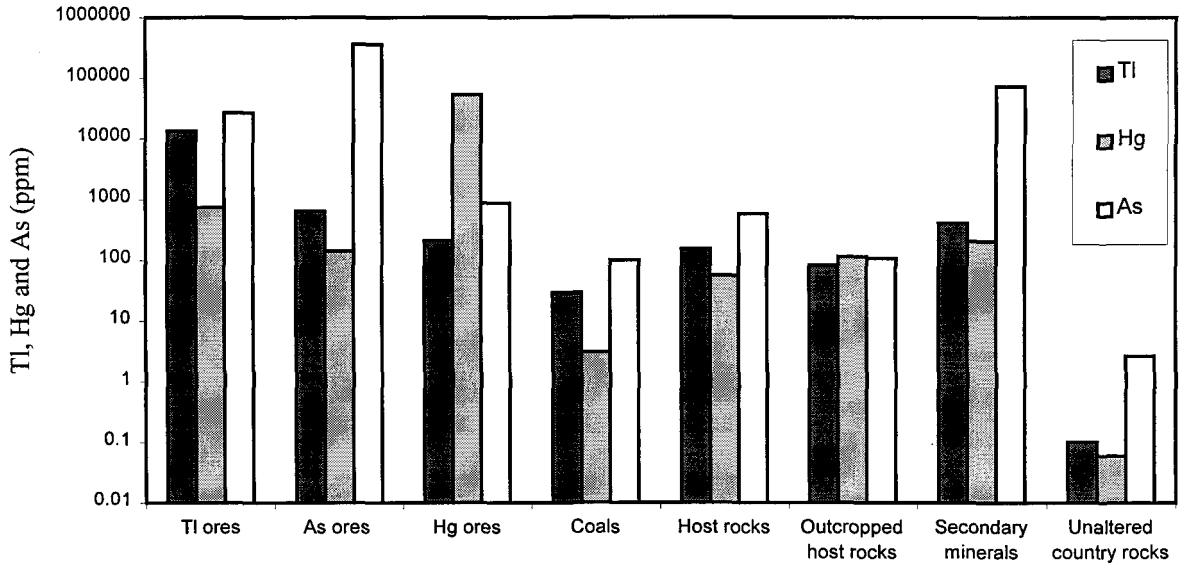

Fig.5-2 Distribution of Tl, Hg and As in rocks/ores

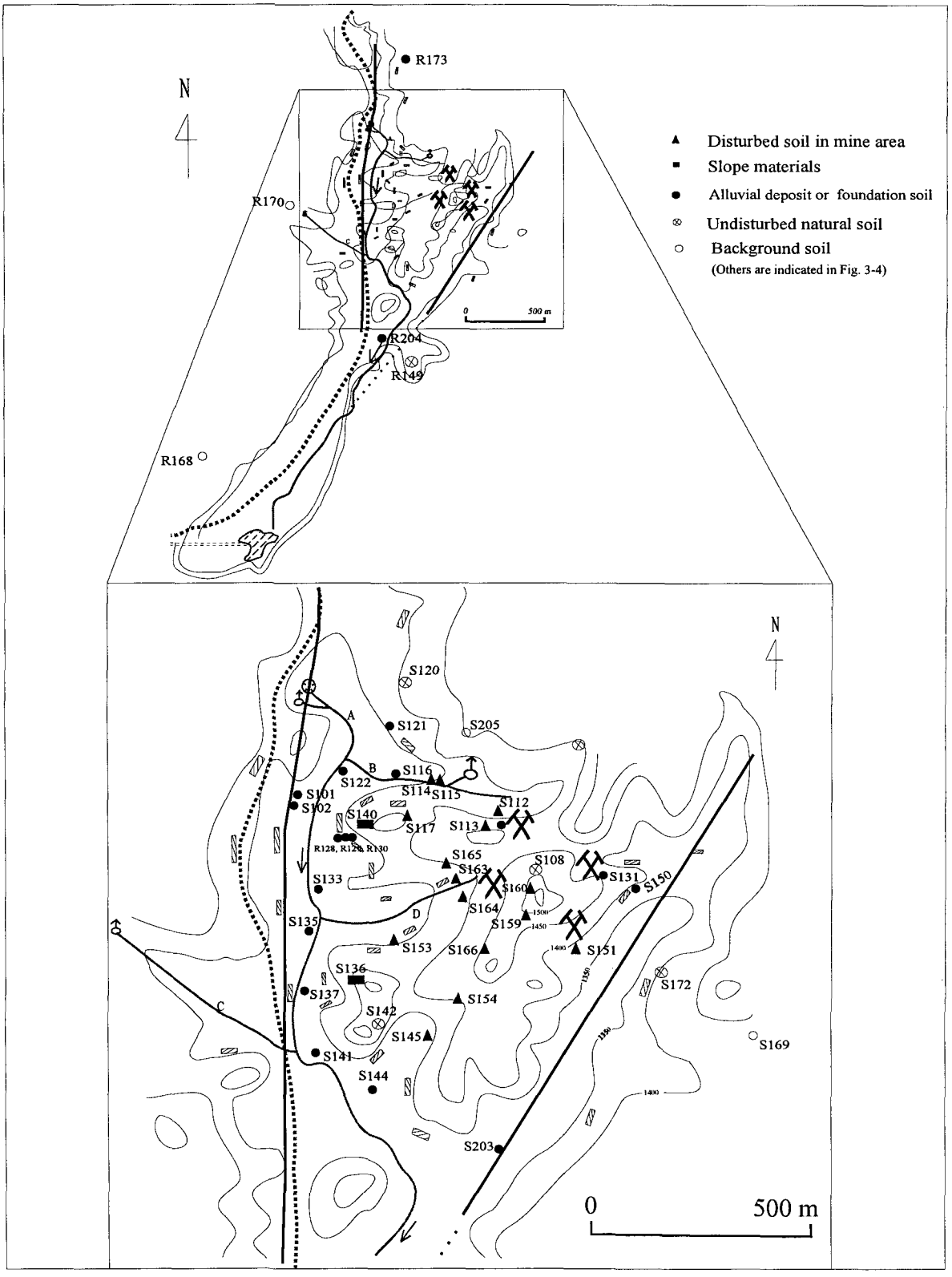

Fig. 5-3 Location of sampling sites of soils

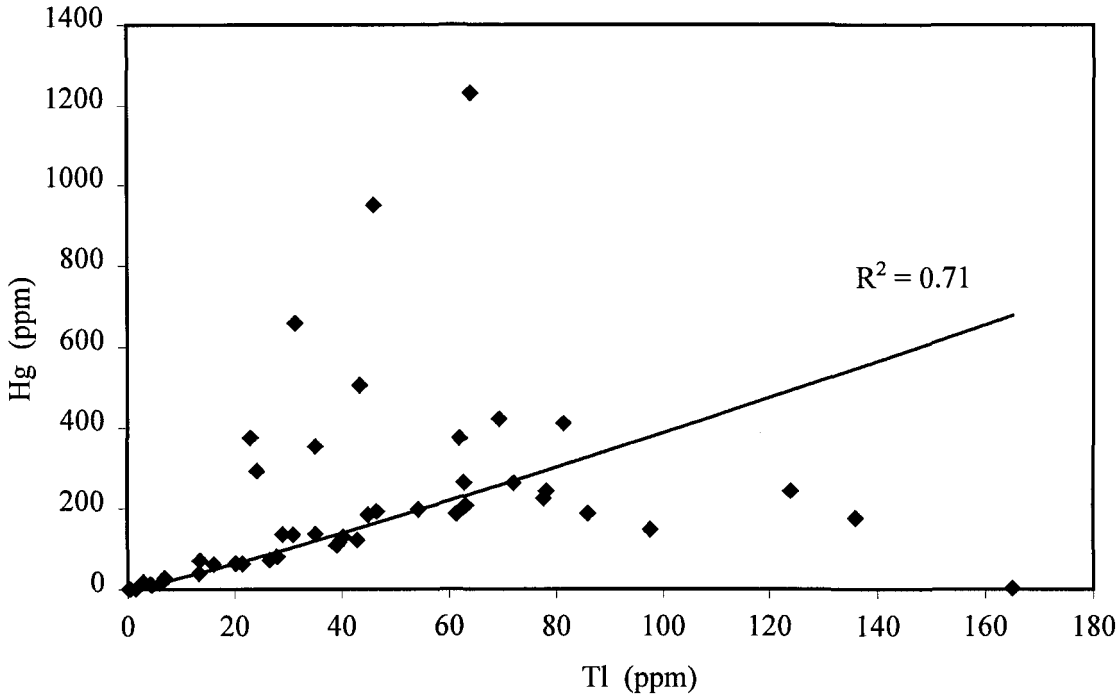

Fig. 5-4 Mercury versus thallium in soils

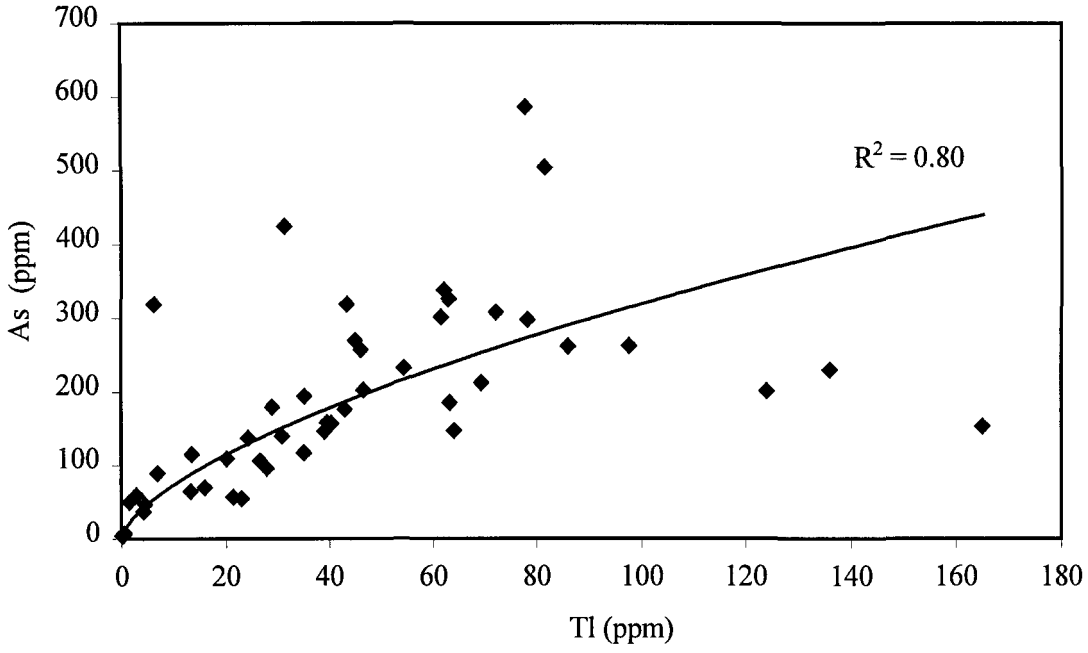

Fig. 5-5 Arsenic versus thallium in soils

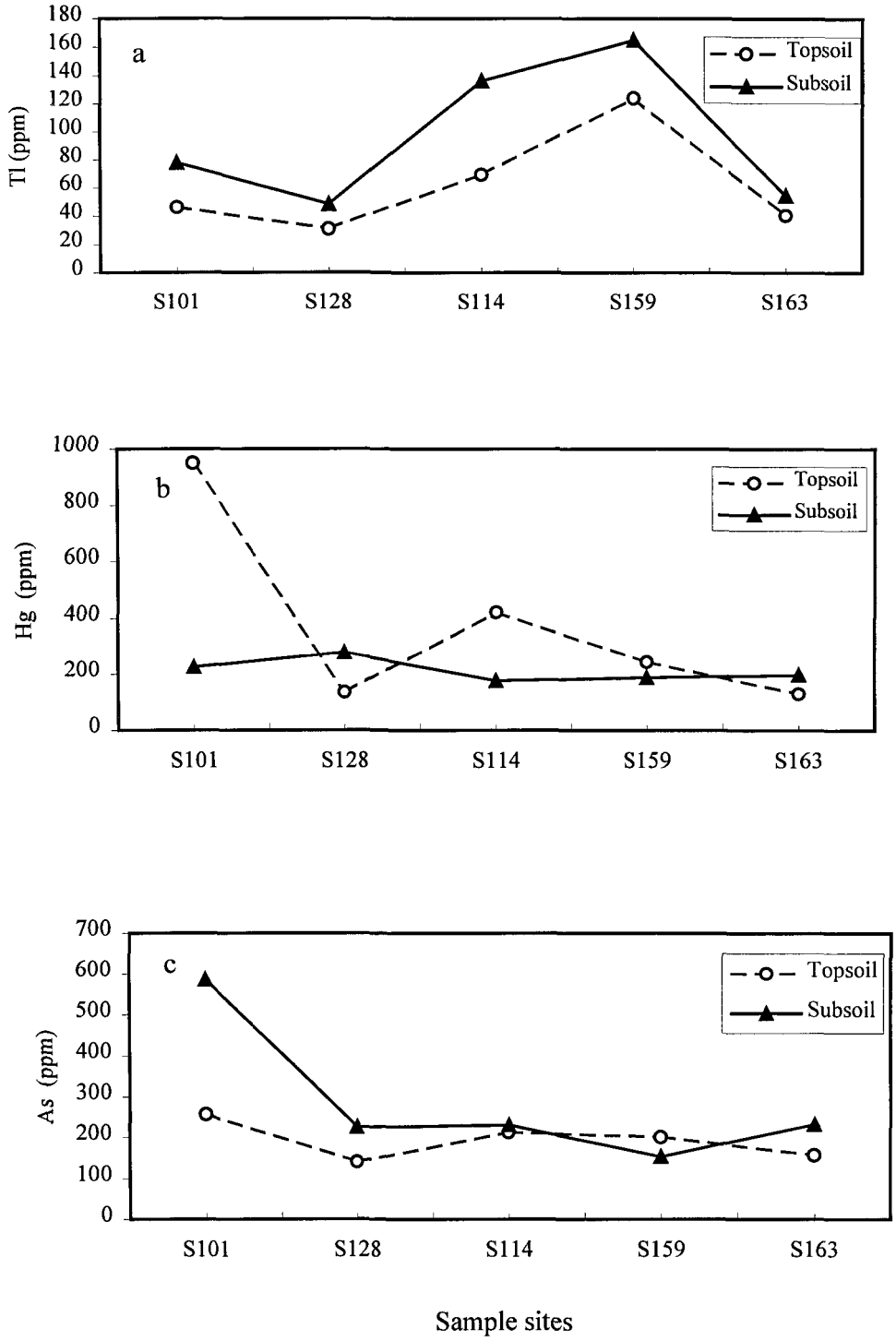

Fig. 5-6 Distribution of metals in topsoil and subsoil: (a) Tl, (b) Hg, and (c) As

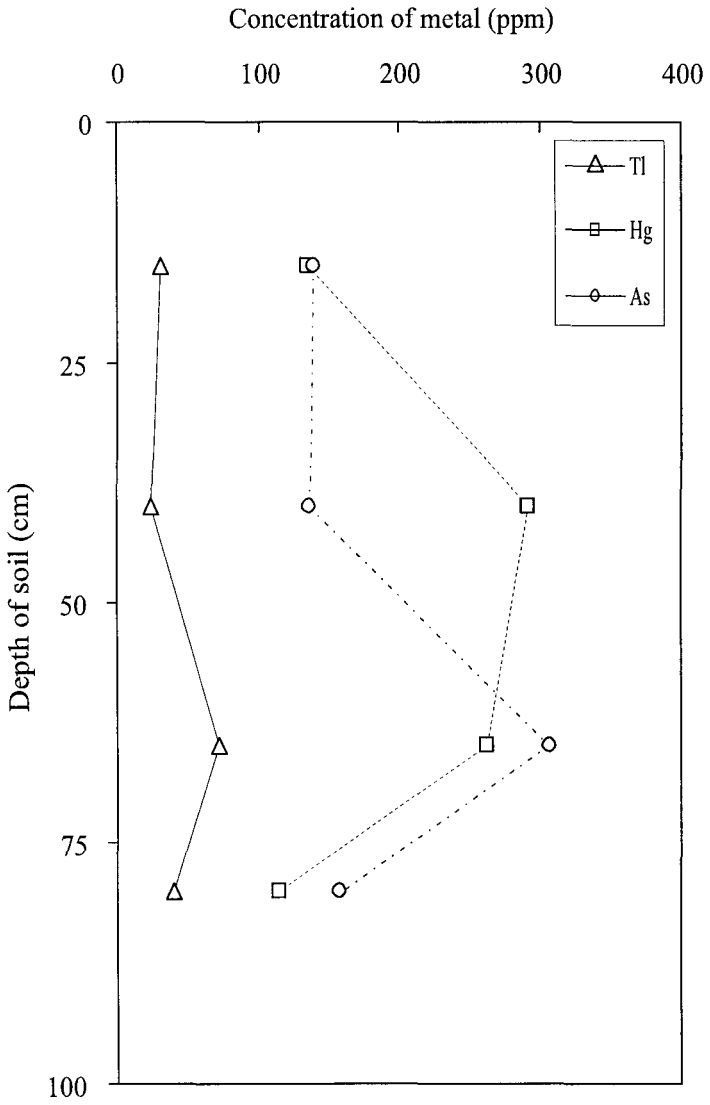

Fig. 5-7 Distribution of Tl, Hg and As in a soil profile

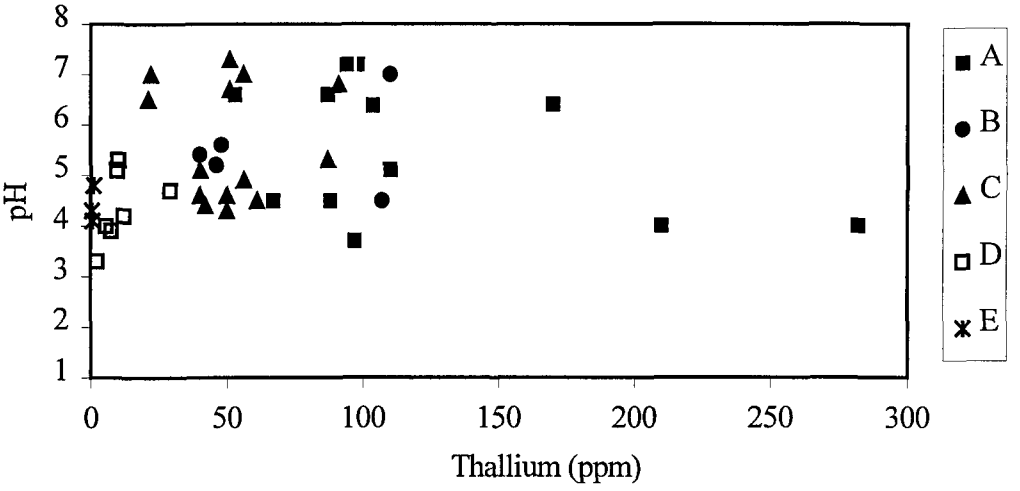

A = Arable soils in mine area; B = Alluvia deposits (up-mid stream);
C = Alluvial deposits (down stream); D =Undisturbed natural soils; E = Background soils

Fig. 5-8 pH value versus Tl concentration in soils

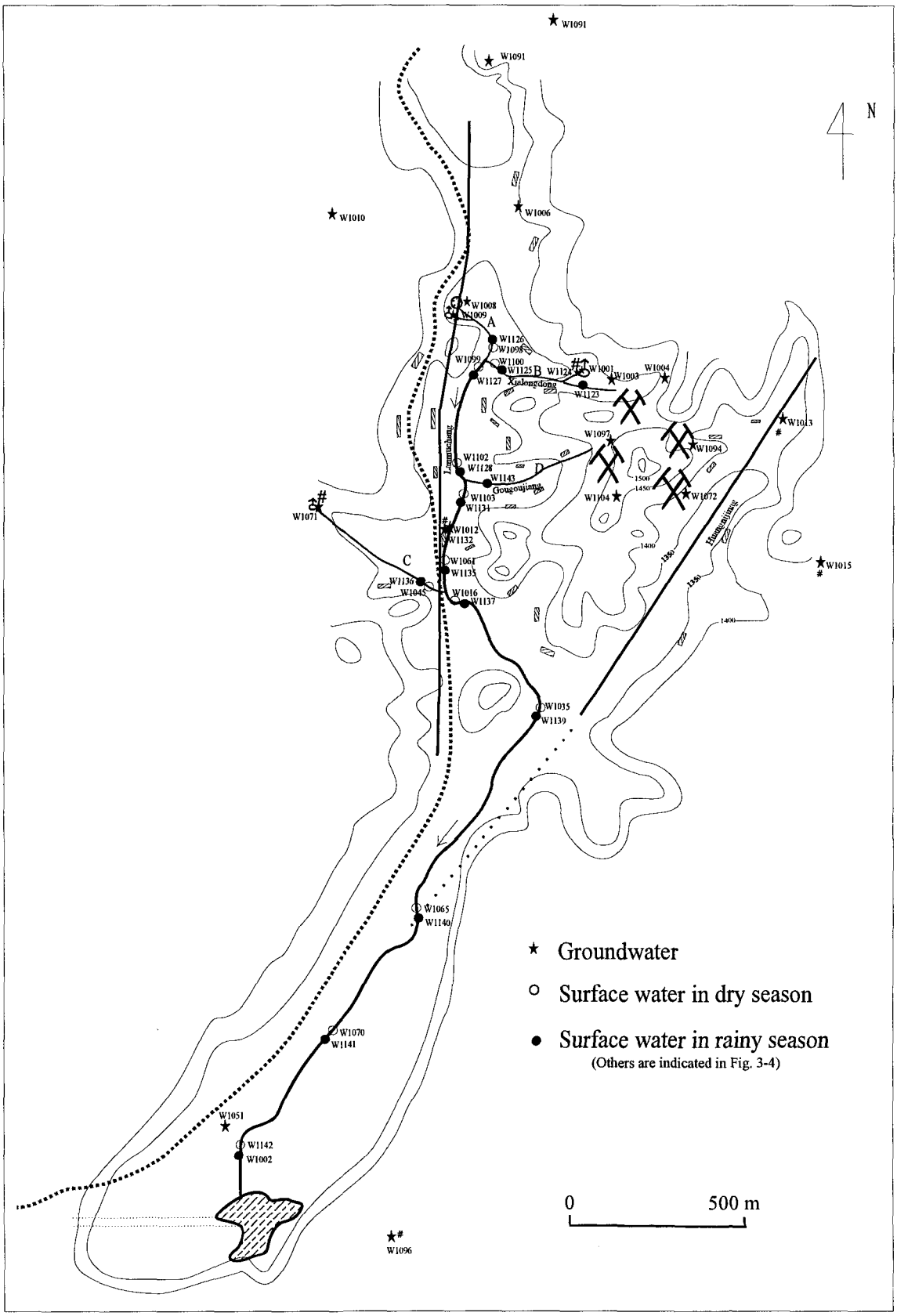

Fig. 5-9 Location of sampling sites of water

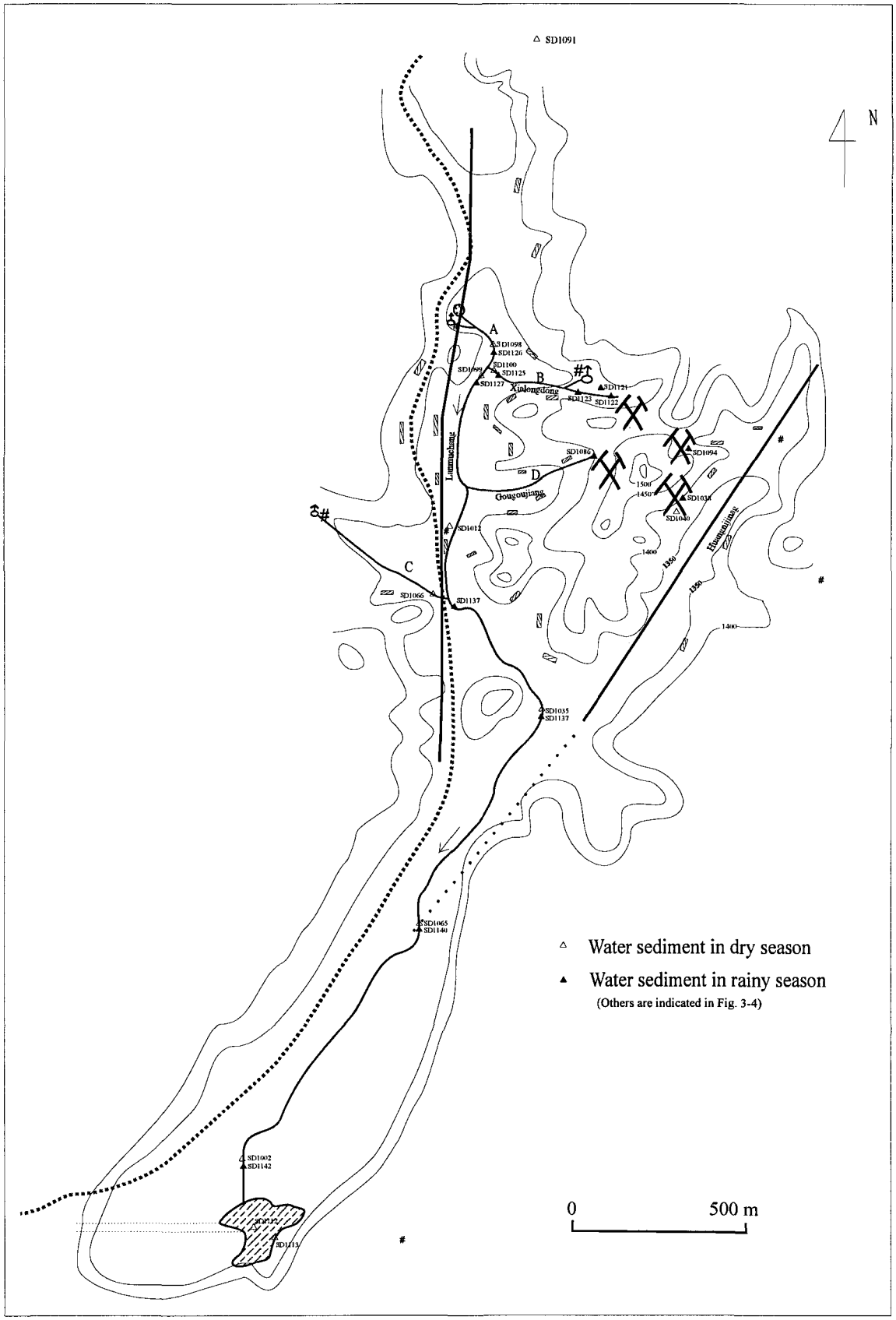

Fig. 5-10 Location of sampling sites of sediments

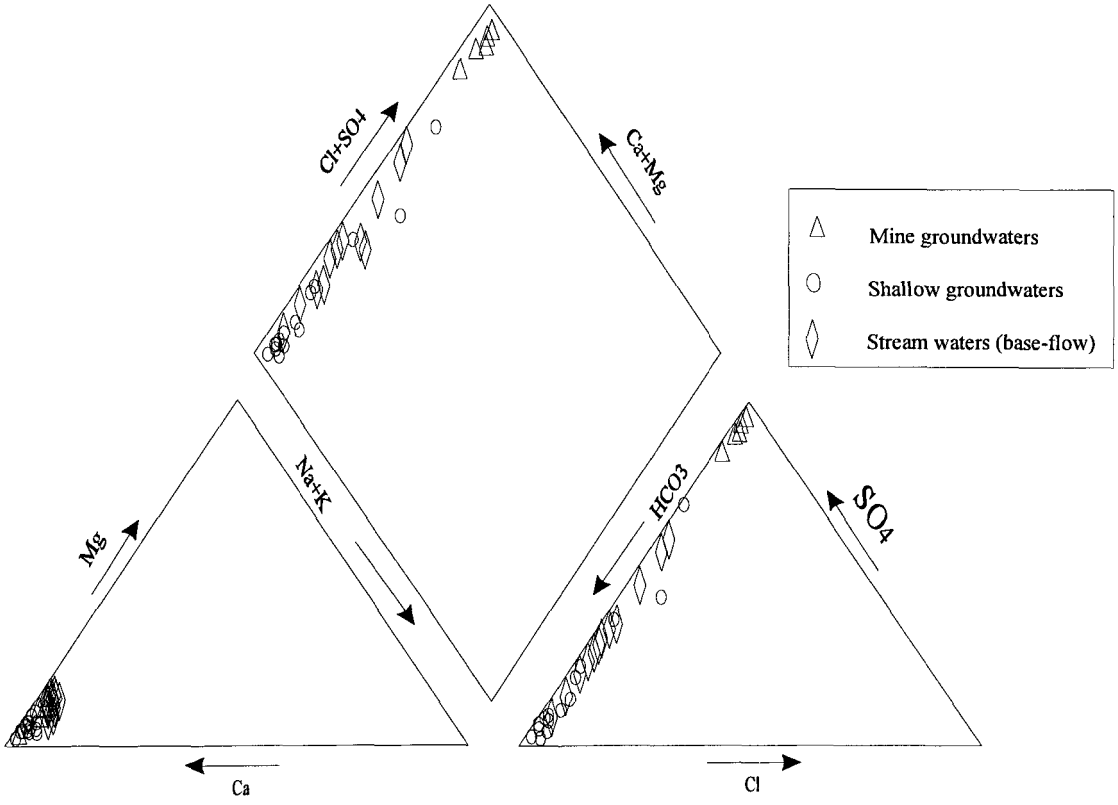

Fig. 5-11 Piper plot showing the variation of major cations and anions for ground- and surface water samples from the Lanmuchang area

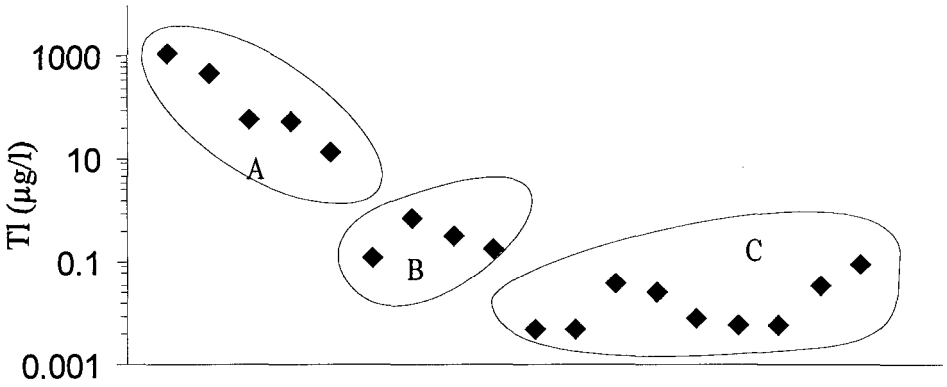

Fig. 5-12 Distribution of Tl in groundwaters

A= deep mine groundwater, B= shallow groundwater close to the Tl mineralized area; C= shallow groundwater outside the Tl mineralized area

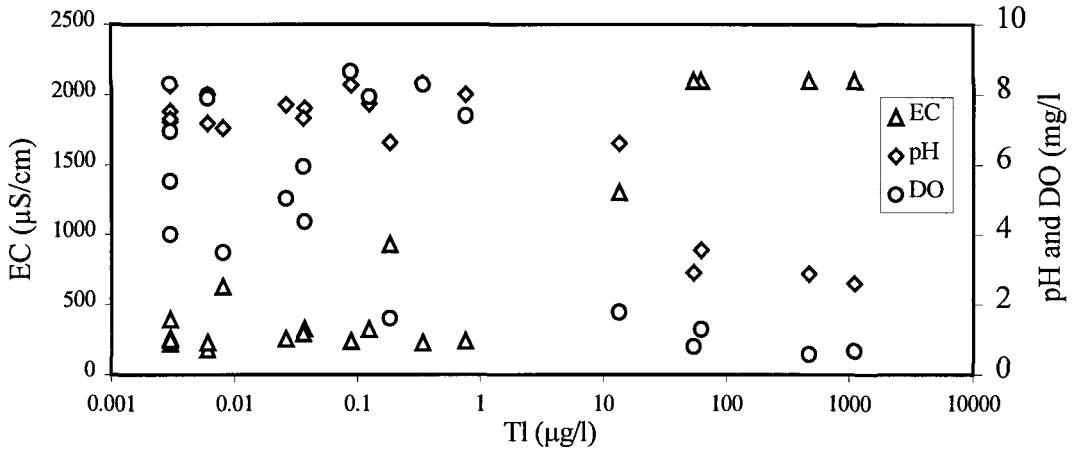

Fig. 5-13 Plot of pH, DO and EC versus Tl in groundwaters

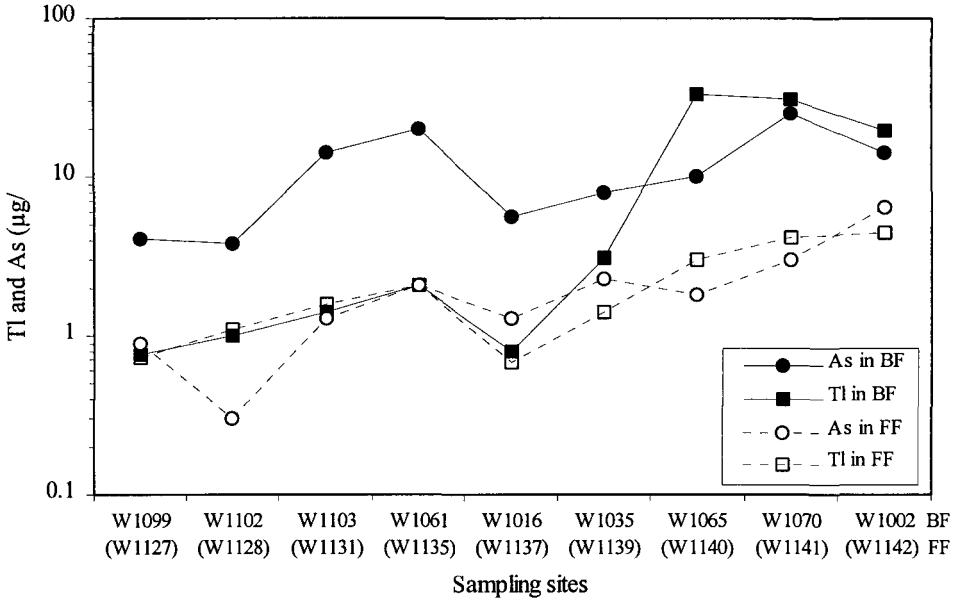

Fig. 5-14 Dispersion pattern of thallium and arsenic in stream water, from upstream (left) to downstream (right); BF = base-flow; FF = flood-flow

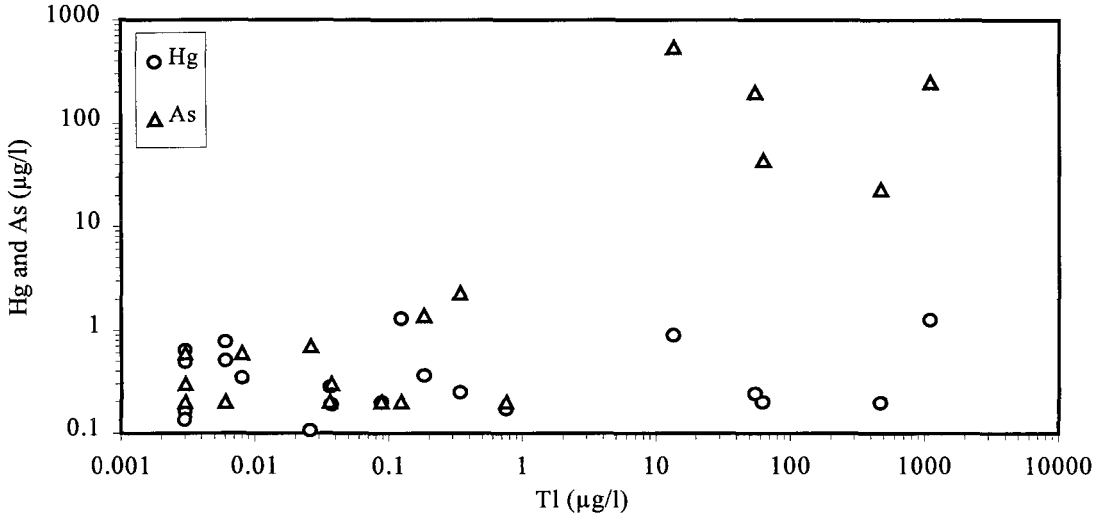

Fig. 5-15 Concentrations of Hg and As versus Tl content in groundwaters

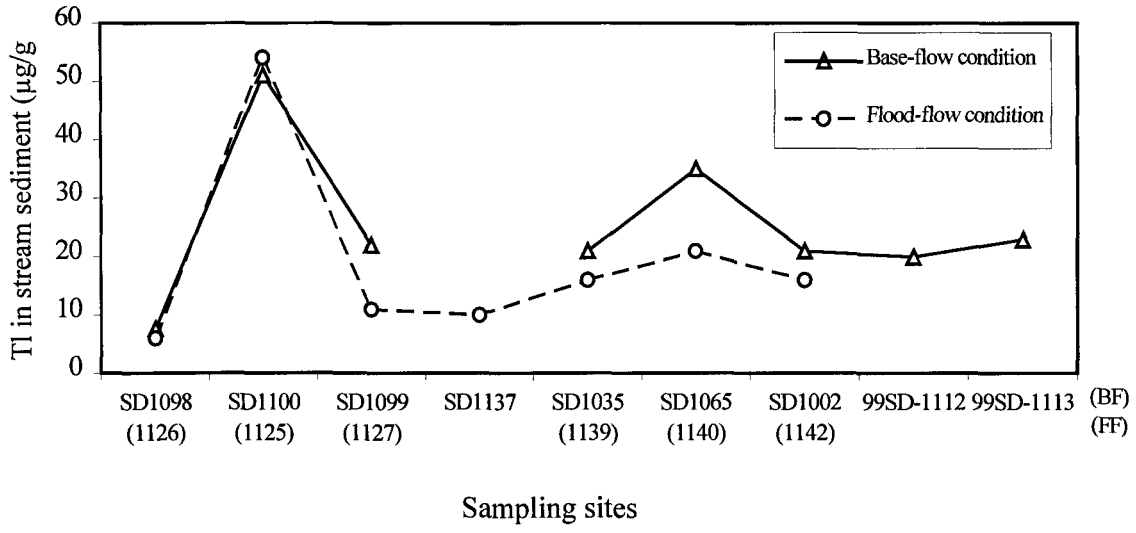

Fig. 5-16 Dispersion of Tl in stream sediments under both base-flow regime and flood-flow regime, from upstream (left) to downstream (right);
BF = base-flow, FF = flood-flow

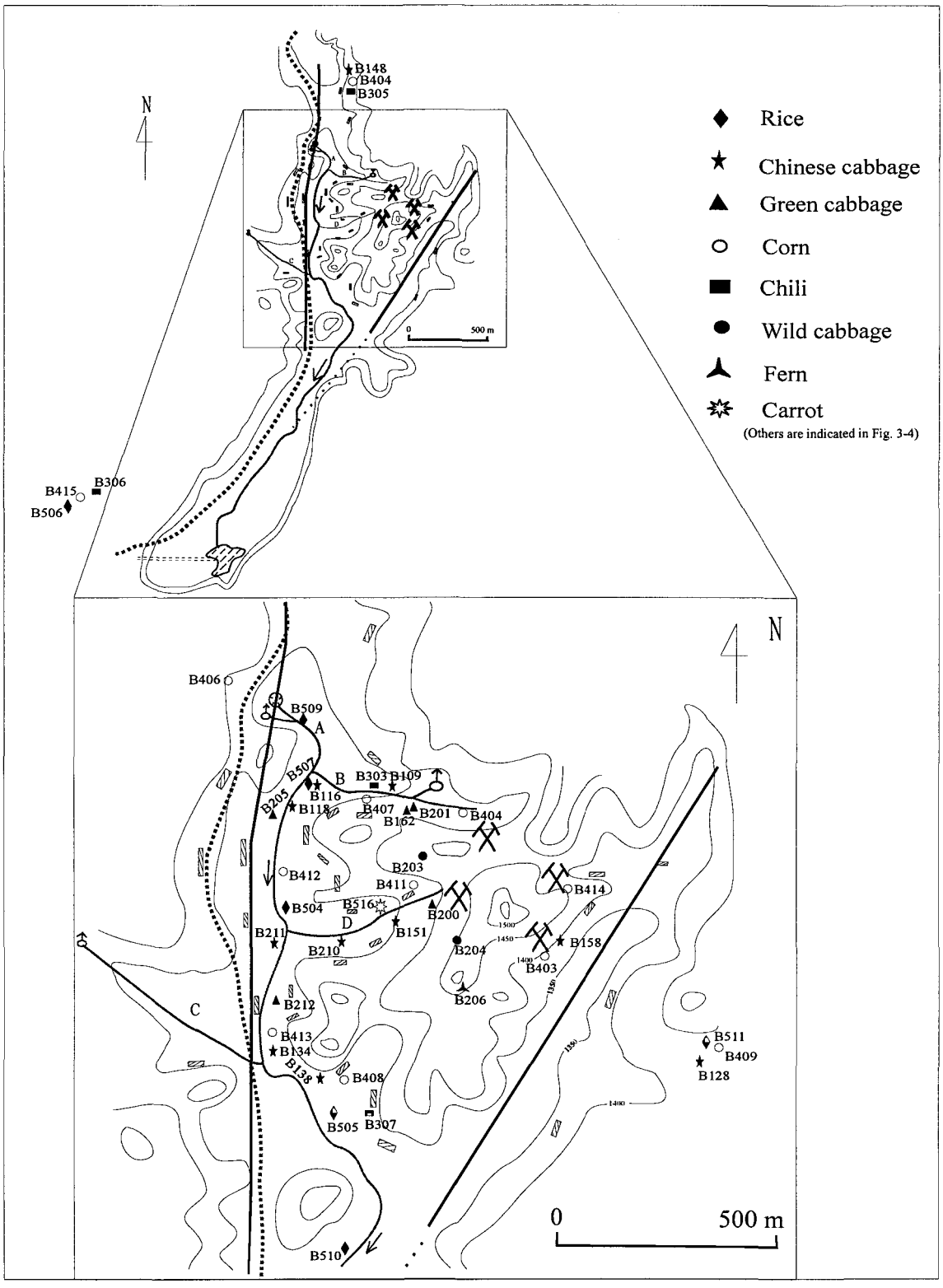

Fig. 5-17 Location of sampling sites of crops and vegetation

CHAPTER 6

INTERPRETATIONS OF THALLIUM DISPERSION IN THE LANMUCHANG AREA

This chapter aims at interpreting the dispersion of Tl together with Hg and As in rocks, soils, sediments, waters and crops in the Lanmuchang Hg-Tl mineralized area as well as in the background area, and at understanding how both the natural processes relating to thallium mineralization and human activities affect the dispersion of thallium.

6.1 Interpretation of Tl dispersion in rocks

6.1.1 Characteristics of thallium mineralization

The primary distribution of thallium can be ascribed to (1) the thallium-bearing sulfide ores, (2) thallium-bearing coals, and (3) thallium mineral-bearing ores.

Thallium occurs as isomorphous additions in the structure of sulfide minerals of mercury ores (cinnabar), arsenic ores (realgar and orpiment) and pyrite or marcasite. The visible thallium minerals (mainly lorandite and minor christite) were not identified associated with these sulfide minerals.

Thallium is also disseminated as isomorphous additions in coals. The enrichment of thallium in coals is up to 12–26 ppm (Table 5-2). The visible thallium minerals (e.g.

lorandite) were not identified in coals. However, the thallium mineral lorandite was initially identified around the coal layers on the on-going coal-mining head face during the field survey of this study in 1999. Two samples collected from the head face contain 100-130 ppm of thallium (Table 5-2).

Thallium finally occurs as independent thallium minerals, mainly lorandite (Li, 1996). The mineral lorandite occurs as individual aggregates or in association with realgar-orpiment, cinnabar, pyrite-marcasite, barite and quartz. Lorandite crystals typically reach sizes of 5–20 mm, exceptionally up to 4 cm. The crystals present needle-like, column-like and radiating forms. They occur as stockworks and bands.

The three types of rocks that host thallium ores are (1) argillaceous rocks, (2) siliceous rocks, and (3) fault gouges made up of siliceous minerals and clay minerals in various proportions. Thallium is enriched in these host rocks either as sulfides (mainly lorandite) or as an isomorphous substitution in their minerals.

Argillaceous rocks are composed of kaolinitic claystone, and carbonaceous shale, and they are a part of products resulting from hydrothermal alteration.

Siliceous rocks contain amounts of matrix and bioclast being chalcedony and quartz. The siliceous rocks are the products of silicification of host rocks in which the hydrothermal silica replaced the original biogenic limestones.

The fault gouges occur in the broken fault and fracture zones in which the siliceous minerals and clay minerals are mixed in various proportions. They are highly altered by argillite, pyrite and enriched in organic matter, and appear dark-gray in color.

The Lanmuchang mineralized area is part of a series of deposits now commonly referred to as "Carlin type deposits" or "sediment hosted gold deposits". The introduction of hydrothermal fluids and interaction with receptive host rocks has been facilitated by faulting, fracturing and brecciation associated with intersecting faults and fractures in all the deposits. In general, the nature of the host lithology is less critical to mineralization than the permeability of each unit of the ore fluids. Hydrothermal alteration typically includes decalcification, silicification, argillization and baritization.

Hydrothermal alteration of the wall rocks began at 250°C in a weakly acidic environment (Chen, 1989b). The first phase is characterized by decalcification which involves the removal of carbonate minerals from the sedimentary host rock by weakly acidic solutions, leading to a general increase in porosity. The importance of early hypogene alteration was to increase porosity and permeability of the host rocks and thus make them more favorable for mineralization. The process of hypogene hydrothermal alteration of carbonate-rich hosts invariably begins with decalcification, which is characteristic of sedimentary-hosted precious metal deposits (Radtke 1985; Berger and Bagby, 1991; Li and Peters, 1998).

The next phase of mineralization is characterized by the silicification of the wallrock (reducing its porosity again) and the precipitation of the sulfide minerals. This silicification is as extensive as that usually observed in the Carlin type gold deposits within the Huijiabao metallegenic belt (Li, 1996; Li and Peters, 1998). Replacement of carbonate with quartz has intensively altered the carbonate-rich host rocks. The silicified rocks are the products of introduction of hydrothermal silica and replacement along faults and fracture

zones of varying orientations. Silica-bearing fluids also moved from fractured zones outward along stratigraphic horizons, resulting in both weak pervasive silicification and micro-stockworks in fracture zones.

During the third stage, the hydrothermal solutions mingled with oxygenated descending waters. These mixed fluids were responsible for host rock alteration, causing deposition of alunite and kaolinite along open fractures.

Finally, supergene alteration led to the formation of sulfate. Supergene alteration is intensively developed in Lanmuchang. The conversion of pyrite to Fe oxides, and the oxidation of small amounts of organic carbon have deeply stained most of the outcrops and abundant sulfates occur in the fractures. The oxidized rock contains mainly quartz and a mixture of clay minerals, and has a very low calcite content. Large amounts of various secondary irons, potassium and magnesium minerals occur as secondary minerals.

6.1.2 Baseline concentrations of Tl, Hg and As

The host rocks sampled from the outcrops contain thallium ranging from 6-330 ppm (Table 5-2), with an average of 82 ppm. These samples were not disturbed by previous mining activities and can represent the natural exposure of the rocks in Lanmuchang area. The sample R146 contains the highest value (330 ppm) (Table 5-2), which can be attributed to the presence of secondary thallium-bearing minerals in the fractures. Thus, the baseline of thallium in the natural exposure of rocks is estimated to be 82 ppm. Similarly, baseline values of Hg and As are estimated to be 113 ppm and 106 ppm, respectively (Table 6-1).

The host rocks exposed to the surface are mainly located on the top or scarps of the hills in the Lanmuchang area. As a result, natural processes, such as physical erosion and chemical weathering, are capable of dispersing thallium into surrounding materials by both physical transport and chemical dispersal. The eroded materials usually still contain thallium-rich sulfides or other minerals, and may migrate into the soils, (sub)surface water in the surrounding or downward areas to enhance the thallium levels in those soils and waters. Therefore, the high baseline values of Tl, Hg and As in the outcropped host rocks can contribute to the enrichment of these toxic metals in the surface environment even during natural processes.

6.1.3 Impacts of natural processes on thallium dispersion

The main thallium-containing minerals in ores (including coals) are composed of lorandite, cinnabar, realgar, orpiment and pyrite. The highest values of thallium in these ores are from the lorandite. Generally, the primary ores of sulfides can produce their primary geochemical haloes around the ore bodies, away from which the strength of halo gradually decreases. The primary metallic halo can even extend to the surface depending upon the physiography of the area in Lanmuchang. Figure 6-1 illustrates the primary halo of thallium from the ore body to the surface. Samples from the surface and the underground ore body at various depths were collected from outcrops and three mining adits. The variations of thallium concentration in this vertical section likely represent the dispersion of thallium primary halo from the ore body to the barren outcrops. The haloes of thallium are the reflection of the extent of primary thallium dispersion into the surrounding rocks. In the

Lanmuchang area, the nature of the terrain prevents the development of progressive high to low thallium haloes, since primary haloes could be centered around local concentrations of thallium ores. However, any of the haloes exposed to the surface or interacting with groundwater can promote a secondary dispersion process into soils and natural groundwaters.

The host rocks of thallium mineralization contain 33–490 ppm of thallium (Table 5-2) with an average of 132 ppm. The host rock samples were collected from the past or present mining adits which often cut the fault or fracture zones, some of which are fault gouges. Thus, they were strongly altered, broken and accompanied by mineralization. These host rocks easily release thallium into the groundwater by meteoric water flowing through the fault or fracture zones. The filtrating groundwater can disperse the thallium to attain deeper groundwater circulation or discharge thallium to surface water through springs or acid mine drainage (AMD).

Secondary minerals are another natural source of thallium. The secondary minerals occur mainly in the fault or fracture zones, due to either the deep weathering or surface weathering (Fig. 6-2, Fig. 6-3). Thallium in these minerals ranges from 25 to 1000 ppm (Table 5-2), with an average of 405 ppm.

According to X-ray diffraction (XRD) analysis (Table 6-2), the secondary minerals are mainly composed of kaolinite, copiapite, epsomite, fibroferrite, pickeringite, zaherite and halotrichite. These minerals are very water-soluble, and they can readily release thallium into the groundwater when groundwater flows through the fault or fracture zones.

The secondary minerals produced due to surface weathering or supergene alteration are also observed in outcropped host rocks where abundant secondary sulfates occur in the fractures. XRD results show that the secondary minerals mainly consist of epsomite, morenosite, fibroferrite, alunogen, ferrocopiate and rozenite (Table 6-2). The outcrop sample R146 contains a large amount of secondary minerals and thallium values reach up to 330 ppm (Table 5-2). All these secondary minerals are also easily water-soluble. Thus, these minerals can readily release thallium into the downhill soils or runoff water by rainwater leaching. On the other hand, the rainwater leaching through the surface fractures can dissolve more thallium from the rocks and may form more secondary minerals in the fractures or rock surface by evaporation after rain leaching. The dual interaction of leaching and evaporation can lead to more thallium sulfates releasing thallium into the ambient ecosystem over the years. The abundance of rainfall and a warm, humid climate facilitate the above cycle.

6.1.4 Impacts of thallium in rocks related to mining activity

The natural dispersion pattern of thallium in rocks can be disturbed by mining activity. The mining impacts are in terms of exposures of mine wastes and AMD. Recent small-scale thallium mining was focused on the easily selected lorandite-rich ores only, while broken up mineralized ores still containing small amount of visible lorandite minerals were discarded as mine wastes and stock piles on hill slopes. A very high thallium level (2600 ppm) was recorded in these waste piles (Table 5-2). The general range of thallium in mine wastes was from 32-2600 ppm (Table 5-2), with an average level of 1092 ppm. These

thallium-rich mine wastes exposed on the surface have become a direct source of thallium contamination easily spreading thallium and other toxic metals in the environment. The water leaching or weathering of these mine wastes easily release thallium into the ambient and downhill soils and (sub)surface waters. These man-made factors overlap the natural processes of thallium dispersion as discussed above and compound the contribution of thallium in the ecosystem.

Coal mining is another way of introducing thallium into the surface environment. Coal contains very high thallium, in the Lanmuchang area, ranging from 12 to 46 ppm (Table 5-2). The coal combustion produces ash which may still contain amounts of thallium, and this ash is used for paving village roads or used as a garden soil additive. The leaching of the coal slags may also enhance the thallium levels in agricultural soils. Moreover, during field work related to this study, the thallium mineral lorandite was also discovered around the currently-mined coal seams, located slightly away from the area where intensive thallium mineralization has been identified. Thallium ranges from 100 to 130 ppm in the lorandite-bearing argillaceous rocks (Table 5-2). The accompanying mineral is cinnabar and realgar, thus Hg is up to 94000 ppm and As up to 996 ppm (Table 5-2). These thallium mineral-rich rocks are transported from the underground coal mining sites and discarded as mine wastes on the surface. Therefore, leaching or weathering of coal mine wastes can also supply thallium into the ambient and downhill soils and (sub)surface waters.

The earlier sporadic mining activities before 1995 were mainly for coal and mercury and large amounts of mine wastes were dumped on the surface. Many of these

wastes migrated downhill during heavy rains or were even used as landfill for terrace cultivation. It is impossible to discriminate between soils mixed with mine wastes and soils formed by the disintegration of thallium bearing rocks. However, what is evident is that both these sources have imparted thallium into soil and water in the area. A detailed discussion regarding this is presented below.

6.2 Interpretation of Tl dispersion in soils

6.2.1 Baseline concentrations of Tl, Hg and As

In general, the undisturbed soils and the slope wash materials are the main component of the arable soils in the Lanmuchang area. Concentrations of Tl, Hg and As in these original soils can provide geochemical baselines of soils of the Lanmuchang Hg-Tl mineralized area.

Soil layers in Lanmuchang area are thin, and widely disturbed by intensive agriculture. Thus, the exposure of undisturbed natural soils within the mineralized area do not spread widely, and only two soil samples (S108 and S142) were collected from the Tl mineralized area in this study. The average concentration of Tl in these two soils is 20 ppm, while the undisturbed soils slightly away from the mine area (S120, S148, S149, S172 and S173) contain much lower thallium concentrations, ranging from 2.2 to 10 ppm (Table 5-6). Three samples of background soils were collected from outside the Lanmuchang area barren of Tl mineralization but in a similar geological setting and thallium contents range from 0.47 to 0.97 ppm (Table 5-2). The above contents for Tl likely indicate the pre-anthropogenic background in the study area, and thus can represent the baseline

concentrations for Tl before mining (Table 6-3). The baseline values for mercury and arsenic are also listed in Table 6-3.

The slope wash materials often accumulate on the slightly to moderately steep slopes due to weathering of outcropped rocks or deforestation, although the soil profiles do not develop. Much of the slope materials are proximal to the bedrock from which they are derived and therefore contain weathering products which reflect that of the bedrock. The slope wash materials are often composed of mud, silt and some talus. Two slope wash materials were sampled. One (R140) is from the foundation of a house downward from the mine area where the soil layers were stripped to expose a stripped slope surface behind the houses. These two slope materials contain thallium ranging from 40 to 46 ppm (Table 5-6), with an average of 43 ppm. The baseline concentrations for Hg and As in these slope materials are also listed in Table 6-3.

According to Table 6-3, the geochemical baseline concentrations for Tl, Hg and As in slope wash materials are slightly higher than in the undisturbed soils in the mineralized area, with a 2-fold enrichment for Tl, 1.5-fold for Hg and 1.5-fold for As, respectively. In detail, the baseline concentrations in undisturbed soils within the mineralized area are 20 ppm for Tl, 40 ppm for Hg and 64 ppm for As. Baseline concentrations in slope materials are 43 ppm for Tl, 73 ppm for Hg and 102 ppm for As. This certainly reflects that the slope wash materials derived from the proximal parent bedrocks were not well sorted and some metal-rich talus was still mixed with them. The concentrations of Tl, As and Hg in the slope materials are very similar with those formed in underground or outcropped host rocks.

The high geochemical baseline concentration for Tl, Hg and As in soils indicates that soils in the Lanmuchang Hg-Tl mineralized area are highly enriched in Tl, As and Hg due to natural processes of chemical/physical weathering and erosion of the highly altered outcrops or near surficial bedrocks. This is true even without the anthropogenic disturbances such as mining operation. The Lanmuchang Hg-Tl deposit is topographically located in a ridge area at high elevations of Zaofan Mountain, and the well-developed fractures and faults result in the intensive surface hydrothermal alteration of the broken bedrock. Moreover, the many steep and moderate slopes around the mountain do not facilitate the formation of soil layers, and slope wash materials can bring large amounts of Tl, Hg and As from surficial bedrocks.

6.2.2 Mode of occurrence of thallium in soils

The mobile fractions of Tl together with Hg and As, extracted by strong acids, have also been determined in this study. All the three toxic metals present large amounts of mobile concentrations in the arable soils (Table 5-6; Fig. 6-4). The mobile fraction by which metals and other chemical species are bound onto solid matter (soils and sediments) may exert an important control on their geochemical behavior. The HNO_3 extraction involves separating a labile fraction from a residual fraction. The mobile fraction includes those associated with hydrous Fe-Mn oxides, absorbed on clays, and occurring in carbonates and sulfides in the soils (Chester et al., 1985; Négrel et al., 2000). The extracted labile fraction represents the part that plays a more important role in environmental impacts, being available for intake by water, soils or plants.

The mobile fraction data of Tl and the major elements distribution in soils (Table 5-6, Table 5-5) indicate that thallium may exist as thallium sulfate, hydrous Fe-Al-Mn oxides, thallium carbonate, thallium sulfide, or adsorbed on clays.

6.2.3 Impacts of thallium in soils related to mining and farming activities

The natural dispersion pattern of thallium in soils can be disturbed by mining operation and agricultural activities. The mining impacts are in terms of exposures of mine waste piles, and AMD. Agricultural activities include transport of soils from upstream sites to fields located downstream, and deforestation for land clearances, enhancing soil erosion.

The human factor affecting the redistribution of metals are well illustrated by the distributions of Tl, Hg and As in arable soils within the mine area. Samples S112, S113, S114, S115, S116 and S117 were collected in the small valley B (called Xialongdong) (Fig. 5-3), where the average concentrations of Tl, Hg and As are up to 96.5 ppm, 327ppm and 263.17 ppm, respectively (Table 5-6). These values are much higher than their baseline concentrations, especially for Hg and As. Mine wastes from the recent thallium mining (1996-1998) (site S111) (Fig. 5-3) contain 32 ppm of Tl, 63.7 ppm of Hg, and 56.4 ppm of As (Table 5-2). These newly-produced wastes are located uphill at a higher elevation and they cannot contribute such higher concentrations in the downward arable soils as observed in valley B. Coal from the old adits contains 12 ppm of Tl, 1.8 ppm of Hg and 15.4 ppm of As (Table 5-2), and so it cannot contribute significantly the high contents of toxic metals found in arable soils. However, the Hg-Tl ores (samples R196 and R333) (Fig. 5-1) identified by this study contain much higher contents of metals, being 100-130 ppm for Tl,

94000 ppm for Hg, and 996 ppm for As (Table 5-2). These ores occur within the coal layers and can probably contribute to the enrichment of Tl, Hg and As in arable soils, through sporadic coal mining. The coal mining which began 300 years ago, has brought large amounts of mine wastes containing metal-rich argillites to the surface. Toxic metals Tl, Hg and As and their host debris are enriched in the fine particles of these wastes, which can migrate through downflow or runoff downwards into farmland or be transported by local farmers to the downward slope for use in farming. These farming soils often contain mine debris, and some subsoil also contains coal ash, which are important evidences of disturbance related to human activity. This probably reflects that mine wastes exposed on surface from the old coal mining operation rather than the recent mine wastes from thallium mining have affected the farmland. The recent mining for Tl and coal can readily introduce further toxic metals into the downward arable soils.

Another possible source of thallium contamination in soils is from the domestic utilization of coal by local villagers. The coals are crushed and mixed with mud from the argillites to make small coal balls for easy storage and combustion. The ash of such coal combustion are often dumped into the arable soils for amendment or used to pave the village roads over the years. This is why some coal ash and mine debris were identified within arable soils during the soil sampling.

Similarly, the human factor affecting the redistribution of metals are also well illustrated by the distributions of Tl, Hg and As in arable soils in the small valley D (called Gougoujiang) (Fig. 5-3). The average concentrations of Tl, Hg and As are as high as 149 ppm, 190 ppm and 189 ppm, respectively (Table 5-6). These values are higher than their

baselines. This is the main old site for Hg and coal mining, and mining for Tl also started in 1996-1998 at the same site. The mine wastes (Sample S162) (Fig. 5-3) at this old mining site contain 136 ppm of Tl, 188 ppm of Hg and 261 ppm of As (Table 5-2). These high concentrations may contribute to the high content of Tl (67-97 ppm), Hg (130-197 ppm) and As (157-232 ppm) at sites S163, S164 and S165 (Fig. 5-3; Table 5-6), although the undisturbed soils or slope wash materials have their natural concentrations of these metals. However, at sites S159 and S160 (Fig. 5-3), located at higher elevation than that of the dump of mine wastes at Gougoujiang valley, the concentrations of Tl, Hg and As in these soils are in the range of 210-282 ppm, 188-243 ppm and 153-210 ppm, respectively (Table 5-6). This is probably due to the slope wash materials from the outcrops at the top of Zaofan Mountain, where secondary mineral-rich outcropped host rocks contain high concentrations of metals, up to 330 ppm of Tl, 130 ppm of Hg and 240 ppm of As (Table 5-2). In addition, mine debris and coal ash deposits can be seen in the soil profiles, also indicating the anthropogenic disturbance from old mining activities.

The arable soil at site S151 (Fig. 5-3) downward from the latest Tl-mining site contain 150 ppm of Tl, 148 ppm of Hg and 262 ppm of As (Table 5-6), and probably reflect the impacts of mine wastes. However, the soils at site S150 (Fig. 5-3), from the garden in front of Huangnijiang village and away from the observable mine wastes, also contain high concentrations of toxic metals, i.e. 100 ppm of Tl, 374 ppm of Hg and 338 ppm of As (Table 5-6). The contents of Hg and As at this site are even more concentrated than in the neighboring soils related to mine wastes (e.g. site S151). The concentrated toxic metals at site S150 are probably related to the construction of a house foundation that has brought

large amounts of slope material and weathered surficial bedrocks to the surface. The fine particles were then used as garden soils, although the natural slope wash materials may contribute greatly high contents of such metals at the same site.

Soils along the bank of Qingshui Stream are intensively cultivated and are the main farmlands for planting vegetables by local residents. These soils were originally produced by alluvial deposition related to the favorable hydro-geomorphological feature (Fig. 3-4). However, topsoils (0-100 cm) are usually disturbed by house and road constructions and intensive cultivation in this densely populated area.

Distributions of Tl, Hg and As in these arable soils vary from one site to another. However, all the arable soils, along the bank of Qingshui Stream within the densely built up area, downwards from the Hg-Tl mineralized area, contain a narrow range of Tl concentration (40-61 ppm) (Table 5-6), with an average level of 50 ppm, except for soils from sites S121, S203 and subsoil S102 and S130 (further discussion for these 4 sites is given below). This range (40-61 ppm) for these soils is very similar to thallium distribution in the near slope wash materials (at sites S136 and S140 with the range of 40-46 ppm of Tl) (Table 5-6). This may imply that the slope wash materials probably contribute to the natural source of thallium in the nearby arable soils.

As is the local custom, house foundation excavations are done by stripping away surface soils and near surficial bedrock (already weathered/broken enough for easily stripping) at the foot of the Lanmuchang Hg-Tl mineralized area. The surface soils and near surficial bedrocks have experienced intensive surface or near surface alteration and chemical/physical weathering, the geochemical baselines of Tl, Hg and As are

pronouncedly high as discussed above. These stripped surface materials were often added to the garden soils, to raise height of the stream bank and improve the soil fertility after removing the gangue. That weathered debris and gravels can be found in the present cultivated garden soils which is the evidence of filling derived from the foundation excavations. This added surface material, together with the natural alluvial deposition at the foot of the Hg-Tl mineralized area along the Qingshui Stream, contributes to the enrichment of Tl in the soils. In other words, even without the foundation excavation disturbance, the soils due to the natural alluvial deposition derived from the Tl-rich slope wash materials and other weathering products can also lead to enrichment of Tl to some extent in these soils.

However, mining also affected the dispersion of Tl in soils along the bank of Qingshui Stream. Soil at site S102 (Fig. 5-3) shows a much higher concentration of Tl (91 ppm) than for other sites (Table 5-6). At sampling site S102, the topsoil (sample S101) contains extremely high Hg, up to 950 ppm, and the subsoil is very high in arsenic (586 ppm) (Table 5-6). The Hg and As values are acid extract fractions, not the "total" content of Hg and As in soils, thus the real "total" contents of Hg and As are expected to be higher. These high values are similar to the concentrations of Hg and As in ores, implying the involvement of mine debris. In fact, the 2-meter depth soil profile shows a number of discontinuity layers of black coal ash mixed with other mine debris from near topsoil to the bottom (Fig. 6-5). This coal ash and mine debris support the finding of mine waste fill used under the present arable soils. The coal ash and mine debris are common in the arable soils between the valleys B and D. As mentioned above, the coal mining and the local domestic

utilization of coals can contribute to another source of enrichment of Tl in soils. The Hg-Tl ores (samples R196 and R333) (Fig. 5-1) identified by this study contain high contents of Tl, Hg and As and can explain why high concentrations of Hg, As and Tl are found in soils mixed with coal ashes and other mine debris.

The arable soils at the middle stream of Qingshui Stream (samples S135, S136 and S141) (Fig. 5-3), containing less coal ashes and mine debris, present less dramatic changes in concentration for Tl, Hg and As. What is noted is that at site S144 (Fig. 5-3) the sample was collected from the top 0-25 cm of the soil layer, and mine wastes were found under this site in which cinnabar was observed. It is therefore obvious that the overlying soils at this site were anthropogenically transported from residence excavation, and not naturally deposited *in situ*.

In summary, the distributions of Tl, Hg and As are controlled by both the natural sources of slope wash materials and weathering products, and the anthropogenic disturbances. The former involves the Tl(As, Hg)-rich weathering products migrating downslope to deposit in the arable soils and thus producing a toxic metal environment. The latter involves mine wastes and coal ash flooded or filled within the soils, and the foundation excavation soils which enhance the concentrations of the three toxic metals. These two processes compound the high enrichment of Tl, Hg and As in the arable soils downward from the Hg-Tl mineralized area.

Compared to the Canadian Environmental Quality Guidelines for thallium, mercury and arsenic (Table 6-4), the arable soils and the undisturbed soils in Lanmuchang area exceed the concentrations of Tl, Hg and As, by 10-126-fold for Tl, 3-38-fold for Hg,

and 8-18-fold for As for both agricultural and residential purposes (except 1-10-fold of Hg for residential purpose). Even without mining disturbance, the concentrations of Tl, As and Hg in soils in Lanmuchang area due to the natural processes present highly contaminated conditions for both agricultural and residential land use, particularly with respect to Tl. The mining activities worsen the situation by introducing more metals into the soils used for farming and residential purposes.

6.3 Interpretation of Tl distribution in sediments

The original source of high Tl in sediments in the Lanmuchang area is from Tl mineralization. High concentrations of Tl and As in sediments indicate that Tl and As in the mineralized rocks in the Lanmuchang area were released through (sub)surface hydrological agents into the aqueous system. The semi-quantitative data for Hg concentration doesn't permit to draw a similar conclusion for Hg. The release of Tl into the sediments can be either caused by the natural processes or enhanced by the mining operations.

Water sediments are mainly composed of a complex mixture of weathered products of geological materials derived within the drainage watershed through discharge of groundwater or surface water runoff.

Groundwater flowing through the broken fault or fracture zones in the mineralized Lanmuchang area can gather large amounts of fine particles into the waters. These fine particles are often Tl-rich clay minerals or amorphous Fe/Al/Mn oxides. Thus, discharging of groundwater can further bring Tl bearing minerals into the stream and deposit them with the stream sediments. High Tl (62 ppm) determined in the bottom sediment of domestic

wells close to the Lanmuchang mineralized area (site SD1012) (Fig. 5-9; Table 5-10) and low Tl determined in well sediments far away from the Lanmuchang area point to a groundwater driven process. Erosion of outcrops or soils by runoff is another natural process controlling the deposition of sediments. The barren outcrops and sloped farmlands are susceptible to weathering and erosion under the warm and humid climate prevailing in the study area.

Tl contents in sediments can be enhanced by mining operations. The AMD involves a metal-rich leachate which contain appreciable Tl-rich amorphous Fe/Al/Mn hydroxides and add to the stream sediments. Water leaching of mine wastes exposed on the surface is another source for the release of Tl into the sediments. The high contents of Tl in the recently formed fine sediments (63 ppm at site SD1122) (Table 5-10) downstream of the waste dumps are clear evidence of contributions from mine wastes.

In the Qingshui Stream, from upstream to downstream, a positive correlation exists for Tl between sediments and stream waters in both the base-flow regime and flood-flow regime (Fig. 6-6; Fig. 6-7). All these correlations indicate an interaction between sediment and water leading to mass exchanges between one another during processes of adsorption/desorption. However, correlation in base-flow regime is better than that in flood-flow regime. This may imply that stream water in base-flow regime has longer time to be in contact with the sediment and the interaction may reach to adsorption/desorption equilibrium.

Furthermore, enzyme leached Tl in sediments shows a much better correlation with its content in stream water under base-flow condition (Fig. 6-7). Enzyme leaching

involves extraction of metals trapped from the amorphous form of Mn and/or Fe oxides that occurs in coatings on mineral grains in sediments (Yeager et al., 1998; Bajc, 1998). The positive correlation from the enzyme leaching data indicates that the Fe/Mn hydroxide coatings on sediment particles are the likely carriers of the mobile fraction of Tl and other metals.

However, the dispersion pattern of Tl in stream water doesn't correspond well to Tl concentrations in sediments, particularly in the downstream section (Fig. 6-8). This implies the existence of other sources rather than sediment release contributing to the high enrichment of thallium in downstream water compared to upper- and middle-stream sections.

High metal contents in sediments have important environmental impacts on the ecosystem (Neumann et al., 1998; CCME, 1999; Ansari et al., 2000). Enrichment of Tl together with other metals due to the natural processes or the mining activities within the Lanmuchang area acts on the environment in two ways. Firstly, the release of Tl can contaminate the water that is used for water supply or irrigation. Particularly in flood-flow conditions, sediments are readily mixed with stream water as indicated by the high turbidity. Secondly, stream bank sediments or dredged stream sediments are often used for cultivation within the enclosed watershed area of Lanmuchang. For instance, stream sediments at the bottom of the sinkhole downstream contain 20 ppm of Tl, whereas the nearby stream bank sediments are enriched in Tl (23 ppm) (Table 5-10). These two sediments show almost the same Tl content. However, soils outside the sinkhole contain much lower Tl levels, down to 0.97-5.5 ppm (Table 5-6). Thus, the stream bank sediments

containing higher Tl are mainly derived from alluvial deposition from upper-middle stream sections.

In summary, the high accumulation of Tl in sediments is one of the important contamination sources in the enclosed watershed of Lanmuchang area. Sediments are the main agents from which Tl from an upstream source area can readily be transported and dispersed to downstream areas. Due to the specific hydro-geomorphological process and topography of Lanmuchang, Tl trapped in sediments can accumulate easily within the enclosed watershed of Lanmuchang, giving rise to a potential thallium contamination and becoming a potential health hazard.

6.4 Interpretation of Tl dispersion in waters

Tl is known to occur in a very dispersed state in nature, and its concentration in natural waters is normally lower as compared to many other metals. However, the concentration of Tl in groundwater and groundwater-recharged stream water in the Lanmuchang study area is much higher than the Tl levels in natural waters reported in the literature (Flegal and Patterson, 1985; Banks et al., 1995; Lin and Nriagu, 1999; Frengstad et al., 2000). Moreover, the occurrence of Tl in the groundwaters in Lanmuchang may be an unparalleled case related to recognizable Tl mineralization (Chen, 1989a,b; Chen et al., 1996; Li, 1996) rather than sulfide mineralization of lead, zinc, iron and copper, polymetallic extracting-processing or cement plant emission (Zitko, 1975b; Dolgner et al., 1983; Schoer, 1984). The general dispersion pattern for Tl in the Lanmuchang aqueous system declines in concentration from mine groundwater → stream water → shallow

groundwater → background water. The occurrences and the dispersions of Tl in the aqueous system are related to the Tl mineralization and water-rock interaction, and can be interpreted to be constrained by hydrogeological conditions.

6.4.1 Contributions of thallium mineralization and water-rock interaction

Tl mineralization is represented by the occurrence of Tl sulfide minerals lorandite, and other Tl-bearing sulfides of arsenic and mercury in the Lanmuchang study area (Chen, 1989b; Li, 1996). The intensive faults and fractures, and mining adits in the supergene zones have likely permitted the O_2-rich and/or the CO_2-rich meteoric waters to migrate through the rock mass to relatively great depths. These waters react with host rocks and Tl ores. The solubility of Tl sulfides is low (0.2 g/l), but the solubility of Tl sulfate is much higher (48.7 g/l) (Sager, 1994). Thus, the weathering processes or breakdown of Tl-bearing sulfides can release significant amounts of Tl into the groundwater and meanwhile decrease the pH values by producing the acid waters. Furthermore, lower pH acidic waters, in turn, may enhance the dissolution of limestone and elevate calcium and the total dissolved solids (TDS) in groundwater.

The groundwater samples with high concentrations of Tl in the study area are restricted within the Tl mineralized strata of P_2l and P_2c. In contrast, shallow groundwater collected from outside the mineralized area contains low Tl, and farther from the mineralized area, some of the samples are below the detection limit (0.005 μg/l). These differences likely reflect the effect of Tl mineralization and its host rocks on the hydrogeochemical composition of groundwater. The concentration of Tl in host rocks

ranges from 33 to 490 ppm, and from 130 to 35000 ppm in ores, whereas the bedrocks outside the mineralized area contain from 0.02 to 0.86 ppm of Tl (Table 5-2). The processes of water-rock interaction are responsible for the strong similarities between rock and water geochemistry (Fig. 6-9).

The geological constraint of Tl mineralization on dispersion of Tl is indicated not only by the enrichment of Tl in groundwater, but also by high sulfate concentrations ranging from 25 to 1200 mg/l (Table 5-8). The elevated contents of SO_4 derived from the primary sulfide minerals or the secondary efflorescent salts, appear to correspond well to the higher Tl levels (Fig. 6-10a). In groundwater, Tl also correlates well to calcium and the TDS (Fig. 6-10b,c). These concomitant increases probably reflect the leaching of the sulfide Tl ore veins by groundwater, enhancing limestone dissolution, and thus elevating the TDS values as well. This is also supported by the negative correlation between Tl and pH values (Fig. 5-13).

The correlations between Tl and Al, Fe and Mn in groundwater also support the idea of contributions from mineralization and water-rock interactions (r values are 0.86 for Tl-Al, 0.93 for Tl-Fe, and 0.83 for Tl-Mn) (Fig. 6-11). These high correlations are related to the fault zones with abundant gouge materials occupying the main groundwater conduit system of the bedrock. These gouge materials are characterized by high amounts of Fe, Al and Mn hydroxides that can contain considerable concentrations of Tl (see Table 5-1 and Table 5-2). Reducing condition indicated by the low dissolved oxygen and acidic condition indexed by low pH values in groundwater (Fig. 5-13) tend to dissolve the Fe, Al and Mn hydroxides and release their adsorbed or coprecipitated contents of Tl to groundwater.

Mobilities of many metals are greatly increased in the acidic waters (Langmuir, 1997). The toxic metal arsenic also shows a similar distribution to Tl, although mercury has no obvious correlation with Tl (Fig. 5-16). These dispersions may be attributed to the fact that the solubility of arsenic sulfides is similar to Tl sulfides, but the low level of mercury in groundwater likely reflect the extremely low solubility and relative resistance of cinnabar to weathering and oxidation (Jonasson and Boyle, 1972; Engler and Patrick, 1975). Rubidium also shows good correlations with Tl in groundwater (Fig. 6-12). This high correlation may reflect the geochemical affinity of the two metals (Heinrichs et al., 1980), and the contribution of water-rock interactions to the water composition.

Tl shows much higher levels in stream water rather than that observed for shallow groundwater discharging to the stream. The average Tl concentration in the stream water in base-flow regime is more than 100 times the value observed for ambient groundwater (Table 5-9). This large difference in concentration could be attributed to either one or a combination of factors such as surface AMD containing high Tl, soil water discharge, Tl-rich stream sediments releasing Tl to the stream water or finally Tl-rich groundwater discharge.

The Qingshui Stream is not substantially recharged by AMD like many streams described in the literature (e.g. Chapman et al., 1983; Fuge et al., 1994; Routh and Ikramuddin, 1996; Paulson, 1997). Indeed, AMD only contributes a small amount to Creek D during a heavy rainfall, modifying its pH value to 3.81 (Table 5-8)but with no apparent effect on the Qingshui Stream. Creeks A, B, C show pH values of 7.94, 7.64 and 8.60, respectively (Table 5-8). A concentration of 59 μg/l of Tl was detected at site W1143 (Fig.

5-9; Table 5-9) in the AMD of Creek D during the rainy season. This value is very similar to that in the deep mine groundwater of site W1097 (54.4 μg/l of Tl) (Fig. 5-9; Table 5-9), but becomes insignificant when mixed with the large volume of stream water as at site W1031 (Fig. 5-9) where the Tl level is only 1.6 μg/l (Table 5-9). This Tl-rich AMD may become an important input of Tl into the stream water when large volumes of Tl mine dewatering for commercial mining is involved.

The water-soil reaction or the soil water seepage may represent one of the factors contributing to the enrichment of Tl in stream water as well. The water in the soil was not analyzed in this study, but very high Tl concentrations ranging from 21 ppm to 100 ppm were detected in the labile fraction of flooded soils along the Qingshui Stream bank, by using strong nitric acid extraction (Table 5-6). The Tl-rich labile portion of soils could facilitate the release of Tl into the soil water, and the stream flow can also enhance the release of Tl during soil erosion along the stream bank. The seepage of Tl-rich soil water and/or the water-soil interaction may thus cause the elevated Tl levels in stream water. This migration mechanism contributes to Tl dispersion in mid-stream, that is, a bit higher concentration of Tl 1.60 μg/l in the flood-flow regime is observed than in the base-flow regime (1.49 μg/l) (Fig. 5-15; Table 5-9), in spite of the fact that water dilution may tend to decrease the Tl concentrations in flooding regime. The elevated concentrations of Tl in Creeks A and B compared to their spring sources (Fig. 5-9) also indicate the contribution of stream bank soil erosion from the upstream section. However, Tl in soils downstream bank is not as high as those upstream and mid-stream banks (Table 5-6), and the soil erosion cannot contribute to the dramatic increases of Tl in downstream waters.

Tl-rich stream sediments releasing Tl to stream water also cannot effectively contribute to higher concentrations of Tl in downstream waters. As illustrated in Fig. 6-8 for the dispersion of Tl in both stream sediments and stream waters, if stream sediments can realistically contribute to high levels of Tl in stream water, there should have been almost the same contributions in both the upstream and downstream where some high Tl values were observed in both stream sediments. However, this is not the case in this study.

Finally, the probable cause contributing to abnormal Tl contents downstream is focused on the Tl-rich groundwater discharge, and is to be discussed below from a hydrogeological perspective.

6.4.2 Hydrogeological constraint

The hydrogeological condition is another constraint on the dispersion and transfer of Tl in the aqueous system of Lanmuchang area. The Tl mineralized area is intensively cut by faults and fractures. As such, the groundwater flowing through the fault/fracture zones can easily leach the Tl ores and enhance migrating of Tl in the aquifers. The groundwater generally flows from the NE to the SW, the same direction as the trend of Tl mineralization-controlling faults (Guizhou Geological Bureau, 1960). Therefore, Tl in groundwater can migrate from the mineralized area to the southwest marginal areas through the NE-SW trending fault zones.

The hydrogeological constraint can be illustrated by the dispersion pattern of Tl in the stream water. As a general fact, it is known that concentrations of metals in stream waters tend to decrease along stream down-gradients. In the case of the Qingshui Stream,

however, if upstream and mid-stream water samplings are compared to downstream water samplings the Tl levels show the opposite trend, that is, the Tl concentrations are much higher downstream than upstream and mid-stream in both base-flow and flooding regimes (Fig. 5-14). The bank sediment/soil erosion as mentioned above cannot satisfactorily explain the unexpected increases of Tl in the downstream section, although they may generally contribute to the enrichment of Tl in stream water. In addition, no AMD drains to the downstream. Therefore, it implies that other sources rather than the soil water seepage and the AMD can explain the significant increase of Tl in the downstream water.

From the above discussion it is evident that the creeks feeding Qingshui Stream cannot account for the higher thallium levels in downstream waters. Topographically, the Huangnijiang fault zone corresponds to a dry valley that only holds the runoff during the heavy rainy season. No water was observed in this valley draining to Qingshui stream during the dry season. So, this excludes the possibility that any surface water bringing Tl from this valley, contributes to the higher Tl concentrations in downstream waters.

Without apparent surface sources, a probable underground source should be considered. Indeed, sites W1065 and W1070, representing very high concentrations of Tl, are within the course of the Huangnijiang fault. Previous hydrogeological drilling data (Guizhou Geological Bureau, 1960) showed that groundwater in deep hydrogeological fractures may discharge outside the Tl mineralized area through the fault zones and flow to the southern margin. Also, the groundwater table is a bit higher at the south margin than elsewhere. The groundwater table elevation, with a 0–20 meter relative elevation above the local streambed and with a fluctuation of 2–5 meter between the dry season and the rainy

season, could facilitate the discharge to the surface streambed if such an outlet of discharge is available. Therefore, unidentified groundwater seepage probably explains the unexpected high Tl contents in the downstream waters, that is, the unidentified groundwater seepage transports the Tl-rich solution or particles from the Tl mineralization area to discharge points at the downstream surface, and subsequently causes the high content of Tl in the downstream waters. The increased concentrations of arsenic, rubidium and sulphate, and the decreased content of bicarbonate also suggest an unidentified groundwater discharge. A similar case study of the Farr Creek drainage basin in Cobalt, Canada, also suggests that in this site, some unidentified groundwater passing through fault zones contributes to the increase in arsenic in downstream waters (Percival et al., 1996).

The hydrogeological constraint can also be illustrated by the higher concentration of Tl (0.337 μg/l) observed in a shallow well water at site W1012 (Fig. 5-9; Table 5-9). This sampling site is close to the Tl mineralization and is located in the terrace of the Lanmuchang fault near the Qingshui Stream bank. Dissolved oxygen (3.49 mg/l) in this well water is much lower than in the ambient stream waters (5.27–8.48 mg/l) (Table 5-8). Higher Tl concentration in this well water indicates that the groundwater may discharge to this well through the fault zones, and/or that the ambient stream water with higher Tl content (1.4 μg/l) at site W1103 may also seep to this well (Fig. 5-9; Table 5-9).

6.4.3 Impacts of groundwater related thallium transfer

Thallium generally exists in natural waters as species of Tl^{+} and Tl^{3+}, but the Tl^{+} species is dominant in the aquatic environment (see Fig. 4-2) (Vink, 1993; Kaplan and

Mattigod, 1998). The solubility of Tl^+ compounds is quite high, suggesting that Tl^+ would not precipitate from solution in most aquatic environment (Sager, 1994). Tl is also expected to move rather readily with groundwater flow and its attenuation by sediments would be very limited (Kaplan and Mattigod, 1998). All these factors would indicate that Tl is a very mobile metal in most natural environments, rather than being locked-up into solid oxides, and Tl disperses easily during oxidation of Tl-bearing sulfides (Vink, 1993).

In this study, the primary sources of Tl in the aqueous environment of the Lanmuchang area are the Tl-rich sulfide minerals. The water-rock interactions through oxidation and/or dissolution of Tl ores raise Tl levels in ground and surface waters. The Lanmuchang watershed receives water from groundwater discharge, and drains surface water to a sinkhole downstream (Fig. 3-4). Groundwater contributes Tl to surface waters in three ways: first, by discharge or seepage through fault zones or soil zones, second, by direct AMD, and third, by de-watering during mining. These groundwater thallium transfer processes have an environmental impact on the ecosystem.

Domestic wells can be easily contaminated by Tl-rich groundwater as it seeps to shallow aquifers where the wells are located. In fact, very high concentrations of Tl (17–40 μg/l) were detected in well waters within the Tl mineralized area in 1977 by Zhou and Liu (1985), and these Tl-rich well waters for drinking supply before the 1980's have caused some chronic Tl poisoning (Zhou and Liu, 1985). At present, some of the wells have been sealed and abandoned, and other wells still supplying drinking water show much lower levels of Tl (0.12–0.34 μg/l, this study) (Table 5-9). For the domestic wells investigated by Zhou and Liu (1985), the locality and the thallium concentration in water for each well

were not specifically indicated. The analytical QA/QC documentation for thallium determination in their study is also unknown. Therefore, it is difficult to compare the thallium data in the drinking water between the present study and the earlier study. It has been shown that groundwater seepage proximal to the fault-mineralized area is the most plausible reason for the Tl distribution pattern in the stream waters. If a single well from the present study is located in the vicinity of a well or just the same well as in the 1985 study, the data in this present study points to a major reduction in the thallium level. If so, it can be argued that the groundwater recharging the wells is restricted to a very localized aquifer having depleted its thallium content over the years. The oxidation process for Tl-bearing rocks or ores actually tend to deplete Tl over the years, and thus release less Tl into the groundwater recharging to the wells.

To date, threshold of Tl in drinking water has not been regulated by the WHO, but it was set as 2 μg/l by the USEPA in 1993 (USEPA, 2000). This concentration is much lower than many other toxic metals (e.g. 50 μg/l for As, 5 μg/l for Cd, 6 μg/l for Sb and 2 μg/l for Pb) (USEPA, 2000). In Russia, the limit is much stricter, down to 0.1 μg/l (Frengstad et al., 2000). The well water in the Lanmuchang area is thus over the Tl safe limit of Russia and lower than that of the USEPA. Therefore, the potential risk of Tl poisoning from drinking water in the Lanmuchang area should be constantly monitored. Furthermore, any future mining in the area must keep in mind the potential Tl contamination to the drinking water through Tl-rich groundwater transfer processes.

Stream water is the only source for domestic use and agricultural irrigation in the Lanmuchang area. The local villagers use the thallium-rich stream water for daily washing

(e.g. washing clothes or vegetables), through which thallium may also enter the villagers' skins. The exposure of thallium to skin causing thallium poisoning was mentioned by Dolgner et al. (1983) and Dmowski et al. (1998), but its effects on skin of people in the Lanmuchang area is not clear. The Tl-rich stream water can also cause Tl contamination in soils. Soils, in turn, contaminate vegetables by uptake of Tl and finally affect the food chain with high Tl contents (Cataldo and Wildung, 1978; Tremet and Mench, 1997). If the totality of Tl sources were summed, irrigation water containing 1 μg/l of Tl would contribute Tl ranging from 0.26 to 1.0 μg/g to plant materials, which can be regarded as the upper limit for human and farm animal consumption (Sager, 1998). At this point, it is worth noting that waters containing Tl at 19.3 μg/l drain to the sinkhole downstream (Fig. 5-9; Table 5-9), and that a new underground irrigation channel was constructed in 1998 to pipe part of the sinkhole waters to a neighboring farming area, south, outside of the studied watershed. Therefore, there is a definite possibility that Tl contamination may extend its impact outside the Lanmuchang watershed. This implies that natural Tl in the aqueous system can multiply its effect through soil and agricultural contamination, and finally reach the food chain.

6.5 Interpretation of Tl dispersion in crops and vegetation

6.5.1 Distribution of Tl, Hg and As in various crops

As described in Section 5.5, thallium shows a distinct dispersion pattern in the edible parts of vegetables and cereals generally cultivated in the Lanmuchang area. The enrichment of Tl is species-dependant (Fig. 6-13). The highest enrichment of Tl is in green

cabbage, 338 ppm (DW) on average (Table 5-14). The second highest enrichment is in carrot root, up to 22 ppm. (Table 5-14). Tl in chili is also concentrated up to 4.1 ppm on average (Table 5-14). In shelled rice and Chinese cabbage, Tl contents slightly decline to 2.4 ppm and 2.2 ppm, respectively (Table 5-14). Finally, Tl in corn is concentrated at an average of 1.5 ppm (Table 5-14). All the crop plants in areas outside the Lanmuchang Hg-Tl mineralized area contain much lower thallium content, generally down to 0.5 ppm (Table 5-14). However, crops growing slightly away from the Hg-Tl mineralized area show Tl concentrations higher than those in areas outside the Lanmuchang but lower than those within the Lanmuchang Hg-Tl mineralized area (Table 5-14). This indicates that thallium concentrations in plants reduce when going downslope and that the concentration is not spread beyond the Lanmuchang mineralized area because of the specific geomorphological context.

The correlations of As-Tl and Hg-Tl in the crops are illustrated in Fig. 6-14 and Fig. 6-15, respectively. The data plots are quite scattered, and good correlations are not observed. This may indicate that the uptake ability of the three metals is different from one another. Indeed, concentrations of Tl, Hg and As in crops differ from one another. Tl is more enriched in crops than its counterparts Hg and As, and As is slightly richer than Hg. This distribution tendency is quite different from that in soils, where the general tendency of distributions is that Hg is slightly higher than As, and Tl presents the lowest concentration (Fig. 6-16). Thus, Tl seems to be taken up preferentially by the crops.

The favorable uptake of Tl into the crops is likely due to the close geochemical affinity between thallium and potassium. These two elements have similar ionic radii of Tl^{+}

(1.59 Å) and K^+ (1.51 Å) (Table 4-1). Because of the very similar ionic radii, thallium can readily substitute for potassium in biota during the biochemical process. Potassium was not detectable in this study (see Appendix), but potassium, as one of the major constituents in biota, should be available for substitution by thallium. The replacement of potassium by thallium and accumulation of thallium in certain crops are widely mentioned by many researchers (Siegel and Siegel, 1976; Schoer, 1984; Tremel and Mench, 1997; Tremel et al., 1997; Leblanc et al., 1999). However, conditions in plants, which are conductive to the substitution of Tl for K, are not very clear.

During the biochemical process, Tl occurs as single-charged, weakly hydrated cation (Tl^+) with ionic radium similar to K^+, and is expected to interfere competitively with K-dependent biological reactions. Tl has the ability to yield complexes with sulfur-containing and phosphorus-containing ligands, leading to a substitution of K at its specific adsorption sites. The Na^+/ K^+-ATPase plays the main role in uptake of K^+ (Edwards et al., 1995). Some explanations for Tl uptake by crops have also been discussed in Section 4.4.1.

The enrichment of Tl in crops is closely related to Tl-rich soils. The soils within the Lanmuchang Hg-Tl mineralized area and along the Qingshui Stream bank are rich in Tl, Hg and As due to both natural processes and human activities as discussed in Section 5.2. These metals can enter the crops growing on these soils through biochemical up-take. The high concentration of Tl in the crops growing in the metal-rich soils in the study area supports the idea of toxic metals being transferred from the soil to the crops. In contrast, crops growing in the uncontaminated soils outside the Lanmuchang area show low concentration of thallium. Concentration of Tl in both green cabbage and Chinese cabbage

correlate with its content in soils on which these crops are growing (Fig. 6-17). Therefore, the high concentrations of Tl in crops within the Lanmuchang Hg-Tl mineralized area directly reflect its source in the contaminated soils.

Thallium presents different concentrations within types of crops and vegetation. Thallium is more enriched in green cabbage than in other crops, generally two orders of magnitude higher (Table 5-14; Fig. 6-13). The pronounced enrichment of Tl in wild cabbage and fern growing in the Lanmuchang Hg-Tl mineralized area was also observed. Enrichment of Tl in green cabbage plants and rape was also noted by many researchers (Lehn and Schoer, 1987; Tremel and Mench, 1997; Schoer, 1984; Kurz et al., 1997). These investigations show marked genotypical differences within the edible parts of common crops in uptake of Tl. However, the possible causes for the genotypical differences in Tl accumulation are unclear.

The enrichment of Tl in green cabbage is not only indicated by high concentrations of Tl but also expressed by the enrichment factor with respect to the concentration of Tl in soils. As listed in Table 5-6, Tl within the Lanmuchang area contains high amounts of labile fraction extracted by nitric acid. Labile fraction of a metal, containing the ionic exchangeable fraction, carbonate fraction and sulfide fraction, is more bioavailable (Ernst, 1996; Tremel et al., 1997). This fraction can be more readily mobilized from soils to vegetation than the total content. Thus, the mobile fraction of Tl in soils within the Lanmuchang area probably reflects the up-take ability of various crops, although the most readily up-take fraction is the water-soluble fraction which was not determined in this study. Using the Tl values of the labile fraction in soils (C_{soil}) and Tl values in vegetation

($C_{vegetation}$) growing on these soils, the enrichment factor of Tl in the vegetations can be defined by the ratio of $C_{vegetation}/C_{soil}$. The enrichment factors for green cabbage and Chinese cabbage are shown in Fig. 6-18. The results show that the enrichment factor is up to 1.13 to 10.73 for green cabbage, whereas Chinese cabbage shows factors under 1. Corn, chili and rice show similar factors as the Chinese cabbage, generally below 1. This clearly illustrates that green cabbage has the highest enrichment factor for Tl among the crops. If the extractable fraction in soils by DTPA-TEA (diethylenetriaminepentaacetic acid–triethanolamine) (Lindsay and Norvell, 1978) or by NH4-acetate (Lehn and Socher, 1987) was used, the enrichment factor of Tl for green cabbage is expected to be much higher than the current range of 1.13-10.73, because it would show lower concentration of the mobile fraction than the nitric acid extractable fraction,

This study only considered the edible parts of the crops, i.e. leaves of green cabbage and Chinese cabbage, chili pods, corn grains, shelled rice or carrot root. The roots of cabbage; leaf, stalk, root of chili; and stalk and hay of rice or corn were not analyzed. Some studies have shown that crop roots (e.g. soybean plants and barley) are enriched in Tl more than the other parts (Kaplan et al., 1990), but some researchers have observed the opposite, that is, thallium is more enriched in shoots than in roots (e.g. rape) (e.g. Al-Attar et al., 1988). The carrot roots containing up to 21.6 ppm of Tl (Table 5-14) may be an indication supporting the above mentioned studies, although the Tl values in carrot leaves are unavailable from the present study. Similarly, the stalk of corn and husks of rice although not analyzed, may also contain high amounts of thallium. If they are used as animal fodder, it is possible that Tl will enter the food chain indirectly. However, Tl in

edible parts of crops can more readily enter the food chain by human consumption and increase the risk of thallium poisoning.

Tl concentrations also differ depending on the period of growth for the same species of crops. For example, young green cabbage contains much lower Tl content than harvested cabbage. Green cabbage labeled B212 (Fig. 5-18) collected one month before the harvest season contained 32 ppm of Tl, whereas harvested cabbage contained 120-494 ppm of Tl (Table 5-14), which is 4-16 times higher. This difference underlines the fact that the accumulation of Tl in vegetation increases with time through the whole biological process of growth.

6.5.2 Evaluation of environmental impacts of Tl, Hg and As in crops

The local villagers in the Lanmuchang Hg-Tl mineralized area consume the crops growing in metal-contaminated soils during the entire year. Chinese cabbage, green cabbage and chili are often freshly consumed, whereas corn and rice are consumed after air-drying. The yield of metals in cabbage and chili from fresh and dried samples were determined by dividing the dry weight by the fresh weight (Table 6-5). Thus, by using the values of dry yield and ash yield, the contents of metals from each crop type consumed by the villagers can be quantitatively estimated by using the following equation:

$$\text{Daily consumption} = \sum_{i=1}^{m} R_i R'_i C_i M_i + \sum_{j=1}^{n} R'_j C_j M_j$$

Where

i = Vegetable

j= Cereal

Ri = Dry yield (Dry weight/Fresh weight, %)

R'_i, R'_j = Ash yield (Ash weight/Dry weight, %)

C_i, C_j =Concentration of metal based on ash weight (Laboratory analysis results, ppm)

M_i = Daily consumption of fresh vegetables (gram)

M_j = Daily consumption of dry cereals

For this study, the amounts of crops harvested from the lands with Tl-Hg-As contamination and consumed by an adult each day are estimated in Table 6-6. The estimation of food consumption are modest, but they could possibly be higher for some families, thus increasing the estimate of ingested thallium. Nevertheless, the daily ingestion of thallium (2.7 mg) through foods calculated within the Lanmuchang area is high compared to areas barren of Tl mineralization outside Lanmuchang (0.043mg, see Table 6-6). The calculated ingestion rate of Tl in human body is up to 39 μg/kg/day on average (body weight of an adult is considered as 70 kg) from the Lanmuchang area, which is 62 times the concentration from the background area barren of Tl mineralization (Table 6-6). However, the daily ingestions for both Hg and As are 0.008 mg and 0.024 mg, respectively, which are much lower than for Tl (Table 6-6). The values of ingestions in the background areas are 0.005 mg for Hg and 0.016 mg for As (Table 6-6), also lower than for Tl. This clearly indicates that the Tl in the contaminated arable soils relative to the Tl mineralization is being readily transferred to the human body through the food chain, whereas the ingestion of Hg and As are less significant.

Very little is known about the threshold levels of Tl that may be harmful to health for different age groups. However, the minimum lethal dose (LD_{LO}) of soluble thallium

salts for an adult has been estimated to be from 0.7 to 1.1 g (from 10-15 mg Tl/kg body weight) (Moeschlin, 1980). Studies of thallium exposure to humans in a wide variety of geographic locations have indicated less than 2 μg as the average daily intake of Tl from environmental sources (Sabbioni et al., 1984). Therefore, the villagers within the Lanmuchang area ingest Tl from food sources, 1350 times higher than the average daily intake (2 μg/day) estimated by Sabbioni et al. (1984). This high ingestion amount of Tl will certainly have adverse effects on human health in the local area of Lanmuchang.

High concentrations of Tl in urine are often a good indicator of abnormal thallium ingested by the body leading to subchronic or chronic thallium intoxication (Bank et al., 1972; Dolgner et al., 1983; Chandler et al., 1990). Distribution of thallium in urines from the local villagers was not determined during this study, but previous epidemiological studies showed high thallium in urines, ranging from 600 to 3000 μg/l in the 1970's (Zhou and Liu, 1985) and 77.7 to 2660 μg/l in the 1990's (Zhang et al., 1999). Within the past three decades, high Tl levels in urine in the villagers of Lanmuchang area have been nearly constant. This likely reflects the continuous ingestion of thallium over the years from foods grown in the Lanmuchang Hg-Tl mineralized area where the arable soils are markedly enriched in thallium.

Concentrations of Hg and As in urine of the local villagers in the Lanmuchang area were also determined by Zhang et al. (1999). Hg ranges from 0.03 to 3.32 μg/l, and As ranges from 0.1 to 6.65 μg/l in the urines analyzed. All the values of Hg and As are significantly lower than thallium values, in fact nearly 2-5 orders of magnitude lower. This illustrates the low daily ingestion of Hg and As through the consumption of food.

Therefore, Hg and As are unlikely to trigger chronic poisoning in the Lanmuchang area as does Tl.

Table 6-1 Estimation of baseline value for Tl, Hg and As in rocks *

Metals	Baselines (ppm)
Tl	82
Hg	113
As	106

Estimation is based on the data of samples from outcropped host rocks

Table 6-2 Composition of some secondary minerals by X-ray diffraction

Sample	Minerals	Chemical formula	Laboratory
M001[a]	Kalinite	$KAl(SO_4)_2 \cdot 11H_2O$	Geological Survey of Canada, Ottawa
M002[a]	Copiapite	$MgFe_4(SO_4)_6(OH)_2 \cdot 20H_2O$	Geological Survey of Canada, Ottawa
AM01[a]	Pickeringite Zaherite	$MgAl_2(SO_4)_4 \cdot 22H_2O$ $Al_{12}(SO_4)_5(OH)_{26}$	Institute of Geochemistry, Guiyang
AM04[b]	Epsomite Morenosite	$MgSO_4 \cdot 7H_2O$ $NiSO_4 \cdot 7H_2O$	Institute of Geochemistry, Guiyang
AM06[a]	Halotrichite Picheringite	$FeAl_2(SO_4)_4 \cdot 22H_2O$ $MgAl_2(SO_4)_4 \cdot 22H_2O$	Institute of Geochemistry, Guiyang
AM07[b]	Fibroferrite Alunogen Ferricopiapite Rozenite	$Fe(SO_4)(OH) \cdot 5H_2O$ $Al_2(SO_4)_3 \cdot 17H_2O$ $Fe_{4.67}(SO_4)_6(OH)_{2.2}$ $FeSO_4 \cdot 4H_2O$	Institute of Geochemistry, Guiyang

a: sampled from underground sites; b: sampled from the fractures of outcropped rocks

Table 6-3 Baseline value of Tl, As and Hg in natural soils

Soils		Tl (ppm)		Hg (ppm)		As (ppm)	
Slope materials	House foundation (N = 2)	40-46	(A = 43)	64.4-81.5	(A = 73)	95.7-109	(A = 102.4)
Undisturbed soils	Close to mine area (N = 2)	12-29	(A=20)	18.8-61.8	(A = 40)	59-69.8	(A = 64)
	Slightly away from mine area (N = 5)	2.2-10	(A=7)	0.8-28	(A = 13.8)	37.1-89.1	(A = 55.6)*
Background soil	Outside Lanmuchang (N = 3)	0.47-0.97	(A=0.69)	0.26-0.87	(A = 0.53)	4.4-7.46	(A = 5.52)

N= number of sample; A= average; * = Sample S173 was not included in calculation due to abnormal As value.

Table 6-4 Canadian environmental quality guidelines for some toxic metals [a]

Metals	Soil (ppm)		Freshwater sediment (ppm)		Fresh water (μg/l)	
	Agricultural land use	Residential/ Parkland use	ISQG [b]	PEL [c]	Community	Aquatic life
Tl	1	1	/	/	2[d]	0.8
Hg	6.6	24	0.17	0.486	1	0.1
As	12	12	5.9	17	25	5.0
Cd	1.4	10	0.6	3.5	5	0.017
Cr	64	64	37.3	90	50	/
Cu	63	63	35.7	197	≤1000	2-4
Pb	70	140	35	91.3	10	1-7
Zn	200	200	123	315	≤5000	30
Ni	50	50	/	/	/	25-150
Ba	750	500	/	/	1000	/

a. Source: CCME, 1999; b. Interim sediment quality guideline; c. Probable effect level; d. US-EPA (2000)

Table 6-5 Dry yield and ash yield of various crops

Crops	Dry yield (Dry weight/Fresh weight;%)	Ash yield (Ash weight/Dry weight; %)
Chinese cabbage	2.51	24.23
Green cabbage	6.67	24.36
Chili	5.32	10.26
Corn	/	1.36
Rice	/	1.57

Table 6-6 Estimation of daily ingestion of Tl, Hg and As from crops in the Lanmuchang area

Crops	Metals	Dry weight (mg/kg)		Converted fresh weight yield (%)	Consumption amounts of foods (kg/day)	Total oral ingestion of metals (mg/day)	
		LMC [a]	BK [b]			LMC	BK
Chinese cabbage	Tl	2.2	0.26	2.51	0.1	0.006	0.0007
	Hg	0.44	0.28			0.001	0.0007
	As	0.89	0.47			0.002	0.0012
Green cabbage	Tl	338	0.39	6.67	0.1	2.25	0.0026
	Hg	0.63	0.33			0.004	0.0022
	As	0.7	0.32			0.005	0.0021
Chili	Tl	4.1	0.27	5.32	0.05	0.011	0.0005
	Hg	0.03	0.01			0.0001	0.0001
	As	0.27	0.19			0.0007	0.0005
Corn	Tl	1.491	0.069	/	0.1	0.149	0.0069
	Hg	<0.005	<0.005			<0.0005	<0.0005
	As	0.020	0.024			0.002	0.0024
Rice	Tl	2.41	0.25	/	0.1	0.24	0.026
	Hg	0.027	0.02			0.003	0.002
	As	0.15	0.09			0.015	0.009
Total	Tl					2.7	0.043
	Hg					0.008	0.005
	As					0.024	0.016

a: LMC = Lanmuchang area; b: BK = Background area outside Lanmuchang

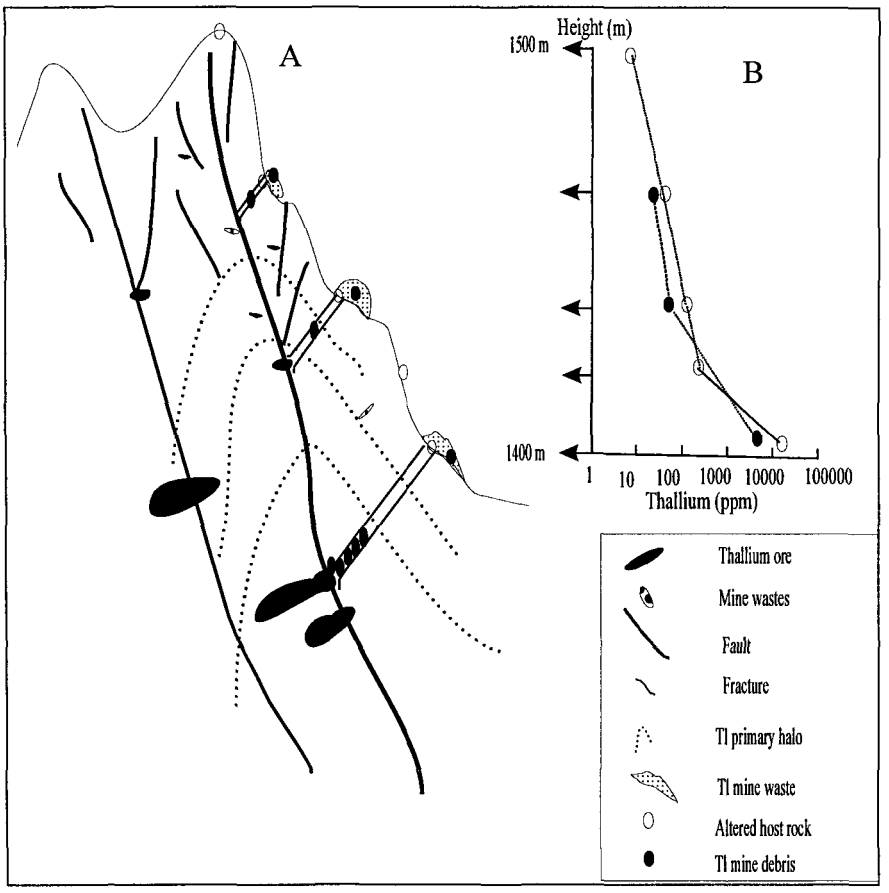

Fig. 6-1 Schematic vertical section of dispersion of thallium(A) and its concentration plot (B) associated with primary ores and mining

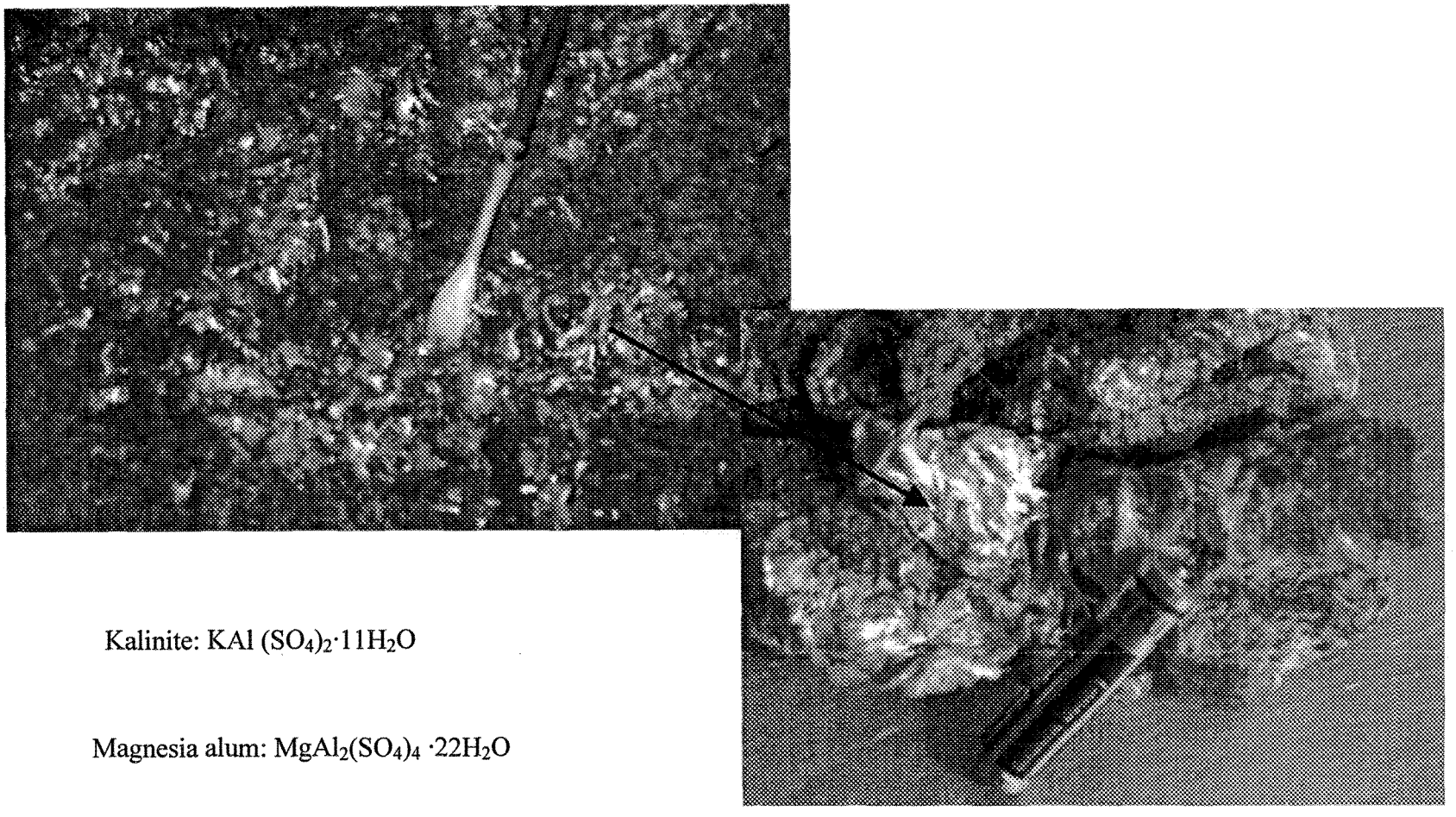

Kalinite: $KAl(SO_4)_2 \cdot 11H_2O$

Magnesia alum: $MgAl_2(SO_4)_4 \cdot 22H_2O$

Fig. 6-2 Some secondary minerals occurring in fault zones in the Lanmuchang mineralized area

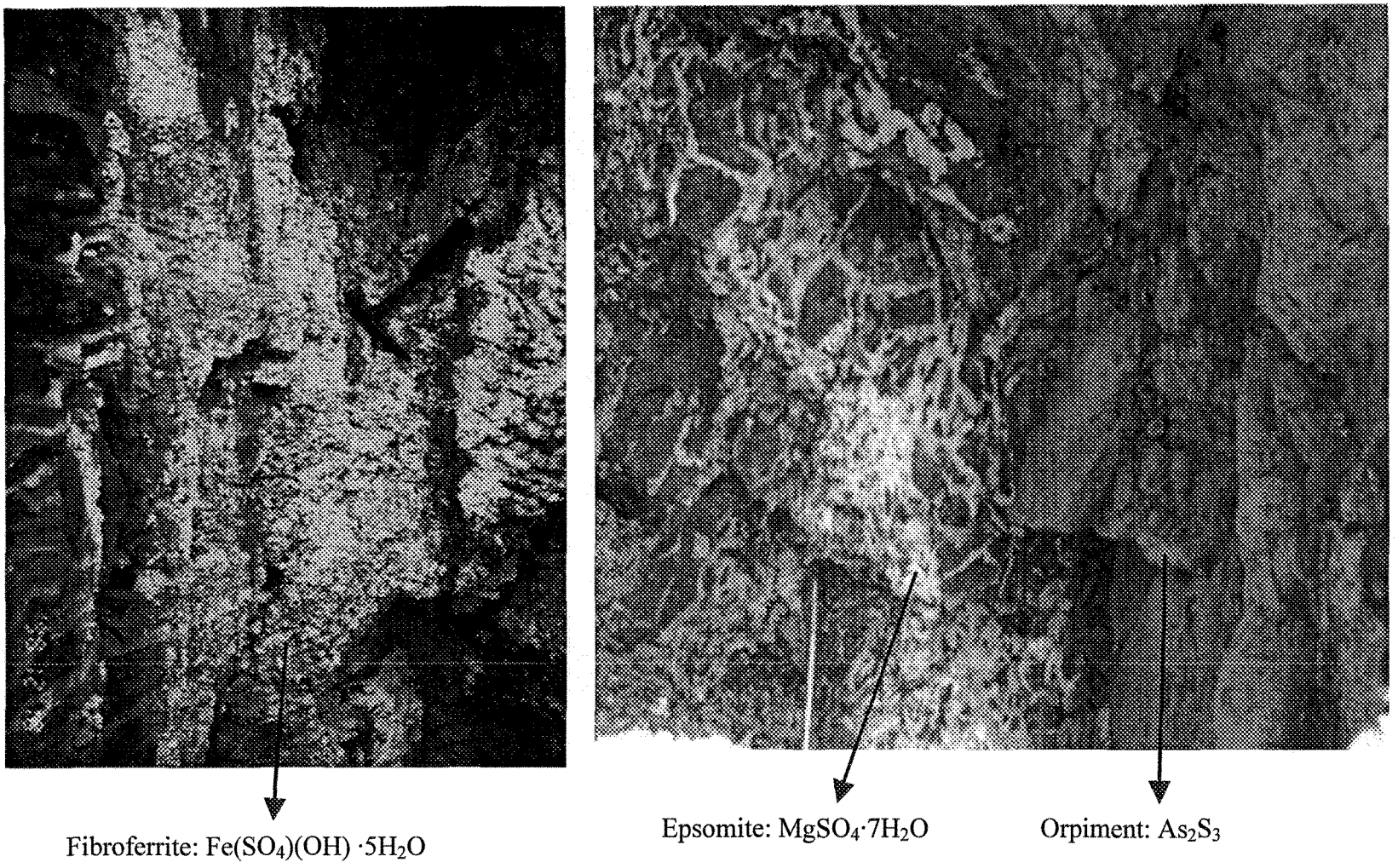

Fig. 6-3 Some secondary minerals occurring in fractures of outcropped host rocks in the Lanmuchang mineralized area

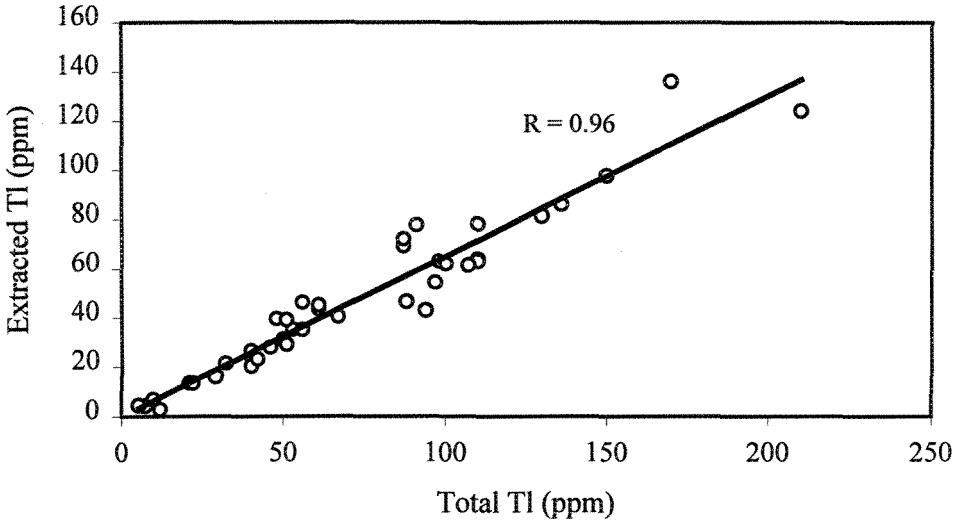

Fig. 6-4 Concentration of mobile fraction of Tl versus total Tl in soils

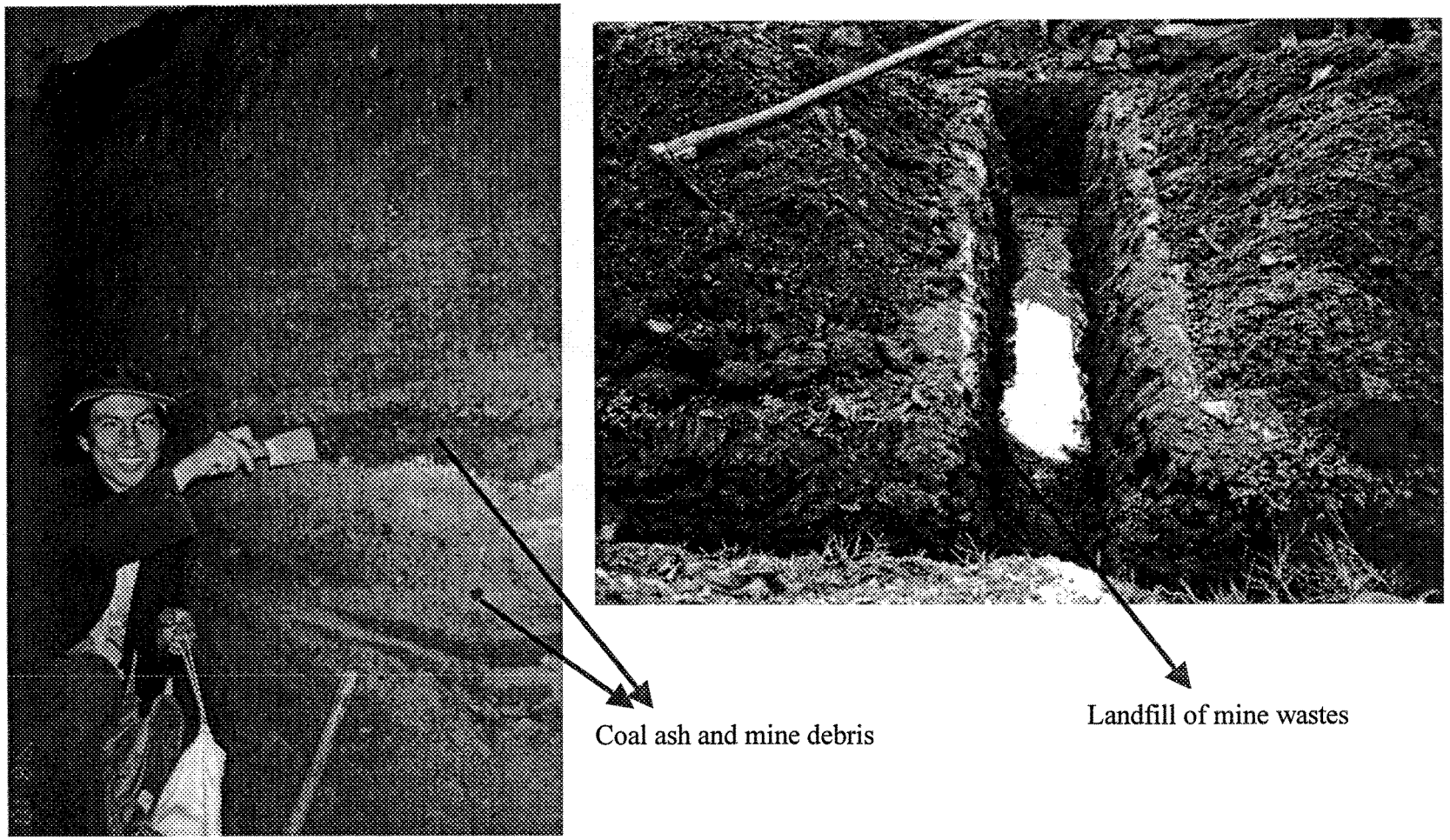

Fig. 6-5 Impacts of mine wastes on arable soils in the Lanmuchang area

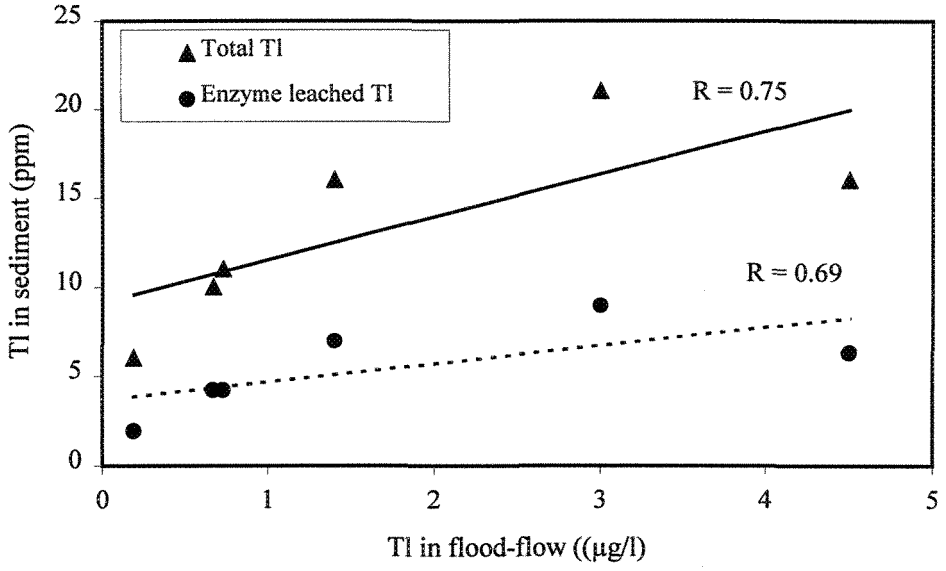

Fig. 6-6 Concentration of Tl in sediments versus stream waters (flood-flow)

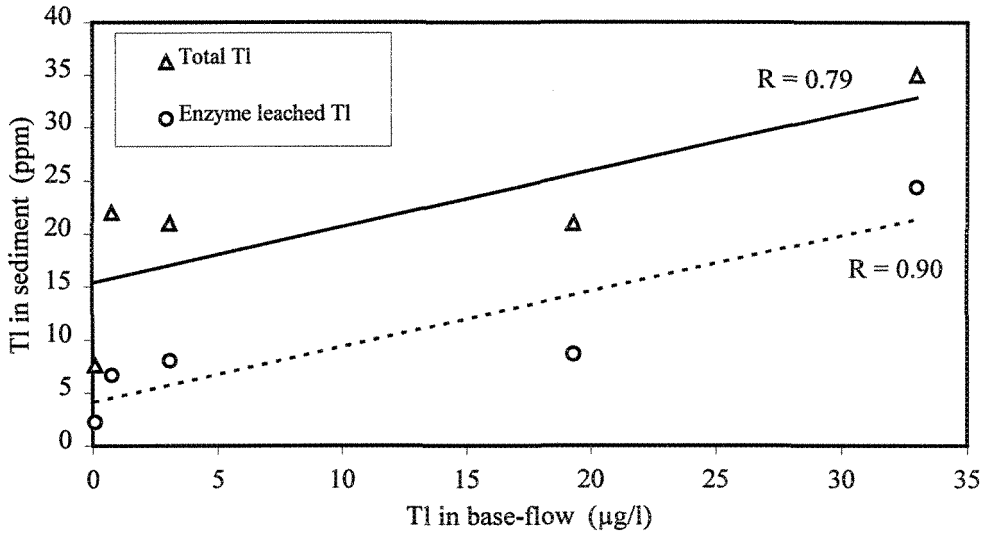

Fig. 6-7Concentration of Tl in sediments versus stream waters (base-flow)

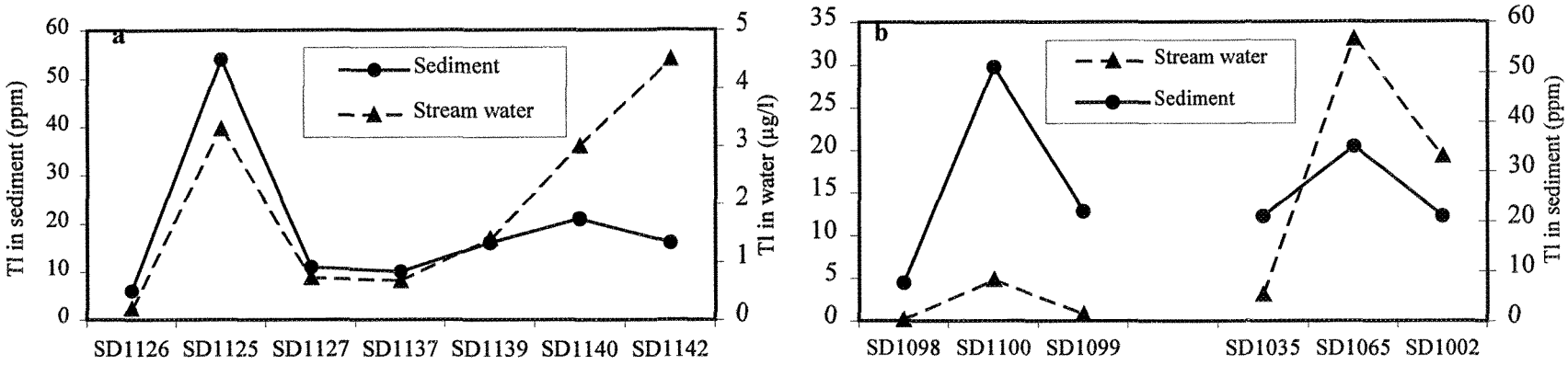

Fig. 6-8 Dispersion pattern of Tl in stream water and sediment in (a) flood-flow regime and (b) base-flow regime

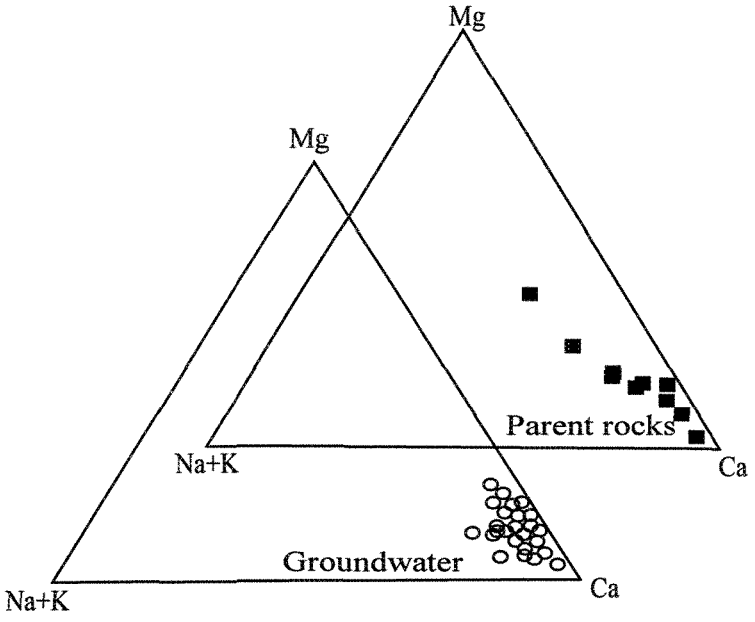

Fig. 6-9 Ternary plot of parent rocks and groundwaters

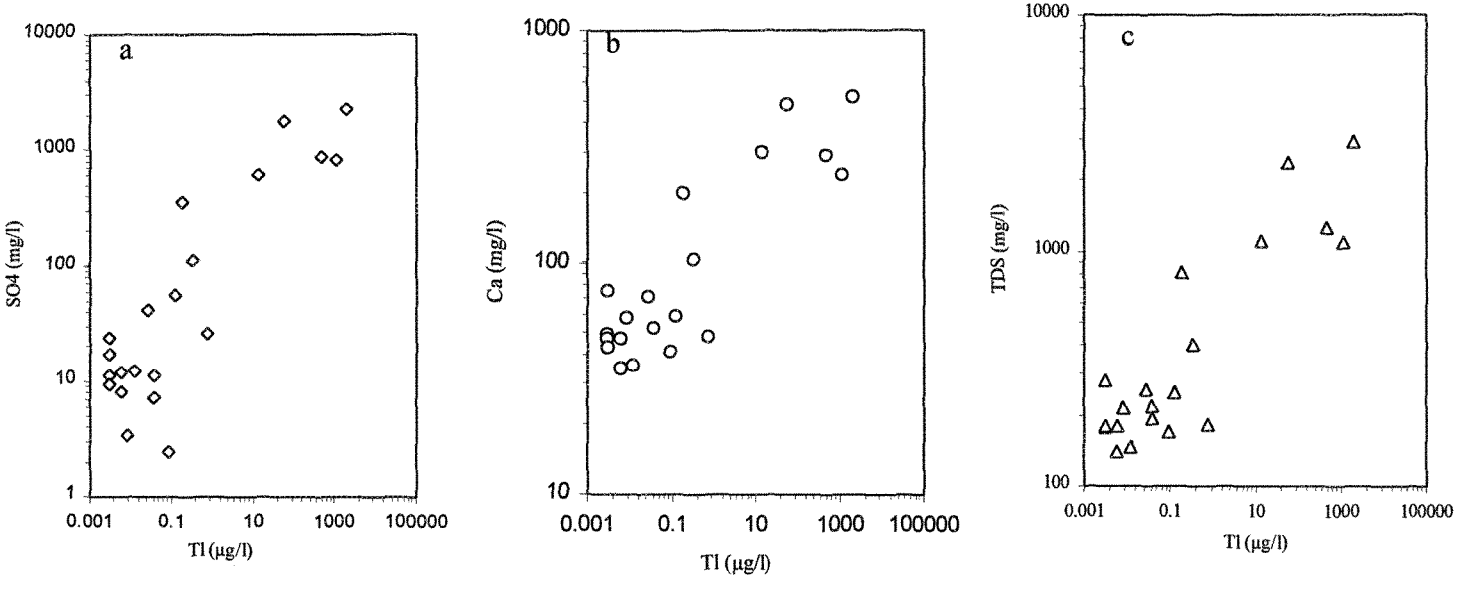

Fig. 6-10 Sulfate (a), calcium (b) and total dissolved solids (c) versus thallium in groundwaters

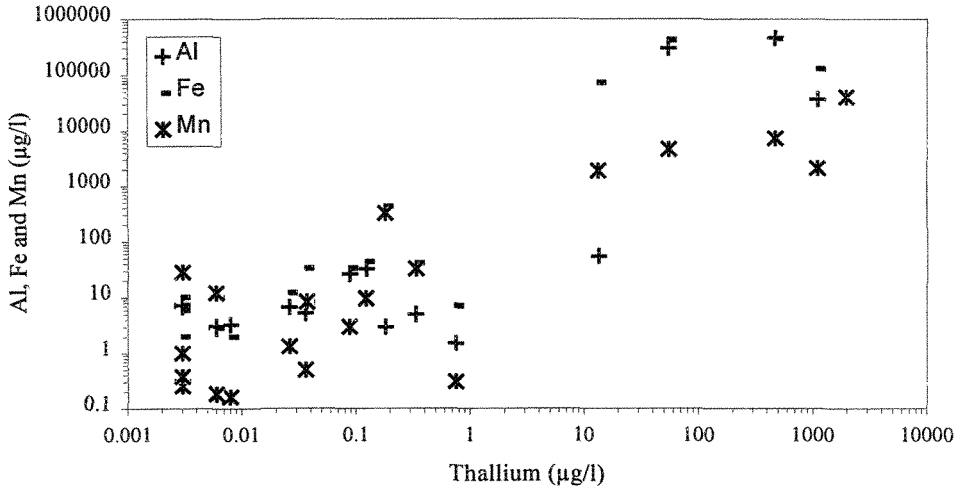

Fig. 6-11 Fe, Mn and Al vs Tl in groundwaters

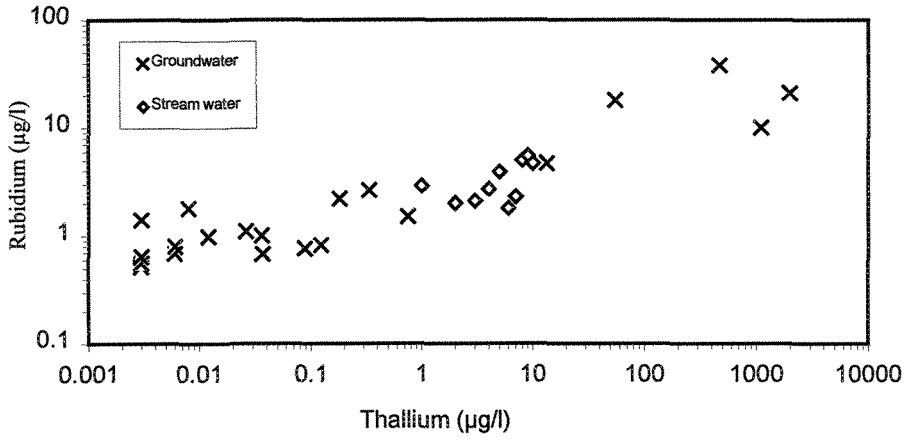

Fig. 6-12 Rb versus Tl in groundwaters and stream waters

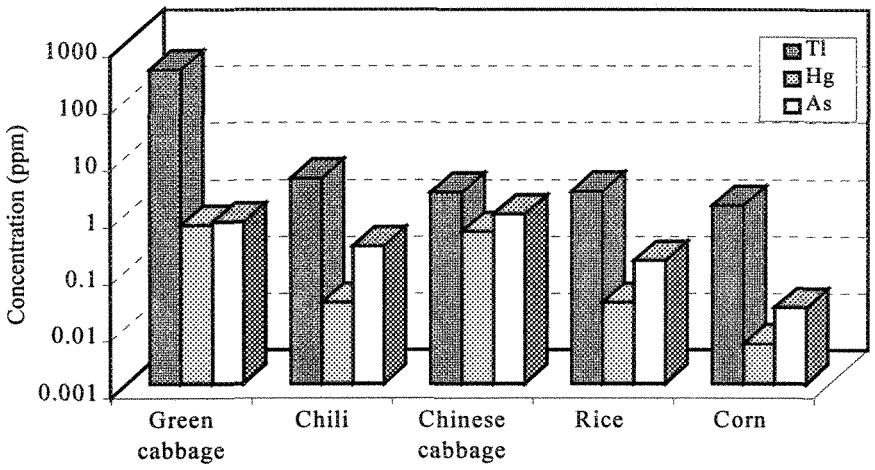

Fig. 6-13 Distribution of Tl, Hg and As in crops

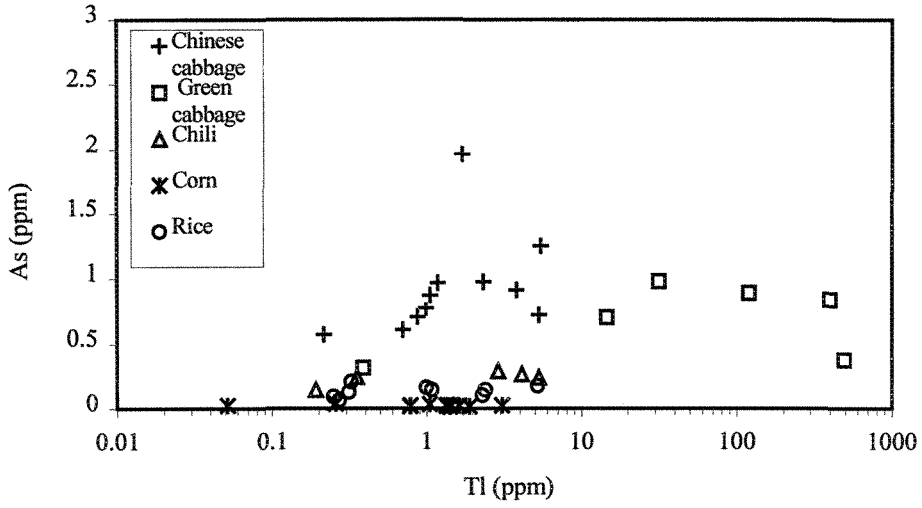

Fig. 6-14 Concentration of arsenic versus thallium in crops

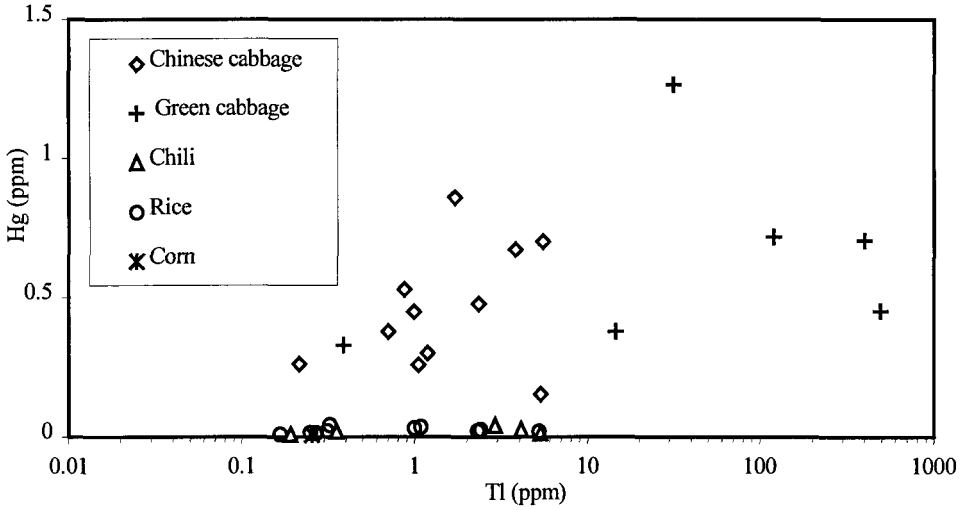

Fig. 6-15 Concentration of Hg vs Tl in crops

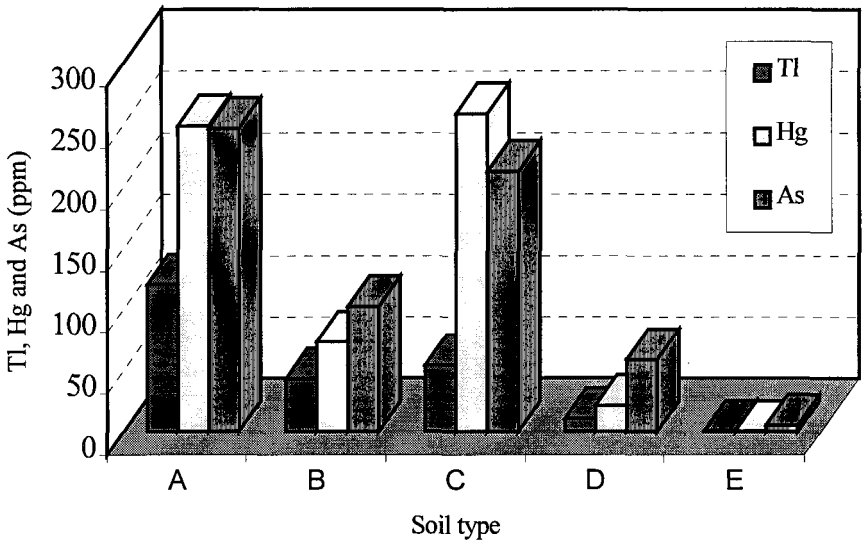

A = Soils in mine area; B = Slope wash materials; C = Alluvium deposits or foundation soils; D = Undisturbed natural soils; E = Background soils

Fig. 6-16 Distribution of Tl, Hg and As in soils

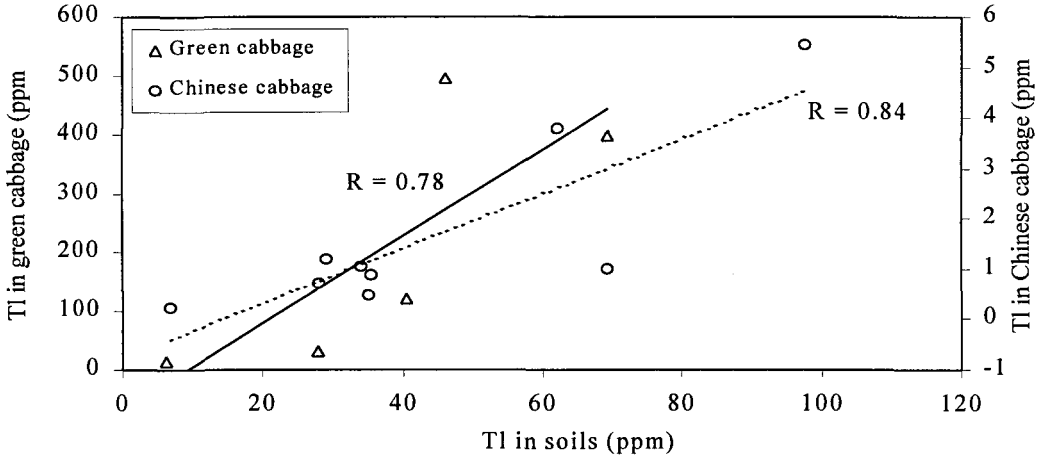

Fig. 6-17 Concentration of Tl in green cabbages and Chinese cabbages versus Tl in soils

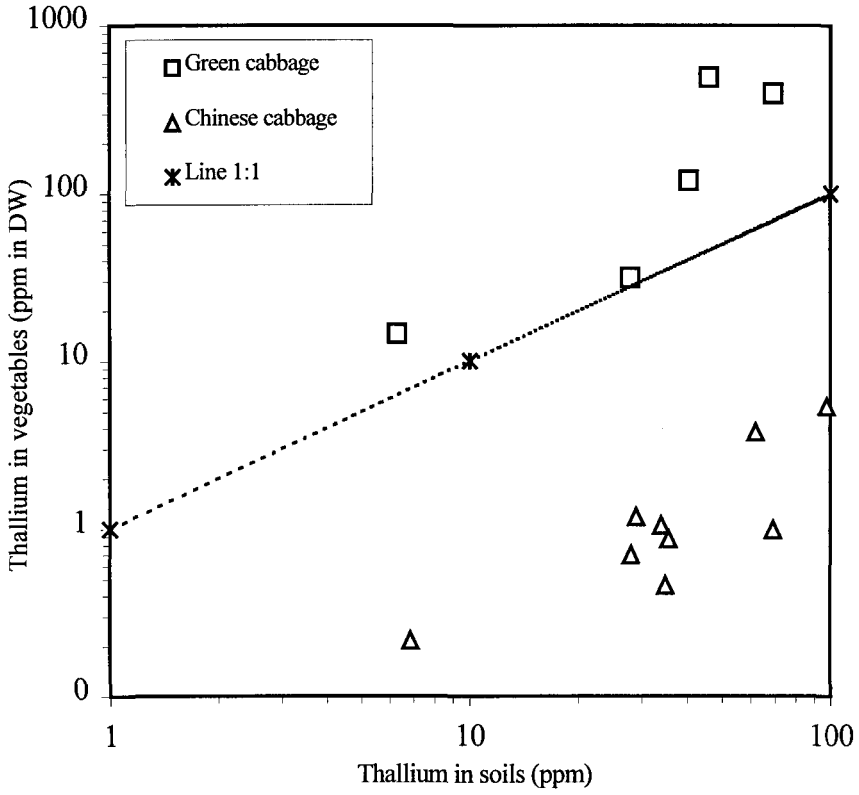

Fig. 6-18 Enrichment factors of Tl in green cabbages and Chinese cabbages with respect to Tl contents in soils

CHAPTER 7

ENVIRONMENTAL IMPACTS OF THALLIUM DISPERSION IN THE LANMUCHANG AREA

7.1 Pathways of thallium into the human body

Pathways of thallium into the human body usually occur by oral, dermal, or inhalation routes. Thallium is released into the atmosphere from industrial operations such as coal-fired power plants, smelting operations, and cement factories. Following the release, thallium can either be inhaled or settle from the atmosphere and contaminate surface water or soil. Because plants readily take up thallium, the primary non-occupational sources of thallium exposure are through the consumption of fruits and vegetables grown in contaminated soil and the use of tobacco products (ATSDR, 1991).

Pathways of Tl into the human body in the Lanmuchang mineralized and community area are mainly through the food chain based on the estimation of daily uptake of thallium through consumption of vegetables and cereals. The local residents rely heavily on local agricultural products of vegetables and cereals grown on the Tl-contaminated soils, and the uptake of thallium through the food chain is continuous over the years.

Drinking water containing elevated Tl is another pathway to human ingestion. However, drinking water from wells in Lanmuchang area has Tl levels below the safe drinking limit. Also drinking water nowadays supplied to the Lanmuchang villages from

outside sources contains low Tl ranging from 0.007 to 0.43 μg/l. These values are much lower than those determined by Zhou and Liu (1985). Their study carried out in the 1960's and 1970's showed a range of 17–40 μg/l. If the highest levels are considered in both studies as the worst case scenario, and 4 liters of water are consumed by adults, then the daily ingestion of Tl through drinking water at present is 1.72 μg as compared to 160 μg in the 1960's –1970's. A value of 160 μg of Tl intake per day can be considered as an important source causing chronic poisoning prevailing at that period. According to this study, however, Tl exposure of 1.72 μg/day through drinking water at present is negligible. Thus, the present drinking water supply cannot pose a threat unless the sources for water supply are damaged by future mining operations.

Animals living within high Tl environment can accumulate appreciable amounts of Tl in the body (Dmowski et al., 1998; Dolgner et al., 1983). Chicken, pigs and buffalos are the three common animals raised by the families in Lanmuchang, and they are prone to accumulate Tl through the ingestion of fodder (e.g. wild cabbage, cabbage roots or old leaves, corn, stalks and rice shells, etc.) grown within the Lanmuchang area. In fact, appreciable amounts of Tl in chicken were determined (APASSGP and EGLIGCAS, 1974), ranging from 5.2 to 25.9 μg/g. This range falls within the range of thallium (2.02 to 44.05 μg/g dry weight) in small mammals living within a high thallium contaminated environment examined by Dmowski et al. (1998). The consumption of chicken or pigs can transfer Tl to humans. Although it may not act pronouncedly, this is another pathway for Tl entering the human body.

Poorly ventilated small scale underground mining of Tl-bearing ores or coals in the Lanmuchang area can disperse many fine particles of Tl-bearing dust into the air. This Tl can easily enter the bodies of miners through the skin or by inhalation. Smelting of Tl or Hg ores, or combustion of coals also can release amounts of thallium into the air. Following release, thallium can either be inhaled or settle from the atmosphere and contaminate surface water or soil. There have been no smelting operations in the Lanmuchang area, so this type of Tl exposure can be excluded. However, domestic combustion of Tl-enriched coals from the Lanmuchang area can readily release Tl into the indoor air which can be either inhaled or dermally absorbed. The quantitative input through coal combustion has not been measured in this study, but continuous utilization of Tl-rich coal indoor will likely enhance Tl exposure to the human body.

Finally, since the mine dumps and outcropped host rocks have high concentrations of Tl, children within the Lanmuchang area playing outdoors may unavoidably touch the thallium minerals in these materials, and uptake of some thallium through skin or orally is possible.

Pathways of thallium into the human body can be conceptually illustrated in Fig. 7-1. Tl in the original rocks or ores can be released into soils, ground and surface water, sediments and crops during natural processes of weathering or erosion, or mining activities. The specific topography and hydro-geomorphology facilitate the dispersion of Tl from the original sources within the Lanmuchang mineralization area to downslope areas within the Lanmuchang watershed. Tl can also further disperse outside the Lanmuchang watershed through water flowing into the sinkhole downstream or through irrigation channels. Tl in

soils, groundwater, surface water, sediment and biota can also be transferred from one another through different interaction processes. Soils and water are the principal agents through which Tl can be readily dispersed. During the geochemical circle, Tl can readily enter the food chain through consumption of Tl-accumulated crops, and Tl-contaminated drinking water.

7.2 Environmental risks of Tl on the human health

The Lanmuchang area characterized by the Hg-Tl-As mineralization is a specific geo-environmental context for accumulation of Tl in the ecosystem on which the local villagers rely heavily for living and farming. Tl is highly enriched in outcropped host rocks, sulfide ores and coals, exposed tailings and mine waste, arable soils, groundwater and surface water as well as stream sediments. The level of occurrence is generally far higher than the environmental quality guidelines. Thus, naturally occurring Tl in the ecosystem compounded by the human activity is posing high environmental risks translated by chronic thallium poisoning within the enclosed watershed of Lanmuchang.

The local villagers suffered from the chronic poisoning prevailing in the 1960's. Thallium poisoning affected a large portion of the population and caused symptoms such as, hair loss, body-aches, weakness, dizzy, tinnitus, poor appetite, reduced vision and blindness. Alopecia is the most common indicator of thallium poisoning, and some patients completely lost their hair like a "cap" removed from the head during an overnight sleep. This chronic Tl intoxication was thought to be largely due to the high concentrations of thallium in vegetables and in drinking water. 189 cases suffering from thallium poisoning

were observed in the endemic study of Zhou and Liu (1985) and others (e.g. Li, 1963; Liu, 1983).

The above symptoms of chronic poisoning are very similar to those in clinical observation (Meggs et al., 1994; Tabandeh et al., 1994; Hirata et al., 1998; Schmidt et al., 1997). The primary targets of thallium toxicity are the nervous, integumentary, and reproductive systems. In humans, acute exposures produce paresthesia, retrobulbar neuritis, ataxia, delirium, tremors, and hallucinations. In both humans and animals, alopecia is the most common indicator of long-term thallium poisoning (Feldman and Levisohn, 1993; Meggs et al., 1994; Tabandeh et al., 1994; Hirata et al., 1998). This supports the presence of Tl chronic poisoning in the community within the Lanmuchang area.

According to the study of Zhou and Liu (1985), the prevalence of thallotoxicosis in the period between 1960 and 1970 was attributed to the increased farming activity following the increase of population after 1958. The increased farming led to severe vegetation degradation, and then severe soil erosion from the mountain slopes. This, in turn, resulted in the deeper deposit of alluvial soils on which crops were planted. Since all 189 patients became ill between March and June, the illness was supposedly related to the season of the year. Zhou and Liu (1985) attributed this to the lower pH values of soils caused by less precipitation in the period of March-June. According to their study, higher quantities of soluble Tl salts remained in soils and Tl uptake by crops increase with the increase in acidity of soils. The above conclusion for the prevalence of thallium intoxication in the 1960's and 1970's by Zhou and Liu (1985) cannot be the only explanation.

High concentrations of Tl in soils as discussed in Section 6.2 are attributed to both human activities (deforestation, farming, mining and preparing foundation for houses, etc.) and natural processes (rock weathering and soil erosion). Even without increased farming from 1958 as mentioned by Zhou and Liu (1985), Tl in high quantities was probably present in soils (at least not less than the baseline values) on which crops were grown. If this is the case, thallium poisoning must have occurred before the 1960's.

The impact of climate alone as discussed by Zhou and Liu (1985) cannot explain the cause of thallium poisoning. Monthly precipitation may have some controls on the uptake of Tl by crops by decreasing pH values in soils. However, the dry season in Lanmuchang area starts from November to March, and precipitation during this period is generally much lower than the period of March-June (Fig. 7-2). If lower precipitation serves to trigger more uptake of Tl by crops as demonstrated by Zhou and Liu (1985), there should have been the same impact on Tl uptake during the period of November-February. Nevertheless, the epidemic cases were not reported in the period of November-February.

Nutritional deficiency combined with exposure to high Tl contents from the Lanmuchang area can probably explain the cause of thallotoxicosis which prevailed in the 1960's and 1970's. Note that severe deforestation occurred everywhere in China in 1958 due to massive cutting down of trees for production of steel evoked by a political movement of that year, and resulted in severe soil erosion. In the early 1960's, the whole country of China experienced harvest failures and famine due to severe drought, and the Lanmuchang community area was also similarly affected. In the 1960's and 1970's, the local population increased to about 1000 people (five members per family on average).

These events led to the nutritional deficiency due to lack of food. In addition, from February to May there was paucity of staple foods because of a bad grain harvest (e.g. rice or corn). This harsh condition caused many families to consume more vegetables (mainly green cabbage and Chinese cabbage) planted in their own Tl-contaminated gardens as their alternate daily staples. Therefore, nutritional deficiency compounded with more consumption of Tl-rich vegetables in 1960's and 1970's triggered the chronic poisoning with the main symptoms being hair loss, body aches, weakness and reduced vision. Nutritional deficiency combined with exposure to high levels of fluorine from domestic coal combustion causing severe bone deformation (one of typical fluorine poisoning symptoms) in Guizhou Province, was also described by Zheng and Huang (1985) and Finkelman et al. (1999).

Agricultural production has been greatly improving since 1980's due to the national reform policy for farmland. The villagers have sufficient staple foods to support their families, and the nutritional deficiency is no longer a severe problem for most of the families, although the Lanmuchang area still ranks as a poor region. As a result, the symptoms of thallium poisoning are not apparent in most of the families, although the arable soils supporting farming still present high thallium contents.

The effect of thallium poisoning can be well illustrated through the case history of one family. Six family members were severely impaired by thallium poisoning in the 1960's and 1970's, leading to body-aches, hair loss and reduced vision affecting all the family members. One member of this family became completely blind, one had pronouncedly reduced vision, and the others experienced slightly reduced vision. At present

in the Lanmuchang area, this family is the poorest with a very low living standard. Thallium poisoning has impaired the family from carrying out manual labor to support itself. Therefore, the family members are still experiencing lack of staple foods and insufficient nutrition. Consequently, some of the family members still have problems of hair loss. The daughter-in-law, a new comer to the family immigrating from an area 10 km from Lanmuchang, together with the other family members experienced severe hair loss even in late 1998-1999. Tl in urine of the family members still contains high level of thallium, ranging from 149.5 to 2530 μg/l (Zhang et al., 1999). The 51-year-old family member, who is completely blind, died in 2000. His death is possibly related to the prolonged Tl poisoning (Qian, J.H., 2001, personal communication). It is important to point out that this family consumes the same drinking water and the same vegetables and cereals grown in their own gardens (along the Qingshui stream bank) that have no obvious difference in Tl contents from other families. The only likely cause for the continuous thallium poisoning can be attributed to nutritional deficiency linked with poverty.

Chronic Tl poisoning seems to be reduced, mainly because of better nutrition enhancement and improvement of drinking water. However, the evidence from Zhang et al. (1999) indicating the presence of high thallium in the urine supports the fact that the family members are still experiencing chronic thallotoxicosis.

This study indicates the magnitude of thallium dispersion in the Lanmuchang area contaminating the food supply. More thallium may be transferred to the surface environment through mining because interest in mining Tl has increased in recent years due to its market value. With more mine wastes and tailings accompanying Tl mining, more Tl

would be introduced into the soils, waters and sediments to enhance the total environmental load of this toxic metal. Therefore, further contamination of Tl in drinking water and farmlands can be predicted in absence of environmental concerns.

Tl in the Lanmuchang watershed area may extend its impacts to areas outside the Lanmuchang due to agricultural expansion or water flowing into the sinkhole. Water containing 4.5 μg/l of Tl in the rainy season drains to the sinkhole downstream, and part of it is piped to neighboring farming areas, south of the Lanmuchang watershed for irrigation through a new underground irrigation channel constructed in 1998. Therefore, the new irrigated areas would be expected to receive significant amounts of Tl and other metals from the Lanmuchang watershed in future, and consequently spread Tl contamination in arable soils and crops. Water containing 19.3 μg/l of Tl during the dry season drains into the ground through the sinkhole downstream, and the behavior and fate of this Tl in further groundwater circulation is unknown. The seepage of Tl-rich water at the sinkhole is an important source of Tl for the groundwater cycle outside the Lanmuchang watershed, probably to the south of the area.

Gold mineralization (known as Carlin-type gold deposits) with accompanying Tl, Hg and As occurs in a number of localities in a geological environment similar to Lanmuchang area (Li and Peters, 1998). Thallium mineralization occurred in low temperature (160°C–250°C) and supergene environment (Chen, 1989b), very similar to that of gold mineralization (150°C–240°C) (Li and Peters, 1998). Therefore, it is geologically reasonable to assume that the introduction of Tl into the host strata of P_2l, P_2c and T_1y is related to gold mineralization. Although, it is outside the scope of the present study to

analyze this situation, it can be inferred from this study that Tl dispersion can be a widespread phenomenon outside the Lanmuchang area. However, the level of Tl concentration will vary depending on the primary dispersion pattern of Tl (Li and Peters, 1998).

7.3 Geo-environmental and socio-economic impacts

The specific geo-environmental context promoting elevated thallium accumulation in the Lanmuchang area exerts a severe constraint on the local socio-economic development since thallium poses high environmental risk in the Lanmuchang community area. As mentioned above, the local residents rely heavily on the local natural resources: Tl-contaminated soils for agricultural and residential use, contaminated water supply for irrigation, and the mining of mineral resources for economic development. All these activities promote thallium as a potential "killer" and will be an obstacle to poverty-reduction and a sound socio-economic development.

The sustainable socio-economic development will be a far away dream without considering effective improvement of the quality of community life. The site-specific natural geo-environment should be considered during the socio-economic development, especially for pursuing a sustainable improvement of community life. The local residents have little knowledge about the potential risks existing in their environment since there has been an absence of detailed investigation. However, even knowing some of the risks, most of the residents cannot culturally and socially change themselves from their old life-customs in appropriate ways to improve their wellbeing.

The local residents have to rely on the contaminated soils for planting vegetables and cereals from year to year, since the alternative farmlands are not easy to find due to the topographical and hydrological condition within the mountainous community of Lanmuchang area. Therefore, remediation of the contaminated soils is a priority to reduce the entry of thallium into the food chain. However, high thallium in soils are derived from both the natural processes and mining activity, and the mobilization of large volumes of metal-bearing materials into soils or alluvium have been and will be taking place for thousands of years even without mining. Therefore, cleanup of high concentration of metals in the arable soils in the Lanmuchang community is a complex task.

Two conventional approaches have been applied to enhance decontamination of soils: (1) *ex situ*, i.e. removal of the toxic metal contaminated soils, their isolation in constructed repositories, or transport to and cleaning in plants with specific techniques; (2) *in situ*, i.e. cleanup at the site itself. The *ex situ* cleanup by conventional technologies is often extremely costly and are often insufficient for reducing the risk. However, this is not economically feasible in the Lanmuchang area. Immobilization procedures for contaminated soils *in situ* often include improving the pH via fertilization with calcium carbonate or input of lime (Mench et al., 1994) or the addition of metal complex agents (Chen and Stevenson, 1986). These *in situ* cleanups may overcome the short-term toxicity in agricultural or residential soils, but they are all insufficient for long-term risk reduction due to plant-microbe interaction. Indeed, addition of lime into the garden soils to raise the pH was advised in the Lanmuchang area (Zhou and Li, 1982), but high concentrations of thallium in various vegetables or cereals are still documented in the current study.

Decontamination by plants (bio-, phytoremediation) of metal contaminated soils is a good alternative by selecting such plant species known to be super accumulators of thallium (Ernst, 1996; Brooks et al., 1998; McGrath, 1998). Planting of some hyperaccumulators of thallium, like *Iberis intermedia* and *Biscutella laevigata* (Brassicaceae) (see Leblanc et al., 1999; Anderson et al., 1999), should be tried in the old mine area, particularly on the hill slope containing Tl-bearing materials. The harvested Tl-accumulated vegetation can be dried and ashed so as to produce a saleable ash (bio-ore) (Brooks and Robinson, 1998). This would remove amounts of thallium from soils and prevent slope soil erosion as well. Re-vegetating the highly metal-resistant plants in heavily contaminated soils is an economically and ecologically important cleanup technique and should be considered for implementation in the Lanmuchang area.

High contents of arsenic and mercury in soils in the Lanmuchang Hg-Tl mineralized area should also be reduced during the soil remediation, although no high uptake of these two toxic metals by vegetables and cereals was determined in this study. Similarly, phytoremediation is a good option to remove these toxic metals. As for the arsenic-contaminated soil remediation, Ma et al. (2001) pointed out that the fern *Pteris vittata* (brake fern) is extremely efficient in extracting arsenic from soils and translocating it into its above-ground biomass, with the highest enrichment up to 2.3%. However, mechanism of hyperaccumulation and transport for As by the brake fern is not clear. As for the mercury-contaminated soil remediation, no hyperaccumulator has been reported in the literature.

Following the arable soil phytoremediation, other steps should be taken to protect further spreading of thallium in the ecosystem of the Lanmuchang area. Firstly, as thallium in highly enriched in green cabbage and rape, these vegetables should not be planted in the contaminated soils. Secondly, sources of drinking water should be carefully guarded against further contamination, since the current level of thallium is not above the safe limit. Thirdly, the exposed mine wastes on slopes from past and future mining should be stabilized to prevent further erosion and migration downslope towards farmland and water systems. Finally, Tl-rich coals should be used carefully with proper stoves with chimneys which are lacking in many households to prevent possible indoor Tl contamination. Finally, the mine wastes or weathered bedrock materials should not be used for local or regional housing constructions, since the sieved fine particles may contain high amounts of thallium and other metals and can produce a potential hazard.

Initiating the above activities for remediation will likely restrain a wider dispersion of thallium in the ecosystem. However, any future mining triggered by market condition for Tl will further disrupt the Lanmuchang area, unless the findings of this study are integrated into planning of future operations.

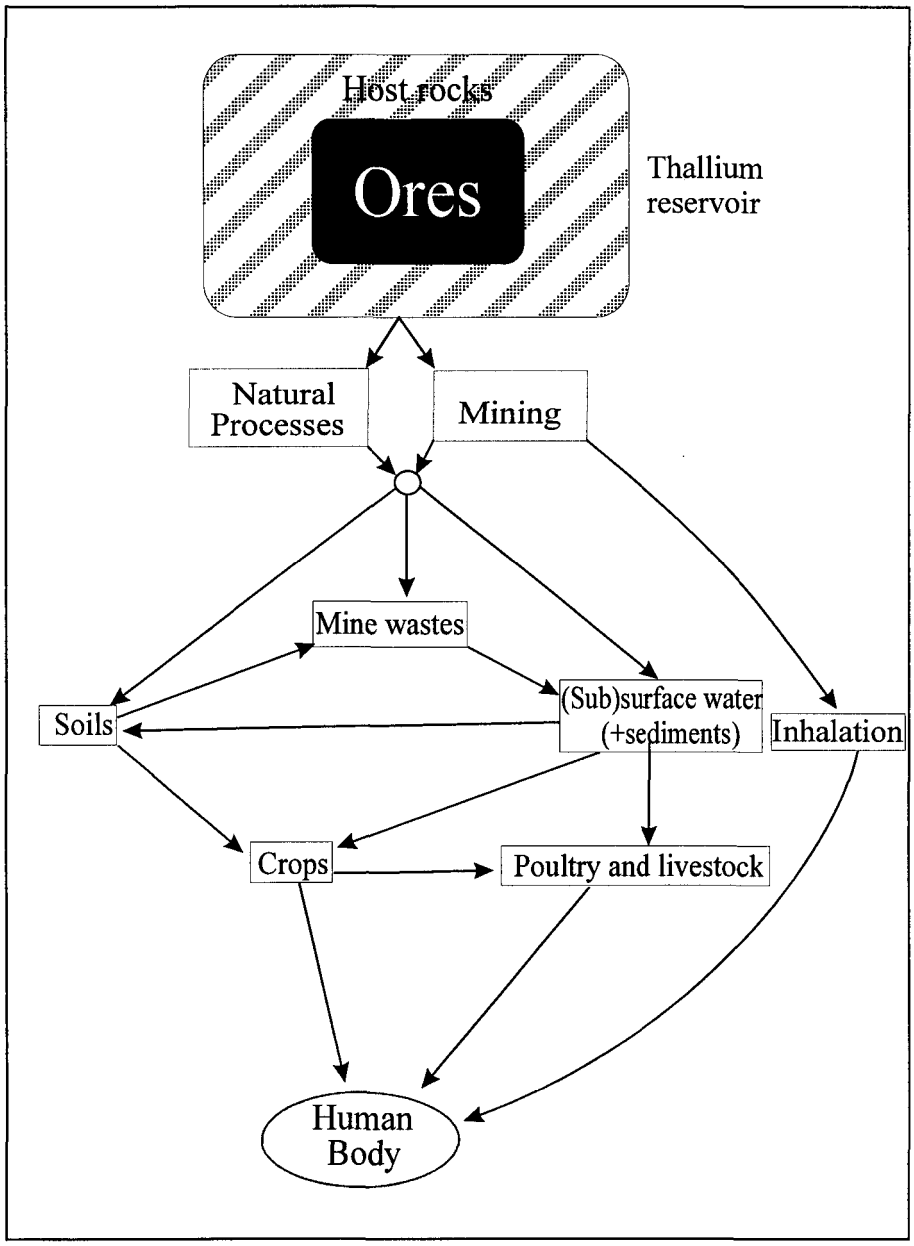

Fig. 7-1 Schematic model of pathways of Tl into the human body

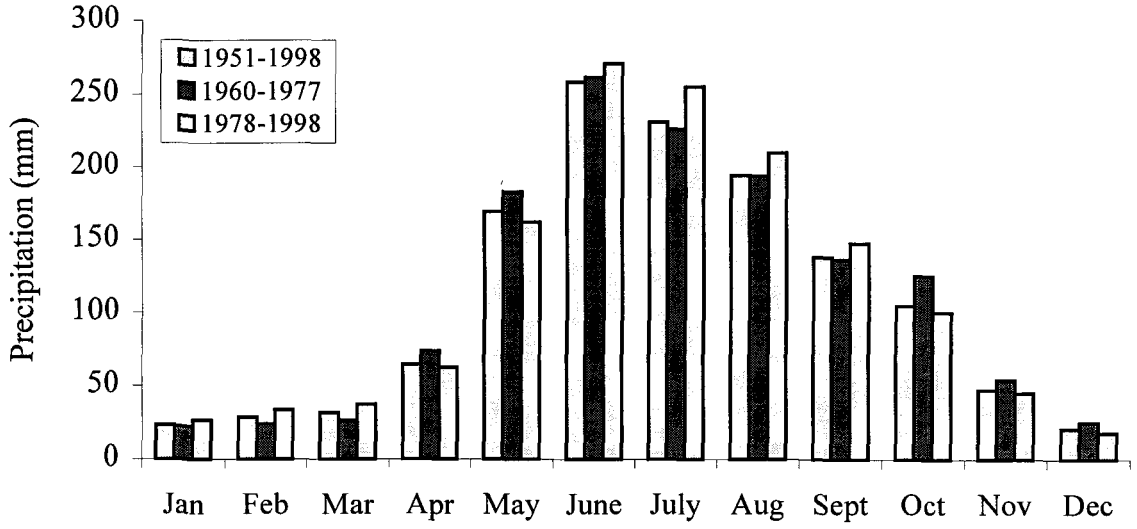

Fig. 7-2 Monthly precipitation during 1951-1998 in the Lanmuchang area

CHAPTER 8

CONCLUSIONS

This study on thallium and its environmental impacts associated with the Hg-Tl-(Au) mineralization in Lanmuchang (Southwestern part of Guizhou, China) have brought to light previously unknown facts related to thallium in the ecosystem. Thallium occurring in a specific geo-environment can become a critical health hazard through dispersion accentuated not only by human activities but also natural geological processes. The findings are summarized below:

(1) The Lanmuchang area is a specific geo-environmental context showing high enrichment of thallium, mercury and arsenic because of the intensive sulfide mineralization of thallium, mercury and arsenic. The sulfide mineralization is mainly characterized by abundant occurrences of thallium sulfide (lorandite), mercury sulfide (cinnabar), and arsenic sulfides (realgar and orpiment). Thallium occurs either as isomorphous substitution within the structure of sulfide minerals of mercury, arsenic ores, pyrite or marcasite, and in coals, or as independent thallium mineral lorandite.

(2) Thallium concentration in sulfide ores ranges from 33-35000 ppm, and 12-46 ppm in coals. Host rocks contain thallium 33-490 ppm, secondary minerals 25-1100 ppm, and outcropped host rocks 6-330 ppm.

(3) High concentrations of thallium in soils are the result of both natural processes and human activity. Thallium contents range from 53 to 282 ppm in soils from mining area, from 21 to 100 ppm in alluvial deposits or foundation soils, from 40-46 ppm in slope wash materials, and from 2.2 to 29 ppm in undisturbed natural soils. These dispersions indicate that the erosion of natural soils from the Tl mineralized area and the mining activity are responsible for the high thallium content.

(4) The concentration of thallium in groundwater sediments and stream sediments ranges from 10 to 3700 ppm. Thallium content in stream sediments in base-flow regime is generally higher than in flood flow regime, but the newly formed fine sediments washed down by rain water contain much higher thallium. The source of high thallium in sediments can be attributed to both the natural erosion or leaching from the mineralized area and mining activities.

(5) The distribution of thallium in waters follows a concentration gradient from high to low in deep groundwater, stream water and shallow groundwater, constrained by thallium mineralization, water-rock interaction and hydrogeological conditions. Thallium occurs at high levels (13.42–1102 μg/l) in deep groundwater within the thallium

mineralized area, and decreases to background levels (0.005 μg/l) away from the mineralization. Thallium in stream water in both base-flow and flood-flow regimes shows higher concentrations than the observed ambient recharged groundwater. Thallium in stream water in both regimes shows abnormally high levels (10 to 100-fold) in downstream rather than in upper and middle-stream. This marked increase in thallium is most likely caused by an unidentified discharge of deep groundwater through fracture zones to the downstream section.

(6) Thallium shows much higher levels in certain crops than Hg and As, and is species-dependent. The enrichment of thallium in the edible parts of crops decreases in the following order: green cabbage > chili > Chinese cabbage > rice > corn. The highest level of thallium in green cabbage is up to 500 μg/g as dry weight. The high accumulation of Tl in crops is due likely to the substitution of Tl for K as these two ions have very similar ionic radii.

(7) Dispersion of thallium together with mercury and arsenic in the specific ecosystem of Lanmuchang takes place within a relatively short distance from the mineralized area and is constrained by the original Tl-Hg-As sulfide mineralization, the specific topography and hydro-geomorphology of the area, and human activity. High thallium is concentrated in the mineralized and mine area, and away from this area, concentration decreases gradually to background level. Thallium from the bedrocks is

transferred to soils, sediments and waters within the enclosed watershed area of Lanmuchang.

(8) Recognition of natural sources and definition of the site-specific geochemical baselines are important to discriminate the relative contribution of high metals in the ecosystem and help insure correct determinations of environmental liabilities and cleanup priorities.

(9) Pathways of Tl into the human body are mainly through the food chain, with dermal and inhalation exposures being less pronounced. Due to high uptake of Tl by crops, the primary natural sources of thallium exposure are through the consumption of vegetables and other crops grown in contaminated soils. The daily uptake of Tl through consumption of locally planted crops rich in Tl has been estimated as 2.659 mg, which is 60 times the daily ingestion in thallium-free background area. Drinking water has Tl levels below the safe drinking limit, and poses no risk to human health. Hg and As play an insignificant role in causing health problem in the Lanmuchang area.

(10) The climate factor triggering the prevalence of chronic thallium poisoning is not supported by this study. Instead, the nutritional deficiency combined with exposure to high Tl contents from the Lanmuchang area can explain the cause of thallotoxicosis which prevailed in the 1960's and 1970's.

(11) The specific geo-environmental context causing high thallium accumulation in the Lanmuchang area imposes a severe constraint on local socio-economic development planning. The site-specific natural geo-environment should be considered during socio-economic development, especially for pursuing a sustainable improvement in community life. Remediation of the contaminated soils becomes a priority to reduce thallium entry into the food chain. Planting vegetation with Tl-hyperaccumulating properties is suggested for an appropriate soil phytoremediation. Green cabbage with a tendency to be highly enriched in thallium should not be planted in the contaminated soils. Several safeguards have also been suggested to prevent further health problems.

(12) The fragility of the eco-environment, the lack of development in local socio-economic conditions, the poor living standard, and the heavy reliance on local natural resources and the community's lack of knowledge and consciousness of the risks of the thallium contamination have limited the improvement of living conditions within the high thallium prone environment. Thus, the knowledge gained from this scientific research should be transferred to the community so that they can apply this knowledge to their daily lives. This is probably one of the appropriate approaches to contribute to poverty-reduction and form the basis for regional sustainable development.

(13) This study not only contributes to the increase of the knowledge-base of geo-environmental hazards related to naturally occurring thallium but also points to

research efforts required for environmentally acceptable sustainable development, since it has been clearly demonstrated that dispersion of thallium into the ecosystem can take place through natural processes with or without mining activities.

REFERENCE

Ahrens, L.H., Willis, J.P. and Oosthuizen, C.O., 1967. Further observations on the composition of manganese nodules with particular reference to some of the rarer elements Geochimica et Cosmochimica Acta 31: 2169–2180

Al-Attar, A.F., Martin, M.H. and Nickless, G., 1988. Uptake and toxicity of cadmium, mercury and thallium to Lolium perenne seedlings. Chemosphere 17: 1219–1225

Allus, M.A., Martin, M.H. and Nickless, G., 1987. Comparative toxicity of thallium to two plant species. Chemosphere 16: 929–932

Analytical Chemistry Laboratories., 2001. Schedule of Analytical Chemistry and Research and Development Services. http://www.nrcan.gc.ca/gsc/mrd/labs/chem_e.html

Anderson, C.W.N., Brooks, R.R., Chiarucci, A., LaCoste, C.J., Leblanc, M., Robinson, B.H., Simcock, R. and Stewart, R.B., 1999. Phytomining for nickel, thallium and gold. Journal of Geochemical Exploration 67: 407–415

Anonymous., 1989. Hair-raising. New Scientist, 28 January 1989, 1649: 28

Ansari, A.A., Singh, I.B. and Tobschall, H.J., 2000. Importance of geomorphology and sedimentation processes for metal dispersion in sediments and soils of the Ganga Plain: identification of geochemical domain. Chemical Geology 162: 245–266

Apambire, W.B., Boyle, D.R. and Michel, F.A., 1997. Geochemistry, genesis and health implications of fluoriferous groundwaters in the upper regions of Ghana. Environmental Geology 33: 13–24

APASSGP and EGLIGCA (Autonomous Prefecture Anti-epidemic Station of Southwest Guizhou Province, Environmental Geology Laboratory, Institute of Geochemistry, Chinese Academy of Sciences), 1974. Thallium enrichment in an ecological circulation—a case report of natural thallotoxicosis. Environment and Health 2: 12–15

Artioli, G. and Kvick, A., 1990. Synchrotron X-ray Rietveld study of perlialite, the natural counterpart of synthetic zeolite-L. European Journal of Mineralogy 2: 749-759

ATSDR (Agency for Toxic Substance and Disease Registry)., 1991. Draft Toxicological Profile for Thallium. Prepared by Clement Assoc., Inc. under contract 205-88-0608. U.S. Public Health service, Agency for Toxic Substance and Disease Registry, Atlants, GA, 91p

Bajc, A.F., 1998. A comparative analysis of enzyme leach and mobile metal ion selective extractions: case studies from glaciated terrain, northern Ontario. Journal of Geochemical Exploration 61: 113–148

Balic Zunic, T., Moele, Y., Loncar, Z. and Micheelsen, H., 1994. Dorallcharite, $(Tl,K)Fe_3^{3+}(SO_4)_2(OH)_6$, a new member of the jarosite-alunite family. European Journal of Mineralogy 6: 255–263

Bank, W.J., Pleasure, D.E., Suzuki, K., Nigro, M. and Katz, R., 1972. Thallium poisoning. Archives of Neurology 26: 456–464

Banks, D., Reimann, C., Royset, O., Skarphagen, H., Sather, O.M., 1995. Natural concentrations of major and trace elements in some Norwegian bedrock groundwaters. Applied Geochemistry 10: 1–16

Batley, G.E. and Florence, T.M., 1975. Determination of thallium in natural waters by anodic stripping voltametry. Electroanalytical Chemistry and Interface Electrochemistry 61: 205–211

Berger, B.R. and Bagby, W.C., 1991. The geology and origin of Carlin-type deposit. In: Foster, R.P. (eds.), Gold Metallogeny and Exploration. Edited by Blackie and Son, Glasgow, United Kingdom, pp. 210–248

Bidoglio, G., Gibson, P.N., O'Gorman, M. and Roberts, K.J., 1993. X-ray absorption spectroscopy investigation of surface redox transformations of thallium and chromium on colloidal mineral oxides. Geochimica et Cosmochimica Acta 57: 2389–2394

Blix, J., Glaser, J., Mink, J., Person, I., Person, P. and Sandstrom, M.J., 1995. Structure of thallium (III) chloride, bromide and cyanide complexes in aqueous solution. Journal of the American Chemical Society 117: 5089–5104

Blix, J., Gyori, B. and Glaser, J., 1989. Determination of stability constant for thallium (III) cyanide complexes in aqueous solution by means of ^{13}C and ^{205}Tl NMR. Journal of the American Chemical Society 111: 7784–7791

Bouska, V., 1981. Geochemistry of Coal. Elsevier Scientific Publishing Company, Amsterdam, 284p

Bowen, H.J.M., 1979. Environmental Chemistry of the Elements. Academic Press, London, 316p

Britten, J.S. and Blank, M., 1968. Thallium activation of the (Na^+–K^+)-activated ATPase of rabbit kidney. Biochimica et Biophysica Acta (Enzymology) 159: 160–166

Brookins, D.G., 1986. Geochemical behaviour of antimony, arsenic, cadmium and thallium: Eh-pH diagrams for 25°C, 1-bar pressure. Chemical Geology 54: 271–278

Brookins, D.G., 1988. Eh-pH Diagrams for Geochemistry. Springer-Verlag, Berlin, 176p

Brooks, R.R. and Ahrens, L.H., 1961. Some observations on the distribution of thallium, cadmium and bismuth in silicate rocks and the significance of covalency on their degree of association with other elements. Geochimica et Cosmochimica Acta 23: 100–115

Brooks, R.R. and Robinson, B.H., 1998. The potential use of hyperaccumulators and other plants for phytomining. In: Brooks, R.R. (eds.), Plants that Hyperaccumulate Heavy Metals; their role in phytoremediation, microbiology, archaeology, mineral exploration and phytomining. CAB International, Wallingford, United Kingdom, pp. 327–356

Brooks, R.R., Ahrens, L.H. and Taylor, S.R., 1960. The determination of trace elements in silicate rocks by a combined spectrochemical-anion exchange technique. Geochimica et Cosmochimica Acta 18: 162–175

Brooks, R.R., Chiarucci, A. and Jaffre, T., 1998. Revegetation and stabilisation of mine dumps. In: Brooks, R.R. (eds.), Plants that Hyperaccumulate Heavy Metals; their role in phytoremediation, microbiology, archaeology, mineral exploration and phytomining. CAB International, Wallingford, United Kingdom pp. 227–248

Byrne, R.H., Kump, L.R. and Cantrell, K.J., 1998. The influence of temperature and pH on trace metal speciation in seawater. Marine Chemistry 25: 163–181

Calderoni, G., Ferri, T., Giannetti, B. and Masi, U., 1985a. The behavior of thallium during alteration of the K-alkaline rocks from the Roccamonfina volcano (Campania, Southern Italy). Chemical Geology 48: 103–113

Calderoni, G., Ferrini, V. and Masi, U., 1985b. Distribution and significance of Pb and Tl in the sulfides and host rocks from the hydrothermal mineralization of the Tolfa Mountains (Latium, Central Italy). Chemical Geology 51: 29–39

Calderoni, G., Giannetti, B. and Masi, U., 1983. Abundance and behavior of thallium in the K-alkaline rocks from the Roccamonfina volcanic (Campania, Southern Italy). Chemical Geology 38: 239–253

Cataldo, D.A. and Wildung, R.E., 1978. Soil and plant factors influencing the accumulation of heavy metals by plants. Environment Health Perspectives 27: 149–160

CCME (Canadian Council of Ministers of the Environment)., 1999. Canadian environmental quality guidelines/ Canadian Council of Ministers of the Environment (Volume 1 and 2). Winnipeg.

Chandler, H.A., Archbold, G.P., Gibson, J.M., O'Callaghan, P., Marks, J.N. and Pethybridge, R.J., 1990. Excretion of a toxic dose of thallium. Clinical Chemistry 36: 1506–1509

Chapman, B.M., Jones, D.R. and Jung, R.F., 1983. Processes controlling metal ion attenuation in acid mine drainage streams. Geochimica et Cosmochimica Acta 47: 1957–1973

Chattopadhyay, A. and Jervis, R.E., 1974. Multi-element determination in market-garden soils by instrumental Photon Activation analysis. Analytical Chemistry 46: 1630–1639

Cheam, V., Desrosiers, R., Sekerka, I., Lawson, G., and Mudroch, A., 1995. Dissolved and total thallium in Great Lakes waters. Journal of Great Lakes Research 21: 384–394

Cheam, V., Lawson, G., Lechner, J., Desrosiers, R. and Nriagu, J., 1996. Thallium and cadmium in recent snow and firn layers in the Canadian Arctic by atomic fluorescence and adsorption spectrometries. Fresenius Journal of Analytical Chemistry 355: 332–335

Chen, D., 1989a. Discovery and research of lorandite in China. Acta Mineralogica Sinica 9: 141–142

Chen, D., 1989b. Discovery of rich-thallium ore body in paragenesis ore deposit of mercury and thallium and its mineralization mechanism. Journal of Guizhou Institute of Technology 18: 1–19

Chen, D., Wang, H. and Ren, D., 1996. Some geochemical problems of ore-forming elements in the ore-host strata of thallium deposits in Southwest Guizhou. Acta Mineralogica Sinica 16: 307–314

Chen, D., Wang, H., Ren, D. and Zou, Z., 1999. Geochemistry of Thallium and its exploration, Southwest Guizhou, China. Bulletin of Mineralogy, Petrology and Geochemistry 18: 57–60

Chen, Y. and Stevenson, J.R., 1986. Soil organic matter interaction with trace elements. In: Chen, Y. and Awnimelech, Y. (eds.), Role of Organic Matter in Modern Agriculture. Nijhoff, Dordrecht, pp. 73–116

Chester, R., Kudoja, W.M., Thomas, A. and Towner, J., 1985. Pollution reconnaissance in stream sediments using non-residual trace metals. Environmental Pollution 10: 213–238

Chou, C.L. and Moffatt, J.D., 1998. Determination of thallium and its species in aquatic environmental samples. In: Nriagu, J.O. (eds.), Thallium in the Environment. New York: John Wiley & Sons, Inc., pp. 121–154

Chowdhury, T.R., Basu, G.K., Mandal, B.K., Biswas, B.K., Samanta, G., Chowdhury, U.K., Chanda, C.R., Lodh, D.L., Roy, S.L., Saha, K.C., Roy, S., Kabir, S., Quamruzzaman, Q. and Chakraborti, D., 1999. Arsenic poisoning in the Ganges delta. Nature 401:545–546

Cleven, R. and Fikkert, L., 1994. Potentionmetric stripping analysis of thallium in natural waters. Analytic Chimica Acta 289: 215–221

Condie, K.C., 1993. Chemical composition and evolution of the upper continental crust; contrasting results from surface samples and shales. Chemical Geology 104: 1–37

Cvetkovic, L., Boronikhin, V.A., Pavicevic, M.K., Krajnovic, D., Grzetic, I., Libowitzky, E., Giester, G. and Tillmanns, E., 1995. Jankovicite, $Tl_5Sb_9(As,Sb)_4S_{22}$, a new Tl-sulfosalt from Allchar, Macedonia. Mineralogy and Petrology 53: 125–131

Dall'Aglio, M., Fornaseri, M. and Brondi, M., 1994. New data on thallium in rocks and natural waters from Central and Southern Italy: insights into application. Miner. Petrogr. Acta XXXVII: 103–112

Davis, L.E., Standefer, J.C., Abercrombie, D.M. and Butler, C., 1981. Acute thallium poisoning: toxicological and morphological studies of the nervous system. Annals Neurology 10: 38–44

Davis, R.D., Beckett, P.H.T. and Wollan, E., 1978. Critical levels of twenty potentially toxic elements in young spring barley. Plant and Soils 49: 395–408

De Albuquereque, C.A.R. and Shaw, D.M., 1972. Thallium. In: Wedepohl, K.H. (eds.), Handbook of Geochemistry, Section 81B–81O. Spring-Verlag, Berlin, pp. 81-D-1–81-D-18

De Ruck, A., Vandecasteele, C. and Dams, R., 1988. Determination of thallium in natural waters by electrothermal atomic absorption spectrometry. Microchimica Acta 2: 187–193

Dean, J.A., 1999. Lang's Handbook of Chemistry (15^{th} edition). McGill-Hill, New York.

Dissanayake, C.B. and Chandrajith, R., 1999. Medical geochemistry of tropical environments. Earth-Science Reviews 47: 219–258

Dissanayake, C.B., 1991. The fluoride problem in the groundwater of Sri Lanka – environmental management and health. International Journal of Environmental Study 38: 137–156

Dmowski, K., Kozakiewicz, A. and Kozakiewicz, M., 1998. Small mammal populations and community under conditions of extremely high thallium contamination in the environment. Ecotoxicology and Environmental Safety 41: 2–7

Dolgner, R., Brockhaus, A., Ewers, U., Wiegand, H., Majewski, F. and Soddemann, H., 1983. Repeated surveillance of exposure to thallium in a population living in the vicinity of a cement plant emitting dust containing thallium. International Archives of Occupational Environmental Health 52: 79–94

Douglas, K.T., Bunni, M.A. and Baindur, S.W., 1990. Thallium in Biochemistry. International Journal of Biochemistry 22: 429–438

Downs, A.J., 1993a. Chemistry of Aluminium, Gallium, Indium and Thallium. New York: Blackie Academic & Professional, 526p

Downs, A.J., 1993b. Chemistry of the Group 13 metals: some themes and variations. In: Downs, A.J. (eds.), Chemistry of Aluminum, Gallium, Indium and Thallium. Blackie Academic & Professional, London, pp. 1–80

Dvornikov, A.G., Ovsyannikova, L.B. and Sidenko, O.G., 1976. Biological uptake factors and biogeochemical coefficients for Donbas hydrothermal deposits; prediction of latent mercury mineralization. Geochemistry International 13: 189–196

Edmunds, W.M. and Smedley, P.L., 1996. Groundwater geochemistry and health: an overview. In: Appleton, J.D., Fuge, R. and McCall, G.J.H. (eds.), Environmental Geochemistry and Health. Geological Society Special Publication, UK No. 113: pp. 91–95

Edwards, R., Lepp, N.W. and Jones, K.C., 1995. Other less abundant elements of potential environmental significance. In: Alloway, B.J. (eds.), Heavy Metals in Soils (2nd Edition). Blackie Academic & Professional, London, pp. 306–352

Emsley, J., 1978. The trouble with thallium. New Scientist, 10 August 1978, 1115: 392–394

Engler, R.M. and Patrick, W.H.J., 1975. Stability of sulphides of manganese, iron, zinc, copper, and mercury in flooded and nonflooded soil. Soil Science 119: 217–221

Ernst, W.H.O., 1996. Bioavailability of heavy metals and decontamination of soils by plants. Applied Geochemistry 11: 163–167

Feldman, J. and Levisohn, D.R., 1993. Acute alopecia: clue to thallium toxicity. Pediatric Dermatology 10: 29–31

Feng, X., Hong, Y., Hong, B. and Ni, J., 1999. Mobility of some potentially toxic trace elements in the coal of Guizhou, China. Environmental Geology 39: 372–377

Fergusson, J.E., 1990. The Heavy Elements: Chemistry, Environmental Impact and Health Effects. Oxford, Pergamon Press, United Kingdom, 614p

Finkelman, R.B., 1981. Modes of occurrence of trace elements in coal. U.S. Geological Survey Open-File Report No. OFR-81-99, 301p

Finkelman, R.B., Belkin, H.E. and Zheng, B., 1999. Health impacts of domestic coal use in China. Proceedings of the National Academy of Sciences of the United States of America 96: 3427–3431

Flegal, A.R. and Patterson, C.C., 1985. Thallium concentration in seawater. Marine Chemistry 15: 327–331

Fletcher, W.K., 1981. Handbook of exploration Geochemistry, Volume 1: Analytical Methods in Geochemical Prospecting. Elsevier, New York, 255p

Frengstad, B. Skrede, A.K.M., Banks, D., Krog, J.R. and Siewers, U., 2000. The chemistry of Norwegian groundwaters: III. The distribution of trace elements in 476 crystalline bedrock groundwaters, as analyzed by ICP-MS techniques. The Science of the Total Environment 246: 21–40

Fuge, R., Pearce, F.M., Pearce, N.J.G. and Perkins, W.T., 1994. Acid mine drainage in Wales and influence of Ochre precipitation on water chemistry. In: Alpers, C.N. and Clowes, D.W. 9eds.), Environmental Geochemistry of Sulfide Oxidation. American Chemical Society, Washington, DC., pp. 261–274

Gassner, G., Tholen, V. and Ternes, W., 2000. Chronic thallium intoxication in five German pointers of one litter. Berliner und Munchener Tierarztliche Wochenschrift, 113: 295–298

Gluskoter, H. J.; Ruch, R.R., Miller, W.G., Cahill, R.A., Drecher, G.B. and Kuhn, J.K., 1977. Trace elements in coal; occurrence and distribution. Circular – Illinois State Geological Survey 499: 1–154

Graeser, S. and Schwander, H., 1992a. Edenharterite ($TlPbAs_3S_8$); a new mineral from Lengenbach, Binntal (Switzerland). European Journal of Mineralogy 4: 1265–1270

Graeser, S., Schwander, H., Wulf, R. and Edenharter, A., 1992b. Erniggliite ($Tl_2SnAs_2S_6$), a new mineral from Lengenbach, Binntal (Switzerland); description and crystal structure determination based on data from synchrotron radiation. Bulletin Suisse de Mineralogie et Petrographie 72: 293–302

Gregotti, C. and Faustman, E.M., 1998. Reproductive and developmental toxicity of thallium. In: Nriagu, J. O. (eds.), Thallium in the Environment. New York: John Wiley & Sons, Inc., pp. 201–214

Gromet, L. P., Dymek, R. F., Haskin, L.A. and Korotev, R.L., 1984. The "North American shale composite"; its compilation, major and trace element characteristics. Geochimica et Cosmochimica Acta 48: 2469–2482

Guha, J., 1999. Geo-environmental management – a conceptual approach. In Abstract Volume, International Conference on Geo-environment Management and Socio-economic Development, Guiyang, China, 13-15 October 1999: 13–14

Guizhou Geological Bureau., 1960. Report of mineral reserves of Lanmuchang mercury-thallium deposit in Xingren County, Guizhou (scale 1/10000), 50p

Guizhou Geological Bureau., 1990a. Report of mineral resources of Zhexiang Quadrangle (G-48-92-A), Dashang Quadrangle (G-48-92-B) and Zhenfeng Quadrangle (G-48-92-C), 210p

Guizhou Geological Bureau., 1990b. Report of regional geological survey of Zhexiang Quadrangle (G-48-92-A), Dashang Quadrangle (G-48-92-B) and Zhenfeng Quadrangle (G-48-92-C)., 222p

Guizhou Hydrogeological Survey., 1985. Report of 1:200 000 Regional Geological Survey of Xingren Quadrangle, Guizhou, China. Beijing, Geological Publishing House, 370p

Hall, G.E.M., and Pelchat, J.C., 1996. Performance of inductively coupled plasma mass spectrometric methods used in the determination of trace elements in surface waters in hydrogeological surveys. Journal of Analytical Atomic Spectrometry 11: 779–786

Heinrichs, H., Schulz-Dobrick, B. and Wedepohl, K.H., 1980. Terrestrial geochemistry of Cd, Bi, Tl, Pb, Zn and Rb. Geochimica et Cosmochimica Acta 44: 1519–1533

Henderson, J.A., Wilkes, G.P., Bragg, L.J. and Oman, C.L., 1985. Analyses of Virginia coal samples collected in 1978-1980. Virginia Division of Mineral Resources Publication 63: 1–56

Hirata, M., Taoda, K., Ono-Ogasawara, M., Takaya, M. and Hisanaga, N., 1998. A probable case of chronic occupational thallium poisoning in a glass factory. Industrial Health 36: 300–303

Hofmann, B.A. and Knill, M.D., 1996. Geochemistry and genesis of the Lengenbach Pb-Zn-As-Tl-Ba-mineralization, Binn Valley, Switzerland. Mineralium Deposita 31: 319–339

Hofmann, B.A., 1994. Formation of a sulfide melt during Alpine metamorphism of the Lengenbach polymetallic sulfide mineralization, Binntal, Switzerland. Mineralium Deposita 29: 439–442

Hugi, T., Fardy, J.J., Morgan, N.C. and Swaine, D.J., 1993. Trace Elements in some Swiss coals. Journal and Proceedings, Royal Society of New South Wales 126: 27–36

Ikramuddin, M., Asmeron, Y., Nordstrom, P.M., Kinart, K.P., Martin, W.M., Digby, S.J.M., Elder, D.D., Nijak, W.F. and Afemari, A.A., 1983. Thallium: a potential guide to mineral deposits. Journal of Geochemical Exploration 19: 465–490

Ikramuddin, M., Besse, L. and Nordstrom, P.M., 1986. Thallium in the carlin-type gold deposits. Applied Geochemistry 1: 493–502

Il'in, V.B. and Konarbayeva, G.A., 2000. Thallium in the soils of southwestern Siberia. Eurasian Soil Science 33: 613–616

Iskowitz, J.M., Lee, J.J.H. and Zeitlin, H., 1982. Determination of thallium in deep-sea ferromanganese nodules. Marine Mining 3: 285–295

Jambor, J.L. and Burke, E.A.J., 1993. New mineral names. American Mineralogist 78: 845–849

Jambor, J.L., Pertsev, N.N. and Roberts, A.C., 1997. New mineral names. American Mineralogist 82: 430–433

Jankovic, S., 1989. Sb-As-Tl mineral association in the Mediterranean region. International Geology Review 31: 262–273

Johan, Z. and Mantienne, J., 1976. Thalliferous mineralization of Jas Roux, Pelvoux Massif, Hautes-Alpes. Reunion Annuelle des Sciences de la Terre 4: 235

Johan, Z., Mantienne, J. and Picot, P., 1981. Chabourneite, a new thalliferous mineral. Bulletin de Mineralogie 104: 10–15

Johnson, C.C., Ge, X., Green, K.A. and Liu, X., 2000. Selenium distribution in the local environment of selected villages of the Keshan disease belt, Zhangjiakou District, Hebei Province, People's Republic of China. Applied Geochemistry 15: 385–401

Jonasson, I.R. and Boyle, R.W., 1972. Geochemistry of mercury and origins of natural contamination of the environment. Canadian Mining and Metallurgical Bulletin 65: 32–39

Jovic, V., 1993. Thallium in rocks, soils and plants: past progress and future need. Neues Jahrbuch fuer Mineralogie Abhandlungen 166: 43–52

Kabata-Pendias, A. and Pendias, H., 1992. Trace Elements in Soils and Plants (2nd Edition). Boca Raton, Florida: CRC Press, 365p

Kaplan, D.I. and Mattigod, S.V., 1998. Aqueous geochemistry of thallium. In: Nriagu, J.O. (eds.), Thallium in the Environment. John Wiley & Sons, Inc., New York, pp. 15–29

Kaplan, D.I., Adriano, D.C. and Sajwan, K.S., 1990. Thallium toxicity in bean. Journal of Environmental Quality 19: 359–365

Krupp, R.E. and Sweard, T.M., 1987. The Rotokawa geothermal system, New Zealand: an active epithermal gold-depositing environment. Economic Geology 82: 1109 –1129

Kurbanayev, M.S., 1966. Thallium in the dispersion aureoles of the Maykain gold-barite polymetallic deposit. Geokhimiya 6: 747–750

Kurz, K.; Schulz, R. and Römheld, V., 1997. Studies on thallium uptake by various crop plants for risk assessment of the food chain. http://www.uni-hohenheim.de/institutes/plant_nutrition/hinstres.htm.

Langmuir, D., 1997. Aqueous Environmental Geochemistry. New Jersey, Englewood Cliffs, Prentice Hall Inc, 600p

Leblanc, G.A. and Dean, J.W., 1984. Antimony and thallium toxicity to embryos and larvae of fathead minnows (*pimephales promelas*). Bulletin of Environmental Contamination and Toxicity 32: 565–569

Leblanc, M., Petit, D., Deram, A., Robinson, B.H. and Brooks, R.R., 1999. The phytomining and environmental significance of hyperaccumulation of thallium by Iberis intermedia from Southern France. Economic Geology 94: 109–114

Lehn, H. and Schoer, J., 1985. Thallium transfer from soils to plants: relations between chemical forms and plant-uptake. In: Lekkas, T.D. (eds.), Proceedings of International Conference on Heavy Metals in the Environment. Athens 2: 286–290

Lehn, H. and Schoer, J., 1987. Thallium-transfer from soils to plants: Correlation between chemical form and plant uptake. Plant and Soils 97: 253–265

Li, G., 1996. A study of ore compositions and thallium occurrence in a mercury-thallium deposit at Lanmuchang in Xingren County in Southwestern Guizhou Province, China. Guizhou Geology 13: 24–37

Li, J.Y., 1963. A report on survey of chronic thallium poisoning in a county. Transactions of Anti-Epidemic Station of Guizhou Province 154–158

Li, X.L., An, X.G. and Nan, J.Y., 1989. The second discovery of christite in nature. Chinese Science Bulletin 34: 942–945

Li, Z. and Peters, S.G., 1998. Comparative Geology and Geochemistry of Sedimentary-Rock-Hosted (Carlin-type) Gold Deposits in the People's Republic of China and in Nevada, USA. U.S. Geological Survey, Open-File Report 98–466, 157p

Lin, T.-S. and Nriagu, J., 1998. Speciation of thallium in natural waters. In: Nriagu, J.O. (eds.), Thallium in the Environment. New York: John Wiley & Sons, Inc., pp. 31–43

Lin, T.-S. and Nriagu, J., 1999. Thallium speciation in the Great Lakes. Environmental Science and Technology 33: 3394–3397

Lindsay, W.L. and Norvell, W.A., 1978. Development of a DTPA soil test for zinc, iron, manganese and copper. Soil Science Society of America 42: 421–428

Liu, J.D., 1983. Report of 4 cases of neuroetinopathy by chronic thallium poisoning. Chinese Journal of Thaumatical Occupation and Ophthalmic Disease 1: 22–23

Logan, P.G., Lepp, N.W. and Phipps, D.A., 1984. Some aspects of thallium uptake by higher plants. In: Hemphill, D.D. (eds.), Trace Substances in Environmental Health. Columbia: University of Missouri, 18: 570–575

Lottermoser, B.G. and Schomberg, S., 1993. Thallium content of fertilizers: environmental implications. Fresenius Environmental Bulletin 2: 53–57

Lu, K.I., 1983. Geology and geochemistry of the Uchinotai-east ore deposit, Kosaka mine, Akita Prefecture, Japan. Mining Geology 33: 367–384

Lu, L.Z., 1981. Report of a case of optic atrophy by chhronic thallium poisoning. Chinese Journal of Opthalmology 17: 247

Lukaszewski, Z., Zembrzuski, W. and Piela, A., 1996. Direct determination of ultratrace of thallium in water by flow-injection-differential-pulse anodic stripping voltammetry. Analytica Chimica Acta 318: 159–165

Ma, L.Q., Komar, K.M., Tu, C., Zhang, W., Cai, Y. and Kennelley, E.D., 2001. A fern that hyperaccumulates arsenic. Nature 409: 579

Magorrian, T.R., Wood, K.G., Michalovic, J.G., Oek, S.L. and Van, M.M., 1974. Water Pollution by Thallium and Related Metals. Calspan Project No. ND-5189-M-1, Calspan Corporation, 182p

Marcus, R.L., 1985. Investigation of a working population exposed to thallium. Journal of the Society of Occupational Medicine 35: 4–9

Mario, D.A., Mario, F. and Mauro, B., 1994. New data on thallium in rocks and natural waters from central and southern Italy; insights into applications. Mineralogica et Petrographica Acta 37: 103–112

Marowsky,G. and Wedepohl, K.H., 1971. General trends in the behaviors of Cd, Hg, Tl and Bi in some major rock forming processes. Geochimica et Cosmochimica Acta 35: 1255–1267

Mathis, B.J. and Kevern, N.R., 1975. Distribution of mercury, cadmium, lead and thallium in a eutrophic lake. Hydrobiology 46: 207–222

Matthews, A.D. and Riley, J.P., 1970. The occurrence of thallium in sea water and marine sediments. Chemical Geology 6: 149–152

McGrath, S.P., 1998. Phytoextraction for soil remediation. In: Brooks, R.R. (eds.), Plants that Hyperaccumulate Heavy Metals; their role in phytoremediation, microbiology,

archaeology, mineral exploration and phytomining. CAB International, Wallingford, United Kingdom, pp. 261–288

Meggs, W.J., Hoffman, R.S., Shih, R.D., Weisman, R.S. and Goldfrank, L.R., 1994. Thallium poisoning from maliciously contaminated food. Journal of Toxicology. Clinical Toxicology 32: 723–730

Mench, M.J., Didier, V.L., Loeffler, M., Gomez, A. and Masson, P., 1994. A mimicked in-situ remediation study of metal-contaminated soils with emphasis on cadmium and lead. Journal of Environmental Quality 23: 58–63

Mermut, A.R., Jain, J.C., Song, L., Kerrich, R., Kozak, L. and Jana, S., 1996. Trace elment concentrations of selected soils and fertilizers in Saskatchewan, Canada. Journal of Environmental Quality 25: 845–853

Moeschlin, S., 1980. Thallium poisoning. Clinic Toxicity 17: 133–146

Moore, D., House, I. and Dixon, A., 1993. Thallium poisoning. British Medical Journal, 306: 1527–1529

Mulkey, J.P. and Oehme, F.W., 1993. A review of thallium toxicity. Veterinary and Human Toxicicology 35: 445–453

Muller, B. and Sigg, L., 1990. Interaction of trace metals with natural particle surface: Comparison between adsorption and desorption experiments and field measurements. Aquatic Sciences 52: 75–92

Murao, S. and Itoh, S., 1992. High thallium content in Kuroko-type ore. Journal of Geochemical Exploration 43: 223–231

Négrel, P., Grosbois, C. and Kloppmann, W., 2000. The labile fraction of suspended matter in the Loire River (France): multi-element chemistry and isotopic (Rb-Sr and C-O) systematics. Chemical Geology 16: 271–285

Neumann, T., Leipe, T. and Shimmield, G., 1998. Heavy-metal enrichment in surficial sediments in the Oder River discharge area: source or sink for heavy metals? Applied Geochemistry 13: 329–337

Nriagu, J.O., 1998. History, production, and uses of thallium. In: Nriagu, J. O. (eds.), Thallium in the Environment. New York: John Wiley & Sons, Inc., pp. 1–4

Nuriyev, A.N. and Dzhabbarova, Z.A., 1973. Abundance of gallium, thallium, germanium and rare earths in the sedimentary rocks and ground waters of petroleum deposits. Geochemistry International 10: 330–335

Parker, D.R., Norvell, W.A. and Chaney, R.L., 1995. GEOCHEM-PC, a chemical speciation program for IBM and compatible personal computers. In: Loeppert, R.H., Schwab, A.P. and Goldberg, S. (eds.), Chemical Equilibrium and Reaction Models. Soil Science Society of America, special Publication 42, Soil Science Society of America, Madison, WI, pp. 245–277

Paulson, A.J., 1997. The transport and fate of Fe, Mn, Cu, Zn, Cd and SO_4 in a groundwater plume and in downstream surface waters in the Cœur d'Alene Mining District, Idaho, U.S.A. Applied Geochemistry 12: 447–464

Percival, J.B., Dumaresq, C.G., Kwong, Y.T.J., Hendry, K.B. and Michel, F.A., 1996. Arsenic in surface waters, Cobalt, Ontario. In: Current Research 1996–C; Geological Survey of Canada, pp. 137–146

Percival, T.J. and Radtke, A.S., 1993. Thallium in disseminated replacement gold deposits of the Carlin-type; a preliminary report. Neues Jahrbuch fuer Mineralogie Abhandlungen 166: 65–75

Percival, T.J. and Radtke, A.S., 1994. Sedimentary-rock-hosted disseminated gold mineralization in the Alsar district, Macedonia. The Canadian Mineralogist 32: 649–665

Plant, J.A. and Raiswell, R., 1983. Principles of environmental geochemistry. In: Thornton, I. (eds.), Applied Environmental Geochemistry. Academic Press, New York, pp. 1–39

Qi, W., Chen, Y. and Cao, J., 1992. Indium and thallium background contents in soils in China. International Journal of Environmental Studies 40: 311–315

Qian, H., Chen, W., Hu, Y., 1995. Features of As, Sb, Hg, Tl and their mineral assemblages in some disseminated gold deposits in Guizhou and Guangxi . Geological Journal of Universities 1: 45–52

Quinby-Hunt, M.S. and Turekian, K.K., 1983. Distribution of elements in sea water. EOS, Transactions, American Geophysical Union 64: 130–131

Radtke, A.S., 1985. Geology of the Carlin gold deposit, Nevada. US Geological Survey of Professional Paper 1267, 124p

Radtke, A.S., Dickson, F.W., Slack, J.F. and Brown, K.L., 1977. Christite, a new thallium mineral from the Carlin gold deposit, Nevada. American Mineralogist 62: 421–425

Reed, D., Cranley, J., Faro, S.N., Pieper, S.J., Kurland, L.T., 1963. Thallotoxicosis. Acute mainifestations and seqelae. Journal of American Medical Association 183: 516–522

Repetto, G., Peso, A.D. and Repetto, M., 1998. Human thallium toxicity. In: Nriagu, J. O. (eds.), Thallium in the Environment. New York: John Wiley & Sons, Inc, pp. 167–199

Rieck, B., 1993. Famous mineral localities; Allchar, Macedonia. The Mineralogical Record 24: 437–447, 449

Riley, J.P. and Siddiqui, S.A., 1986. The determination of thallium in sediments and natural waters. Analytica Chimica Acta 118: 117–123

Routh, J. and Ikramuddin, M., 1996. Trace-element geochemistry of Onion Creek near Van Stone lead-zinc mine (Washington, U.S.A.)– Chemical analysis and geochemical modeling. Chemical Geology 133: 211–224

Sabbioni, E., Ceotz, L. and Bignoli, G., 1984. Health and environmental implications of trace metals released from coal-fired power plants: An assessment study of the situation in the European Community. The Science of the Total Environment 40: 141–154

Sager, M., 1992. Speciation of thallium in river sediments by consecutive leaching techniques. Mikrochimica Acta 106: 241–251

Sager, M., 1994. Thallium. Toxicological and Environmental Chemistry 45: 11–32

Sager, M., 1998. Thallium in agricultural practice. In: Nriagu, J. O. (eds.), Thallium in the Environment. New York: John Wiley & Sons, Inc., pp. 59–87

Savenko, V.S., 2001. Physicochemical state of thallium(I) and thallium(III) in seawater. Geochemistry International 39: 88–91

Schmidt, D., Bach, M. and Gerling, J.A., 1997. case of localized retinal damage in thallium poisoning. International Ophthalmology 21: 143–147

Schoer, J., 1984. Thallium. In: Hutzinger, O. (eds.). The Handbook of Environmental Geochemistry. Berlin: Springer-Verlag 3: 143–214

Shah, M.T., Ikramuddin, M. and Shervais, J.W., 1994. Behavior of Tl relative to K, Rb, Sr and Ba in mineralized and unmineralized metavolcanics from the Dir area, northern Pakistan. Mineralium Deposita 29: 422–426

Shannon, R.D., 1976. Revised effective ionic radii and systematic studies of interatomic distances in halides and chalcogenides. Acta Crytallographica A32: 751–767

Shaw, D.M., 1952. The geochemistry of thallium. Geochimica et Cosmochimica Acta 2: 118–154

Shaw, D.M., 1957. The geochemistry of gallium, indium, thallium – a review. Physics and Chemistry of the Earth 2: 154–164

Shaw, D.M., Dostal, J. and Keays, R.R., 1976. Additional estimates of continental surface Precambrian shield composition in Canada. Geochimica et Cosmochimica Acta 40: 73–83

Siegel, B.Z. and Siegel, S.M., 1976. Effect of potassium on thallium toxicity in cucumber seedlings: further evidence for potassium-thallium ion antagonism. Bioinorganic Chemistry 6: 341–270

Slepnev, Y.S., 1961. The relationship of thallium and rubidium, cesium and potassium in metamorphic rocks, granites and rare-metals pegmatites of Sayan. Geokhimiya 4: 359–361

Smith, B., Chenery, S.R.N., Cook, J.M., Styles, M.T., Tiberindwa, J.V., Hampton, C., Freers, J., Rutakinggirwa, M., Sserunjogi, L., Tomkins, A. and Brown, C.J., 1998. Geochemical and environmental factors controlling exposure to cerium and magnesium in Uganda. Journal of Geochemical Exploration 65: 1–15

Smith, I.C. and Carson, B.L., 1977. Trace Metals in the Environment. Volume 1– Thallium. Ann Arbor Science Publishers Inc., Michigan, 307p

Sobott, R.J., 1995. Minerals and calculated low-temperature phase equilibrium in the pseudoternary system Tl_2S-As_2S_3-Sb_2S_3. Mineralogy and Petrology 53: 277–284

Sobott, R.J., Klaes, R. and Moh, G.H., 1987. Thallium-containing mineral systems. Part I: Natural assemblages of Tl-sulfosalts and related laboratory experiments. Chemie der Erde 47: 195–218

Stetzenbach, K.J., Amano, M., Kreamer, D.K. and Hodge, V.F., 1994. Testing the limits of ICP-MS: Determination of trace elements in ground water at the per-per-million level. Ground Water 32: 976–985

Swaine, D.J., 1990. Trace Elements in Coal. Butterworths, London, 278p.

Tabandeh, H., 1998. Effect of thallium toxicity on the visual system. In: Nriagu, J. O. (eds.), Thallium in the Environment. New York: John Wiley & Sons, Inc., pp. 263–199

Tabandeh, H., Crowston, J.G. and Thompson, G.M., 1994. Ophthalmologic features of thallium poisoning. American Journal of Ophthalmology 117: 243–245

Taylor, S.R., 1964. Abundance of chemical elements in the continental crust: a new table. Geochimica et Cosmochimica Acta 28: 1273–1285

Taylor, S.R., 1966. The application of trace element data to problem in petrology. Physics and Chemistry of the Earth 6: 133–213

Thompson, C., Dent, J. and Saxby, P., 1988. Effects of thallium poisoning on intellectual function. British Journal of Psychiatry 153: 396–399

Tremel, A. and Mench, M., 1997. Le thallium dans les sols et les végétaux supérieurs. II. Le thallium dans les végétaux supérieurs. Agronomie 17: 261–269

Tremel, A., Masson, P., Sterchemán, T., Baize, D. and Mench, M., 1997. Thallium in French Agrosystems – I. Thallium contents in arable soils. Environmental Pollution 95: 293–302

Tseng, W.P., Chu, H.M., How, S.W., Fong, J.M., Lin, C.S. and Yeh, S., 1968. Prevalence of skin cancer in an endemic area of chronic arsenicism in Taiwan. Journal National Cancer Institute 40: 453–463

Tunney, T., 2001. Chinese and Canadian researchers reduce arsenic poisoning in China. UniWorld, February 2001: 11

Turekian, K.K. and Wedepohl, K.H., 1961. Distribution of the elements in some major units of the earth's crust. Bulletin of Geological Society of America 72: 175–191

Turner, D.R., Whitfield, M. and Dickson, A.G., 1981. The equilibrium speciation of dissolved components in freshwater and seawater at 25°C and 1 atm pressure. Geochimica et Cosmochimica Acta 45: 855–881

U.S. Geological Survey., 1999. Metal Prices in the United States through 1998, pp. 151–153

USEPA (United States Environmental Protection Agency)., 2000. National Primary Drinking Water Regulations. http://www.epa.gov/OGWDW/dwh/t-ioc/thallium.html.

Valiyev, Y.Y., Pachadzhanov, D.N., Adamchuk, I.P. and Korsum, V.I., 1984. Geochemistry of bisbush and thallium in Mesozoic carbonate rocks in the Gissar Range. Geokhimiya 3: 384–389

Van Loon, J.C. and Barefoot, R.R., 1989. Analytical Methods for Geochemical Exploration. Academic Press, San Diego, 344p

Vink, B.W., 1993. The behaviour of thallium in the (sub)surface environment in terms of Eh and pH. Chemical Geology 109: 119–123

Vink, B.W., 1998. Thallium in the (sub)surface environment: its mobility in terms of Eh and pH. In: Nriagu, J. O. (eds.), Thallium in the Environment. New York: John Wiley & Sons, Inc., pp. 45–58

Vlasov, K.A., 1966. Geochemistry and Mineralogy of Rare Elements and Genetic Types of Their Deposits. Vol I. Geochemistry of Rare Elements. Israel Program for Scientific Translation

Voskresenskaya, N.T. and Karpova, I.S., 1958. Thallium in ore minerals of the Verkhyaya Kvaisa. Geochemistry 5: 552–559

Voskresenskaya, N.T., 1961. Thallium in some hydrothermal deposits of the Greater Caucasus. Geochemistry 8: 731–739

Voskresenskaya, N.T., 1969. Thallium in sedimentary sulfides. Geokhimiya 3: 261–272

Voskresenskaya, N.T., Timofeyeva, N.V. and Topkhana, M., 1962. Thallium in some minerals and ores of sedimentary origins. Geochemistry International: 851-859

Wainwright, A.P., Kox, W.J., House, I.M., Henry, J.A., Heaton, R. and Seed, W.A., 1988. Clinical features and therapy of acute thallium poisoning. Quarterly Journal of Medicine 69: 939–944

Wang, Y., Suo, S., Zhang, M., 1994. Tectonic and Carlin-Type Gold Deposits in Southwestern Guizhou, China (in Chinese with abstract in English). Geological Publishing House, Beijing, 115p

Warren, H.V. and Horsky, S.J., 1986. Thallium, a biogeochemical prospecting tool for gold. Journal of Geochemical Exploration 26: 215–221

Weeks, M.E., 1968. Discovery of the Elements (7^{th} edition). Journal of Chemical Education, Inc. Easton, Pennsylvania, 908p

Weissberg, B.G., 1969. Gold-silver ore-grade precipitates from New Zealand thermal waters. Economic Geology 64: 95–108

Wilson, J.R., Robinson, P.D., Wilson, P.N., Stanger, L.W. and Salmon, G.L., 1991. Gillulyite, $Tl_2(As,Sb)_8S_{13}$, a new thallium arsenic sulfosalt from the Mercur gold deposit, Utah. American Mineralogist 76: 653–656

Wilson, J.R., Sen Gupta, P.K., Robinson, P.D., and Griddle, A.J., 1993. Fangite, Tl_3AsS_4, a new thallium arsenic sulfosalt from the Mercur Au deposit, Utah, and revised optical data for gilluyite. American Mineralogist 78: 1096–1103

Yang, G. and Xia, M., 1995. Studies on human dietary requirements and safe range of dietary intakes of selenium in China and their application to the prevention of related endemic diseases. Biomedical and Environmental Sciences 8: 187–201

Yang, K., and Dong, Z., 1994. Carlin gold deposits in Yunnan, Guizhou, Guangxi and northwestern Sichuan, China. In: Gao, Z.M. (eds.). New Advances of Gold Deposits researches in China. Seismic Press, Beijing, pp. 284–348.

Yeager, J.R., Clark, J.R., Mitchell, W. and Renshaw, R., 1998. Enzyme leach anomalies associated with deep Mississippi Valley-type zinc ore bodies at the Elmwood Mine, Tennessee. Journal of Geochemical Exploration 61: 103–112

Zhang, B., Zhang, Z., Zhang, X. and Chen, G., 1997. A research into environmental Geochemistry of Lanmuchang thallium deposit in Xingren of Guizhou Province. Guizhou Geology 14: 71–77

Zhang, Z., Chen, G., Zhang, B., Chen, Y. and Zhang, X., 1999. Lanmuchang Tl deposit and its environmental geochemistry. Science in China (Series D) (In Chinese) 29: 433–440

Zhang, Z., Zhang, B., Long, J., Zhang, X. and Chen, G., 1998. Thallium pollution associated with mining of thallium deposits. Science in China (Series D) 41: 75–81

Zhang, Z., Zhang, X., Zhang, B., Chen, Y. and Gong, G., 1996. Topomorphic characteristics of realgar in the Nanhua As-Tl deposit. Acta Mineralogica Sinica, 16: 315–320

Zheng, B and Huang, R., 1985. Environmental geochemistry study of the fluorosis caused by burning coal indoors in southwest China. News Dispatch of Endemic Diseases 3: 49–51

Zheng, B., Ding, Z., Huang, R., Zhu, J., Yu, X., Wang, A., Zhou, D., Mao, D. and Su, H., 1999. Issues of health and disease relating to coal use in southwestern China. International Journal of Coal Geology 40: 119–132

Zhou, D.X. and Li, S.S., 1980. Determination of trace thallium in water, soil and biologic specimens. Journal of Environmental Science 3: 29–34

Zhou, D.X. and Li, S.S., 1982. Preliminary investigation on control and prevention of soil pollution by thallium. Acta Pedologica Sinca 19: 409–411

Zhou, D.X. and Liu, D.N., 1985. Chronic thallium poisoning in a rural area of Guizhou Province, China. Journal of Environmental Health 48: 14–18

Zhou, W., 1998. Thallium poisoning occurring in two universities of Beijing. Popular Medicine 8: 36

Zhuang, X., Yang, S., Zeng, R. and Xu, W., 1999. Characteristics of trace elements in coals from several main coal districts in China. Geological Science and Technology Information 18: 63–66

Zitko, V., 1975a. Chemistry, Application, Toxicity, and Pollution Potential of Thallium. Department of the Environment, Fisheries and Marine Service Research Development, Research and Development Directorate, Biological Station, St. Andrew, New Brunswick, Canada. Technical Report No. 518, 41p

Zitko, V., 1975b. Toxicity and pollution potential of thallium. The Science of the Total Environment 4: 185–192

Zitko, V., Carson, W.V. and Carson, W.G., 1975. Thallium occurrence in the environment and toxicity to fish. Bulletin of Environmental Contamination and Toxicity 13: 23–30

Zubovic, P., Bragg, L.J., Rega, N.H., Lemaster, N.H., Rose, M.E., Golightly, D.W. and Puskas, J., 1980. Chemical analysis of 659 coal samples from the eastern United States. United States Geological Survey, Open–File Report No.-80-2003, 513p

Zyka, V., 1971. Thallium in plants from Alsar. Journal of Geological Sciences, Series TG 10: 91–96

APPENDIX

A1 Sampling protocol

A1.1 Rock sampling

Rocks were sampled from both the underground mining sites and outcrops. The ores of mercury, thallium and arsenic, their wall rocks, and coals were collected in the old and present underground mining sites. The outcrops of rocks and some tailings were also collected. Some secondary minerals were sampled in both underground and outcrops. The sampling pattern is shown in Fig. 5-1.

A1.2 Soil sampling

Soil samples were collected using a stainless steel shovel from the mining sites and natural sites around the mine area so as to represent the natural soils and farm lands on which the locally consumed crops are grown.

At each sampling site, three subsamples were taken over an area of 5 square meters to form a final composite. In some sampling sites, both topsoil (0-20 cm) and subsoil (20-30 cm) were collected to investigate the variation in contents of metals. Samples in a soil profile (77 cm depth) were also collected. All the soil samples were kept in polyethylene bags and air-dried in the laboratory until further processing.

In order to estimate the reproducibility of the sampling procedure, duplicate samples at 10% of the sites were taken at a distance of 5 m from the original sample location.

A1.3 Sediment sampling

The stream sediments were sampled throughout the Qingshui Stream from upstream to downstream. In downstream, one bank sediment sample was also collected. The fresh sediments were stored in cloth bags and air-dried until further processing

A1.4 Water sampling

During the 1998 dry season (October–December), the groundwater was sampled from the springs, the domestic shallow wells and adit water which discharges from hydraulically conductive fractures and in drainage ditches on the mine adit floor; and the stream water was collected through out the Qingshui Stream. In the 1999 wet season (June–August), the surface water was also collected through out the Qingshui Stream, just after two days of a flood event. Waters for geochemical analysis were filtered on site by using Millipore Sterivex syringe capsules containing 0.45 μm cellulose acetate filters. Three filtered sub-samples of water were sealed in pre-cleaned 60 ml Nalgene® bottles, one for anion analysis, one for cation determination (preserved with 0.4 % ultra pure HNO_3 to acidify the sample pH to 2.0), and the third one for mercury determination particularly (preserved with ultra pure HNO_3 + BrCl solution). A field duplicate was collected for every 10 sites. Water temperature, pH, electric conductivity and dissolved oxygen were measured

in the field. All samples were sealed with screw caps and stored in coolers at 4°C and then shipped to the laboratory where they were kept in coolers at the same temperature. The water samples were finally air-shipped to the laboratory of the Geological Survey of Canada in Ottawa for geochemical analysis.

A1.5 Crops and vegetation sampling

Sampled crops are mainly composed of vegetables, and cereals. The edible parts of these crops were the focus of the thallium investigation. The vegetables are Chinese cabbage and green cabbage, mainly collected during the harvest season, but a few were sampled during their early growing stage. All the corn, rice and chili were collected in the harvesting seasons. Some wild grasses and ferns were also collected in the mine area. The sampling sites of crops correspond to the locations of soil samples, that is, around the crops, the soils on which the crops were growing were also collected. The vegetable samples were cleaned using de-ionized water in the field and air-dried in labeled paper bags, whereas the samples of corn, rice and chili were kept air dry in paper bags before shipment to the laboratory.

A2 Treatment of samples prior to analysis

A2.1 Rocks

All the rock samples were prepared for geochemical analysis by jaw crushing to 1.5 cm, sub-sampling and pulverizing in a Bico ceramic disc grinder followed by reduction to <100 mesh powder in a ceramic ball mill. Final product is a 20 grams vial of

representative powder suitable for acid dissolution or fusion. Approximately 5 grams of total rock powder was used for a standard whole-rock and trace-metal analysis.

A2.2 Soils and sediments

All the soil and sediment samples were prepared for geochemical analysis by air-drying at room temperature and by disaggregating to pass through a 2 mm sieve. The sieved fractions were then ground in a Bico ceramic disc grinder followed by reduction to < 80-mesh (< 180 μm) powder in a ceramic ball mill. An 80-mesh screen is usually used because the minus 80-mesh fraction is commonly found to give good anomaly contrast and is sufficiently abundant in most soils and sediments providing the few grams needed for analysis presented no difficulty (Fletcher, 1981). Similarly, in view of common geochemical stream sediment surveys (Van Loon and Barefoot, 1989), the < 180 μm size fraction of the sediments was selected as the fraction most likely to reflect hydromorphically dispersed metals and metalloids and mine site pollution.

A2.3 Waters

The water samples were kept at the laboratory coolers under 4°C, and no additional treatment was carried out prior to on-line determination.

A2.4 Crops and vegetation

All crops and vegetation samples except corn and rice were cut into small pieces (1-2cm long). The rice was treated so its outer sheath was moved. The pure rice samples,

the pure corn samples and the cut vegetable samples were then kept in labeled paper bags and air-dried in an electric drying cabinet in the laboratory at about 25°C until completely dry.

A3 Geochemical analytical methods

A3.1 Rocks

All the rock samples were analyzed at the Analytical Chemistry Laboratories of the Geological Survey of Canada in Ottawa, Canada (Analytical Chemistry Laboratories, 2001).

The analysis of major elements was undertaken by fused disk wavelength dispersive X-ray Fluorescence (XRF). However, for samples containing greater than 5% sulfur, because of problems to produce a fused disc, major elements were determined by Inductively Coupled Plasma–Emission Spectrometry (ICP–ES). For the ICP–ES method, analysis was done by fusing the sample with a mixed lithium metaborate-lithium tetraborate flux, dissolution of the fusion melt followed by analysis by ICP–ES.

Ferrous iron was determined using the Wilson Method (titrimetric). H_2O (total), CO_2 (total) and S (total) were determined using combustion followed by infrared spectrometry using a LECO SC444-DR Sulphur/Carbon Determinator. CO_2 (carbonate carbon) was determined by acid evolution (10 % HCl) of CO_2 which was subsequently analyzed by a LECO CR-12 Carbon Determinator. Reported C (total non-carbonate carbon) was calculated as $C = (CO_{2t}-CO_2)/3.66$. Loss on ignition was determined by gravimetry at 900° C.

For the analysis of trace elements (except for As and Hg), the determinations were based on the total dissolution of the sample using nitric, perchloric and hydrofluoric acids followed by a lithium metaborate fusion of any residual material, and using ICP-ES and ICP-MS. Hg, As and W are determined by INAA at the Activation Laboratories Ltd. in Ancaster, Ontario, Canada.

A3.2 Soils

All the soil samples were analyzed at both the Analytical Chemistry Laboratories of the Geological Survey of Canada in Ottawa and the Norwest Labs in Calgary, Canada.

The determinations of major elements by XRF or ICP-ES and the total trace elements (except for As and Hg) by ICP-ES are the same as the determination of rocks at the Geological Survey of Canada in Ottawa. The results represent the total concentrations of the elements.

The determination of trace metals at the Norwest Labs (Calgary) employs nitric acid and hydrogen peroxide on a hot plate or nitric acid in a closed vessel and microwave digestion. The digestible solution was measured by ICP-ES for determination of Tl, As, Ba, Be, Cd, Cr, Co, Cu, Pb, Mo, Ni, Se, V, Zn plus Hg by cold vapor, and the results are the strong acid extractable concentrations of metals, not the total concentrations, representing the mobile or labile fraction of metals in soils.

The major elements of Ca, Mg, Na, K, cation exchange capacity (CEC), total exchange cation (TEC) and base saturation implying the soil characterization were also determined at the Norwest Labs.

The soil pH values were measured by means of soil in $CaCl_2$ solution at the Analytical Chemistry Laboratories of the Geological Survey of Canada in Ottawa.

A3.3 Sediments

All the sediment samples were analyzed at both the Analytical Chemistry Laboratories of the Geological Survey of Canada in Ottawa and the Norwest Labs in Calgary Canada.

The multiple-elements were determined by ICP-MS following an oxalic acid leach from the Activation Laboratories Ltd. The leachable concentrations of metals represent the mobile or labile fraction in soils.

The determinations of major elements by XRF or ICP-ES and the total trace elements (except for As and Hg) by ICP-MS are the same as the determination of soils at the Geological Survey of Canada in Ottawa. The results represent the total concentrations of the elements.

A3.4 Waters

All the water samples were analyzed at the Analytical Chemistry Laboratories of the Geological Survey of Canada in Ottawa (Analytical Chemistry Laboratories, 2001).

The trace metals were analyzed by direct inductively coupled plasma–mass spectrometry (ICP–MS) while the mercury by cold vapor ICP–MS. The major elements of Na, K, Ca, Mg and Si were determined by ICP–ES, the anions of Cl and SO_4 by ion chromatography, and HCO_3 by acid-base titration. The analytical precision, assured by the

quality assurance/quality control through the duplicates, the blanks and the reference sample OTT96 (Geological Survey of Canada, Ottawa), is better than 15% for major ions and trace metals.

A3.5 Crops and vegetation

All the crops and vegetation samples were analyzed at the Activation Laboratories Ltd. in Ancaster, Ontario, Canada.

The air-dried samples were ashed at 475°C for 36 hours. 0.25 grams of ash was dissolved in 1 ml of concentrated HNO_3 and 1 ml of concentrated H_2O_2 at 90°C for 2 hours and then diluted to 10 with 18 megohm water. The samples were further diluted so that the final dilution is 1000. Samples were spiked with internal standards and analyzed by ICP-MS using a Perkin Elmer SCIEX ELAN 6000.

The ash yield, i.e. the ratio of ash weight to dry weight of crops and vegetation samples, was measured after ashing.